Photo-crosslinked biodegradable polymer networks for controlled intraocular drug delivery

Janine Jansen

Photo-crosslinked biodegradable polymer networks for controlled intraocular drug delivery

Janine Jansen

PhD thesis with references and summaries in English and Dutch
University of Twente, Enschede, The Netherlands
October 2011

The research described in this thesis was carried out between February 2008 and October 2011 in the research group Biomaterials Science and Technology of the MIRA institute for Biomedical Technology and Technical Medicine, University of Twente, Enschede, The Netherlands. The research in this thesis was financially supported by DSM.

Printed by Wöhrmann Print Service, Zutphen, the Netherlands

PHOTO-CROSSLINKED BIODEGRADABLE POLYMER NETWORKS FOR CONTROLLED INTRAOCULAR DRUG DELIVERY

PROEFSCHRIFT

ter verkrijging van
de graad van doctor aan de Universiteit Twente,
op gezag van de rector magnificus,
Prof. Dr. H. Brinksma
volgens besluit van het College van Promoties
in het openbaar te verdedigen
op donderdag 26 januari 2012 om 16.45 uur

door

Janine Jansen

geboren op 29 december 1983
te Brummen

Dit proefschrift is goedgekeurd door de promotoren:
Prof. Dr. Jan Feijen
Prof. Dr. Dirk W. Grijpma

ISBN: 978-90-365-3291-4

Samenstelling van de commissie:

Voorzitter	prof. dr. G. van der Steenhoven
Promotor	prof. dr. J. Feijen
Promotor	prof. dr. D.W. Grijpma
Leden	prof. dr. J.J.L.M. Cornelissen Universiteit Twente, Nederland
	prof. dr. P.J. Dijkstra Universiteit Twente, Nederland en Soochow University, China
	prof. dr. P. Dubruel Universiteit Gent, België
	prof. dr. J.M.M. Hooymans Rijksuniversiteit Groningen, Nederland
	prof. dr. G. Storm Universiteit Utrecht, Nederland
	prof. dr. S. van der Wal Universiteit van Amsterdam, Nederland
	dr. G. Mihov DSM, Nederland

Table of contents

Chapter 1

General introduction

The ageing of our population and the rise in the prevalence of diabetes have increased the number of patients with diseases of the back of the eye such as age related macula degeneration (AMD) and diabetic macular edema (DME). These two diseases are the major causes of blindness in industrialized nations [1]. AMD and DME may require drug delivery to the posterior segment of the eye, which can be achieved most efficiently by direct injection into the vitreous. As these diseases are chronic conditions, repeated injections are often necessary. These injections can be stressful for patients and might lead to complications like endophthalmitis. Patients with AMD or DME would benefit considerably from the development of drug delivery systems that can provide sustained intraocular delivery for months to years.

At the moment several devices for drug delivery to the posterior segment of the eye are commercially available [2, 3]. However, only one of these devices is biodegradable. This device, called Ozurdex®, is an injectable rod-shaped poly(lactic-co-glycolic acid) implant that releases dexamethasone and is applied for the treatment of DME [4]. Degradable drug delivery systems overcome the need to remove the implant after the drug is released. Importantly, no systems are available for the controlled and sustained intraocular release of protein drugs. However, now that more and more recombinant protein therapeutics become available, there clearly is a need for advanced drug delivery systems that can increase the stability and bioavailability of these drugs [5]. Also in the treatment of AMD and other diseases of the back of the eye, protein drugs have proven their use and are frequently used [6]. However, due to their large size and relative instability the controlled release of protein drugs is more complicated than that of low molecular weight drugs.

Many biodegradable polymers have been studied for application in controlled drug delivery systems [7]. Due to their versatility, photo-crosslinked polymer networks are an interesting class of polymeric materials for application in drug delivery systems [8]. The drug release profiles of these materials can be tuned by varying the crosslink density or hydrophilicity of the networks. Moreover, networks can easily be loaded with drugs by

dispersing or dissolving the drug in a macromer solution prior to the photo-crosslinking process. Since photo-polymerization is rapid and can be accomplished with minimal heat generation, the incorporation of heat-sensitive compounds such as proteins is feasible. Samples with different shapes can simply be prepared using molds while crosslinked micro- and nanoparticles can be prepared by irradiating emulsions.

Photo-crosslinked polymer networks are often prepared from oligomers that are end-functionalized with double bond-containing groups. Besides the frequently used methacrylate and acrylate derivatives, fumaric acid derivates are also attractive compounds for end-functionalization of oligomers [9]. It can be expected that residual unreacted fumarate end-groups will not lead to toxicity upon implantation since fumaric acid generated after hydrolysis is a compound naturally found in the body [10].

Scope of the studies

In this thesis two main issues are addressed. First the potential of fumaric acid derivatives in the preparation of photo-crosslinked polymer networks will be explored. Different degradable oligomers are end-functionalized with fumaric acid monoethyl ester (FAME). These end-groups are compared to the more frequently used methacrylate end-groups and several different network materials are prepared and characterized. Secondly, the potential of photo-crosslinked polymer networks for intraocular drug delivery is studied. The release of model drugs from several different photo-crosslinked polymer networks is evaluated and the intraocular degradation behavior of several materials is investigated.

Outline of the thesis

In **Chapter 2** an introduction to biodegradable photo-crosslinked polymer networks is given. Current approaches for intraocular drug delivery are reviewed and several examples of the application of biodegradable photo-crosslinked polymer networks in drug delivery systems are presented.

Chapter 3 describes the preparation of photo-crosslinked polymer networks from FAME-functionalized poly(trimethylene carbonate) (PTMC) oligomers. The reaction kinetics are evaluated and N-vinyl-2-pyrrolidone (NVP) and vinyl acetate are used as reactive diluents. The release of vitamin B12, a model drug, from networks with different hydrophilicites is investigated.

In **Chapter 4** the release of two model proteins, lysozyme and albumin, from networks prepared from FAME-functionalized PTMC oligomers is studied. NVP is used as a reactive diluent and oligomers of different molecular weights are used to vary the network mesh-size.

Chapter 5 is focused on the preparation of photo-crosslinked polymer networks from FAME-functionalized poly(D,L-lactic acid) (PDLLA) oligomers. The molecular weight of the oligomers and the NVP content are varied to obtain networks with different mesh-sizes and hydrophilicities. The release of lysozyme and albumin from the networks is assessed.

In **Chapter 6** the preparation of photo-crosslinked hydrogels is described. The hydrogels are prepared from FAME-functionalized triblock oligomers with a hydrophilic poly(ethylene glycol) middle block. The hydrophobic blocks consist of PTMC, PDLLA or a copolymer of the two monomers. The length and composition of the hydrophobic blocks are varied to tune degradation and protein release profiles.

In **Chapter 7** attention is paid to the kinetic chain length of PDLLA-methacrylate networks. 2-Mercaptoethanol is used as a chain transfer agent to control the kinetic chain length. Network specimens are degraded and the molecular weights of the non-degradable carbon-carbon kinetic chains are determined.

Chapter 8 describes the intraocular degradation behavior of linear and crosslinked PTMC and PDLLA. Rod-shaped samples are implanted in the vitreous of rabbits and the degradation process is followed in time.

In **Chapter 9** the preparation of photo-crosslinked microspheres is described. These are prepared from FAME- and methacrylate-functionalized PDLLA oligomers using the emulsion solvent evaporation method.

References

[1] C. Bunce, W. Xing, R. Wormald, Causes of blind and partial sight certifications in England and Wales: April 2007-March 2008. Eye 24(11) (2010) 1692-1699.

[2] E. Eljarrat-Binstock, J. Pe'er, A. Domb, New techniques for drug delivery to the posterior eye segment. Pharm Res 27(4) (2010) 530-543.

[3] T.R. Thrimawithana, S. Young, C.R. Bunt, C. Green, R.G. Alany, Drug delivery to the posterior segment of the eye. Drug Discov Today 16(5-6) (2011) 270-277.

[4] J.A. Haller, F. Bandello, R. Belfort Jr, M.S. Blumenkranz, M. Gillies, J. Heier, A. Loewenstein, Y.-H. Yoon, M.-L. Jacques, J. Jiao, X.-Y. Li, S.M. Whitcup, Randomized, sham-controlled trial of dexamethasone intravitreal implant in patients with macular edema due to retinal vein occlusion. Ophthalmology 117(6) (2010) 1134-1146.

[5] A.K. Pavlou, J.M. Reichert, Recombinant protein therapeutics - success rates, market trends and values to 2010. Nat Biotechnol 22(12) (2004) 1513-1519.

[6] W.R. Freeman, Avastin and new treatments for AMD: Where are we? Retina 26(8) (2006) 853-858.

[7] B.D. Ratner, A.S. Hofmann, F.J. Schoen, J.E. Lemons, Biomaterials Science, Elsevier, 2004.

[8] B. Baroli, Photopolymerization of biomaterials: issues and potentialities in drug delivery, tissue engineering, and cell encapsulation applications. J Chem Technol Biot 81(4) (2006) 491-499.

[9] D.W. Grijpma, Q. Hou, J. Feijen, Preparation of biodegradable networks by photo-crosslinking lactide, ε-caprolactone and trimethylene carbonate-based oligomers functionalized with fumaric acid monoethyl ester. Biomaterials 26(16) (2005) 2795-2802.

[10] H. Shin, J.S. Temenoff, A.G. Mikos, In vitro cytotoxicity of unsaturated oligo[poly(ethylene glycol) fumarate] macromers and their cross-linked hydrogels. Biomacromolecules 4(3) (2003) 552-560.

Chapter 2

Photo-crosslinked biodegradable polymer networks for controlled intraocular drug delivery

Photo-crosslinked biodegradable polymer networks

Biodegradable polymer networks can be formed through photo-initiated crosslinking of degradable macromers that contain two or more double bonds (Figure 1). In this way a macromer solution or melt is converted to a solid three-dimensional network via a chain polymerization mechanism. This reaction follows the characteristic steps of chain polymerizations, with photo-initiation, propagation and termination [1]. Upon illumination a photo-initiator dissociates and (most often) forms two radicals. These radicals react with the carbon-carbon double bonds of the macromer, forming a growing kinetic chain. These kinetic chains are carbon-carbon chains that remain present after degradation of the network. Termination occurs by combination, disproportionation or chain transfer.

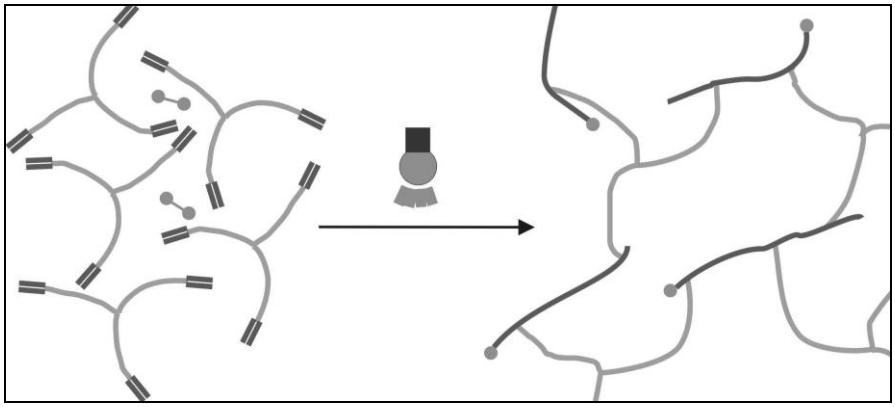

Figure 1. *Polymer network formation through photo-initiated crosslinking of functionalized oligomers.*

Biodegradable photo-crosslinked polymer networks are often prepared from degradable oligomers that are end-functionalized with double bond-containing groups (Figure 1). Many degradable oligomers have been used in the preparation of photo-crosslinked

polymer networks. Examples are poly(trimethylene carbonate) (PTMC) [2, 3] and aliphatic polyesters, such as poly(lactic acid) (PLA) [4], poly(ε-caprolactone) (PCL) [5, 6] and poly(propylene fumarate) (PPF) [7]. Also block copolymers of poly(ethylene glycol) (PEG) and aliphatic polyesters have been frequently used in the preparation of photo-crosslinked hydrogels [8]. PLA, PCL and PTMC can be synthesized by ring opening polymerization of cyclic monomers. By changing the amount and functionality of the alcohol used as a co-initiator, the molecular weight and number of arms of the synthesized oligomer can be controlled [9].

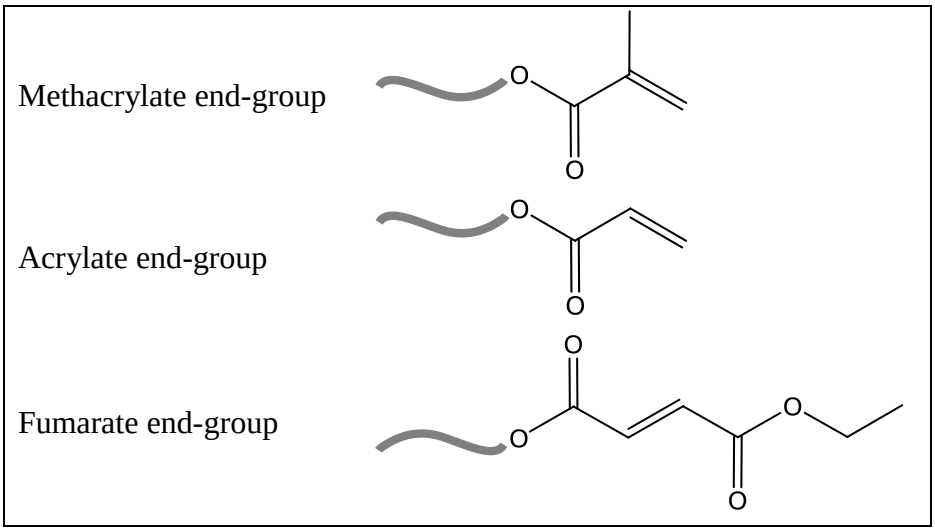

Figure 2. *Photo-polymerizable methacrylate, acrylate and fumarate end-groups.*

To allow for network preparation by photo-initiated crosslinking, degradable oligomers need to be functionalized with double bond-containing groups to obtain macromers (Figure 2). However, poly(propylene fumarate) is an example of a biodegradable polymer that needs no further functionalization, because the backbone already contains double bonds. Methacrylate- and acrylate derivatives have been most frequently used in end-functionalization reactions. Fumaric acid derivatives are also attractive compounds for end-functionalization. Fumaric acid is a compound naturally found in the body as a component of the citric acid cycle, therefore it can be expected that residual unreacted fumarate end-groups will not lead to toxicity upon implantation after hydrolysis [10]. Compared to (meth)acrylate-functionalized oligomers, the reactivity of fumarate-functionalized oligomers is relatively low [11]. By copolymerization with a suitable comonomer, the fumarate crosslinking reaction can be accelerated significantly. N-vinyl-2-pyrrolidone (NVP) is often used as a comonomer in the photo-polymerization of fumaric acid derivatives [12, 13].

Photo-crosslinked biodegradable polymer networks are an interesting class of materials for biomedical applications, as photo-crosslinking is rapid and can be accomplished with minimal heat generation [14]. A wide range of substances and even cells can be entrapped in the networks [15] and spatial and temporal control over the polymerization process allows for the fabrication of polymer matrices with complex shapes [16]. Therefore, photo-crosslinked biodegradable polymer networks have been studied frequently for application in drug delivery devices [17] and as scaffolding materials for tissue engineering [18].

Intraocular drug delivery

In ophthalmology, several chronic diseases may require repeated drug delivery to the posterior segment of the eye. Examples are age-related macula degeneration (AMD), diabetic macular edema, and uveitis (inflammation of the uvea, the middle vascular layer of the eye). AMD is the leading cause of blindness in the developed world [19]. Drug delivery to the posterior segment of the eye is challenging and several barriers need to be overcome [20]. Topical ocular medications such as eye drops hardly reach the posterior segment and the blood-retinal barriers prevent most systemically delivered drugs from achieving therapeutic levels in the posterior segment of the eye. Pharmacologically, the most efficient way to deliver drugs to the posterior segment is direct administration into the vitreous. Following injection, drugs are cleared from the vitreous within days or weeks, depending on the drug [20-22]. The repeated injections that are often required can be stressful for patients and might lead to complications such as endophthalmitis.

Developments in protein and gene therapy have highlighted the need for advanced drug delivery systems capable of increasing the stability and bioavailability of these new therapeutic agents [23]. For example, since a few years AMD is treated with anti-VEGF (vascular endothelial growth factor**)** antibodies (Lucentis® (Ranibizumab) and Avastin® (Bevacizumab, used off-label)) through monthly intraocular injections [24]. In patients with severe AMD, choroidal neovascularization occurs. Exudates and bleeding from these vessels lead to scar formation in the macula and irreversible vision loss. Lucentis® and Avastin® prevent the formation of new blood vessels trough the inhibition of VEGF. The development of an intraocular sustained release system, capable of maintaining a therapeutic level of these drugs within the vitreous cavity for several months or even years would be a significant advance in the treatment of AMD. However, the controlled release of protein drugs is more complicated than that of low molecular weight drugs due to their large size and relative instability.

Non-biodegradable systems

Several controlled release systems have been developed to achieve sustained intraocular drug levels [25-28]. In 1996 Vitrasert® (Baush & Lomb) (Figure 3, C) was the first implantable drug delivery system to be approved by the FDA for the treatment of posterior segment disease [29]. The non-biodegradable implant is used to treat cytomegalovirus retinitis which is common in patients with AIDS. The reservoir-type device, composed of the drug and a coating of poly(vinyl alcohol) (PVA) and poly(ethylene vinyl acetate) (PEVA), releases ganciclovir over an 8 month period. Because the device is non-degradable, the empty device must be removed during a second surgery. A second commercially available non-degradable implant very similar to Vitrasert® is a fluocinolone acetonide implant (Retisert®, Baush & Lomb) applied for the treatment of uveitis [30]. This device was approved by the FDA in 2005. Several other less invasive non-degradable implants are currently being evaluated in clinical trials [28]. These include I-vation™ (SurModics) [31], a scleral plug (Figure 3, B) releasing triamcinolone acetonide, and Illuvien™ (Alimera Sciences) [32], an injectable rod-shaped implant (Figure 3, A) delivering fluocinolone acetonide, both for the treatment of diabetic macular edema.

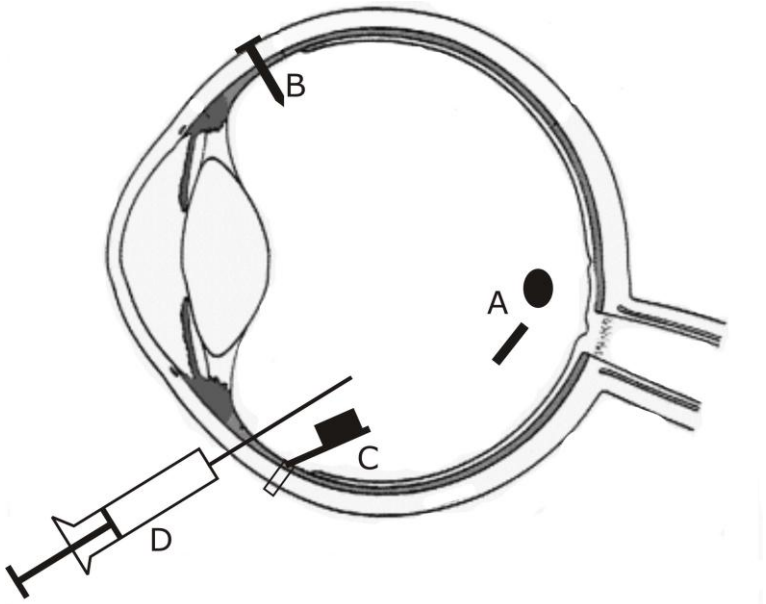

Figure 3. *Controlled intraocular drug delivery. A - Rod or disc shaped implants. Small rods can be injected. B - Scleral plug. C - Vitrasert®/Retisert® implant. D- Intravitreal injection of microspheres.*

Biodegradable systems

Degradable inserts overcome the need to remove the implant after the drug is released. Ozurdex® (formerly Posurdex®, Allergan Inc.) [33], which was FDA approved in 2009, is the only degradable device for drug delivery to the posterior segment of the eye currently on the market. The injectable rod-shaped PLGA (poly(lactic-co-glycolic acid)) implant releases dexamethasone and is applied for the treatment of diabetic macular edema. Several other degradable systems designed for drug delivery to the posterior segment of the eye are currently under investigation [34-38]. Biodegradable systems under investigation are typically the matrix (monolithic) type, consisting of a homogeneous rod or pellet made from biodegradable polymer and drug, although core-shell and microparticle systems have also been studied. Most of the current literature on intraocular use of biodegradable polymers refers to PLA or PLGA. For example Kunou *et al.* [39] developed a poly(D,L-lactic acid) (PDLLA) scleral plug for the release of ganciclovir. A mixture of high and low molecular weight PDLLA was used to obtain optimal *in vivo* drug release profiles in the vitreous over a period of 25 wk. More recently a donut-shaped PLGA implant was developed by Choonara *et al.* [40]. This device, also designed to release ganciclovir, is sutured to the sclera and was found to be well tolerated in the rabbit vitreous. Also several microparticle systems based on PLA and PLGA have been studied. For example, Peyman *et al.* [41] investigated the use of PLGA microspheres for the intraocular release of cytosine arabinoside and 5-fluorouracil, two antimetabolic drugs, in primates. It was found that both drugs could be detected in the vitreous 11 d after injection of the microspheres. Mordenti *et al.* [42] studied the intraocular release of a humanized monoclonal antibody (a 148 kDa model protein) from PLGA microspheres. It was shown that it is possible to release proteins inside the vitreous from PLGA microspheres. However, only approximately 30% of the loaded protein was released, which was also observed in *in vitro* experiments. Furthermore, the PLGA formulation did not offer any pharmacokinetic advantage over the solution formulation since the release of the antibody from the microspheres was relatively fast and the protein has a long half-life in the vitreous (approximately 6 d). These results point out that achieving controlled and sustained release of proteins from biodegradable polymers is often a lot more challenging than achieving controlled and sustained release of low molecular weight drugs.

Currently a sustained release formulation based on PLGA microspheres is being developed for Macugen® (pegabtanib sodium), a PEGylated anti-VEGF aptamer (a single strand oligonucleotide) that is used in the treatment of AMD [43]. *In vitro* release of this 50 kDa drug over a period of several weeks without loss of activity was achieved.

Besides PLA and PLGA also other degradable polymers have been investigated for use in intraocular drug delivery systems. Silva-Cunha *et al.* [44] studied the intravitreal release of dexamethasone from a disk-shaped poly(ε-caprolactone) implant. The degradation of PCL is slow compared to that of PLA and PLGA and it was found that after 55 wk 79 % of the drug was still present in the implant. The devices were well tolerated in the rabbit eye. It was suggested that these slowly degrading devices could be suitable for sustained intraocular drug delivery over months or even years.

Heller *et al.* [45] investigated the use of poly(ortho esters) for intraocular delivery of 5-fluorouracil. Two different poly(ortho esters), both viscous injectable materials, were found to be well tolerated in the rabbit vitreous. One of the materials degraded rapidly, within approximately 5 d, while the lifetime of the other material was approximately 3 months. Although *in vitro* release of 5-fluorouracil from poly(ortho esters) over periods of several days to a few months has been shown to be feasible, drug delivery to the posterior segment of the eye has yet to be investigated.

Mikos and coworkers [46, 47] developed rod-shaped photo-crosslinked monolithic drug delivery devices consisting of PPF and NVP for the release of several low molecular weight ophthalmic drugs. *In vitro* the drugs were released from the matrix over a period of several months to a year. An initial 2 wk implantation study showed that the PPF/NVP implants were well tolerated in the rabbit vitreous.

Drug delivery from photo-crosslinked biodegradable polymer networks

Biodegradable photo-crosslinked polymer networks are an interesting class of materials for application in drug delivery [14]. Networks can be easily loaded with drugs by dispersing or dissolving the drug in a crosslinkable macromer solution prior to the crosslinking process (Figure 4). In this way, large amounts of drug can be loaded into a matrix at high efficiencies. By varying parameters such as the crosslink density and network hydrophilicity, release profiles can be controlled. By the use of molds devices with different geometries can be prepared. It is also possible to prepare crosslinked micro- or nanoparticles [48-50].

Photo-crosslinked polymer networks are attractive for the release of sensitive drugs such as proteins, since networks are formed with minimal heat generation. However, protein stability issues that are known for all polymeric protein delivery systems are also relevant for photo-crosslinked polymer networks. During preparation, storage and release, a range of conditions may affect the stability of the protein [51, 52]. For example, the use of organic solvents and exposure to water-oil interfaces may lead to protein denaturation. Interaction with hydrophobic polymer surfaces and a drop in pH as a result of polymer

degradation may lead to protein aggregation or denaturation. All of these factors should be considered when a new protein release device is developed.

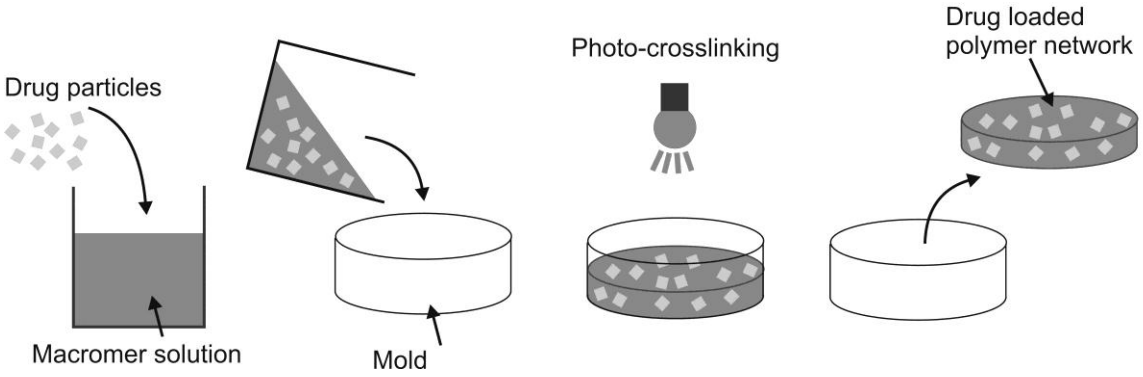

Figure 4. *Preparation of a drug loaded photo-crosslinked polymer network.*

In photo-crosslinked polymer networks the network is formed through free-radical chain polymerization. Free radicals may undergo side reactions with the incorporated proteins which can result in protein denaturation or covalent attachment of the protein to the network [14, 53]. Several approaches have been suggested to prevent these effects. First of all, the photo-crosslinking reaction should be rapid to minimize exposure of the protein to the radicals. Also, the concentration of double bonds is important, since it was found that damage to proteins is limited if sufficient double bond-containing groups are present to react with the radicals [54]. If proteins are encapsulated in a photo-crosslinked hydrogel, the protein is protected from the free radicals if the polymerization reaction takes place in the hydrophobic domains, while the protein resides in the hydrophilic domains. This can be achieved if good phase separation occurs prior to the crosslinking reaction and a relatively hydrophobic photo-initiator is used that is mainly present in the hydrophobic domains (Figure 5) [53].

Baroli *et al.* [55] proposed a method where a protein was first incorporated in gelatin particles before encapsulation in a photo-crosslinked hydrogel. In their system, Gu *et al.* [54] dispersed solid protein particles in an organic phase that contains the macromers and the initiator. The researchers remark that if proteins are in solution during crosslinking it is likely that side reactions with free radicals occur, whereas if a protein is present in the form of solid particles during the polymerization reaction, contact with free radicals is limited.

Photo-crosslinked hydrogels

Many researchers have studied PEG copolymer based photo-crosslinked networks for controlled release applications. These networks are generally highly swollen hydrogels that degrade by hydrolytic bulk degradation. Hubbell and coworkers were the first to prepare biodegradable photo-crosslinked hydrogels from water soluble macromers with a central PEG block and D,L-lactide or glycolide hydrophobic blocks terminated with acrylate groups [8]. Several proteins were dissolved in the macromer solution prior to crosslinking and their release from disk-shaped hydrogel specimens was studied [56]. Proteins were released from the hydrogels in several days and proteins with a low molecular weight were released faster than proteins with a high molecular weight. It was found that the release of protein from the hydrogel was controlled by both diffusion and degradation. The researchers state that the macromer must be matched to molecular weight of the drug if drug release is to be controlled by degradation. If the incorporated drug is much smaller than the hydrogel mesh-size, release will be diffusion controlled.

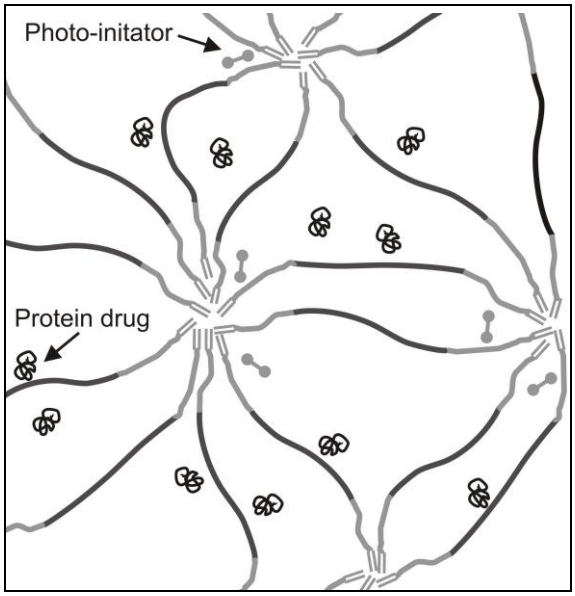

Figure 5. *A phase separated macromer solution prior to hydrogel formation through photo-crosslinking. The incorporated protein resides in the hydrophilic domains while photo-polymerization takes place in the hydrophobic domains.*

In a later study Anseth and coworkers investigated the release of lysozyme, bovine serum albumin (BSA) and FITC-labeled (fluorescein isothiocyanate) dextran from the same degradable PEG-based hydrogels [57]. The initial mesh-size of the different hydrogels was calculated and followed in time as hydrolytic degradation simultaneously occurred. Based on these data and the size of the incorporated model drug the release profiles could

be modeled. The three model compounds were released from the hydrogels within several days. The small protein lysozyme (14.6 kDa) was released faster than the high molecular weight FITC-dextran (77 kDa). In the same research group the release of DNA from photo-crosslinked hydrogels prepared from methacrylated triblock oligomers was investigated [58]. Again the hydrophilic block was PEG and the hydrophobic block was either PDLLA or PCL. DNA could be released over periods of 6 to 100 days. It was found however that maintaining the biological activity of the encapsulated DNA during photo-encapsulation and the release period was challenging.

More recently another type of photo-crosslinked degradable hydrogels was developed by Hennink and coworkers [59, 60]. These hydrogels consist of triblock copolymers with a hydrophilic PEG middle block and methacrylated poly(N-(2-hydroxypropyl) methacrylamide lactate) hydrophobic blocks. These hydrophobic blocks are thermosensitive and a hydrogel is formed when a macromer solution is heated above a certain temperature. These gels can then be further stabilized by photo-crosslinking of the methacrylate groups. The release of lysozyme, bovine serum albumin and IgG from these hydrogels was studied. It was found that the proteins were released from the hydrogels in several days to one month, depending on the size of the protein. Release of the proteins was controlled by diffusion only and degradation of the gels did not play a role. Importantly, complete release of the proteins was found and the released lysozyme was fully active. The release rate of the proteins could be tuned by varying the macromer concentration in the crosslinked solution. More concentrated macromer solutions resulted in slower release. Also the molecular weight of the PEG block and the degree of methacrylation were found to affect the release profiles.

Photo-crosslinked hydrophobic networks

As can be seen from these examples, photo-crosslinked hydrogels are mainly suitable for short term drug release. For sustained drug release more hydrophobic networks are required. Several more hydrophobic photo-crosslinked biodegradable polymer networks have been investigated for controlled release applications. Amsden and coworkers have extensively studied the use of acrylated star-shaped ε-caprolactone-co-D,L-lactide oligomers for the controlled and sustained release of proteins [54, 61-63]. In their system, solid drug particles were dispersed in the macromer solution prior to crosslinking. If sensitive proteins were encapsulated the solid particles were prepared by lyophilizing the protein with bovine serum albumin and/or trehalose. These compounds protect the protein from side reactions and denaturation during crosslinking and release. Interferon-γ, VEGF and interleukin-2 could be released over periods of a few weeks. Release from the

photo-crosslinked elastomers was driven by osmotic pressure and protein bioactivity was maintained to a large extent (60-90 %).

In other studies acrylated star-shaped ε-CL-co-DLLA oligomers were combined with acrylated PEG-based oligomers to tune network hydrophilicity [64, 65]. Vitamin B12, goserelin acetate and MFFD (an anti-atherosclerotic peptide) were incorporated in these networks as solid particles and were released over periods of several weeks to 3 months. Release rates could be tuned by varying the amount of PEG incorporated and the PEG molecular weight. For these networks drug release was diffusion controlled.

Recently, photo-crosslinked acrylated TMC-based oligomers were investigated for application in drug delivery [66, 67]. Networks prepared from acrylated star-shaped trimethylene carbonate-co-ε-caprolactone-co-D,L-lactide oligomers were applied for releasing VEGF and hepatocyte growth factor (HGF). Protein particles that were incorporated in the networks were prepared by colyophilization with trehalose, albumin and/or NaCl. The proteins were released through osmotic pressure driven release over a period of approximately 1 month and 70-90 % of the bioactivity was maintained. In another study bovine serum albumin, colyophilized with trehalose and/or NaCl, was incorporated in networks prepared from acrylated star-shaped TMC and TMC-co-DLLA oligomers. It was found that networks prepared from TMC macromers were not suitable for osmotic pressure driven protein release due to their high tear resistance. BSA incorporated in networks prepared from acrylated star poly(TMC-co-DLLA) macromers was released in approximately 1 month.

As described above, Mikos and coworkers investigated photo-crosslinked PPF/NVP networks for use in intraocular drug delivery [46, 47, 68]. Several low molecular weight drugs were incorporated in and released from these networks over periods of up to 1 year. Drug release was controlled by diffusion and network degradation. Unfunctionalized PEG was added and the PPF/NVP ratio was adjusted to tune network hydrophilicity and drug release. An injectable ocular drug delivery system based on PPF was also developed [69]. Here PPF and the drug, fluocinolone acetonide, were dissolved in N-methyl pyrrolidone, a water-miscible non-reactive solvent. Upon injection of the solution the matrix precipitates and can be stabilized further by visible light initiated photo-polymerization. No NVP was incorporated in the formulation and therefore photo-crosslinking of the PPF chains is slow. *In vitro*, fluocinolone acetonide was released over a period of approximately 1 year.

Sharifi *et al.* prepared macromers from ε-caprolactone oligomers linked by fumarate groups [70]. Networks were prepared by photo-crosslinking these macromers using NVP

as a comonomer. Tamoxifen citrate particles were incorporated in the networks. The drug was released over a period of approximately 2 wk and release was diffusion controlled.

Materials that degrade by surface erosion are attractive for application in drug delivery devices, since linear release profiles can be obtained and release rates are not dependent on the size and hydrophilicity of the incorporated drug. Quick *et al.* studied DNA release from photo-crosslinked polyanhydride networks prepared from methacrylated sebacic acid (MSA) and methacrylated 1,6-bis(carboxyphenoxy)hexane (MCPH) [71]. The networks degraded by surface erosion and linear release profiles were obtained. By changing the ratio of the two components degradation and release rates could be controlled. Release periods varied from several days to one month. When the DNA was mixed into the precursor solution as solid particles DNA recovery was limited to 25 %. This could be improved to 70 % by pre-encapsulation of the DNA in alginate particles.

Weiner *et al*. combined MSA and MCPH with PEG diacrylate to obtain more hydrophilic polyanhydride networks [72]. Two model proteins, horseradish peroxidase and FITC labeled BSA, were incorporated and released. The proteins were protected by pre-encapsulation in gelatin particles. As these networks are more hydrophilic than the polyanhydride networks studied by Quick *et al*., they do not degrade by surface erosion and release is controlled by diffusion and matrix degradation. The proteins were released in 1 wk to 4 months, depending on the amount of PEG and the MSA to MCPH ratio. Although active horseradish peroxidase was released, the release of both FITC-BSA and horseradish peroxidase was incomplete.

Recently Seppälä and coworkers prepared photo-crosslinked surface eroding poly(ester anhydride) networks from stars-shaped poly(ε-caprolactone) oligomers first reacted with succinic anhydride and then functionalized with methacrylate end-groups [73, 74]. Propranolol HCl, a low molecular weight model drug, and dextran, a high molecular weight model drug, were incorporated. Both drugs were released by surface erosion controlled release within 1 to 3 d, illustrating that for surface eroding materials drug release rates are not affected by the size of the drug. Surface erosion and drug release rates could be tuned to some extent by using alkenyl succinic anhydrides with different alkenyl chain lengths.

Lendlein and coworkers illustrated that photo-crosslinked polymer networks are versatile materials by combining drug release, degradation and shape memory behavior in one material [75]. Low molecular weight model drugs where released from their networks prepared from methacrylated ε-caprolactone-co-glycolide oligomers within a few months by diffusion controlled release.

Conclusions

The literature reviewed in this chapter illustrates that photo-crosslinked biodegradable polymer networks are versatile materials that have been studied frequently for application in controlled drug delivery. Also for intraocular drug delivery these materials could very well be used. Small injectable rods can be prepared by photo-crosslinking in molds and also photo-crosslinked microspheres can be prepared. Controlled and sustained release of protein drugs remains challenging due to the large size and instability of these molecules. When incorporating protein drugs in photo-crosslinked polymer networks, care should be taken to prevent side reactions of free radicals with the protein during crosslinking.

References

[1] G. Odian, Principles of Polymerization, Wiley-Interscience, 2004.

[2] Q. Hou, D.W. Grijpma, J. Feijen, Creep-resistant elastomeric networks prepared by photocrosslinking fumaric acid monoethyl ester-functionalized poly(trimethylene carbonate) oligomers. Acta Biomater 5(5) (2009) 1543-1551.

[3] T. Matsuda, I.K. Kwon, S. Kidoaki, Photocurable biodegradable liquid copolymers: Synthesis of acrylate-end-capped trimethylene carbonate-based prepolymers, photocuring, and hydrolysis. Biomacromolecules 5(2) (2004) 295-305.

[4] F.P.W. Melchels, J. Feijen, D.W. Grijpma, A poly(D,L-lactide) resin for the preparation of tissue engineering scaffolds by stereolithography. Biomaterials 30(23-24) (2009) 3801-3809.

[5] A.O. Helminen, H. Korhonen, J.V. Seppälä, Crosslinked poly(ester anhydride)s based on poly(ε-caprolactone) and polylactide oligomers. J Polym Sci A Polym Chem 41(23) (2003) 3788-3797.

[6] M.P K. Turunen, H. Korhonen, J. Tuominen, J.V. Seppälä, Synthesis, characterization and crosslinking of functional star-shaped poly(ε-caprolactone). Polym Int 51(1) (2002) 92-100.

[7] J.P. Fisher, M.D. Timmer, T.A. Holland, D. Dean, P.S. Engel, A.G. Mikos, Photoinitiated cross-linking of the biodegradable poly(propylene fumarate). Part I. Determination of network structure. Biomacromolecules 4(5) (2003) 1327-1334.

[8] A.S. Sawhney, C.P. Pathak, J.A. Hubbell, Bioerodible hydrogels based on photopolymerized poly(ethylene glycol)-co-poly(α-hydroxy acid) diacrylate macromers. Macromolecules 26(4) (1993) 581-587.

[9] H. Korhonen, A. Helminen, J.V. Seppälä, Synthesis of polylactides in the presence of co-initiators with different numbers of hydroxyl groups. Polymer 42(18) (2001) 7541-7549.

[10] H. Shin, J.S. Temenoff, A.G. Mikos, In vitro cytotoxicity of unsaturated oligo[poly(ethylene glycol) fumarate] macromers and their cross-linked hydrogels. Biomacromolecules 4(3) (2003) 552-560.

[11] D.W. Grijpma, Q. Hou, J. Feijen, Preparation of biodegradable networks by photo-crosslinking lactide, ε-caprolactone and trimethylene carbonate-based oligomers functionalized with fumaric acid monoethyl ester. Biomaterials 26(16) (2005) 2795-2802.

[12] J. Jansen, F.P.W. Melchels, D.W. Grijpma, J. Feijen, Fumaric acid monoethyl ester-functionalized poly(D,L-lactide)/N-vinyl-2-pyrrolidone resins for the preparation of tissue engineering scaffolds by stereolithography. Biomacromolecules 10(2) (2009) 214-220.

[13] A.S. Sarvestani, W. Xu, X. He, E. Jabbari, Gelation and degradation characteristics of in situ photo-crosslinked poly(L-lactide-co-ethylene oxide-co-fumarate) hydrogels. Polymer 48(24) (2007) 7113-7120.

[14] B. Baroli, Photopolymerization of biomaterials: issues and potentialities in drug delivery, tissue engineering, and cell encapsulation applications. J Chem Technol Biot 81(4) (2006) 491-499.

[15] S.J. Bryant, K.S. Anseth, Hydrogel properties influence ECM production by chondrocytes photoencapsulated in poly(ethylene glycol) hydrogels. J Biomed Mater Res 59(1) (2002) 63-72.

[16] F.P.W. Melchels, J. Feijen, D.W. Grijpma, A review on stereolithography and its applications in biomedical engineering. Biomaterials 31(24) (2010) 6121-6130.

[17] K. Davis, Controlled release from crosslinked degradable networks. Crit Rev Ther Drug Carrier Syst 19(4-5) (2002) 385-423.

[18] J.L. Ifkovits, J.A. Burdick, Review: Photopolymerizable and degradable biomaterials for tissue engineering applications. Tissue Eng 13(10) (2007) 2369-2385.

[19] C. Bunce, W. Xing, R. Wormald, Causes of blind and partial sight certifications in England and Wales: April 2007-March 2008. Eye 24(11) (2010) 1692-1699.

[20] A. Urtti, Challenges and obstacles of ocular pharmacokinetics and drug delivery. Adv Drug Deliv Rev 58(11) (2006) 1131-1135.

[21] S.J. Bakri, M.R. Snyder, J.M. Reid, J.S. Pulido, R.J. Singh, Pharmacokinetics of intravitreal Bevacizumab (Avastin). Ophthalmology 114(5) (2007) 855-859.

[22] T.U. Krohne, N. Eter, F.G. Holz, C.H. Meyer, Intraocular pharmacokinetics of Bevacizumab after a single intravitreal injection in humans. Am J Ophthalmol 146(4) (2008) 508-512.

[23] A.K. Pavlou, J.M. Reichert, Recombinant protein therapeutics - success rates, market trends and values to 2010. Nat Biotechnol 22(12) (2004) 1513-1519.

[24] R. Jager, W. Mieler, J. Miller, Medical progress: Age-related macular degeneration. N Engl J Med 358(24) (2008) 2606-2617.

[25] M.J. Colthurst, R.L. Williams, P.S. Hiscott, I. Grierson, Biomaterials used in the posterior segment of the eye. Biomaterials 21(7) (2000) 649-665.

[26] E.M. del Amo, A. Urtti, Current and future ophthalmic drug delivery systems: A shift to the posterior segment. Drug Discov Today 13(3-4) (2008) 135-143.

[27] E. Eljarrat-Binstock, J. Pe'er, A. Domb, New techniques for drug delivery to the posterior eye segment. Pharm Res 27(4) (2010) 530-543.

[28] T.R. Thrimawithana, S. Young, C.R. Bunt, C. Green, R.G. Alany, Drug delivery to the posterior segment of the eye. Drug Discov Today 16(5-6) (2011) 270-277.

[29] B. Dhillon, A. Kamal, C. Leen, Intravitreal sustained-release ganciclovir implantation to control cytomegalovirus retinitis in AIDS. Int J STD AIDS 9(4) (1998) 227-230.

[30] G.J. Jaffe, D. Martin, D. Callanan, P.A. Pearson, B. Levy, T. Comstock, Fluocinolone acetonide implant (Retisert) for noninfectious posterior uveitis - Thirty-four-week results of a multicenter randomized clinical study. Ophthalmology 113(6) (2006) 1020-1027.

[31] P.U. Dugel, H.L. Cantrill, D. Eliott, T. Mahmoud, R. Avery, S.E. Varner, Clinical safety and preliminary efficacy of an intravitreal triamcinolone implant (I-vationTM TA) in DME. Invest Ophthalmol Vis Sci 48(5) (2007) 1413.

[32] F.E. Kane, J. Burdan, A. Cutino, K.E. Green, Iluvien (TM): a new sustained delivery technology for posterior eye disease. Expert Opin Drug Deliv 5(9) (2008) 1039-1046.

[33] J.A. Haller, F. Bandello, R. Belfort Jr, M.S. Blumenkranz, M. Gillies, J. Heier, A. Loewenstein, Y.-H. Yoon, M.-L. Jacques, J. Jiao, X.-Y. Li, S.M. Whitcup, Randomized, sham-controlled trial of dexamethasone intravitreal implant in patients with macular edema due to retinal vein occlusion. Ophthalmology 117(6) (2010) 1134-1146.

[34] R. Herrero-Vanrell, I.T. Molina-Martinez, PLA and PLGA microparticles for intravitreal drug delivery: an overview. J Drug Deliv Sci Technol 14(1) (2007) 11-17.

[35] R. Herrero-Vanrell, M.F. Refojo, Biodegradable microspheres for vitreoretinal drug delivery. Adv Drug Deliv Rev 52(1) (2001) 5-16.

[36] N. Kuno, S. Fujii, Biodegradable intraocular therapies for retinal disorders progress to date. Drugs Aging 27(2) (2010) 117-134.

[37] S.S. Lee, P. Hughes, A.D. Ross, M.R. Robinson, Biodegradable implants for sustained drug release in the eye. Pharm Res 27(10) (2010) 2043-2053.

[38] T. Yasukawa, H. Kimura, Y. Tabata, Y. Ogura, Biodegradable scleral plugs for vitreoretinal drug delivery. Adv Drug Deliv Rev 52(1) (2001) 25-36.

[39] N. Kunou, Y. Ogura, T. Yasukawa, H. Kimura, H. Miyamoto, Y. Honda, Y. Ikada, Long-term sustained release of ganciclovir from biodegradable scleral implant for the treatment of cytomegalovirus retinitis. J Control Release 68(2) (2000) 263-271.

[40] Y.E. Choonara, V. Pillay, T.R. Carmichael, L.C.R. Meyer, L.C. Du Toit, S. Naylor, C. Wanblad, In vivo evaluation of a biodegradable donut-shaped minitablet for prolonged posterior segment drug delivery in the rabbit eye model. J Pharm Sci 100(5) (2011) 1819-1832.

[41] G.A. Peyman, M. Conway, B. Khoobehi, K. Soike, Clearance of microsphere-entrapped 5-fluorouracil and cytosine-arabinoside from the vitreous of primates. Int Ophthalmol 16(2) (1992) 109-113.

[42] J. Mordenti, K. Thomsen, V. Licko, L. Berleau, J.W. Kahn, R.A. Cuthbertson, E.T. Duenas, A.M. Ryan, C. Schofield, T.W. Berger, Y.G. Meng, J. Cleland, Intraocular pharmacokinetics and safety of a humanized monoclonal antibody in rabbits after intravitreal administration of a solution or a PLGA microsphere formulation. Toxicol Sci 52(1) (1999) 101-106.

[43] G.P. Cook, L. Burgess, J. Wing, T. Dowie, P. Calias, D.T. Shima, K. Campbell, D. Allison, S. Volker, P. Schmidt, Preparation and characterization of Pegaptanib sustained release microsphere formulations for intraocular application. Invest Ophthalmol Vis Sci 47(5) (2006) 5123.

[44] A. Silva-Cunha, S.L. Fialho, M.C. Naud, F. Behar-Cohen, Poly-ε-caprolactone intravitreous devices: an in vivo study. Invest Ophthalmol Vis Sci 50(5) (2009) 2312-2318.

[45] J. Heller, Ocular delivery using poly(ortho esters). Adv Drug Deliv Rev 57(14) (2005) 2053-2062.

[46] M.C. Hacker, A. Haesslein, H. Ueda, W.J. Foster, C.A. Garcia, D.M. Ammon, R.N. Borazjani, J.F. Kunzler, J.C. Salamone, A.G. Mikos, Biodegradable fumarate-based drug-delivery systems for ophthalmic applications. J Biomed Mater Res A 88A(4) (2009) 976-989.

[47] A. Haesslein, H. Ueda, M.C. Hacker, S. Jo, D.M. Ammon, R.N. Borazjani, J.F. Kunzler, J.C. Salamone, A.G. Mikos, Long-term release of fluocinolone acetonide using biodegradable fumarate-based polymers. J Control Release 114(2) (2006) 251-260.

[48] C. Esen, G. Schweiger, Preparation of monodisperse polymer particles by photopolymerization. J Colloid Interface Sci 179(1) (1996) 276-280.

[49] Z. Gao, E. Grulke, A. Ray, Synthesis of monodisperse polymer microspheres by photopolymerization of microdroplets. Colloid Polym Sci 285(8) (2007) 847-854.

[50] D. Missirlis, N. Tirelli, J.A. Hubbell, Amphiphilic hydrogel nanoparticles. Preparation, characterization, and preliminary assessment as new colloidal drug carriers. Langmuir 21(6) (2005) 2605-2613.

[51] S.P. Schwendeman, H.R. Constantino, R.K. Gupta, R. Langer, in: K. Park (Ed.), Controlled Drug Delivery, Challenges and Strategies, 1997.

[52] M. van de Weert, W.E. Hennink, W. Jiskoot, Protein instability in poly(lactic-co-glycolic acid) microparticles. Pharm Res 17(10) (2000) 1159-1167.

[53] C.-C. Lin, S.M. Sawicki, A.T. Metters, Free-radical-mediated protein inactivation and recovery during protein photoencapsulation. Biomacromolecules 9(1) (2007) 75-83.

[54] F. Gu, R. Neufeld, B. Amsden, Maintenance of vascular endothelial growth factor and potentially other therapeutic proteins bioactivity during a photo-initiated free radical cross-linking reaction forming biodegradable elastomers. Eur J Pharm Biopharm 66(1) (2007) 21-27.

[55] B. Baroli, V.P. Shastri, R. Langer, A method to protect sensitive molecules from a light-induced polymerizing environment. J Pharm Sci 92(6) (2003) 1186-1195.

[56] J.L. West, J.A. Hubbell, Photopolymerized hydrogel materials for drug delivery applications. React Polym 25(2-3) (1995) 139-147.

[57] S. Lu, K.S. Anseth, Release behavior of high molecular weight solutes from poly(ethylene glycol)-based degradable networks. Macromolecules 33(7) (2000) 2509-2515.

[58] D.J. Quick, K.S. Anseth, DNA delivery from photocrosslinked PEG hydrogels: encapsulation efficiency, release profiles, and DNA quality. J Control Release 96(2) (2004) 341-351.

[59] R. Censi, T. Vermonden, H. Deschout, K. Braeckmans, P. di Martino, S.C. De Smedt, C.F. van Nostrum, W.E. Hennink, Photopolymerized thermosensitive poly(HPMAlactate)-PEG-based hydrogels: Effect of network design on mechanical properties, degradation, and release behavior. Biomacromolecules 11(8) (2010) 2143-2151.

[60] R. Censi, T. Vermonden, M.J. van Steenbergen, H. Deschout, K. Braeckmans, S.C. De Smedt, C.F. van Nostrum, P. di Martino, W.E. Hennink, Photopolymerized thermosensitive hydrogels for tailorable diffusion-controlled protein delivery. J Control Release 140(3) (2009) 230-236.

[61] F. Gu, R. Neufeld, B. Amsden, Osmotic-driven release kinetics of bioactive therapeutic proteins from a biodegradable elastomer are linear, constant, similar, and adjustable. Pharm Res 23(4) (2006) 782-789.

[62] F. Gu, R. Neufeld, B. Amsden, Sustained release of bioactive therapeutic proteins from a biodegradable elastomeric device. J Control Release 117(1) (2007) 80-89.

[63] F. Gu, H.M. Younes, A.O.S. El-Kadi, R.J. Neufeld, B.G. Amsden, Sustained interferon-γ delivery from a photocrosslinked biodegradable elastomer. J Control Release 102(3) (2005) 607-617.

[64] B. Amsden, G. Misra, M. Marshall, N. Turner, Synthesis and characterization of biodegradable networks providing saturated-solution prolonged delivery. J Pharm Sci 97(2) (2008) 860-874.

[65] B. Amsden, B. Qi, Anti-atherosclerotic peptide delivery from a photocrosslinkable biodegradable network. Int J Pharm 388(1-2) (2010) 32-39.

[66] R. Chapanian, B.G. Amsden, Combined and sequential delivery of bioactive VEGF165 and HGF from poly(trimethylene carbonate) based photo-cross-linked elastomers. J Control Release 143(1) (2010) 53-63.

[67] R. Chapanian, B.G. Amsden, Osmotically driven protein release from photo-cross-linked elastomers of poly(trimethylene carbonate) and poly(trimethylene carbonate-co-D,L-lactide). Eur J Pharm Biopharm 74(2) (2010) 172-183.

[68] A. Haesslein, M.C. Hacker, H. Ueda, D.M. Ammon, R.N. Borazjani, J.F. Kunzler, J.C. Salamone, A.G. Mikos, Matrix modifications modulate ophthalmic drug delivery from photo-cross-linked poly(propylene fumarate)-based networks. J Biomater Sci Polym Ed 20(1) (2009) 49-69.

[69] H. Ueda, M.C. Hacker, A. Haesslein, S. Jo, D.M. Ammon, R.N. Borazjani, J.F. Kunzler, J.C. Salamone, A.G. Mikos, Injectable, in situ forming poly(propylene fumarate)-based ocular drug delivery systems. J Biomed Mater Res A 83A(3) (2007) 656-666.

[70] S. Sharifi, H. Mirzadeh, M. Imani, Z. Rong, A. Jamshidi, M. Shokrgozar, M. Atai, N. Roohpour, Injectable in situ forming drug delivery system based on poly(ε-caprolactone fumarate) for tamoxifen citrate delivery: Gelation characteristics, in vitro drug release and anti-cancer evaluation. Acta Biomater 5(6) (2009) 1966-1978.

[71] D.J. Quick, K.K. Macdonald, K.S. Anseth, Delivering DNA from photocrosslinked, surface eroding polyanhydrides. J Control Release 97(2) (2004) 333-343.

[72] A.A. Weiner, E.A. Bock, M.E. Gipson, V.P. Shastri, Photocrosslinked anhydride systems for long-term protein release. Biomaterials 29(15) (2008) 2400-2407.

[73] R.A. Hakala, H. Korhonen, V.V. Meretoja, J.V. Seppälä, Photo-cross-linked biodegradable poly(ester anhydride) networks prepared from alkenylsuccinic anhydride functionalized poly(ε-caprolactone) precursors. Biomacromolecules 12(7) (2011) 2806-2814.

[74] J. Mönkäre, R.A. Hakala, M.A. Vlasova, A. Huotari, M. Kilpeläinen, A. Kiviniemi, V. Meretoja, K.H. Herzig, H. Korhonen, J.V. Seppälä, K. Järvinen, Biocompatible photocrosslinked poly(ester anhydride) based on functionalized poly(ε-caprolactone) prepolymer shows surface erosion controlled drug release in vitro and in vivo. J Control Release 146(3) (2010) 349-355.

[75] A.T. Neffe, B.D. Hanh, S. Steuer, A. Lendlein, Polymer networks combining controlled drug release, biodegradation, and shape memory capability. Adv Mater 21(32-33) (2009) 3394-3398.

Chapter 3

Rapid photo-crosslinking of fumaric acid monoethyl ester functionalized poly(trimethylene carbonate) oligomers for drug delivery applications*

Janine Jansen[1], Mark J. Boerakker[2], Jean Heuts[3], Jan Feijen[4] and Dirk W. Grijpma[1,5]

1) MIRA Institute for Biomedical Technology and Technical Medicine, Department of Biomaterials Science and Technology, Faculty of Science and Technology, University of Twente, P.O. Box 217, 7500 AE, Enschede, The Netherlands
2) DSM Ahead, P.O Box 18, 6160 MD, Geleen, The Netherlands
3) DSM Resolve R&D Solutions, P.O Box 18, 6160 MD, Geleen, The Netherlands
4) MIRA Institute for Biomedical Technology and Technical Medicine, Department of Polymer Chemistry and Biomaterials, Faculty of Science and Technology, University of Twente, P.O. Box 217, 7500 AE, Enschede, The Netherlands
5) W.J. Kolff Institute, Department of Biomedical Engineering, University Medical Center Groningen, University of Groningen, Antonius Deusinglaan 1, 9713 AV, Groningen, The Netherlands

* J Control Release 147(1) (2010) 54-61.

Abstract

Photo-crosslinkable, fumaric acid monoethyl ester-functionalized poly(trimethylene carbonate) oligomers were synthesized and copolymerized with N-vinyl-2-pyrrolidone (NVP) and vinyl acetate (VAc) to form biodegradable polymer networks. The copolymerization reactions were much faster than homopolymerization of the fumarate end-groups of the macromers. The hydrophilicity of the networks could by varied by mixing NVP and VAc at different ratios. The prepared network extracts were compatible with NIH 3T3 fibroblasts. Release of vitamin B12, used as a model drug, could be tuned by varying network hydrophilicity and macromer molecular weight. A more hydrophilic and less densely crosslinked network resulted in faster release.

Introduction

Photo-crosslinked degradable polymer networks are a unique class of materials for application in drug delivery [1]. Such networks can easily be loaded with drugs by dispersing or by dissolving the drug in a crosslinkable macromer solution prior to the crosslinking process. In this way, large amounts of drug can be loaded into a matrix at high efficiencies. Furthermore, photo-crosslinking can be accomplished very rapidly and with minimal heat generation.

Poly(trimethylene carbonate) (PTMC) is a flexible, biodegradable and biocompatible polymer. *In vitro* high molecular weight PTMC degrades slowly by hydrolysis of the carbonate linkages, while *in vivo* the degradation of PTMC occurs much faster by enzymatic surface erosion [2, 3]. In contrast to poly(lactide) and poly(glycolide) (co)polymers, PTMC degrades without the formation of acidic compounds. This may be an advantage in protein delivery, since a drop in pH that could lead to denaturation of the protein [4, 5], does not occur. Despite their advantageous degradation properties, only few examples of the application of TMC-based polymers in drug delivery systems can be found [6-8].

Networks based on PTMC can be prepared by photo-initiated crosslinking of functionalized PTMC oligomers. Methacrylate derivatives have been most frequently used in functionalization reactions. Fumaric acid derivatives are also attractive compounds for end-functionalization. Fumaric acid is a compound naturally found in the body, therefore it can be expected that residual unreacted fumarate end-groups will not lead to toxicity upon implantation [9]. However, compared to methacrylate-functionalized oligomers, the reactivity of fumarate-functionalized oligomers is relatively low [10]. In drug delivery applications, rapid crosslinking reactions are desired to

minimize exposure of the drug to UV light and to the radicals formed [11, 12]. By copolymerization with a suitable comonomer, the fumarate crosslinking reaction can significantly be accelerated.

N-vinyl-2-pyrrolidone (NVP) is a monomer that can copolymerize with fumaric acid derivatives at high rates [13-15]. With use of the Q-e scheme [16, 17], the calculated copolymerization constants for diethyl fumarate and NVP are 0.0004 and 0.0007, respectively. This implies that alternating copolymers will form when fumaric acid derivatives and NVP are copolymerized. It should be noted that poly(N-vinyl-2-pyrrolidone) (PVP) is a biocompatible polymer that is often used as an additive in pharmaceutics [18]. Vinyl acetate (VAc) can also be expected to copolymerize at high rates with fumaric acid derivatives. The calculated copolymerization constants for diethyl fumarate and VAc are 0.008 and 0.007, respectively. VAc copolymers have been frequently used in drug delivery devices as well [19].

Drug release profiles can be tuned by varying the crosslink density or by adjusting the hydrophilicity of crosslinked polymer networks. Several authors have described the use of poly(ethylene glycol) (PEG) to adjust drug release profiles of photo-crosslinked polymer networks [20-22]. Recently Haesslein *et al.* [23, 24] have shown that varying the NVP content of poly(propylene fumarate) networks has a similar effect.

In this paper the development of a rapidly crosslinking fumaric acid-based system is described. The photo-crosslinking kinetics of fumaric acid monoethyl ester derivatized PTMC oligomers with hydrophilic NVP or hydrophobic VAc comonomers were studied. By using mixtures of NVP and VAc at different ratios, PTMC networks with different hydrophilicities could be prepared. To illustrate the potential of these networks in drug delivery applications, release experiments were conducted using vitamin B12 as a model drug.

Materials and methods

Materials

Trimethylene carbonate (TMC) was purchased from Boehringer Ingelheim (Germany). Tin 2-ethylhexanoate ($Sn(Oct)_2$), trimethylol propane (TMP), glycerol, fumaric acid monoethyl ester (FAME), vinyl acetate (VAc) and MTT (3-(4,5-dimethyl-2-thiazolyl)-2,5-diphenyl tetrazolium bromide) were obtained from Sigma Aldrich (U.S.A.). Methacryloyl chloride (MACl) was obtained from Alfa Aesar (Germany). N-vinyl-2-pyrrolidone (NVP), 1,3-dicyclohexylcarbodiimide (DCC) and triethyl amine (TEA) were purchased from Fluka (Switzerland). 4-Dimethylaminopyridine (DMAP) was purchased

from Merck (Germany). Irgacure 2959 (2-hydroxy-1-[4-(2-hydroxyethoxy)phenyl]-2-methyl-1-propanone) was obtained from Ciba Specialty Chemicals (Switzerland). Phosphate buffered saline (PBS, pH 7.4) was obtained from B. Braun (Germany). Fetal bovine serum (FBS) and DMEM (Dulbecco's Modified Eagle's Medium) were obtained from Gibco (U.S.A.). Penicillin/streptomycin and trypsin were purchased from Lonza (Switzerland).

Analytical grade dichloromethane (DCM) and dimethyl sulfoxide (DMSO) were obtained from Biosolve (the Netherlands). DCM was dried over CaH_2 and distilled, other solvents were of technical grade and were used as received (Biosolve, the Netherlands).

Synthesis and characterization of 3-armed MA- and FAME-functionalized PTMC oligomers

Three-armed poly(trimethylene carbonate) oligomers were synthesized by ring opening polymerization of trimethylene carbonate in the presence of glycerol or trimethylol propane as a trifunctional initiator. The oligomer syntheses were carried out at a 30 to 60 gram scale. TMC, initiator and $Sn(Oct)_2$ (approximately 0.2 mmol/mol monomer) as a catalyst were reacted in the melt at 130 ^{o}C for 48 h under argon. The targeted molecular weights were 3100 g/mol and 9100 g/mol, corresponding to approximately 10 and 30 TMC units per arm respectively. To achieve this, 30 and 90 mol of monomer were used per mol of initiator.

The oligomers were functionalized by coupling fumaric acid monoethyl ester to the hydroxyl termini of the oligomers [10, 25]. An amount of oligomer was charged into a three-necked flask and dried for 2 h at 110 ^{o}C *in vacuo* and cooled to room temperature under argon. The oligomers were dissolved in dried DCM, and after addition and dissolution of FAME the system was further cooled to 0 ^{o}C. Then a dichloromethane solution of DCC and DMAP was added drop-wise to the vigorously stirred oligomer solution. In the coupling reaction, 1.2 moles of FAME and DCC and 0.03 moles of DMAP were used per mole of hydroxyl end-groups. The coupling reaction was continued overnight, letting the contents slowly warm up to room temperature. After completion of the reaction, the formed dicyclohexylurea was removed by filtration and the macromer was purified by washing with water, precipitation in cold ethanol, and drying under vacuum.

The oligomers were also functionalized by coupling methacryloyl chloride to the hydroxyl end-groups of the oligomers. An amount of oligomer was charged into a three-necked flask and dried for 2 h at 110 ^{o}C *in vacuo* and then cooled to room temperature under argon. The oligomer was dissolved in dry DCM, TEA was added and the flask was

cooled to 0 ^{o}C. MACl was added drop-wise to the vigorously stirred oligomer solution. Per mole of hydroxyl groups 1.2 moles of MACl and TEA were used. The coupling reaction was continued for 24 h, letting the contents slowly warm up to room temperature. The TEA.HCl salt that had formed was removed by filtration and the macromers were purified by washing with water, precipitation in cold ethanol, and drying under vacuum. The oligomer synthesis and the functionalization reactions are schematically shown in Figure 1. The oligomers are labeled as PTMC 3XMW, in which 3 is the number of arms (the same for all oligomers) and MW is the molecular weight per arm. Macromers are denoted as PTMC 3XMW-FAME or PTMC 3XMW-MA. For example, a PTMC 3X1K-MA macromer has a molecular weight of 1000 g/mol per arm and methacrylate end-groups.

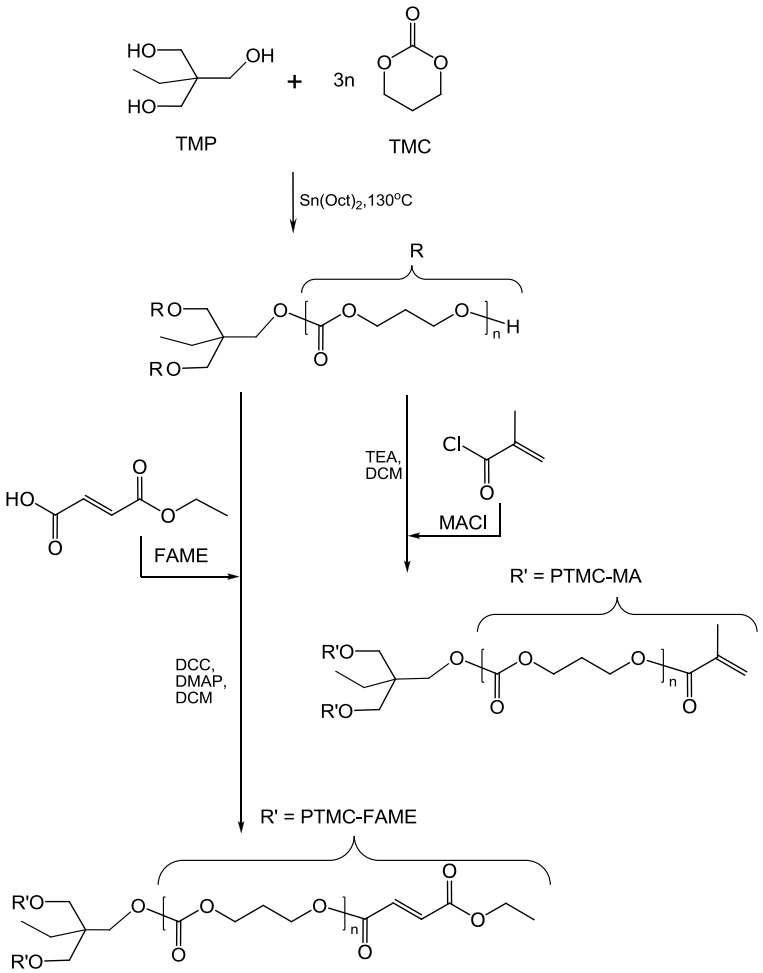

Figure 1. *Synthesis of PTMC oligomers functionalized with FAME and with MACl.*

Proton nuclear magnetic resonance (^{1}H-NMR) spectra were recorded on a Varian Inova 300 MHz NMR spectrometer. Deuterated chloroform was used as a solvent. The

oligomer and macromer molecular weights (M_n) and the degrees of functionalization of the macromers were determined from the spectra.

Photo-crosslinking kinetics

The photo-crosslinking kinetics of the macromers were studied using different methods. Double bond conversion was followed using photo- differential scanning calorimetry (photo-DSC) and real time Fourier-transform infrared spectroscopy (rt-FTIR), gel contents were determined after different crosslinking times.

Four different macromer formulations were evaluated: PTMC 3X1K-FAME macromers were dissolved in NVP (30 wt% of total) and VAc (30 wt% of total). PTMC 3X1K-MA and PTMC 3X1K-FAME formulations not containing reactive diluent were prepared by dissolving the macromers in DCM (0.2 g/ml). Each formulation contained 1 wt% (relative to the amount of macromer) Irgacure 2959 photo-initiator. When DCM was used to dissolve the macromers, it was left to evaporate before the crosslinking reaction.

Photo-DSC experiments in which the samples were illuminated at a constant temperature (25 ^{o}C) were performed using a Perkin Elmer Diamond DSC equipped with an Exfo OmniCure 2000 curing unit (200 W mercury lamp, 250-450 nm). The light intensity was set at 4.5-5.5 mW/cm^2. The exothermal heat flow of the polymerization reaction was measured as a function of time. Sample masses of 0.5-3 mg were used. For samples containing NVP or VAc, the DSC pans were covered with quartz windows to limit evaporation of the monomers. After completion of the polymerization reaction in the first run, a second run was taken to establish the baseline. Polymerization rates and conversions were estimated from the heat of polymerization evolved per double bond functionality (ΔH_{pol}, Table 1).

The rates of polymerization (the rates of double bond conversion) were calculated using:

$$R_p(t) = \frac{|Q(t)|}{\Delta H_{max}}$$

R_p (s^{-1}) is the polymerization rate and Q (mW) is the heat flow. ΔH_{max} (mJ) is the maximum heat that evolves if all double bond-containing groups have reacted. ΔH_{max} is the heat evolved per mol of double bond-containing groups (ΔH_{pol}) times the number of moles present in the sample. The conversion was calculated by integrating the polymerization rate over time.

Table 1. *Overview of literature values of heats of polymerization (ΔH_{pol}).*

Functional group or compound	ΔH_{pol} (kJ/mol)	Reference
Methacrylates	54.8	[16, 26-28]
Fumarates	65	[16]
Vinyl acetate	89.5	[16]
N-vinyl-2-pyrrolidone	53.9	[29]

Real-time FTIR spectra were recorded on a Bruker Vertex 70 FTIR spectrometer with a transflection (transmission/reflection) cell accessory in a nitrogen atmosphere. The light source was a Dr. Hönle Bluepoint UV lamp with a light guide (327-373 nm, 6.6 mW/cm^2). The macromer solutions were applied on gold sputtered aluminum plates. In the case of the PTMC 3X1K-FAME/VAc system, a closed transmission cell was used to limit evaporation of vinyl acetate.

In the PTMC 3X1K-MA, PTMC 3X1K-FAME and PTMC 3X1K-FAME/VAc systems double bond conversions of the methacrylate end-groups, fumarate end-groups and VAc were determined from the C=C stretching vibrations at 1680-1600 cm^{-1}. In the PTMC 3X1K-FAME/NVP system the conversions of the fumarate end-groups and NVP were determined from the C=C–H stretching vibrations at 3100-3020 cm^{-1}. These stretching vibrations allowed the most accurate determinations. Conversions were calculated from the decrease in peak heights in time by:

$$\text{conversion}(t) = \frac{H_{max} - H(t)}{H_{max}}$$

In which H is the peak height and H_{max} is the peak height in the spectrum at the beginning of the polymerization reaction.

The formation of a network, as a result of the conversion of macromer and reactive diluent double bonds, was also followed in time. After exposure of the formulations to UV light for different periods of time in an Ultralum crosslinking cabinet (100-200 mg drops on a glass substrate exposed to 365 nm at 3-5 mW/cm^2), the gel contents were measured. Specimens of the formed networks (n=3) were weighed (m_0), extracted with acetone overnight and dried at 90 ^{o}C until constant weight. The mass of the dry network (m_1) was then determined. The gel content is defined as:

$$\text{gel content} = \frac{m_1}{m_0} \times 100\%$$

Preparation and characterization of PTMC networks

Network films were prepared from FAME- and MA-functionalized PTMC oligomers. FAME-functionalized macromers were dissolved in DCM (0.2 g/ml), or in NVP (30 wt% of total) or VAc (30 wt% of total). Solutions in mixtures of NVP and VAc, at different ratios, were also prepared (the total amount of reactive diluent was kept constant at 30 wt%). MA-functionalized macromers were dissolved in DCM (0.2 g/ml) only. To each formulation 1 wt% (with respect to the macromer) of Irgacure 2959 photo-initiator was added, and films with a thickness of about 0.5 mm were cast on glass microscopy slides. When DCM was used to dissolve the macromers, it was left to evaporate before the crosslinking reaction.

Photo-crosslinking was carried out at room temperature in a nitrogen atmosphere in a crosslinking cabinet, as described above. MA-functionalized oligomers and FAME-functionalized oligomers dissolved in NVP and/or VAc as reactive diluents were crosslinked for 15 min. FAME-functionalized oligomers not dissolved in a reactive diluent were crosslinked for 3 h.

Gel contents were determined as described above. Water uptake experiments were carried out using network samples that were extracted with acetone overnight and dried at 90 ^{o}C until constant weight. Specimens (n=3) were weighed (m_d) and incubated in distilled water for 1 d, the samples were then removed from the water, blotted dry, and weighed again (m_s). The water uptake was calculated using:

$$\text{water uptake} = \frac{m_s - m_d}{m_d} \times 100\%$$

The thermal properties of oligomers, macromers and non-extracted networks (in the dry and in the wet state), were evaluated using a Perkin Elmer Pyris 1 differential scanning calorimeter. Samples were heated from -60 ^{o}C to 100 ^{o}C at a heating rate of 10 ^{o}C/min and quenched rapidly at 300 ^{o}C/min to -60 ^{o}C. After 5 min a second heating scan was recorded. The glass transition temperature (T_g) was taken as the midpoint of the heat capacity change in the second heating run. The melting temperature (T_m) was determined as the maximum of the endotherm peak in the first heating run.

Network films were dried at room temperature under vacuum for 2 d prior to the DSC measurements. Also wet films (swollen in distilled water for 1 d) were analyzed in the same manner, in the temperature range of -100 ^{o}C to 20 ^{o}C.

Cytocompatibility of PTMC network films

Non-extracted PTMC network films were dried at room temperature under vacuum for 2 d and cut into samples with a surface area of 4 cm^2. The materials were disinfected in isopropanol (2×15 min), washed with PBS (2×15 min) and left to dry in a laminar flow hood. Samples were placed in square polystyrene wells (2×2 cm^2) and extracted with serum free culture medium (DMEM (Dulbecco's modified Eagle's medium), 1 ml per 3 cm^2) at 37 ^{o}C for 24 h. The supernatants were stored at -20 ^{o}C until further use.

NIH 3T3 fibroblasts were cultured in T175 cell culture flasks in DMEM medium supplemented with 10 % fetal bovine serum and 1 % penicillin/streptomycin. The cells were cultured for 5 d at 37 ^{o}C in a 5 % CO_2 atmosphere, trypsinized for about 5 min at 37 ^{o}C, and redispersed in medium (25×10^4 cells/ml). Cells were then seeded in 96 well tissue culture polystyrene (TCPS) plates at a density of 5×10^4 cells per well and cultured for 1 d. Then the medium was aspirated from the wells, and 100 μl of extract was added to the cells (n=3), followed by 100 μl of culture medium containing 20 % FBS. Normal culture medium (containing 10 % FBS) and 50 % v/v DMSO were used as controls. The cells were cultured at 37 ^{o}C, in a 5 % CO_2 atmosphere for 1 d.

The metabolic activity of the cells was analyzed using the MTT (3–(4,5-dimethylthiazol-2-yl)-2,5-diphenyltetrazolium bromide) assay. The medium was aspirated from the cells and replaced by 200 μl of fresh medium and 20 μl of MTT solution (5 mg/ml). After 4 h of incubation, the supernatant was removed and the formed crystals were dissolved in 200 μl DMSO. The contents of the wells were centrifuged at 13000 rpm for 2 min, and the supernatants were transferred to a 96 well plate. The absorbance was read on a Tecan Safire^2 microplate reader at 540 nm.

A direct contact experiment was also conducted. The network specimens were placed on top of a confluent layer of NIH 3T3 cells for 1 d, then the samples were removed and the cells were fixed and stained with methylene blue. The cell density and morphology were examined using an inverted light microscope.

Drug release from crosslinked PTMC films

Vitamin B12 (cyanocobalamin) was used as a model drug, it was grinded and sieved into particles smaller than 106 μm. Vitamin B12 (1 wt%) was dispersed in different solutions

of FAME-functionalized PTMC oligomers (30 wt% reactive diluent, with different NVP to VAc ratios, and 1 wt% Irgacure 2959). The mixtures were stirred, vortexed and poured into Teflon moulds (diameter 15 mm, height 0.5 mm). As the light penetration decreases upon addition of vitamin B12 particles to the macromer solutions, the dispersions were crosslinked in a nitrogen atmosphere for 30 min at 14-20 mW/cm^2 (Ultralum crosslinking cabinet, 365 nm). Crosslinking was done immediately after preparing the dispersions, therefore sedimentation of the particles did not occur.

The drug-loaded specimens (n=3) were taken from the moulds and immersed in 2 ml of PBS (pH 7.4, 37 ^oC) containing 0.02 wt% NaN_3 as a bactericide. In the release experiments aliquots of 0.5 ml were taken at different time points and replaced by 0.5 ml of fresh PBS. The concentration of the released vitamin B12 was determined using a SLT 340 ATCC microplate reader (340 nm). For this, a vitamin B12 calibration curve was prepared in the concentration range of 25 to 1000 μg/ml.

Results and discussion

Synthesis and characterization of 3-armed FAME- and MA-functionalized PTMC oligomers

Trimethylene carbonate was polymerized by ring opening polymerization with a trifunctional initiator to yield three-armed oligomers with targeted molecular weights of 3100 g/mol and 9100 g/mol. The obtained molecular weights were 3.0×10^3 g/mol and 9.8×10^3 g/mol, as determined from the initiator to TMC ratios in ^{1}H-NMR spectra. Different double bond-containing groups were coupled to the oligomers to obtain crosslinkable macromers. The successful coupling of fumaric acid monoethyl ester to the PTMC 3X1K and PTMC 3X3K oligomers was confirmed by the appearance of the –CH=CH– and the $–CH_3$ peaks of FAME at δ 6.85 and δ 1.32 and by the disappearance of $–CH_2–$ PTMC end-groups at δ 1.92. The degree of functionalization of the PTMC 3X1K-FAME macromer was determined using the integral values of the $–CH_3$ peak of FAME at δ 1.32 and the $–CH_3$ of TMP at δ 0.91 and could be calculated to be 0.97. For the PTMC 3X3K-FAME macromer, the degree of functionalization was 1.00. In both cases PTMC end-groups could not be discerned, and it can be concluded that the functionalization reactions were essentially complete.

The coupling of methacryloyl chloride to the PTMC 3X1K oligomer was confirmed by the appearance of $=CH_2$, and the $–CH_3$ peaks of the methacrylate group at δ 5.58 and δ 6.11, and at δ 1.95 respectively. The degree of functionalization was calculated using

the integrals of the $-CH_3$ of the methacrylate peak at δ 1.95 and the $-CH_3$ of TMP at δ 0.91 and was 0.91. Here too, PTMC end-groups could not be discerned, suggesting that the functionalization was essentially complete.

Photo-crosslinking kinetics

The kinetics of the crosslinking reaction of PTMC 3X1K-FAME macromers, and the effect of adding a comonomer (reactive diluent) were studied using different methods. The reaction rates were compared with those of PTMC 3X1K-MA.

Conversion of double bonds

The photo-crosslinking kinetics of the macromers were determined by following the double bond conversion as a function of time. Graphs of the conversion versus time obtained by rt-FTIR and the reaction rate versus time obtained by photo-DSC are shown in Figure 2.

It can be observed in Figure 2a that PTMC 3X1K-FAME macromers crosslink much slower than the PTMC 3X1K-MA macromers. While the conversion of the PTMC 3X1K-MA system as calculated from the FTIR data is essentially complete, the low reactivity of fumarates has resulted in a lower final conversion (approximately 60 %) of the FAME-functionalized macromers. (Note that determined conversions higher than 100% and irregularities in the curves are related to the difficulty of precisely quantifying the infrared absorption spectra as a result of shifts in the baseline and position of the peaks, small sizes of the peaks, (partially) overlapping peaks, and shrinkage of the specimens due to polymerization).

By copolymerizing PTMC 3X1K-FAME with NVP as a reactive diluent, a much faster reacting system is obtained. This is likely due to the formation of alternating comonomer sequences in the polyaddition chain. The figure shows, that the curing kinetics are similar to those of PTMC 3X1K-MA. In the PTMC 3X1K-FAME/NVP system, maximum conversion is also reached. Although the NVP and fumarate absorptions in the spectra could not be quantified separately, due to overlap of the peaks and the high amounts of NVP (30 wt%), analysis using the Multivariate Curve Resolution technique (MCR) [30] revealed that the final conversions of NVP and fumarate were both close to 100 %.

Also when VAc is used as a reactive diluent, the photo-polymerization reaction of PTMC 3X1K-FAME is much accelerated. Although PTMC 3X1K-FAME/VAc crosslinks somewhat slower than PTMC 3X1K-MA and the PTMC 3X1K-FAME/NVP system, the reaction is significantly faster than the crosslinking reaction of PTMC 3X1K-FAME (Figure 2a). Maximum conversion is approximately 75 %.

For diethylfumarate and NVP, both copolymerization constants calculated using the Q-e scheme are a factor 10 lower than the copolymerization constants for diethylfumarate and vinyl acetate. This may explain the higher effectivity of NVP in accelerating the PTMC 3X1K-FAME photo-crosslinking reaction.

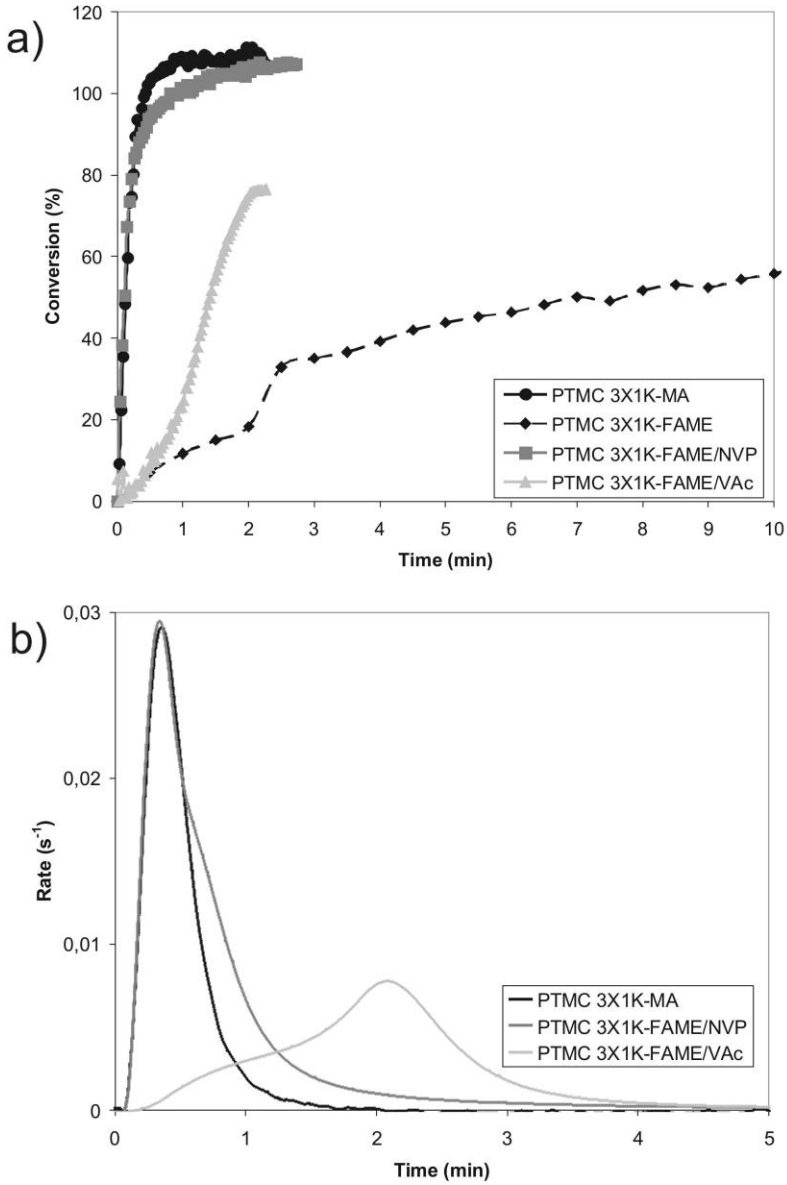

Figure 2. *Double bond conversion versus time determined by rt-FTIR(a) and reaction rate versus time determined by photo-DSC (b) during photo-crosslinking of PTMC 3X1K-MA macromers, PTMC 3X1K-FAME macromers, and of mixtures of PTMC 3X1K-FAME macromers with NVP and VAc (30 wt%) as comonomers (reactive diluents).*

The progress of the (crosslinking) reaction could also be evaluated by measuring heat effects. The results of DSC experiments, where the different macromers and their

mixtures with reactive diluent are photo-polymerized, are shown in Figure 2b. Here the polymerization rates (calculated from the measured heat flows and heats of polymerization (see Table 1)) are given as a function of time. Although it was not possible to determine polymerization rates of PTMC 3X1K-FAME macromers by photo-DSC, due to the small amounts of heat released per time unit, the PTMC 3X1K-FAME/NVP system shows comparable crosslinking behaviour as PTMC 3X1K-MA macromers. In both cases, the maximum polymerization rates are reached within 30 s. For PTMC 3X1K-FAME/VAc, the highest rates of polymerization are reached at a later time point (2 min). Shoulders in photo-polymerization rate curves have been observed before [26]. From these experiments, the accelerating effect of copolymerizing PTMC 3X1K-FAME with NVP and VAc can also be seen.

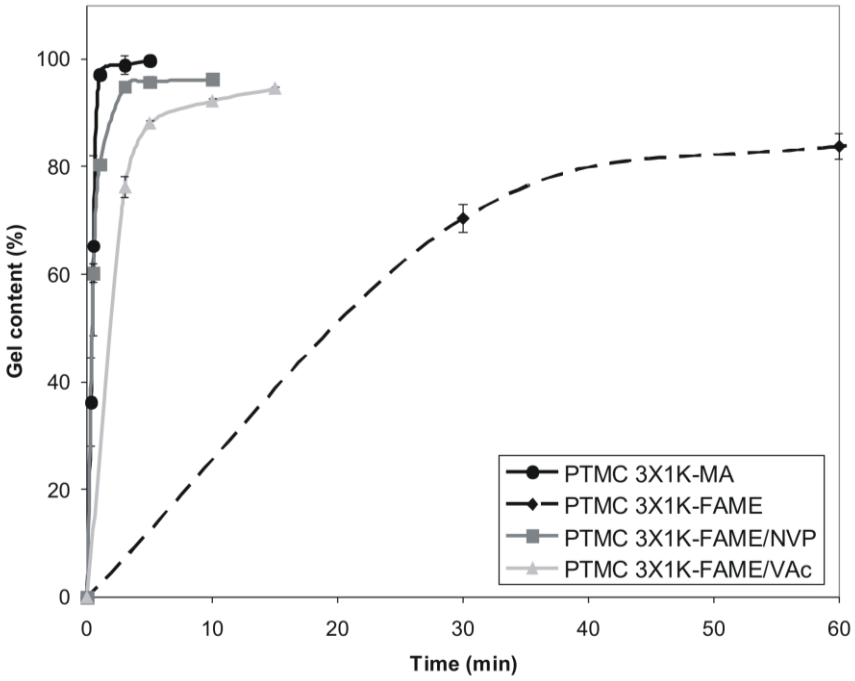

Figure 3. *Gel content as a function of crosslinking time for PTMC 3X1K-MA macromers, PTMC 3X1K-FAME macromers, and of mixtures of PTMC 3X1K-FAME macromers with NVP and VAc (30 wt%) as comonomers (reactive diluents).*

Formation of networks

The photo-crosslinking kinetics were also studied on a larger scale by determining gel contents of network films after different periods of crosslinking in an Ultralum crosslinking cabinet. In Figure 3 the gel content of the networks is given as a function of time for the different systems.

Although the reaction conditions (irradiation intensity and wavelength) are slightly different, similar trends are observed as in rt-FTIR and photo-DSC experiments. The PTMC 3X1K-MA and PTMC 3X1K-FAME/NVP systems crosslink fastest. The PTMC 3X1K-FAME/VAc system is slightly slower, but still much faster than the PTMC 3X1K-FAME macromers crosslinked without reactive diluent. The accelerating effect of copolymerizing reactive diluents can clearly be seen. The maximal gel contents obtained are high for all systems, although double bond conversions might not always have been complete (see Figure 2). Networks with a gel content of 100 % can be obtained without all double bonds being polymerized, as every macromer molecule has 3 double bond-containing groups.

Characterization of network films

To vary the hydrophilicity of PTMC networks, FAME-functionalized PTMC oligomers were crosslinked in the presence of NVP, VAc or a mixture of these two. Different NVP to VAc ratios were used, the total amount of reactive diluent was kept constant at 30 wt%. The properties of the networks were compared to the properties of PTMC 3X1K-MA networks and PTMC 3X1K-FAME networks prepared without a copolymerizing reactive diluent.

The PTMC 3X1K-MA networks showed a gel content of 93 %. The PTMC 3X1K-FAME networks showed a slightly lower gel content (88 %), while PTMC networks crosslinked in the presence of a reactive diluent showed gel contents above 93 % as can be seen in Figure 4. Networks with different NVP to VAc ratios were prepared from PTMC 3X1K-FAME and PTMC 3X3K-FAME macromers. Networks prepared from the higher molecular weight macromers seem to have the highest gel contents. The figure also shows that by varying the NVP to VAc ratio, the hydrophilicity of the resulting networks could readily be tailored. This is due to differences in hydrophilicty: NVP polymers are hydrophilic while VAc polymers are hydrophobic. Water uptake varied from 2 % for PTMC 3X1K-FAME/NVP/VAc networks containing only VAc as reactive diluent, to 29 % for PTMC 3X1K-FAME/NVP/VAc networks containing only NVP as reactive diluent. The PTMC 3X1K-FAME and the PTMC 3X1K-MA networks (which were prepared in the absence of a reactive diluent) absorbed approximately 5 % water. For PTMC 3X3K-FAME/NVP/VAc networks the water uptake varied from 1 % for networks containing only VAc, to 42 % for networks containing only NVP. When comparing the swelling behavior of PTMC 3X1K-FAME/NVP/VAc networks with that of PTMC 3X3K-FAME/NVP/VAc networks, it can be observed that the networks prepared from

the macromers with the higher molecular weights absorb more water. This is the result of the larger mesh-sizes in the latter networks.

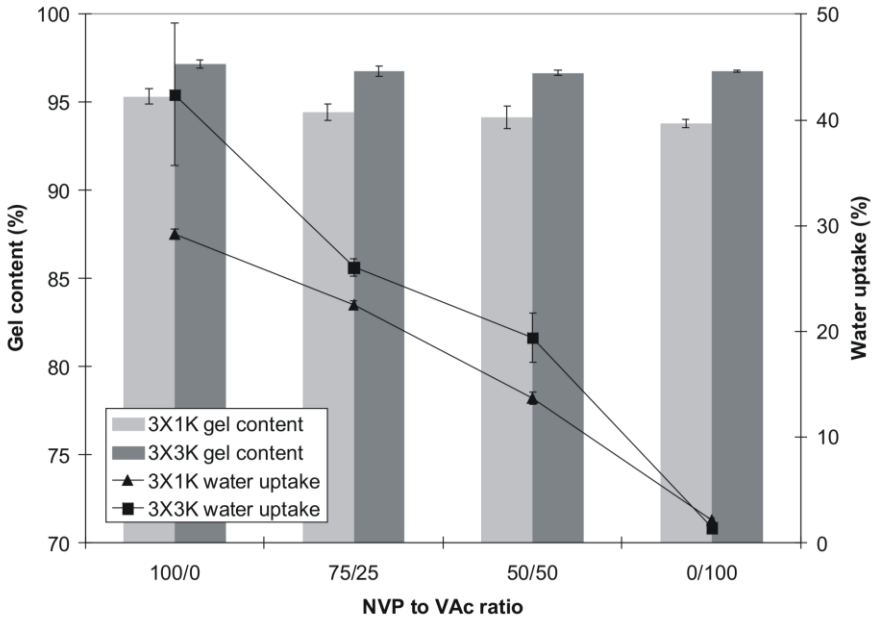

Figure 4. *Gel content and water uptake of networks prepared from PTMC 3X1K-FAME and PTMC 3X3K-FAME macromers with 30 wt% NVP and/or VAc as a reactive diluent.*

The thermal properties of oligomers, macromers, and of dry- and wet networks were determined by DSC, and values are listed in Table 2. The glass transition temperature of PTMC 3X1K-FAME networks dry is slightly lower than the T_g of dry PTMC 3X1K-MA networks. This is possibly due to a higher number of dangling chain ends (a lower double bond conversion) resulting from the lower reactivity of the fumarate end-group. All dry networks prepared by copolymerization with 30 wt% NVP and/or VAc showed a higher T_g than networks prepared without a reactive diluent. The glass transition temperatures of poly(N-vinyl-2-pyrroldione) and poly(vinyl acetate) are 109-179 ^oC and 23-31 ^oC respectively [18], which in both cases is higher than that of PTMC (-17 ^oC). For these copolymer networks, a single T_g was observed (also when scanning to 200 ^oC), this indicates that NVP and vinyl acetate have formed a single phase with the macromers and with each other. For dry networks no clear relationship between T_g and NVP to VAc ratio was observed, while for hydrated PTMC 3X1K-FAME/NVP/VAc networks, T_g decreased with increasing NVP content. Networks with high NVP contents absorb more water, and therefore show a somewhat lower T_g in the wet state than networks with low NVP contents.

Table 2. *Thermal properties of oligomers, macromers and (non-extracted) networks in the dry state and after incubation in water.*

	NVP to VAc ratio	T_g (^oC) dry	T_m (^oC)	ΔH_m (J/g)	T_g (^oC) wet[a]
PTMC 3X1K oligomer		-30.3			
PTMC 3X1K-MA		-35.7	29.3	13.2	
PTMC 3X1K-FAME		-23.2	38.9	35.9	
PTMC 3X1K-MA network [b]		-7.9			-17.4
PTMC 3X1K-FAME network [b]		-15.5			-17.8
PTMC 3X1K-FAME/NVP/VAc network	100/0	2.4			-17.6
PTMC 3X1K-FAME/NVP/VAc network	75/25	-6.3			-16.5
PTMC 3X1K-FAME/NVP/VAc network	50/50	-2.2			-14.2
PTMC 3X1K-FAME/NVP/VAc network	25/75	-1.7			-11.9
PTMC 3X1K-FAME/NVP/VAc network	0/100	-4.3			[c]

[a] Samples were incubated in distilled water for 1 d (Figure 4). The PTMC 3X1K-FAME/NVP/VAc 25/75 network had a gel content of 94 % and absorbed 5 % water.

[b] Prepared using dichloromethane to dissolve the macromers and initiator, followed by evaporation of the solvent.

[c] Could not be determined due to overlap of the glass transition and the water melting peak.

The cytocompatibility of soluble fractions of the prepared networks was assessed in an indirect assay. NIH 3T3 fibroblasts cultured in the presence of extracts of the networks showed high metabolic activity, comparable to cells cultured in normal culture medium (Figure 5). Cells cultured in the presence of DMSO showed significantly lower metabolic activity. These results indicate that extracts from the networks were not toxic for NIH 3T3 fibroblasts. Additionally, initial direct contact experiments, where the networks were placed on top of a confluent layer of cells, also did not show any indication of toxicity.

Vitamin B12 release

To investigate the drug release behavior from networks prepared from FAME-functionalized PTMC oligomers and NVP and/or VAc as a reactive diluent, the networks were loaded with vitamin B12 particles. By dispersing solid vitamin B12 particles in the macromer solutions, loaded networks could easily be obtained after photo-crosslinking. Disks measuring 15 mm in diameter that weighed approximately 120 mg and contained 1 wt% (approximately 1.2 mg) vitamin B12 were prepared.

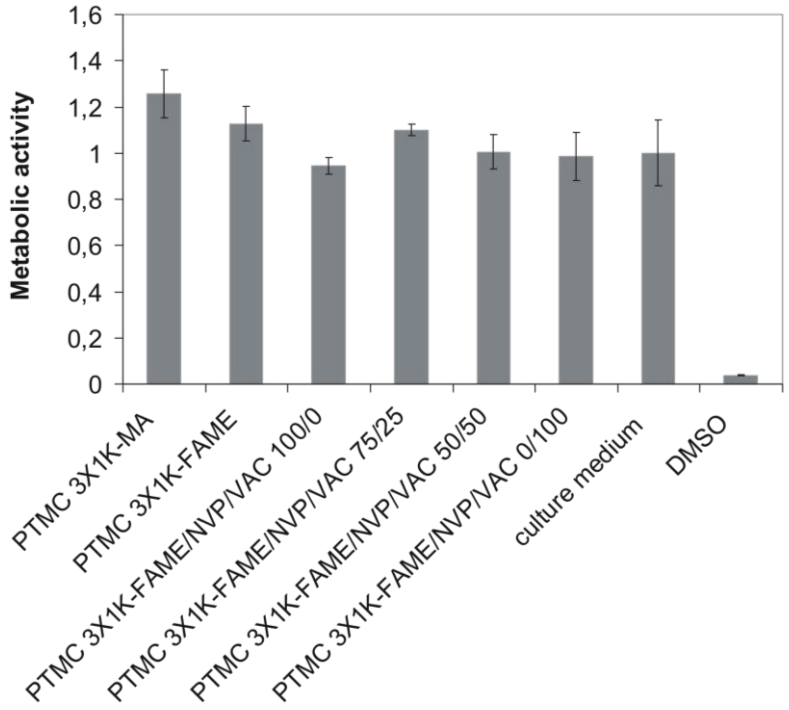

Figure 5. *Results of MTT assays, where NIH 3T3 fibroblasts were cultured in medium containing extracts from PTMC networks copolymerized with different NVP to VAc ratios. Values are relative to the control (culture medium).*

Vitamin B12 was used as a model drug, since it has a relatively high molecular weight (1355 g/mol) that is comparable to the molecular weight of several peptide drugs [20]. Furthermore, it can easily be detected spectrophotometrically due to its pink color.

The results of the release experiments are shown in Figure 6. Networks were prepared from two different macromers: PTMC 3X1K-FAME and PTMC 3X3K-FAME, using different NVP to VAc ratios.

Figure 6a shows, that for PTMC 3X1K-FAME/NVP/VAc networks the system containing only VAc showed the largest burst release. This is followed by a short period of linear release that levels off after 2 wk. It seems likely that the hydrophilic vitamin B12 is not able to diffuse through the hydrophobic matrix, and only vitamin B12 in particles at the outside of the specimens is released. The three NVP-containing networks prepared from the PTMC 3X1K-FAME macromers, show a smaller burst release that corresponds to approximately 6 % of the loaded vitamin B12. In the first week, the release behaviour of the networks is comparable. After 1 wk the release from the more hydrophilic networks is faster than the release from the less hydrophilic networks. The release from the 50/50 NVP/VAc and 75/25 NVP/VAc systems levels off after about 5 wk when only approximately 10 % of the loaded vitamin B12 was released. However,

from the PTMC 3X1K-FAME/NVP/VAc networks with only NVP, vitamin B12 is released in a controlled and sustained way. After 23 wk, approximately 70 % of the loaded vitamin B12 was released.

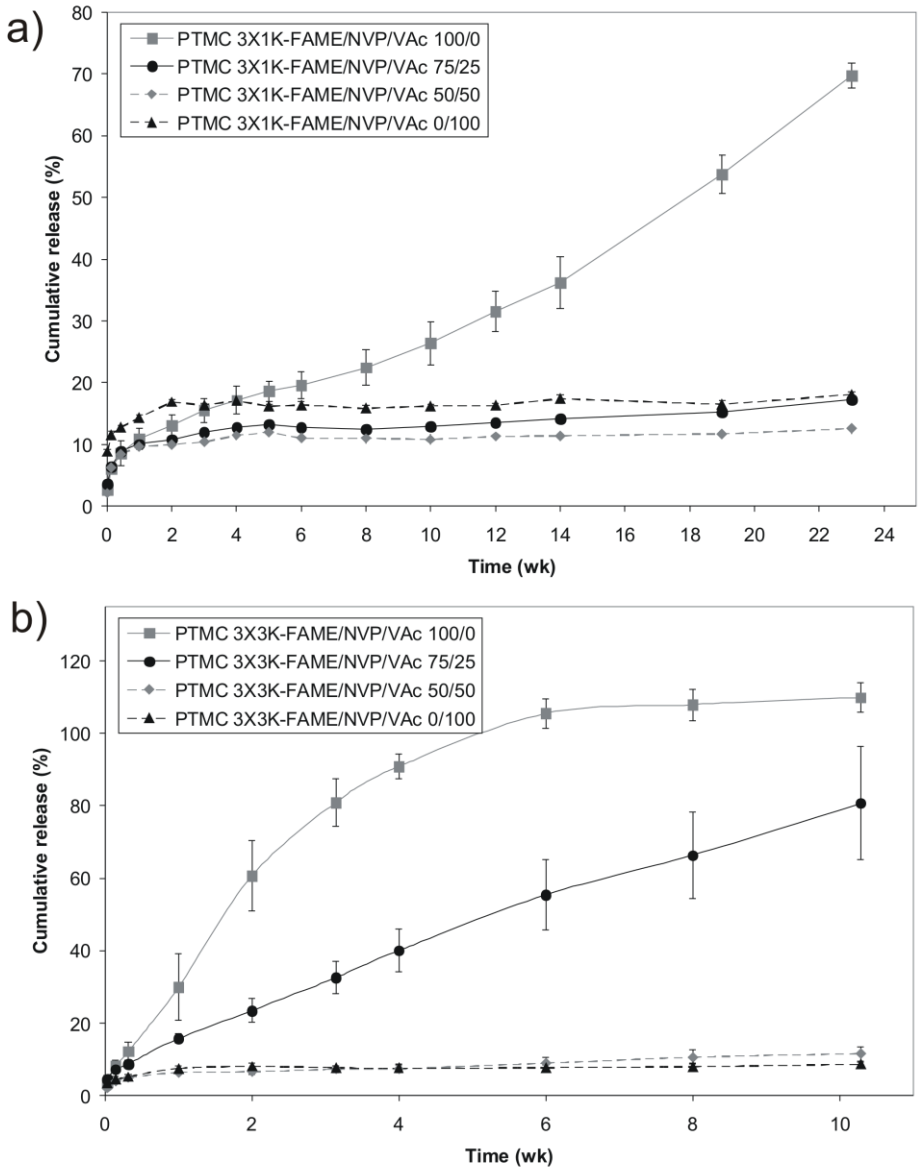

Figure 6. *Vitamin B12 release from a) PTMC 3X1K-FAME/NVP/VAc networks, b) PTMC 3X3K-FAME/NVP/VAc networks. In all cases the amount of reactive diluent was 30 wt%.*

Figure 6b shows that vitamin B12 is released faster from the less densely crosslinked PTMC 3X3K-FAME/NVP/VAc networks, this is in agreement with the water-uptake values presented in Figure 4. From PTMC 3X3K-FAME/NVP/VAc 100/0 networks, approximately 100 % of the loaded vitamin B12 was released within 6 wk, while the

75/25 NVP/VAc networks released approximately 81 % of the loaded vitamin B12 in 10 wk. For the other more hydrophobic networks, the release was limited to less than 10 %.

In the time period of 2 to 14 wk close to zero-order release of vitamin B12 can be observed from PTMC 3X1K-FAME/NVP/VAc 100/0 matrices. Also for the PTMC 3X3K-FAME/NVP/VAc 75/25 and the PTMC 3X3K-FAME/NVP/VAc 100/0 systems zero-order kinetics are observed until approximately 80% of the compound has been released. In our case, where the drug is dispersed in a polymer matrix, the release is expected to scale with the square root of time according to the Higuchi model [31]. A possible explanation for the observed zero-order release profiles is that the diffusivity of the drug in the matrix increases in time, *e.g.* due to hydrolytic degradation of the matrix. This was verified by weighing the samples after the release experiments. Mass losses ranged from 3 to 7 % for the PTMC 3X1K-FAME/NVP/VAc systems after 25 wk and 1.4 to 5 % for the PTMC 3X3K-FAME/NVP/VAc systems after 15 wk. The mass loss was highest for networks which contained 30 wt% NVP, as these are the most hydrophilic ones. Although degradation of the networks is relatively slow, this can be an advantage when controlled and sustained release of drugs over a period of months to years is desired. *In vivo,* enzymatic surface erosion might also play a role and the degradation characteristics of the networks might be somewhat different.

From these results, it can be concluded that drug release can be tuned by adjusting the hydrophilicity of these networks. A more hydrophilic network results in a faster vitamin B12 release. Furthermore, lower crosslinking densities also lead to more rapid release. Currently these photo-crosslinked systems are being optimized for the release of larger hydrophilic molecules such as proteins. Their degradation behavior, drug release characteristics and the tissue reaction to PTMC networks are being evaluated *in vivo*.

Conclusions

A fast crosslinking system based on FAME-functionalized PTMC oligomers was developed. When copolymerizing with a suitable reactive diluent, such as NVP or VAc, the system shows comparable crosslinking kinetics to MA-functionalized PTMC oligomers. Network hydrophilicity can be adjusted by combining NVP and VAc at different ratios. Extracts from PTMC 3X1K-FAME/NVP/VAC networks do not appear to be toxic to NIH 3T3 fibroblasts. The release of vitamin B12 as a model drug can be tuned by adjusting the hydrophilicity and the crosslink density of the network. Controlled and sustained release could be achieved. The more hydrophilic and less densely crosslinked networks released vitamin B12 at a faster rate.

Acknowledgements

We would like to acknowledge Peter Tummers for performing the MCR analysis and Sandra Da Silva Teixeira for help with the cell culturing experiments.

References

[1] K. Davis, Controlled release from crosslinked degradable networks. Crit Rev Ther Drug Carrier Syst 19(4-5) (2002) 385-423.

[2] A.P. Pêgo, M.J.A. van Luyn, L.A. Brouwer, P.B. van Wachem, A.A. Poot, D.W. Grijpma, J. Feijen, In vivo behavior of poly(1,3-trimethylene carbonate) and copolymers of 1,3-trimethylene carbonate with D,L-lactide or ε-caprolactone: Degradation and tissue response. J Biomed Mater Res A 67A(3) (2003) 1044-1054.

[3] Z. Zhang, R. Kuijer, S.K. Bulstra, D.W. Grijpma, J. Feijen, The in vivo and in vitro degradation behavior of poly(trimethylene carbonate). Biomaterials 27(9) (2006) 1741-1748.

[4] T. Uchida, A. Yagi, Y. Oda, Y. Nakada, S. Goto, Instability of bovine insulin in poly(lactide-co-glycolide) (PLGA) microspheres. Chem Pharm Bull 44(1) (1996) 235-236.

[5] M. van de Weert, W.E. Hennink, W. Jiskoot, Protein instability in poly(lactic-co-glycolic acid) microparticles. Pharm Res 17(10) (2000) 1159-1167.

[6] U. Edlund, A.-C. Albertsson, Copolymerization and polymer blending of trimethylene carbonate and adipic anhydride for tailored drug delivery. J Appl Polym Sci 72(2) (1999) 227-239.

[7] H. Wang, J.H. Dong, A.Y. Qiu, Z.W. Gu, Studies on properties and drug delivery systems of PTMC-b-PEG-b-PTMC block copolymers. J Macromol Sci Pure Appl Chem A35(5) (1998) 811-820.

[8] Z. Zhang, D.W. Grijpma, J. Feijen, Poly(trimethylene carbonate) and monomethoxy poly(ethylene glycol)-block-poly(trimethylene carbonate) nanoparticles for the controlled release of dexamethasone. J Control Release 111(3) (2006) 263-270.

[9] H. Shin, J.S. Temenoff, A.G. Mikos, In vitro cytotoxicity of unsaturated oligo[poly(ethylene glycol) fumarate] macromers and their cross-linked hydrogels. Biomacromolecules 4(3) (2003) 552-560.

[10] D.W. Grijpma, Q. Hou, J. Feijen, Preparation of biodegradable networks by photo-crosslinking lactide, ε-caprolactone and trimethylene carbonate-based oligomers functionalized with fumaric acid monoethyl ester. Biomaterials 26(16) (2005) 2795-2802.

[11] B. Baroli, V.P. Shastri, R. Langer, A method to protect sensitive molecules from a light-induced polymerizing environment. J Pharm Sci 92(6) (2003) 1186-1195.

[12] F. Gu, R. Neufeld, B. Amsden, Maintenance of vascular endothelial growth factor and potentially other therapeutic proteins bioactivity during a photo-initiated free radical

cross-linking reaction forming biodegradable elastomers. Eur J Pharm Biopharm 66(1) (2007) 21-27.

[13] J. Jansen, F.P.W. Melchels, D.W. Grijpma, J. Feijen, Fumaric acid monoethyl ester-functionalized poly(D,L-lactide)/N-vinyl-2-pyrrolidone resins for the preparation of tissue engineering scaffolds by stereolithography. Biomacromolecules 10(2) (2009) 214-220.

[14] S. Sharifi, H. Mirzadeh, M. Imani, M. Atai, F. Ziaee, Photopolymerization and shrinkage kinetics of in situ crosslinkable N-vinyl-pyrrolidone/poly(ε-caprolactone fumarate) networks. J Biomed Mater Res A 84A(2) (2008) 545-556.

[15] M.J. Yaszemski, R.G. Payne, W.C. Hayes, R. Langer, A.G. Mikos, In vitro degradation of a poly(propylene fumarate)-based composite material. Biomaterials 17(22) (1996) 2127-2130.

[16] J. Brandrup, E.H. Immergut, A. Abe, D.R. Bloch, Polymer Handbook, Wiley-Interscience New York, 1999.

[17] G. Odian, Principles of Polymerization, Wiley-Interscience, 1991.

[18] Polymer Data Handbook, Oxford University Press, New York, 1999.

[19] R. Langer, J. Folkman, Polymers for the sustained release of proteins and other macromolecules. Nature 263(10) (1976) 797-800.

[20] B. Amsden, G. Misra, M. Marshall, N. Turner, Synthesis and characterization of biodegradable networks providing saturated-solution prolonged delivery. J Pharm Sci 97(2) (2008) 860-874.

[21] A.A. Weiner, E.A. Bock, M.E. Gipson, V.P. Shastri, Photocrosslinked anhydride systems for long-term protein release. Biomaterials 29(15) (2008) 2400-2407.

[22] D. Wu, X. Zhang, C.-C. Chu, Synthesis, characterization and drug release from three-arm poly(ε-caprolactone) maleic acid/poly(ethylene glycol) diacrylate hydrogels. J Biomater Sci Polym Ed 14(8) (2003) 777-802.

[23] A. Haesslein, M.C. Hacker, H. Ueda, D.M. Ammon, R.N. Borazjani, J.F. Kunzler, J.C. Salamone, A.G. Mikos, Matrix modifications modulate ophthalmic drug delivery from photo-cross-linked poly(propylene fumarate)-based networks. J Biomater Sci Polym Ed 20(1) (2009) 49-69.

[24] A. Haesslein, H. Ueda, M.C. Hacker, S. Jo, D.M. Ammon, R.N. Borazjani, J.F. Kunzler, J.C. Salamone, A.G. Mikos, Long-term release of fluocinolone acetonide using biodegradable fumarate-based polymers. J Control Release 114(2) (2006) 251-260.

[25] A. Hassner, V. Alexanian, Direct room temperature esterification of carboxylic acids. Tetrahedron Lett 19 (1978) 4475-4478.

[26] K.S. Anseth, C.M. Wang, C.N. Bowman, Reaction behaviour and kinetic constants for photopolymerizations of multi(meth)acrylate monomers. Polymer 35(15) (1994) 3243-3250.

[27] A.K. Burkoth, K.S. Anseth, A review of photocrosslinked polyanhydrides: in situ forming degradable networks. Biomaterials 21(23) (2000) 2395-2404.

[28] K.A. Davis, J.A. Burdick, K.S. Anseth, Photoinitiated crosslinked degradable copolymer networks for tissue engineering applications. Biomaterials 24(14) (2003) 2485-2495.

[29] T.J. White, W.B. Liechty, C.A. Guymon, The influence of N-vinyl pyrrolidone on polymerization kinetics and thermo-mechanical properties of crosslinked acrylate polymers. J Polym Sci A Polym Chem 45(17) (2007) 4062-4073.

[30] P. Gemperline, Practical Guide to Chemometrics, CRC Taylor & Francis, 2006.

[31] T. Higuchi, Rate of release of medicaments from ointment bases containing drugs in suspension. J Pharm Sci 50(10) (1961) 874.

Chapter 4

Photo-crosslinked poly(trimethylene carbonate)-fumarate/ N-vinyl-2-pyrrolidone networks for the controlled release of proteins*

Janine Jansen[1], Mirjam B. Bosman[1], Mark J. Boerakker[2], Jan Feijen[3] and Dirk W. Grijpma[1,4]

1) MIRA Institute for Biomedical Technology and Technical Medicine, Department of Biomaterials Science and Technology, Faculty of Science and Technology, University of Twente, P.O. Box 217, 7500 AE, Enschede, The Netherlands
2) DSM Ahead, P.O Box 18, 6160 MD, Geleen, The Netherlands
3) MIRA Institute for Biomedical Technology and Technical Medicine, Department of Polymer Chemistry and Biomaterials, Faculty of Science and Technology, University of Twente, P.O. Box 217, 7500 AE, Enschede, The Netherlands
4) W.J. Kolff Institute, Department of Biomedical Engineering, University Medical Center Groningen, University of Groningen, Antonius Deusinglaan 1, 9713 AV, Groningen, The Netherlands

*J Control Release 148(1) (2010) e79-e80.

Abstract

Networks were prepared from fumaric acid monoethyl ester functionalized PTMC macromers of molecular weights ranging from 3000 to 15000 g/mol and N-vinyl-2-pyrrolidone (NVP). At a constant NVP content of 50 wt%, water uptake increased with increasing macromer molecular weight. Two model proteins, lysozyme and albumin, were incorporated into the networks. The proteins were released fastest from the networks with the highest crosslink density, probably due to osmotic pressure induced microcracks. The networks prepared from the macromers with higher molecular weights are most suited for the controlled release of proteins over longer periods of time.

Introduction

Photo-crosslinked degradable polymer networks are an interesting class of materials for application in drug delivery. A polymer network wherein a drug is dispersed can be prepared by mixing solid drug particles into a macromer solution prior to crosslinking. In this way, large amounts of drug can be loaded at high efficiencies. By varying parameters such as the crosslink density and the network hydrophilicity, release profiles can be tuned.

Poly(trimethylene carbonate) (PTMC) is a biodegradable and biocompatible material that degrades without the formation of acidic compounds. This is advantageous for application in protein delivery, since low pH may lead to protein denaturation. To make PTMC oligomers suitable for photo-crosslinking they need to be functionalized with polymerizable (crosslinkable) entities. Fumarate derivatives are attractive compounds for functionalization of oligomers, since fumaric acid is a component of the citric acid cycle. The relatively low reactivity of fumarate-functionalized oligomers can be overcome by choosing an appropriate comonomer for the photo-initiated crosslinking reaction, such as N-vinyl-2-pyrrolidone.

Methods

Trimethylene carbonate was polymerized by ring opening polymerization, using trimethylol propane as a trifunctional initiator to yield three-armed PTMC oligomers. Oligomers with three different molecular weights were prepared; 1000 g/mol (PTMC 3X1K), 3000 g/mol (PTMC 3X3K) and 5000 g/mol (PTMC 3X5K) per arm. Oligomers were functionalized by coupling with fumaric acid monoethyl ester (FAME) [1].

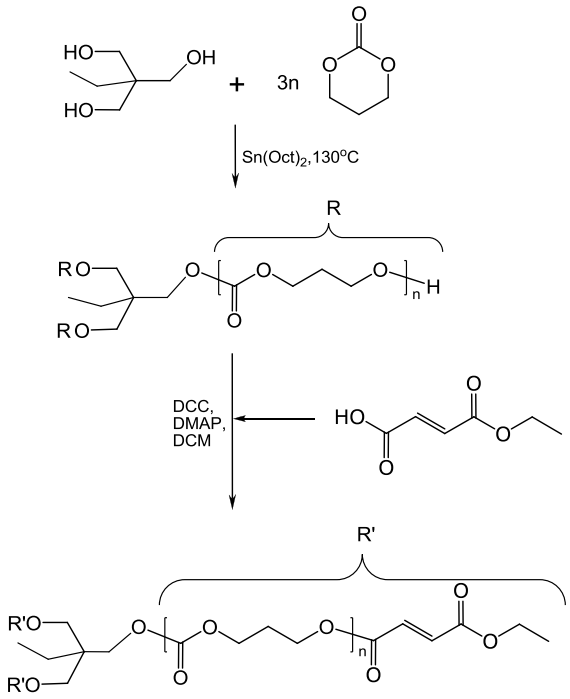

Figure 1. *Synthesis of FAME-functionalized PTMC oligomers.*

Solutions containing 50 wt% macromer and 1 wt% (with respect to the macromer) Irgacure 2959 photo-initiator in NVP were prepared. After photo-crosslinking (365 nm, 3-5 mW/cm^2, 15 min), the networks were characterized with respect to their gel contents and water uptake properties.

To obtain protein-loaded networks, 10 wt% of solid protein particles (<106 μm) was mixed into the macromer solutions prior to crosslinking. Two different proteins were used: lysozyme and bovine serum albumin. Disk-shaped samples with a diameter of 15 mm and a thickness of 0.75 mm were prepared by crosslinking the dispersions in a mold. The samples were immersed in 5 ml PBS (phosphate-buffered saline) containing 0.02 wt% NaN_3. At different time points aliquots were taken and replaced by fresh PBS. Protein concentrations were determined using a BCA (bicinchoninic acid) protein assay.

Results and discussion

PTMC macromers of different molecular weights were synthesized successfully and photo-crosslinked using NVP as a hydrophilic comonomer. All networks showed gel contents above 90 % (Figure 2). The figure also shows that water uptake increased with increasing macromer molecular weight, although all networks contained the same amount of NVP.

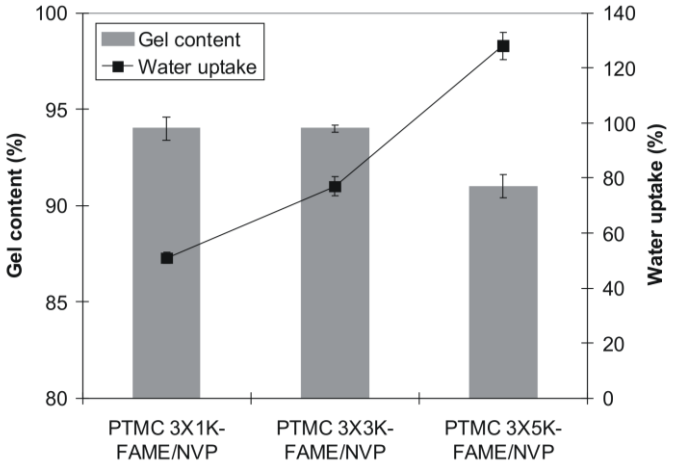

Figure 2. *Gel content and water uptake for networks prepared from FAME-functionalized PTMC macromers with different molecular weights.*

The release of two model proteins, lysozyme (14 kDa) and albumin (66 kDa) from these networks was investigated (Figure 3). Proteins could easily be loaded into the networks by dispersing solid protein particles into the macromer solutions prior to the photo-crosslinking reaction.

For both proteins, release was fastest from the PTMC 3X1K-FAME/NVP networks. This was not expected, as these networks have the lowest water uptake and the smallest mesh-size. Possibly water that is attracted by the incorporated proteins causes the formation of microcracks in the densely crosslinked and somewhat brittle PTMC 3X1K-FAME/NVP networks. Interestingly, albumin (the protein with the higher molecular weight) is released faster from these networks than lysozyme. This could be the result of the high osmotic activity of albumin; it is known for example that serum albumin is essential for maintaining the osmotic pressure of blood.

The PTMC 3X3K-FAME/NVP and PTMC 3X5K-FAME/NVP networks are less densely crosslinked and less brittle than the PTMC 3X1K-FAME/NVP networks. Figure 3a shows that the release of lysozyme from the PTMC 3X3K-FAME/NVP network is significantly slower than from the PTMC 3X5K-FAME/NVP network, apparently diffusion in these networks is of importance. Also the release of albumin, Figure 3b, from these networks is sustained. Albumin release is significantly slower than that of lysozyme, in accordance with the difference in size of the proteins. The difference between the PTMC 3X3K-FAME/NVP and PTMC 3X5K-FAME/NVP networks is limited; here also effects of osmotic pressure might play a role.

A bacteria lysis experiment indicated that the activity of lysozyme released after 7 and 21 d was 77 % and 72 %, respectively. This indicates that the effect of the photo-polymerization process on the protein was limited.

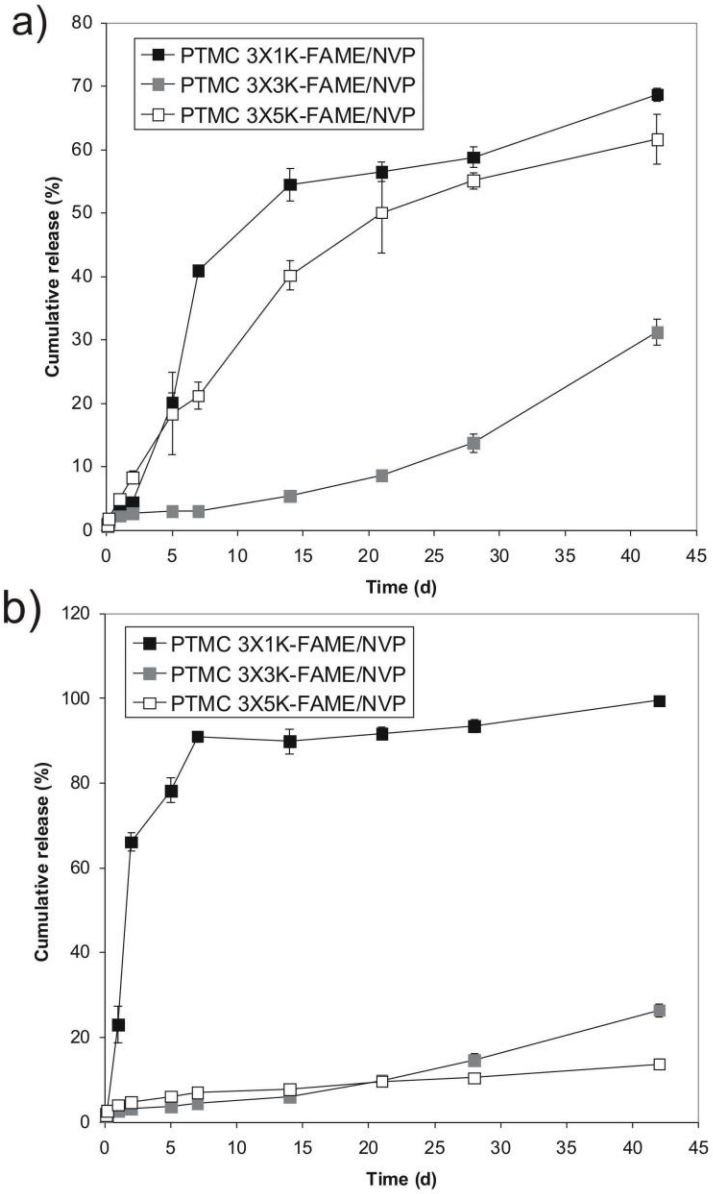

Figure 3. *Cumulative release of lysozyme (a) and albumin (b) from networks prepared from PTMC macromers with different molecular weights and NVP.*

Conclusions

PTMC 3X3K-FAME/NVP and PTMC 3X5K-FAME/NVP networks appear to be suitable for the controlled and sustained release of proteins. PTMC 3X1K/NVP networks release

lysozyme and albumin faster than the other networks, most likely because the water attracted by the proteins results in rupture of these densely crosslinked networks.

References

[1] D.W. Grijpma, Q. Hou, J. Feijen, Preparation of biodegradable networks by photo-crosslinking lactide, ε-caprolactone and trimethylene carbonate-based oligomers functionalized with fumaric acid monoethyl ester. Biomaterials 26(16) (2005) 2795-2802.

Chapter 5

Photo-crosslinked networks prepared from fumaric acid monoethyl ester-functionalized poly(D,L-lactic acid) oligomers and N-vinyl-2-pyrrolidone for the controlled and sustained release of proteins

Janine Jansen[1], Martijn P. Tibbe[1], George Mihov[2], Jan Feijen[3] and Dirk W. Grijpma[1,4]

1) MIRA Institute for Biomedical Technology and Technical Medicine, Department of Biomaterials Science and Technology, Faculty of Science and Technology, University of Twente, P.O. Box 217, 7500 AE, Enschede, The Netherlands
2) DSM Ahead, P.O. Box 18, 6160 MD, Geleen, The Netherlands
3) MIRA Institute for Biomedical Technology and Technical Medicine, Department of Polymer Chemistry and Biomaterials, Faculty of Science and Technology, University of Twente, P.O. Box 217, 7500 AE, Enschede, The Netherlands
4) W.J. Kolff Institute, Department of Biomedical Engineering, University Medical Center Groningen, University of Groningen, Antonius Deusinglaan 1, 9713 AV, Groningen, The Netherlands

Abstract

Photo-crosslinked networks were prepared from fumaric acid monoethyl ester-functionalized poly(D,L-lactic acid) oligomers and N-vinyl-2-pyrrolidone. Two model proteins, lysozyme and albumin, were incorporated into the network films as solid particles and their release behavior was studied. By varying the NVP content and macromer molecular weight, degradation behavior and protein release profiles of the prepared networks could be tuned. The more hydrophilic and less densely crosslinked networks released albumin and lysozyme at a faster rate. Although active lysozyme was released from the networks over the complete release period, lysozyme release was often incomplete. This was most likely caused by electrostatic and/or hydrophobic interactions between the protein and the degrading polymer network.

Introduction

In the past decade, several researchers investigated the use of photo-crosslinked biodegradable polymer networks for controlled drug delivery applications [1, 2]. A major advantage of photo-crosslinking is that a drug can easily be entrapped in a network by dispersing or dissolving it in a macromer solution prior to crosslinking. In this way, large amounts of drug can be loaded at high efficiencies. Furthermore, photo-polymerization is rapid and can be accomplished with minimal heat generation, allowing for the incorporation of heat-sensitive compounds such as proteins.

Poly(D,L-lactic acid) (PDLLA) is a well known polymer that has been studied extensively for application in biodegradable drug delivery systems [3]. Networks based on PDLLA can be prepared by photo-initiated crosslinking of functionalized PDLLA oligomers. Besides the frequently used methacrylate derivatives, fumaric acid derivates are also attractive compounds for end-functionalization reactions. It can be expected that residual unreacted fumarate end-groups will not lead to toxicity upon implantation since fumaric acid is a compound naturally found in the body [4]. The relatively low reactivity of fumarate end-groups can be overcome by choosing an appropriate comonomer for the photo-initiated crosslinking reaction, such as N-vinyl-2-pyrrolidone (NVP) [5].

Previously, many photo-crosslinked polymer networks have been studied as drug delivery systems. These include photo-crosslinked highly swollen hydrogels [6-8] and more hydrophobic networks based on PDLLA, poly(ε-caprolactone), poly(trimethylene carbonate) (PTMC) or copolymers of these three [9-12]. Drug release profiles can be tuned by varying the crosslink density or by adjusting the hydrophilicity of crosslinked polymer networks. Several authors have used the incorporation of poly(ethylene glycol) (PEG) to increase network hydrophilicity and adjust drug release profiles [13-15].

Increasing the NVP content of networks prepared from fumaric acid derivatives was shown to also increase network hydrophilicity and drug release rates [16-18].
Controlled and sustained release of protein drugs is challenging due to the large size and the relative instability of these molecules. During preparation, storage and release, a range of conditions may affect the stability of a protein [19, 20]. When incorporating protein drugs in photo-crosslinked polymer networks, care should be taken to prevent side reactions of free radicals with the protein [21]. However, when solid protein particles are dispersed in an organic phase containing the macromer and photo-initiator, contact with free radicals is limited since the protein remains in the solid form during the photo-polymerization reaction [22].
In previous research we prepared tissue engineering scaffolds by stereolithography from fumaric acid monoethyl ester (FAME) functionalized PDLLA oligomers and NVP [18]. Furthermore, we investigated PTMC oligomers functionalized with FAME end-groups for the controlled release of model drugs and proteins [5, 23]. In this paper we describe the preparation of photo-crosslinked polymer networks from PDLLA-FAME macromers and NVP. The crosslink density and hydrophilicity of the networks were varied by using macromers of different molecular weights and different NVP concentrations. The degradation behavior of the networks was investigated and the release of two model proteins, lysozyme and bovine serum albumin, from the prepared networks was studied.

Materials and methods

Materials

D,L-lactide (DLLA) was purchased from Purac Biochem (The Netherlands). Tin 2-ethylhexanoate ($Sn(Oct)_2$), trimethylol propane (TMP), fumaric acid monoethyl ester (FAME), deuterated chloroform, bovine serum albumin, lysozyme, *micrococcus lysodeikticus* and acetate buffer solution (pH 4.7) were obtained from Sigma Aldrich (U.S.A.). N-vinyl-2-pyrrolidone (NVP) and 1,3-dicyclohexylcarbodiimide (DCC) were purchased from Fluka (Switzerland). 4-Dimethylaminopyridine (DMAP) was purchased from Merck (Germany). Irgacure 2959 (2-hydroxy-1-[4-(2-hydroxyethoxy)phenyl]-2-methyl-1-propanone) was obtained from Ciba Specialty Chemicals (Switzerland). The BCA (bicinchoninic acid) protein assay kit was obtained from Thermo Fisher Scientific (U.S.A.). Phosphate buffered saline (PBS, pH 7.4) was obtained from B. Braun (Germany). Analytical grade dichloromethane (DCM) was obtained from Biosolve (The Netherlands). DCM was dried over CaH_2 and distilled, and other solvents were of technical grade and were used as received (Biosolve, The Netherlands).

Synthesis and characterization of 3-armed FAME-functionalized PDLLA oligomers

Three-armed poly(D,L-lactide) oligomers were synthesized by ring opening polymerization of D,L-lactide in the presence of trimethylol propane (TMP) as a trifunctional initiator (Figure 1). The oligomer syntheses were carried out on a 40 g scale. DLLA, initiator and $Sn(Oct)_2$ (approximately 0.2 mmol/mol monomer) as a catalyst were reacted in the melt at 130 ^{o}C for 48 h under argon. The targeted molecular weights were 6.1 kg/mol, 9.1 kg/mol and 12.1 kg/mol corresponding to approximately 14, 21 and 28 D,L-lactide units per arm respectively. To achieve this, 42, 63 and 84 mol of monomer were used per mol of initiator.

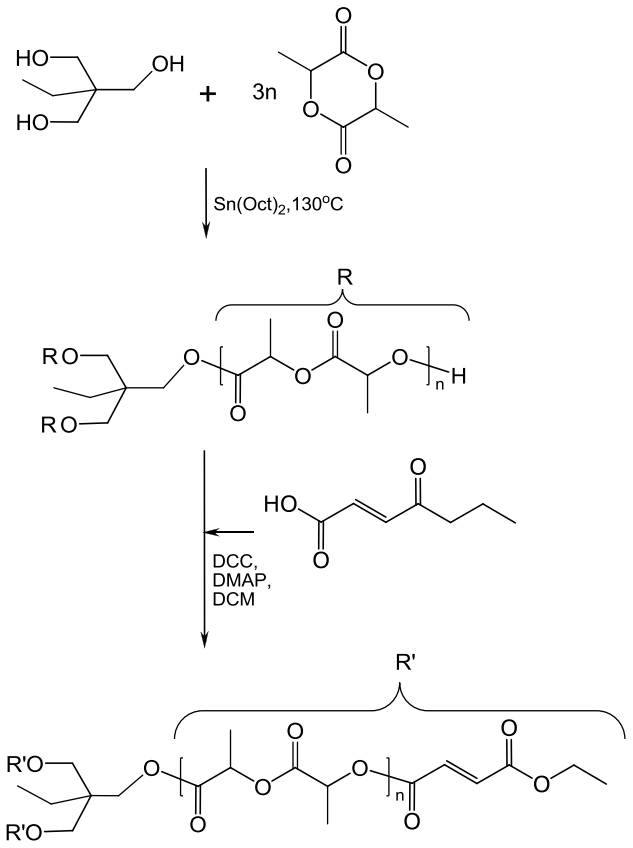

Figure 1. *Synthesis of FAME-functionalized PDLLA oligomers.*

The oligomers were functionalized by coupling fumaric acid monoethyl ester to the hydroxyl termini of the oligomers (Figure 1) [24, 25]. An amount of oligomer was charged into a three-necked flask and dried for 2 h at 110 ^{o}C *in vacuo* and cooled to room temperature under argon. The oligomers were dissolved in dried DCM, and after addition and dissolution of FAME the system was further cooled to 0 ^{o}C. Then a dichloromethane solution of DCC and DMAP was added drop-wise to the vigorously stirred oligomer solution. In the coupling reaction, 1.2 moles of FAME and DCC and 0.03 moles of

DMAP were used per mole of hydroxyl end-groups. The coupling reaction was continued overnight, letting the contents slowly warm up to room temperature. After completion of the reaction, the formed dicyclohexylurea was removed by filtration. The macromers were purified by precipitation in cold isopropanol, washing with water and freeze-drying.
The macromers are labeled as PDLLA 3XMW-FAME, in which 3 is the number of arms (the same for all macromers) and MW is the molecular weight per arm. For example, a PDLLA 3X3K-FAME macromer has a molecular weight of 3000 g/mol per arm and an overall molecular weight of approximately 9000 g/mol.
Proton nuclear magnetic resonance (^{1}H-NMR) spectra were recorded on a Varian Inova 300 MHz NMR spectrometer. Deuterated chloroform was used as a solvent. The oligomer and macromer number average molecular weights (M_n) and the degrees of functionalization of the macromers were determined from the spectra.

Preparation and characterization of PDLLA-FAME/NVP network films

Disk-shaped network specimens were prepared from FAME-functionalized PDLLA oligomers. Macromers were dissolved in NVP at different concentrations (30, 40 and 50 wt% NVP of the total mass). To each formulation 1 wt% (with respect to the macromer) of Irgacure 2959 photo-initiator was added. The solutions were poured into a Teflon mould, covered with a thin FEP (fluorinated ethylene propylene) foil, and photo-crosslinked in an Ultralum crosslinking cabinet (365 nm, 3-5 mW/cm^2, 15 min). Disk-shaped samples with a diameter of approximately 10 mm and thickness of approximately 0.5 mm were obtained.
To determine the gel content after crosslinking, a network specimen (n=3) was weighed (m_0), extracted with acetone overnight and dried at 90 ^{o}C until constant weight. The mass of the dry network (m_1) was then determined. The gel content is defined as:

$$\text{gel content} = \frac{m_1}{m_0} \times 100\%$$

To determine the water uptake, a network specimen (non-extracted, n=3) was dried at 90 ^{o}C overnight, weighed (m_d) and incubated in distilled water for 1 d. Then the samples were removed from the water, blotted dry, and weighed again (m_s). The water uptake was calculated using:

$$\text{water uptake} = \frac{m_s - m_d}{m_d} \times 100\%$$

The thermal properties of macromers and non-extracted networks were evaluated using a Perkin Elmer Pyris 1 differential scanning calorimeter. Network specimens were dried at 90 ^{o}C over night prior to the measurements. Samples were heated from -50 ^{o}C to 150 ^{o}C at a heating rate of 10 ^{o}C/min and quenched rapidly at 300 ^{o}C/min to 70 ^{o}C. After 5 min a second heating scan was recorded. The glass transition temperature (T_g) was taken as the midpoint of the heat capacity change in the second heating run.

Hydrolytic degradation of PDLLA-FAME/NVP network films

To study the hydrolytic degradation of the photo-crosslinked networks disk-shaped specimens (non-extracted, diameter = 10 mm, thickness = 0.5 mm) were immersed in 2 ml PBS (37 ^{o}C) containing 0.02 wt% NaN_3 as a bactericide. At different time points specimens (n=2) were blotted dry and weighed to determine the wet mass, dried at 90 ^{o}C under a nitrogen flow until constant weight, and then weighed to determine the dry mass.

Protein release from PDLLA-FAME/NVP network films

Lysozyme (14 kDa) and bovine serum albumin (66 kDa) were used as model protein drugs, and were grinded and sieved into particles smaller than 106 μm. The proteins (10 wt%) were dispersed in different solutions of FAME-functionalized PDLLA oligomers (30, 40 or 50 wt% NVP and 1 wt% Irgacure 2959). The mixtures were stirred and poured into Teflon moulds (diameter 10 mm, height 0.5 mm). The dispersions were crosslinked in a nitrogen atmosphere for 15 min at 3-5 mW/cm^2 (Ultralum crosslinking cabinet, 365 nm). Crosslinking was done immediately after preparing the dispersions; therefore sedimentation of the particles did not occur.

The protein-loaded specimens (n=3) were taken from the moulds and immersed in 3 ml of PBS (pH 7.4, 37 ^{o}C) containing 0.02 wt% NaN_3 as a bactericide. In the release experiments aliquots of 0.5 ml were taken at different time points and replaced by 0.5 ml of fresh PBS. Lysozyme and albumin concentrations were determined using the BCA (bicinchoninic acid) protein assay [26]. To determine the activity of the released lysozyme additional lysozyme loaded specimens were incubated in 2 ml PBS and all PBS was replaced each week. The lysozyme concentration in these solutions was determined using the BCA assay and the lysozyme activity was determined using the *micrococcus lysodeikticus* lysis assay [27].

Scanning electron microscopy (SEM; Philips XL30 operated at 2 kV) was used to analyze the protein particles and protein loaded specimens. Samples were sputter-coated with gold prior to analysis.

Results and discussion

Synthesis and characterization of 3-armed FAME-functionalized PDLLA oligomers

With trimethylol propane as a trifunctional initiator, D,L-lactide was polymerized by ring opening polymerization to yield three-armed oligomers with targeted molecular weights of 2000, 3000 and 4000 g/mol per arm. The obtained molecular weights, as determined from the TMP to D,L-lactide ratios in ^{1}H-NMR spectra, were close to the targeted molecular weights (Table 1).

Fumaric acid monoethyl ester was coupled to the oligomers to obtain crosslinkable macromers. The successful coupling of FAME to the PDLLA oligomers was confirmed by the appearance of the –CH=CH–, $-CH_2-$ and $-CH_3$ peaks of FAME at δ 6.91, δ 4.28, and δ 1.22 in the ^{1}H-NMR spectra of the precipitated reaction products. The degrees of functionalization (p) of the macromers were determined using the integral values of the $-CH_3$ peak of FAME at δ 1.22 and the $-CH_3$ of TMP at δ 0.88. For all macromers, functionalization degrees close to 100 % were obtained (Table 1).

The glass transition temperatures of the macromers were determined by DSC and are presented in Table 1. As expected, the glass transition temperatures of the macromers increase with increasing molecular weight.

Table 1. *Characteristics of the prepared macromers.*

Macromer	M_n (kg/mol per arm)[a]	p (%)[a]	T_g (^oC)[b]
PDLLA 3X2K-FAME	2.3	100	44.7
PDLLA 3X3K-FAME	3.0	97	47.7
PDLLA 3X4K-FAME	3.8	100	49.6

[a] Determined by ^{1}H-NMR

[b] Determined by DSC

Characterization of PDLLA-FAME/NVP network films

Networks were formed from FAME-functionalized PDLLA oligomers by UV irradiation using NVP as a reactive diluent and Irgacure 2959 as a photo-initiator. Macromers of different molecular weights were used and the NVP content was varied from 30 to 50 wt%. The influence of NVP content and macromer molecular weight on the network properties was evaluated.

In all cases the network gel content was close to 90 % (Figure 2), indicating efficient network formation. As was previously found [18], the water uptake of the networks

increased with increasing NVP content. This is due to the hydrophilic character of NVP. When networks with a same NVP content prepared from PDLLA 3X2K-FAME macromers and PDLLA 3X3K-FAME macromers are compared, it can be seen that the networks prepared from the higher molecular weight macromers absorb more water. This is in agreement with previous findings [5, 23] and is most likely a result of the larger mesh-size of these networks. However, if the molecular weight of the macromers is increased from 3000 g/mol per arm to 4000 g/mol per arm no further increase in water uptake is observed. Possibly phase separation plays a role here. With increasing macromer molecular weight, the network mesh-size increases and the number of FAME groups per FAME/NVP chain decreases. This may enable some phase separation of the hydrophobic PDLLA chains and the hydrophilic FAME/NVP chains and lead to a different network structure in the swollen state. Another possible explanation can be that in networks prepared from higher molecular weight macromers more entanglements are present that can restrict network swelling.

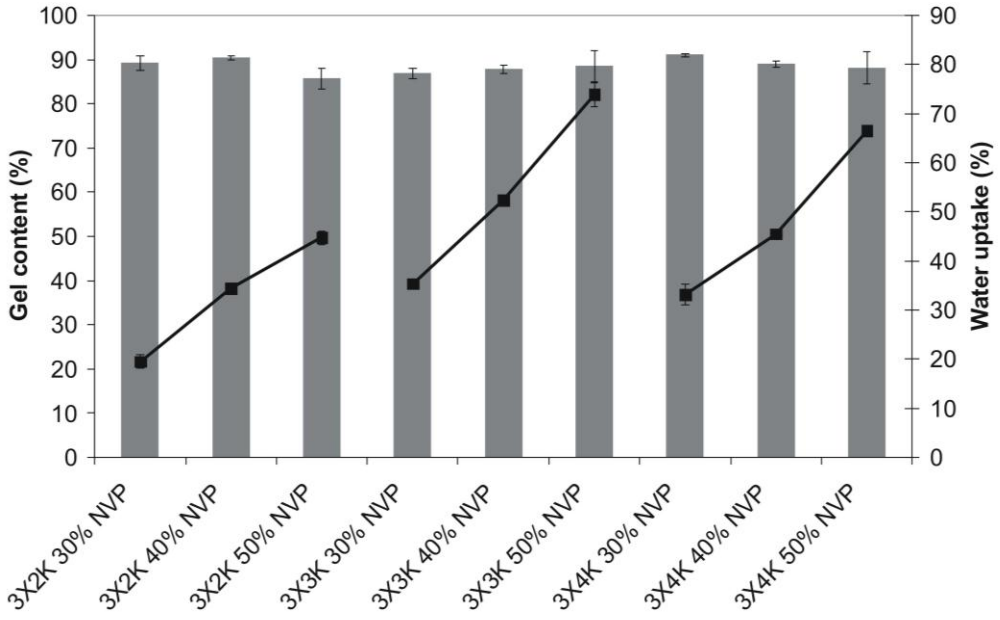

Figure 2. *Gel content (bars) and water uptake (lines) of networks prepared from PDLLA-FAME macromers of different molecular weights and with different amounts of NVP.*

The glass transition temperatures of dry non-extracted networks were determined by DSC and are presented in Table 2. It can been seen that the networks show higher T_g values than the macromers (Table 1). Furthermore, the T_g increases with increasing NVP content and the T_g values found are higher than that of high molecular weight PDLLA. It is expected that in the dry state the T_g of the networks will increase with increasing NVP

content, because the T_g of high molecular weight poly(N-vinyl-2-pyrrolidone) (PVP) is relatively high (T_g is 170 ^oC) For all networks, a single T_g was observed, which indicates that the NVP containing chains formed a single phase with the macromers. All PDLLA-FAME/NVP networks show T_g values between 56 ^oC and 70 ^oC. No clear trend as a function of macromer molecular weight was found. Although it could be expected that networks prepared from lower molecular weight macromers would have higher crosslink densities and would therefore display a higher T_g [28], this was not observed. It should be noted that non-extracted samples were analyzed and any unreacted NVP may have acted as a plasticizer and have decreased the T_g. Furthermore, the glass transitions of these networks are rather broad and therefore small differences between samples are difficult to detect.

Table 2. *Glass transition temperatures of dry, non-extracted network specimens.*

Macromer	NVP content (wt%)	T_g (^oC)
PDLLA 3X2K-FAME	30	56.9
PDLLA 3X2K-FAME	40	66.0
PDLLA 3X2K-FAME	50	66.3
PDLLA 3X3K-FAME	30	59.1
PDLLA 3X3K-FAME	40	60.5
PDLLA 3X3K-FAME	50	60.9
PDLLA 3X4K-FAME	30	62.8
PDLLA 3X4K-FAME	40	65.6
PDLLA 3X4K-FAME	50	69.1
High MW PDLLA[a]	0	55.1
High MW PVP[a,b]	100	179

[a] T_g values of high MW PDLLA and high MW PVP are given as a reference.

[b] Data from reference [29] $M_w = 9\times10^5$ g/mol.

Hydrolytic degradation of PDLLA-FAME/NVP network films

In the prepared networks, both the NVP content and the macromer molecular weight were varied. To understand the effect of these factors on network degradation a clear view of the network structure is required. In Figure 3 the proposed network structure and the effect of macromer molecular weight and NVP content are depicted schematically.

The networks consist of hydrophobic, degradable PDLLA chains and hydrophilic, non-degradable FAME/NVP chains. These FAME/NVP chains are formed when FAME and

NVP copolymerize through a light induced radical polymerization to form the network. Based on the copolymerization constants of fumaric acid and NVP the formation of alternating copolymers would be expected [29]. However, the number of NVP molecules present is much higher than the number of FAME end-groups and the mobility of the FAME end-groups is restricted. Furthermore, in a previous study we found that both FAME and NVP are consumed throughout the polymerization reaction [5]. We therefore expect that the network structure is as depicted in Figure 3: PDLLA chains connected by FAME/NVP copolymer chains in which the FAME end-groups are separated by a number of NVP moieties.

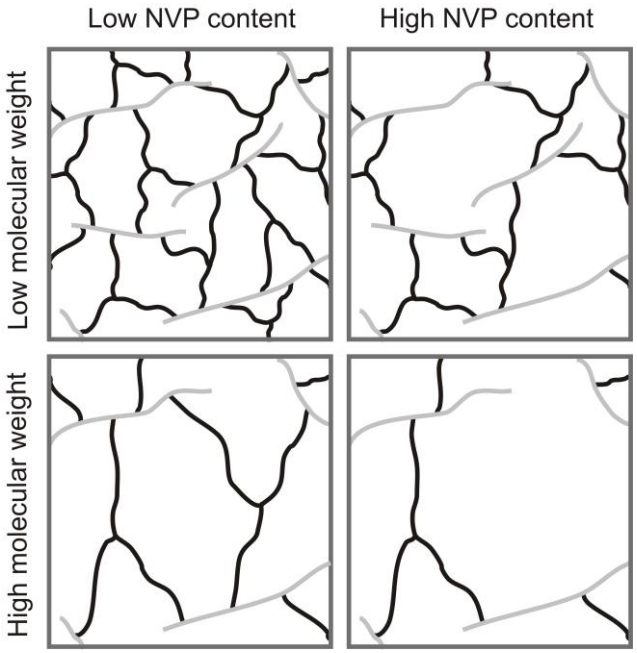

Figure 3. *Proposed structure of the synthesized networks. PDLLA chains are shown in black, FAME/NVP chains are shown in gray.*

To investigate the degradation behavior of PDLLA-FAME/NVP network films, specimens were incubated in PBS at 37 ^{o}C. At regular time intervals samples were weighed to determine their wet mass and dried and weighed to determine their dry mass. The results are shown in Figure 4.

The networks prepared with more NVP lose more dry mass over time (Figure 4d). Since these networks are most hydrophilic and therefore display the highest water uptake (Figure 2) they show relatively fast degradation. Furthermore, the networks prepared with high amounts of NVP contain a large amount of hydrophilic FAME/NVP chains that can readily go into solution as hydrolytic degradation of the PDLLA chains occurs. Additionally, in the networks prepared with high amounts of NVP, less FAME groups are

present in the FAME/NVP chains, which connect the PDLA chains in the network (Figure 3). This means that the extent of degradation required before these FAME/NVP chains can go into solution is lower compared to networks prepared with a smaller amount of NVP. No clear effect of the macromer molecular weight on the dry mass loss was found. The NVP content appears to be the most important factor in determining degradation behavior.

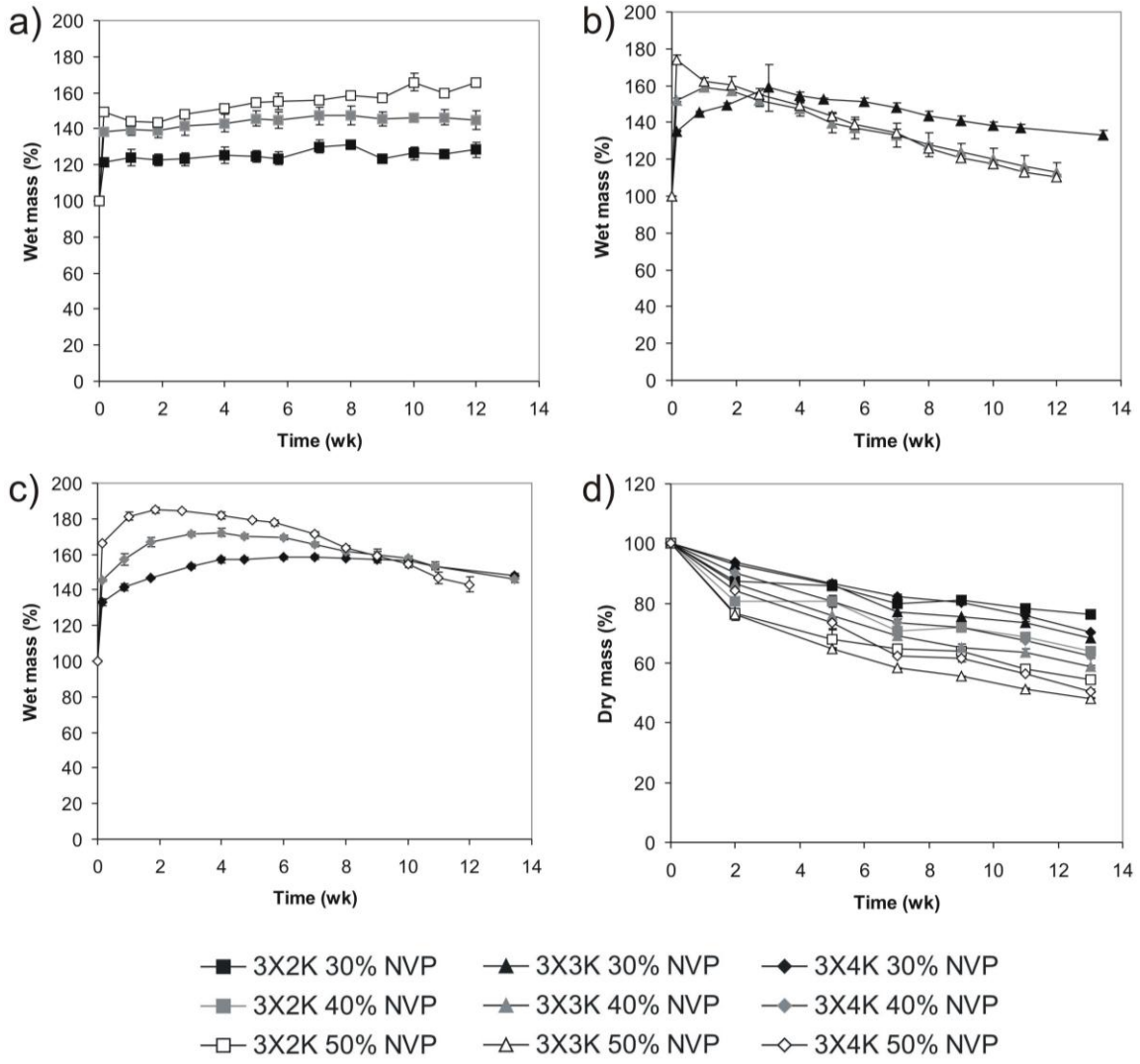

Figure 4. *Degradation of PDLLA-FAME/NVP networks. Wet mass in PBS (a-c) and dry mass (d) as a function of time.*

In the wet mass profiles in time, not only the NVP content but also the macromer molecular weight seems to play an important role (Figure 4a-c). For the networks prepared from PDLLA 3X3K-FAME and PDLLA 3X4K-FAME macromers, first a

maximum in the wet mass is observed followed by a steady decrease (Figure 4b and c). The initial increase in the wet mass can be caused by hydrolytic chain scission of the PDLLA chains that results in an increased mesh-size and network swelling. When this process continues, the hydrophilic FAME/NVP chains and other degradation products start to go into solution and the wet mass decreases. Again it is found that degradation is fastest for the networks with the highest NVP contents.

Networks prepared from the PDLLA 3X2K-FAME macromers show different wet mass profiles in time than the networks prepared from higher molecular weight macromers. Although the dry mass of these networks is decreasing in time (Figure 4d), the wet mass does not decrease, but stays more or less constant, or even slightly increases over time (Figure 4a). This may be related to the high crosslink density of these networks. As chain scission occurs, the mesh-size increases and the network can take up more water. On the other hand, soluble degradation products leave the network, decreasing the wet mass. Most likely these effects cancel each other out, leading to relatively stable wet masses in time.

These results indicate that the degradation behavior of these network films is affected by both the macromer molecular weight and the NVP content.

Protein release from PDLLA-FAME/NVP network films

To investigate the drug release behavior from different networks prepared from PDLLA-FAME macromers and NVP, the networks were loaded with protein particles. By dispersing solid protein particles in the macromer solutions, loaded networks could easily be obtained after photo-crosslinking (Figure 5). Disks measuring 10 mm in diameter and approximately 0.5 mm in thickness that contained 10 wt% protein were prepared. Lysozyme (14 kDa) and bovine serum albumin (66 kDa) were used as model proteins. The effect of the NVP content and macromer molecular weight on the protein release profiles was investigated. The results of the release experiments are shown in Figure 6 and Figure 7.

Figure 6 shows that the NVP content of PDLLA-FAME/NVP networks has a large influence on the protein release profiles. Proteins are released fastest from the networks with the highest NVP content. This is a result of the high water uptake of these networks (Figure 2). Both lysozyme and albumin are released from the networks containing 50 % NVP already within a few weeks. Release from the networks containing 30 or 40 % NVP is more sustained. Lysozyme is not released much faster than albumin, although it is a smaller protein. While often the major part of the loaded albumin was released, in many cases, lysozyme release was found to be incomplete.

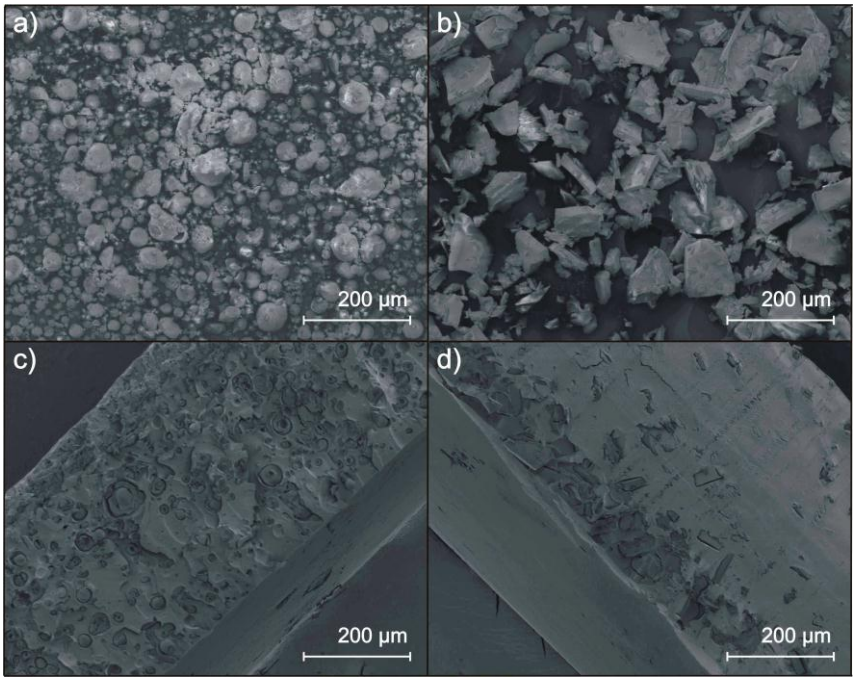

Figure 5. *SEM images of lysozyme particles (a), albumin particles (b), a PDLLA 3X2K-FAME/40% NVP network specimen loaded with lysozyme particles (c) and a PDLLA 3X2K-FAME/40% NVP network specimen loaded with albumin particles (d).*

Both degradation and diffusion can play a role in the release from these PDLLA-FAME/NVP networks. These networks degrade during the release period, resulting in an increasing mesh-size over time. The release of albumin from the PDLLA 3X2K-FAME networks containing 30 % NVP is initially slow, while after approximately 8 wk the release rate starts to increase, caused by the increased mesh-size. Diffusion of the protein becomes less restricted and the release rate increases.

In Figure 7 the release of lysozyme and albumin from networks prepared from PDLLA-FAME macromers of different molecular weights is displayed. All these networks contain 40 % NVP. Protein release is slowest from the PDLLA 3X2K-FAME/NVP networks, which is due to the high crosslink density and low water uptake of these networks (Figure 2). Differences between the PDLLA 3X3X-FAME/NVP and PDLLA 3X4K-FAME/NVP networks are small, which is in agreement with the water uptake measurements (Figure 2) and degradation characteristics (Figure 4).

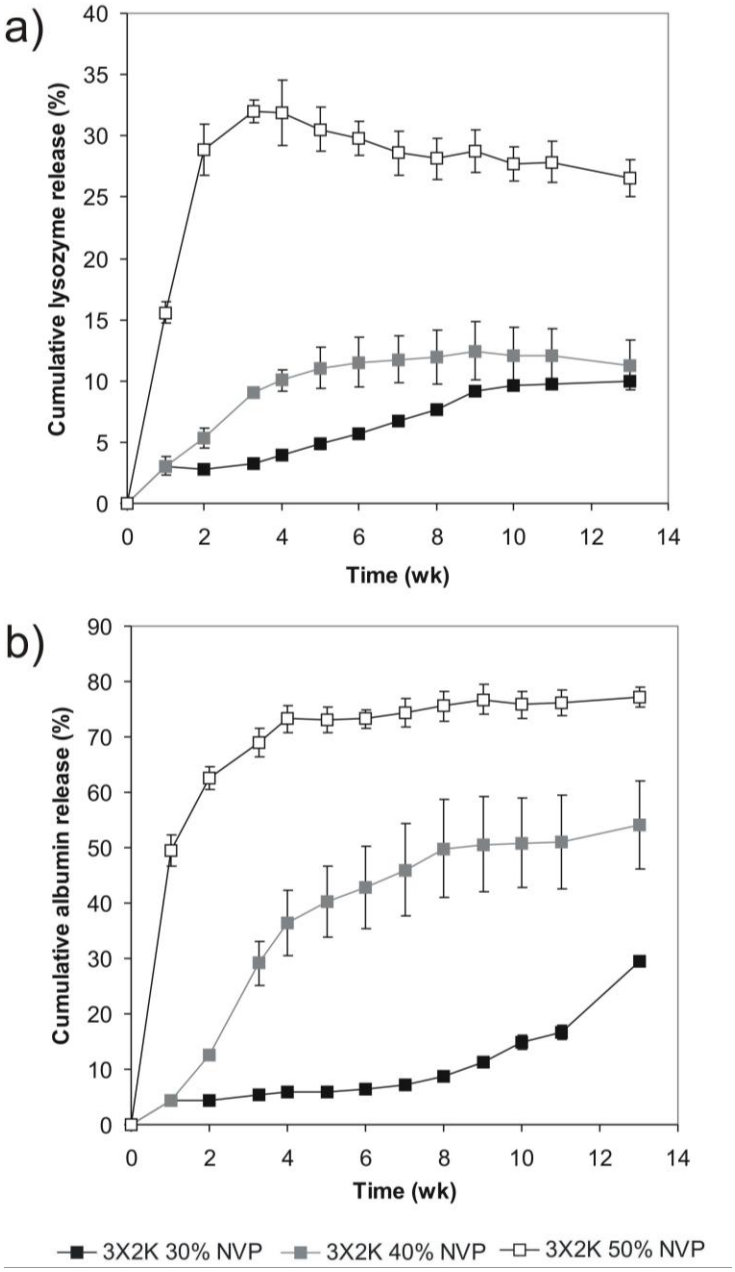

Figure 6. *Influence of the NVP content of PDLLA 3X2K-FAME/NVP networks on the release of lysozyme (a) and albumin (b).*

From these results it can be concluded that the used model proteins can be released from PDLLA-FAME/NVP networks over prolonged periods of time ranging from several weeks to a few months. Both the NVP content and the macromer molecular weight can be varied to obtain optimal release profiles.

Since it is of great importance that a released protein has retained is activity, the activity of the released lysozyme was determined (Figure 8). It was found that during the complete release period active lysozyme was released. This indicated that the protein

does remain active within the polymer matrix. The activity of the released lysozyme varied from 60 to 100 %. No clear effects of the composition of the network films on the activity of the released protein were found.

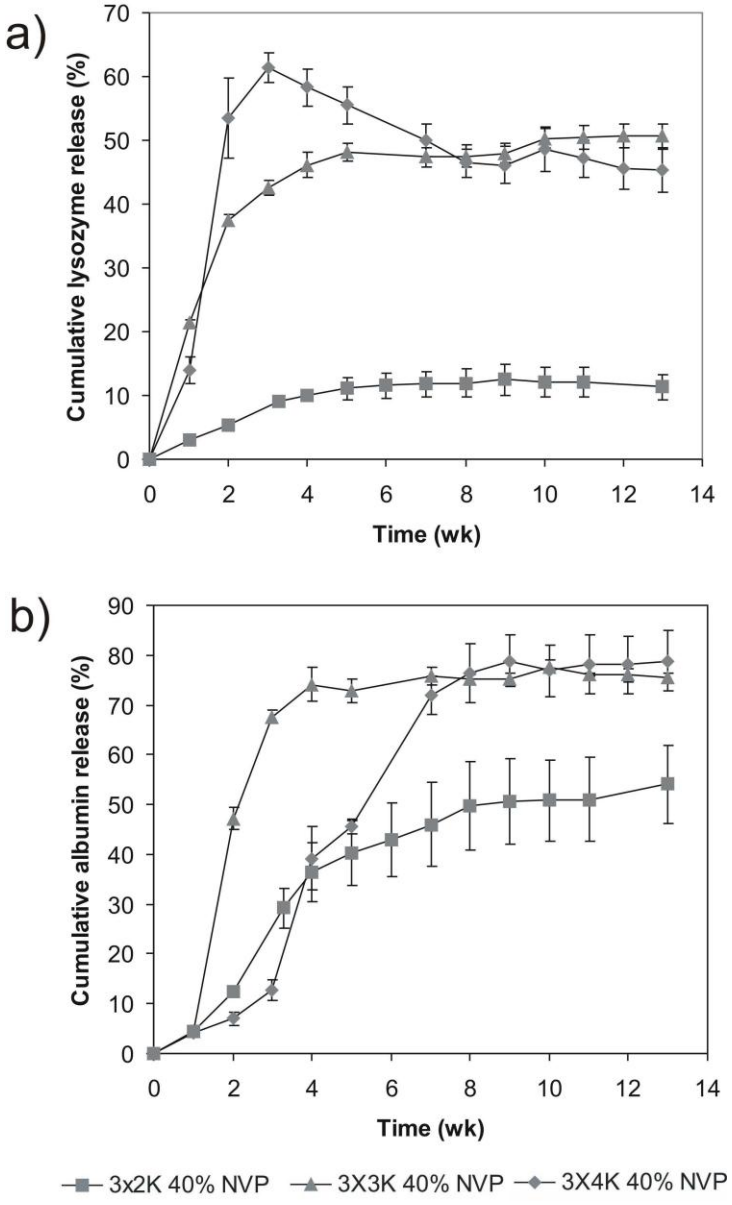

Figure 7. *Influence of the macromer molecular weight of PDLLA-FAME/NVP networks containing 40 % NVP on the release of lysozyme (a) and albumin (b).*

While in case of albumin often most of the protein was released, lysozyme release was frequently incomplete (Figure 6 and Figure 7). Incomplete release of lysozyme from release systems based on poly(lactic-co-glycolic acid) has been repeatedly observed and investigated [30-33]. Many factors during device preparation, storage and release can

play a role [19, 20]. Since photo-initiated free radical polymerization was used to prepare the protein loaded network films, side reactions may have occurred between the radicals and the proteins, which may lead to incomplete protein release [21]. However, in this case, the protein was incorporated in the form of solid particles, minimizing the contact between protein and radicals [22]. It is therefore expected that interaction of the protein with the polymer matrix, through hydrophobic or electrostatic interactions, is a more important explanation for the incomplete release. In some cases the lysozyme concentration in the media even decreases over time (Figure 6a), also indicating lysozyme adsorption to the polymer matrix. To investigate the effect of lysozyme adsorption on the release profile, the release study was repeated in different release media (Figure 9). If was found that a release medium with a lower pH and the addition of extra salt both resulted in a significant increase in overall lysozyme release.

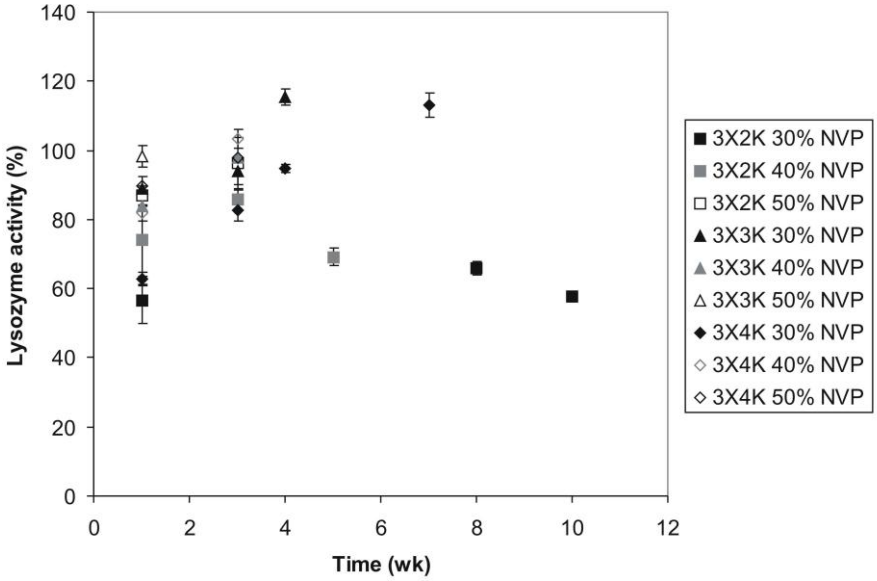

Figure 8. *Lysozyme activity after release from different networks prepared from FAME-functionalized PDLLA oligomers and NVP.*

Lysozyme is a basic protein that is positively charged at neutral pH (isoelectric point at pH 11). In contrast, albumin has an isoelectric point of 5. When chain scission of PDLLA occurs, negatively charged carboxyl end-groups are formed that may interact with the positively charged amino acids of lysozyme [33, 34]. To confirm that ionic interactions play a role in the incomplete release of lysozyme, sodium chloride was added to the release medium. Salt ions present in the release medium reduce the ionic interactions by shielding the charged groups. An increase in salt concentration was indeed found to

increase the amount of lysozyme released (Figure 9), indicating that electrostatic interactions play an important role in the incomplete protein release.

A release medium of a lower pH (acetate buffer, pH 4.7) also resulted in the release of more lysozyme when compared to release in PBS (Figure 9). At a lower pH the carboxylic acid end-groups present in the networks are protonated leading to a lower extent of ionic interaction with lysozyme [33]. This may explain why a release medium of a lower pH results in more complete release of lysozyme. However, it has also been suggested that lysozyme is not optimally folded at pH 7.4 and that its hydrophobic domains are partially exposed at this pH [31]. This may result in enhanced adsorption of the protein to the hydrophobic polymer matrix through hydrophobic interactions. This suggests that hydrophobic interactions may also play a role in the incomplete release of lysozyme from PDLLA-FAME/NVP networks.

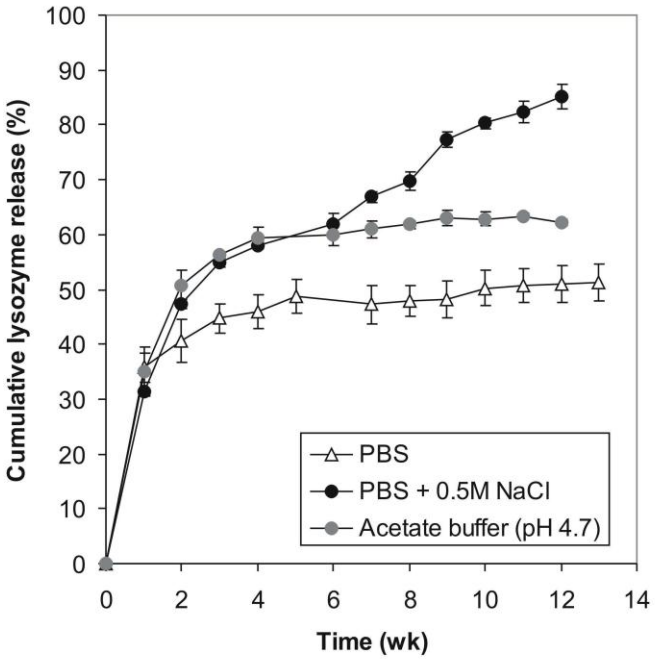

Figure 9. *Effect of the release medium on the lysozyme release from PDLLA 3X3K-FAME/50% NVP networks.*

These results indicate that the controlled and sustained release of proteins from degradable polymer matrices remains challenging. Release kinetics do not only depend on the polymer characteristics and protein size, but also on other properties of the protein such as charge and stability under the release conditions. Therefore, every protein release system based on degradable polymers needs careful optimization to obtain the desired release profile and complete release of active protein.

Conclusions

Photo-crosslinked networks were prepared from PDLLA-FAME macromers and NVP. By changing the NVP content and macromer molecular weight, degradation behavior and protein release profiles of the prepared networks could be controlled. Two model proteins, lysozyme and albumin, could be released from the networks in a controlled and sustained way. The more hydrophilic and less densely crosslinked networks released the proteins at a faster rate. Although active lysozyme was released from the networks over the complete release period, lysozyme release was often incomplete. This was most likely caused by electrostatic and/or hydrophobic interactions between the protein and the degrading polymer network.

References

[1] B. Baroli, Photopolymerization of biomaterials: issues and potentialities in drug delivery, tissue engineering, and cell encapsulation applications. J Chem Technol Biot 81(4) (2006) 491-499.

[2] K. Davis, Controlled release from crosslinked degradable networks. Crit Rev Ther Drug Carrier Syst 19(4-5) (2002) 385-423.

[3] B.D. Ratner, A.S. Hofmann, F.J. Schoen, J.E. Lemons, Biomaterials Science, Elsevier, 2004.

[4] H. Shin, J.S. Temenoff, A.G. Mikos, In vitro cytotoxicity of unsaturated oligo[poly(ethylene glycol) fumarate] macromers and their cross-linked hydrogels. Biomacromolecules 4(3) (2003) 552-560.

[5] J. Jansen, M.J. Boerakker, J. Heuts, J. Feijen, D.W. Grijpma, Rapid photo-crosslinking of fumaric acid monoethyl ester-functionalized poly(trimethylene carbonate) oligomers for drug delivery applications. J Control Release 147(1) (2010) 54-61.

[6] R. Censi, T. Vermonden, M.J. van Steenbergen, H. Deschout, K. Braeckmans, S.C. De Smedt, C.F. van Nostrum, P. di Martino, W.E. Hennink, Photopolymerized thermosensitive hydrogels for tailorable diffusion-controlled protein delivery. J Control Release 140(3) (2009) 230-236.

[7] S. Lu, K.S. Anseth, Release behavior of high molecular weight solutes from poly(ethylene glycol)-based degradable networks. Macromolecules 33(7) (2000) 2509-2515.

[8] J.L. West, J.A. Hubbell, Photopolymerized hydrogel materials for drug delivery applications. React Polym 25(2-3) (1995) 139-147.

[9] R. Chapanian, B.G. Amsden, Combined and sequential delivery of bioactive VEGF165 and HGF from poly(trimethylene carbonate) based photo-cross-linked elastomers. J Control Release 143(1) (2010) 53-63.

[10] F. Gu, H.M. Younes, A.O.S. El-Kadi, R.J. Neufeld, B.G. Amsden, Sustained interferon-γ delivery from a photocrosslinked biodegradable elastomer. J Control Release 102(3) (2005) 607-617.

[11] J. Mönkäre, R.A. Hakala, M.A. Vlasova, A. Huotari, M. Kilpeläinen, A. Kiviniemi, V. Meretoja, K.H. Herzig, H. Korhonen, J.V. Seppälä, K. Järvinen, Biocompatible photocrosslinked poly(ester anhydride) based on functionalized poly(ε-caprolactone) prepolymer shows surface erosion controlled drug release in vitro and in vivo. J Control Release 146(3) (2010) 349-355.

[12] S. Sharifi, H. Mirzadeh, M. Imani, Z. Rong, A. Jamshidi, M. Shokrgozar, M. Atai, N. Roohpour, Injectable in situ forming drug delivery system based on poly(ε-caprolactone fumarate) for tamoxifen citrate delivery: Gelation characteristics, in vitro drug release and anti-cancer evaluation. Acta Biomater 5(6) (2009) 1966-1978.

[13] B. Amsden, G. Misra, M. Marshall, N. Turner, Synthesis and characterization of biodegradable networks providing saturated-solution prolonged delivery. J Pharm Sci 97(2) (2008) 860-874.

[14] A.A. Weiner, E.A. Bock, M.E. Gipson, V.P. Shastri, Photocrosslinked anhydride systems for long-term protein release. Biomaterials 29(15) (2008) 2400-2407.

[15] D. Wu, X. Zhang, C.-C. Chu, Synthesis, characterization and drug release from three-arm poly(ε-caprolactone) maleic acid/poly(ethylene glycol) diacrylate hydrogels. J Biomater Sci Polym Ed 14(8) (2003) 777-802.

[16] A. Haesslein, M.C. Hacker, H. Ueda, D.M. Ammon, R.N. Borazjani, J.F. Kunzler, J.C. Salamone, A.G. Mikos, Matrix modifications modulate ophthalmic drug delivery from photo-cross-linked poly(propylene fumarate)-based networks. J Biomater Sci Polym Ed 20(1) (2009) 49-69.

[17] A. Haesslein, H. Ueda, M.C. Hacker, S. Jo, D.M. Ammon, R.N. Borazjani, J.F. Kunzler, J.C. Salamone, A.G. Mikos, Long-term release of fluocinolone acetonide using biodegradable fumarate-based polymers. J Control Release 114(2) (2006) 251-260.

[18] J. Jansen, F.P.W. Melchels, D.W. Grijpma, J. Feijen, Fumaric acid monoethyl ester-functionalized poly(D,L-lactide)/N-vinyl-2-pyrrolidone resins for the preparation of tissue engineering scaffolds by stereolithography. Biomacromolecules 10(2) (2009) 214-220.

[19] S.P. Schwendeman, H.R. Constantino, R.K. Gupta, R. Langer, in: K. Park (Ed.), Controlled Drug Delivery, Challenges and Strategies, 1997.

[20] M. van de Weert, W.E. Hennink, W. Jiskoot, Protein instability in poly(lactic-co-glycolic acid) microparticles. Pharm Res 17(10) (2000) 1159-1167.

[21] C.-C. Lin, S.M. Sawicki, A.T. Metters, Free-radical-mediated protein inactivation and recovery during protein photoencapsulation. Biomacromolecules 9(1) (2007) 75-83.

[22] F. Gu, R. Neufeld, B. Amsden, Maintenance of vascular endothelial growth factor and potentially other therapeutic proteins bioactivity during a photo-initiated free radical

cross-linking reaction forming biodegradable elastomers. Eur J Pharm Biopharm 66(1) (2007) 21-27.

[23] J. Jansen, M.B. Bosman, M.J. Boerakker, J. Feijen, D.W. Grijpma, Photo-crosslinked poly(trimethylene carbonate)-fumarate/n-vinyl pyrrolidone networks for the controlled release of proteins. J Control Release 148(1) (2010) e79-e80.

[24] D.W. Grijpma, Q. Hou, J. Feijen, Preparation of biodegradable networks by photo-crosslinking lactide, ε-caprolactone and trimethylene carbonate-based oligomers functionalized with fumaric acid monoethyl ester. Biomaterials 26(16) (2005) 2795-2802.

[25] A. Hassner, V. Alexanian, Direct room temperature esterification of carboxylic acids. Tetrahedron Lett 19 (1978) 4475-4478.

[26] P.K. Smith, R.I. Krohn, G.T. Hermanson, A.K. Mallia, F.H. Gartner, M.D. Provenzano, E.K. Fujimoto, N.M. Goeke, B.J. Olson, D.C. Klenk, Measurement of protein using bicinchoninic acid. Anal Biochem 150(1) (1985) 76-85.

[27] P. Shih, B. Malcolm, S. Rosenberg, J. Kirch, A. Wilson, Reconstruction and testing of ancestral proteins. Methods Enzymol 224 (1993) 576-590.

[28] T.G. Fox, S. Loshaek, Influence of molecular weight and degree of crosslinking on the specific volume and glass temperature of polymers. J Polym Sci 15(80) (1955) 371-390.

[29] J. Brandrup, E.H. Immergut, A. Abe, D.R. Bloch, Polymer Handbook, Wiley-Interscience New York, 1999.

[30] D. Blanco, M.J. Alonso, Protein encapsulation and release from poly(lactide-co-glycolide) microspheres: effect of the protein and polymer properties and of the co-encapsulation of surfactants. Eur J Pharm Biopharm 45(3) (1998) 285-294.

[31] G. Jiang, B.H. Woo, F. Kang, J. Singh, P.P. DeLuca, Assessment of protein release kinetics, stability and protein polymer interaction of lysozyme encapsulated poly(lactide-co-glycolide) microspheres. J Control Release 79(1-3) (2002) 137-145.

[32] A. Paillard-Giteau, V.T. Tran, O. Thomas, X. Garric, J. Coudane, S. Marchal, I. Chourpa, J.P. Benoît, C.N. Montero-Menei, M.C. Venier-Julienne, Effect of various additives and polymers on lysozyme release from PLGA microspheres prepared by an s/o/w emulsion technique. Eur J Pharm Biopharm 75(2) (2010) 128-136.

[33] T.G. Park, H. Yong Lee, Y. Sung Nam, A new preparation method for protein loaded poly(D,L-lactic-co-glycolic acid) microspheres and protein release mechanism study. J Control Release 55(2-3) (1998) 181-191.

[34] J. Chesko, J. Kazzaz, M. Ugozzoli, D.T. O'Hagan, M. Singh, An investigation of the factors controlling the adsorption of protein antigens to anionic PLG microparticles. J Pharm Sci 94(11) (2005) 2510-2519.

Chapter 6

Photo-crosslinked biodegradable hydrogels prepared from fumaric acid monoethyl ester-functionalized oligomers for protein delivery

Janine Jansen[1], George Mihov[2], Jan Feijen[3] and Dirk W. Grijpma[1,4]

1) MIRA Institute for Biomedical Technology and Technical Medicine, Department of Biomaterials Science and Technology, Faculty of Science and Technology, University of Twente, P.O. Box 217, 7500 AE, Enschede, The Netherlands
2) DSM Ahead, P.O. Box 18, 6160 MD, Geleen, The Netherlands
3) MIRA Institute for Biomedical Technology and Technical Medicine, Department of Polymer Chemistry and Biomaterials, Faculty of Science and Technology, University of Twente, P.O. Box 217, 7500 AE, Enschede, The Netherlands
4) W.J. Kolff Institute, Department of Biomedical Engineering, University Medical Center Groningen, University of Groningen, Antonius Deusinglaan 1, 9713 AV, Groningen, The Netherlands

Abstract

Photo-crosslinkable, fumaric acid monoethyl ester-functionalized triblock oligomers were synthesized and copolymerized with N-vinyl-2-pyrrolidone to form biodegradable photo-crosslinked hydrogels. Poly(ethylene glycol) was used as the middle hydrophilic segment and the hydrophobic segments were based on D,L-lactide, trimethylene carbonate or a mixture of these monomers. Two model proteins, lysozyme and albumin, were incorporated in the hydrogels and their release was studied. The composition of the hydrophobic segments could be used to tune degradation behavior and release rates. Careful optimization of photo-polymerization conditions is needed to limit conjugation of proteins to the hydrogels and protein denaturation.

Introduction

Hydrogels are hydrophilic polymer networks that are able to retain large volumes of water. Due to their crosslinked structure, formed by either chemical bonds or physical interactions, they do not dissolve in water. Their high water content and biocompatibility make hydrogels attractive for biomedical applications such as tissue engineering and controlled drug delivery [1].

To form hydrogels hydrophilic polymers can be covalently crosslinked by different methods [2]. An attractive crosslinking method is photo-polymerization of oligomers that are functionalized with double bond-containing groups. Photo-polymerization offers the advantage of spatial and temporal control, and even *in situ* gel formation by transdermal photo-polymerization has been shown to be feasible [3]. Photo-crosslinked hydrogels are interesting for drug delivery applications since they can easily be loaded with drugs by dissolving the drug in the crosslinkable macromer solution prior to the crosslinking process [4]. The encapsulation of low molecular weight drugs, proteins, DNA and even cells has been reported [5, 6].

Di(meth)acrylated triblock copolymers of poly(ethylene glycol) (PEG) and degradable hydrophobic polyesters such as poly(lactic acid) (PLA) and poly(glycolic acid) (PGA) have been extensively used for the preparation of photo-crosslinked hydrogels. Hubbell and coworkers [7, 8] were the first to prepare this type of hydrogel. The degradation behavior of these gels is determined by the crosslink density and the hydrolytic susceptibility of the hydrophobic blocks. Release of model proteins from these networks is controlled by diffusion and degradation.

Poly(trimethylene carbonate) (PTMC) is a flexible, biodegradable and biocompatible polymer. Although the *in vitro* degradation of PTMC is slow [9], the degradation of PTMC *in vivo* has been shown to be much faster due to the presence of enzymes and

reactive oxygen species [10-12]. However, this will most likely not occur when PTMC is incorporated in hydrogels since the enzymatic degradation rate of PTMC decreases dramatically when the PTMC containing polymer becomes more hydrophilic [13]. Therefore, PTMC may be an interesting hydrophobic block for the preparation of slowly degrading hydrogels [14].

Although methacrylate derivatives have been most frequently used to functionalize water soluble oligomers with double bond-containing groups, fumaric acid derivatives are also attractive compounds for end-functionalization. Fumaric acid is a compound naturally found in the body as a component of the citric acid cycle and it can therefore be expected that residual unreacted fumarate end-groups after cleavage will not lead to toxicity upon implantation [15]. Compared to methacrylate-functionalized oligomers, the reactivity of fumarate-functionalized oligomers is relatively low [16] and therefore N-vinyl-2-pyrrolidone (NVP) is often used as a comonomer in the photo-polymerization reaction [17].

Fumaric acid derivatives have been used before for the preparation of hydrogels. Heller *et al.* [18] prepared hydrogels from polyesters obtained by polycondensation of fumaric acid and PEG. Suggs *et al.* [19] used poly(propylene fumarate-co-ethylene glycol) copolymers to prepare hydrogels by heat induced radical polymerization. Sarvestani *et al.* [20] prepared hydrogels by redox initiated radical polymerization of macromers consisting of PLA and PEG blocks linked by fumaric acid. In these three studies fumaric acid is incorporated into the main chain of the polymer. It is also possible to use fumaric acid monoethyl ester to end-functionalize oligomers [16]. In our group initial experiments were performed on the preparation of hydrogels by photo-crosslinking of fumarate end-functionalized PEG-PTMC block copolymers [21].

In this study hydrogels prepared from fumarate end-functionalized triblock oligomers were investigated. PEG with a molecular weight of 4000 g/mol was used as the hydrophilic segment. PTMC, poly(D,L-lactide) (PDLLA), which contains ester bonds that are more susceptible to hydrolysis than the PTMC carbonate bonds [9], and a 50/50 copolymer of TMC and D,L-lactide were used as hydrophobic segments. The composition of the hydrophobic block and the block length were varied to tune degradation rate and protein release profiles.

Materials and methods

Materials

Trimethylene carbonate (TMC) was purchased from Boehringer Ingelheim (Germany). D,L-lactide (DLLA) was purchased from Purac Biochem (The Netherlands). Tin 2-ethylhexanoate ($Sn(Oct)_2$), fumaric acid monoethyl ester (FAME), deuterated chloroform, poly(ethylene glycol) (M_n 4000 g/mol), 2,2-dimethoxy-2-phenylacetophenone (Irgacure 651), bovine serum albumin, lysozyme and *micrococcus lysodeikticus* were obtained from Sigma Aldrich (U.S.A.). N-vinyl-2-pyrrolidone (NVP) and 1,3-dicyclohexylcarbodiimide (DCC) were purchased from Fluka (Switzerland). 4-Dimethylaminopyridine (DMAP) was purchased from Merck (Germany). Irgacure 2959 (2-hydroxy-1-[4-(2-hydroxyethoxy)phenyl]-2-methyl-1-propanone) was obtained from Ciba Specialty Chemicals (Switzerland). The BCA (bicinchoninic acid) protein assay kit was obtained from Thermo Fisher Scientific (U.S.A.). Phosphate buffered saline (PBS, pH 7.4) was obtained from B. Braun (Germany). Analytical grade dichloromethane (DCM) was obtained from Biosolve (The Netherlands). DCM was dried over CaH_2 and distilled, and other solvents were of technical grade and were used as received (Biosolve, The Netherlands).

Synthesis and characterization of macromers

Six different triblock oligomers were synthesized by the ring opening polymerization of D,L-lactide, trimethylene carbonate, or a 50/50 mixture of these two, using PEG as a difunctional initiator. PEG (M_n = 4000 g/mol) was dried at 110 ^oC for 2 h. Monomer (D,L-lactide, trimethylene carbonate or a 50/50 mixture), PEG and stannous octoate catalyst were reacted in the melt at 130 ^oC for 2 d under argon. The intended molecular weights of the hydrophobic blocks were 400 and 800 g/mol per arm. Unpurified oligomers were used in the coupling reaction to prepare macromers.

Oligomers were functionalized by coupling fumaric acid monoethyl ester (FAME) to their hydroxyl termini [16, 22]. An amount of oligomer was charged into a three-necked flask, dried for 2 h at 110 ^oC *in vacuo* and cooled to room temperature under argon. The oligomers were then dissolved in dried DCM, and after addition and dissolution of FAME the system was further cooled to 0 ^oC. Then a dichloromethane solution of DCC and DMAP was added drop-wise to the vigorously stirred oligomer solution. In the coupling reaction, 1.2 moles of FAME and DCC and 0.03 moles of DMAP were used per mole of hydroxyl end-groups. The coupling reaction was continued overnight, letting the contents slowly warm up to room temperature. After completion of the reaction, the

formed dicyclohexylurea (DCU) was removed by filtration and the macromers were purified by precipitation in cold diethyl ether and drying under vacuum.

Proton nuclear magnetic resonance (^{1}H-NMR) spectra were recorded on a Varian Inova 300 MHz NMR spectrometer. Oligomers and macromers were dissolved in deuterated chloroform. NMR spectra of the reaction mixtures were used to determine molar masses and degrees of functionalization.

The thermal properties of the macromers were studied using a Perkin Elmer Pyris 1 differential scanning calorimeter (DSC) connected to a liquid nitrogen cooling accessory. Samples were heated from -60 ^{o}C to 100 ^{o}C at a heating rate of 10 ^{o}C/ min and cooled at 10 ^{o}C/min to -60 ^{o}C. After 5 min a second heating scan was recorded. The glass transition temperature (T_g) was taken as the midpoint of the heat capacity change in the second heating run. The melting temperature (T_m) was determined as the temperature of the maximum of the endotherm in the first heating run.

Preparation of hydrogels by photo-crosslinking in solution

The macromers were dissolved in PBS at a concentration of 30 wt%. To investigate the effect of the macromer concentration on network properties, the macromers were also dissolved in PBS at other concentrations. The concentration of NVP and photo-initiator were kept constant with respect to the macromer. The Irgacure 2959 photo-initiator was dissolved in NVP, this solution was then added to the macromer solutions in PBS to obtain an NVP concentration of 10 wt% (depending on the macromer molecular weight, this corresponds to 2.3 or 2.6 moles of NVP per mole of FAME end-groups) and a photo-initiator concentration of 1 wt% (both with respect to the macromer). The solutions were poured into a Teflon mould, covered with a thin FEP (fluorinated ethylene propylene) foil, and photo-crosslinked in an Ultralum crosslinking cabinet (365 nm, 3-5 mW/cm^2, 15 min). Disked-shaped samples with a diameter of approximately 10 mm and thickness of approximately 0.5 mm were obtained.

Hydrogel characterization

To determine the gel content after crosslinking, a network specimen (n=3) was weighed, and the total mass of the network and unreacted macromer and NVP was determined (m_0) using the macromer and NVP fractions in the crosslinking solution. Afterwards the sample was swollen and extracted in distilled water for 1 d, blotted dry and weighed (m_s). Then the sample was freeze-dried and the mass of the dry network (m_1) was determined. Gel content is defined as:

$$\text{Gel content} = \frac{m_1}{m_0} \times 100\%$$

Water uptake was calculated using:

$$\text{Water uptake} = \frac{m_s - m_0}{m_0} \times 100\%$$

The water uptake of the hydrogels was determined at different temperatures. For this the swollen gels were incubated at a certain temperature for 1 h before they were blotted dry and weighed (m_s). The water uptake was calculated as described above.

The mechanical properties of the hydrogels were studied using a Physica MCR 301 rheometer (Anton Paar). The gap of the parallel plates was adjusted to obtain a normal force of approximately 40 N and to assure optimal contact between the sample and the plates [23]. A frequency of 1 Hz and a strain of 1 % were applied. All experiments were performed at 37 ^{o}C. Disk shaped specimens (n=3) with a thickness of approximately 0.5 mm were prepared by photo-crosslinking the macromer solutions in a mold. Specimens were swollen in distilled water for 1 d prior to the measurements. Specimens with a diameter equal to the diameter of the rheometer setup (25 mm) were punched out off the swollen specimens. The molecular weight between effective cross-links (M_c) was calculated from the storage modulus (G′) using the following equation, which is an adaptation of the rubber elasticity theory [24, 25]:

$$G' = \frac{\rho RT}{M_c}$$

where ρ is the polymer concentration (g/m^3), R is the gas constant and T is the absolute temperature.

When it is assumed that the hydrophobic segments and FAME/NVP crosslinks form small crosslink zones with PEG in between these crosslink points, the mesh-size of the hydrogels can be approximated from the molecular weight between crosslinks using [26, 27]:

$$\xi = \varphi_p^{-1/3} l (nC_\infty)^{1/2}$$

where ξ is the mesh-size in angstrom, φ_p is the polymer volume fraction in the equilibrium swollen state. l is the bond length, taken as 1.50 Å (the average of one carbon-carbon and two carbon-oxygen bonds). C_∞ is the characteristic ratio (3.8 for PEG [28]) and n is the average number of bonds between crosslinks which can be calculated using:

$$n = 3\frac{x_{PEG} M_c}{M_r}$$

where x_{PEG} is the weight fraction of PEG in the macromer and M_r is the molecular weight of the PEG repeating unit (44 g/mol). The polymer volume fraction, φ_p, is taken as 1/Q in which Q is the equilibrium volume swelling ratio calculated using:

$$Q = 1 + \frac{m_s - m_0}{m_0} \times \frac{\rho_{macr}}{\rho_{water}}$$

m_s and m_0 were determined as described above. ρ_{macr} is the density of the macromers, taken as 1.2 g/ml for all macromers.

To study the degradation of hydrogels (n=3) prepared from 30 wt% macromer solutions the swelling ratio was followed in time. The swelling ratio was determined from the initial mass after preparation of the hydrogel by photo-crosslinking (m_0) and the mass of the swollen gel after a certain time t at 37 ^oC in PBS (m_t):

$$\text{Swelling ratio} = \frac{m_t}{m_0}$$

Protein release

Lysozyme (14 kDa, 41 Å [29]) and bovine serum albumin (66 kDa, 72 Å [29]) loaded hydrogels were prepared by adding 0.25 ml of protein solution in PBS (40 mg/ml) to a solution of 0.5 g macromer in 0.92 ml PBS. The final macromer concentration in PBS was adjusted to 30 wt%. The Irgacure 2959 photo-initiator was dissolved in NVP and this solution was then added to the macromer solutions in PBS to obtain a NVP concentration of 10 wt% and a photo-initiator concentration of 1 wt% (both with respect to the macromer). The solutions were poured into a Teflon mould and photo-crosslinked for 15 min in an Ultralum crosslinking cabinet (365 nm, 3-5 mW/cm^2). The obtained

specimens (diameter approximately 10 mm, thickness approximately 0.5 mm, n=3) were immersed in 2 ml of PBS (pH 7.4, 37 ^{o}C) containing 0.02 wt% NaN_3. Samples of 0.5 ml were removed and replaced with fresh PBS regularly. Lysozyme and albumin concentrations were determined using the BCA (bicinchoninic acid) protein assay [30]. Lysozyme activity was determined using the *micrococcus lysodeikticus* lysis assay [31].

Results and discussion

Macromer synthesis

A number of triblock oligomers was synthesized by ring opening polymerization of trimethylene carbonate, D,L-lactide or a mixture of the two using $Sn(Oct)_2$ as a catalyst. PEG with a molecular weight of 4000 g/mol (M_n = 3.99×10^3 g/mol, determined by ^{1}H-NMR) was used as a bifunctional initiator and oligomers with two different hydrophobic segment lengths were prepared by varying the monomer to initiator ratio. The obtained hydrophobic block lengths calculated from ^{1}H-NMR spectra are slightly lower than the intended molecular weights (Table 1). Possibly small amounts of water were present that also initiated polymerization leading to somewhat shorter PDLLA and PTMC blocks. This can be due to the fact that PEG was dried only by vacuum drying at elevated temperature and not by azeotropic distillation.

To obtain crosslinkable macromers, fumaric acid monoethyl ester was coupled to the oligomers. Examples of ^{1}H-NMR spectra of purified PEG-PDLLA-FAME and PEG-PTMC-FAME macromers with peak assignment are shown in Figure 1 and Figure 2. The coupling of FAME to the oligomers was identified specifically by the appearance of the peaks of the =CH– (d) at δ 6.85, and the –CH_3 (f) at δ 1.34 of the FAME. The degrees of functionalization of the macromers summarized in Table 1 were determined using the integral values of the –CH_3 peak of FAME at δ 1.32 (f) and the –CH_2– of PEG at δ 3.64 (c). For all macromers the functionalization degrees were adequate to allow effective crosslinking. The calculated degrees of functionalization are lowest for the PEG-PTMC-FAME macromers. However, PTMC end-groups (a' in Figure 2) were barely visible, and it can therefore be concluded that the degree of functionalization was high for these macromers. The degrees of functionalization calculated for the PEG-PDLLA-FAME and the PEG-PDLLA/PTMC-FAME macromers were above 100%. This may possibly be explained by some overlap of peak f of FAME at δ 1.34 with other peaks, such as peak a of PDLLA at δ 1.54, resulting in difficulties in peak integral value determination.

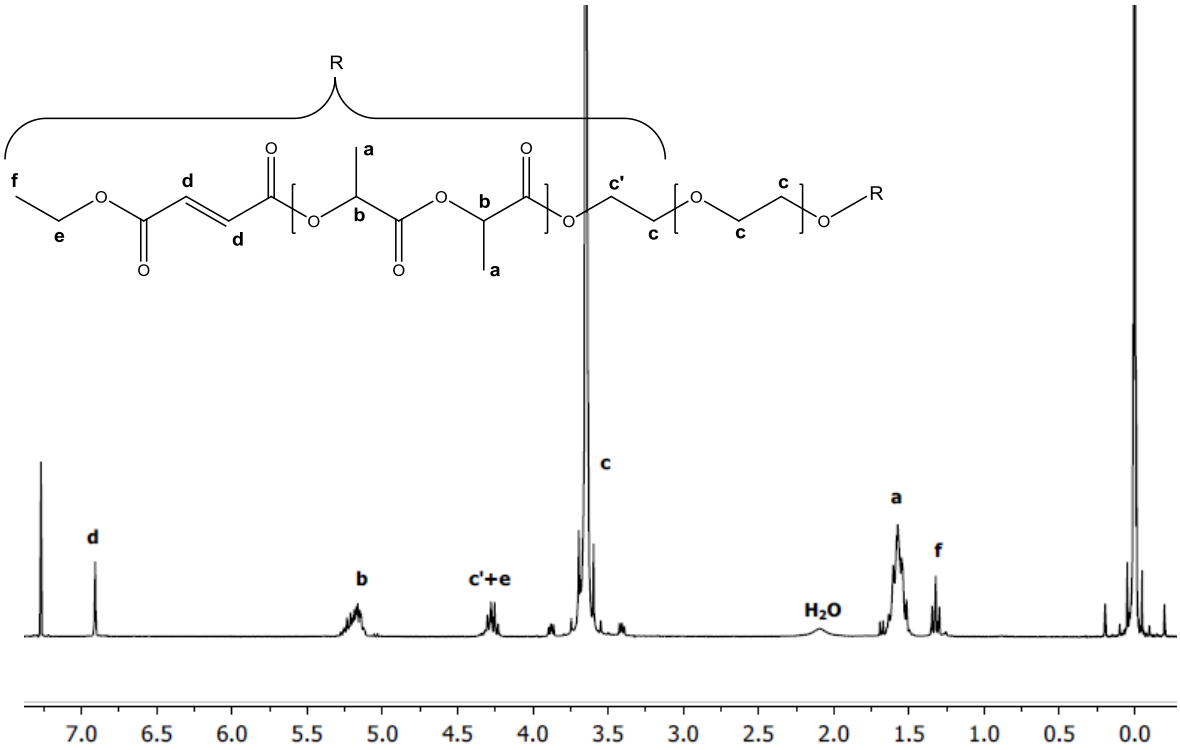

Figure 1. *[1]H-NMR spectrum of PEG4K-PDLLA2X0.8K-FAME macromers.*

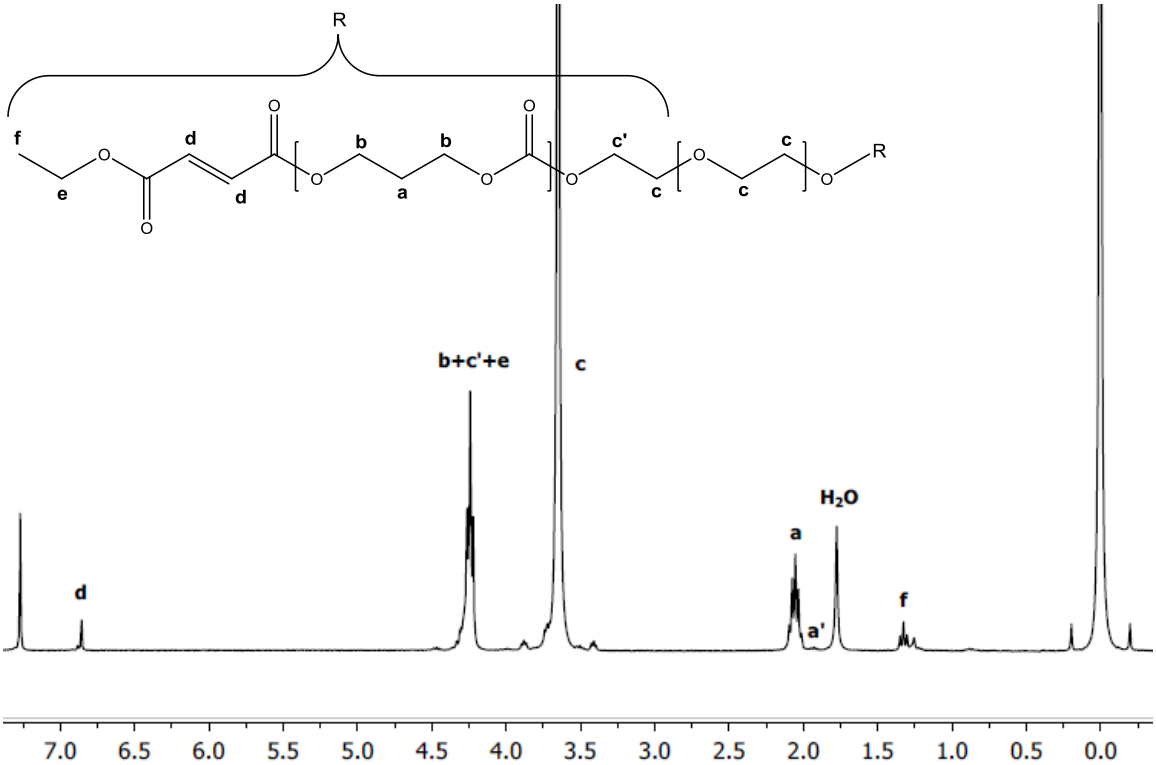

Figure 2. *[1]H-NMR spectrum of PEG4K-PTMC2X0.8K-FAME macromers.*

Table 1. *Characteristics of PEG-PTMC-FAME, PEG-PDLLA-FAME and PEG-PDLLA/PTMC-FAME macromers.*

	Targeted			^{1}H-NMR				
Macromer[a]	n_{TMC}[b]	n_{LA}[b]	PEG%[c]	n_{TMC}[b]	n_{LA}[b]	M_n[d] (g/mol)	PEG%[c]	p[e] (%)
PEG4K-PDLLA2X0.4K-FAME	-	2.8	79	-	1.8	2.6×10^2	84	106
PEG4K-PDLLA2X0.8K-FAME	-	5.6	68	-	3.7	5.3×10^2	75	104
PEG4K-PTMC2X0.4K-FAME	3.9	-	79	2.4	-	2.5×10^2	84	72
PEG4K-PTMC2X0.8K-FAME	7.8	-	68	6.1	-	6.2×10^2	73	76
PEG4K-PDLLA/PTMC2X0.4K-FAME	2.0	1.4	79	1.7	1.0	3.2×10^2	82	124
PEG4K-PDLLA/PTMC2X0.8K-FAME	3.9	2.8	68	3.2	2.1	6.3×10^2	73	124

[a] Example illustrating the nomenclature used: the PEG4K-PDLLA2X0.4K-FAME macromer contains a middle PEG block (4000 g/mol), two hydrophobic PDLLA blocks (400 g/mol) and FAME end-groups.

[b] Number of trimethylene carbonate/lactide units per block

[c] wt% (PEG/(PEG+PTMC/PDLLA+FAME))

[d] Molecular weight of the hydrophobic blocks

[e] Degree of functionalization

The thermal properties of the PEG-PDLLA-FAME, PEG-PTMC-FAME and PEG-PDLLA/PTMC-FAME macromers were studied using DSC. The results are summarized in Table 2. For all macromers the melting temperature of the PEG block is lower than that of pure PEG (62.7 ^oC). This can be explained by partial mixing of the hydrophilic and hydrophobic phases. The T_g of the PDLLA blocks was not found. Most likely because this transition is close to the melting peak of PEG and the PDLLA content is relatively low. The T_g of the PTMC segments in the PEG-PTMC-FAME macromers was detected.

The T_g's of the PDLLA/PTMC blocks are somewhat higher than that of the PTMC blocks due to the higher T_g of PDLLA. Both for PTMC and PDLLA/PTMC blocks the T_g increases with increasing segment molecular weight.

Table 2. *Thermal properties of PEG-PDLLA-FAME, PEG-PTMC-FAME and PEG-PDLLA/PTMC-FAME macromers.*

	T_g (^oC)	T_m (^oC)	ΔH_m (J/g)
PEG4K-PDLLA2X0.4K-FAME	-	51.4	119.7
PEG4K-PDLLA2X0.8K-FAME	-	50.4	106.1
PEG4K-PTMC2X0.4K-FAME	-39.8	52.5	117.2
PEG4K-PTMC2X0.8K-FAME	-37.1	50.3	95.1
PEG4K-PDLLA/PTMC2X0.4K-FAME	-28.6	50.5	114.9
PEG4K-PDLLA/PTMC2X0.8K-FAME	-22.2	49.4	112.1
PEG4K	-	62.6	186.0

Hydrogel properties

Hydrogels were prepared from the synthesized macromers by photo-polymerization. The macromers were dissolved in PBS at different concentrations. A solution of photo-initiator in NVP was added and the macromer solutions were irradiated to obtain photo-crosslinked hydrogels. The hydrogels were characterized with respect to their gel content and water uptake (Figure 3).

All hydrogels show gel contents above 90 %, illustrating that photo-polymerization of the fumarate end-groups with NVP as a comonomer and Irgacure 2959 as an initiator was quite effective. Water uptake of the hydrogels decreased with increasing macromer concentration used in the crosslinking. Most likely in the hydrogels prepared from concentrated macromer solutions more entanglements are present that restrict swelling. In addition, the FAME conversion may be somewhat higher for the gels prepared from more concentrated macromer solutions. For all hydrophobic block compositions hydrogels with 800 g/mol hydrophobic segments absorbed less water than hydrogels with 400 g/mol hydrophobic segments. For PEG-PTMC-FAME/NVP hydrogels the difference in water uptake between the two segment lengths was largest. When PEG-PTMC-FAME/NVP and PEG-PDLLA-FAME/NVP hydrogels with the same hydrophobic block lengths are compared, it can be seen that the PEG-PTMC-FAME/NVP networks absorb more water. High molecular weight PTMC is slightly less hydrophobic than high molecular weight PDLLA due to the lower T_g [32] and PTMC oligomers with a molecular weight up to approximately 400 g/mol have even been shown to be water soluble [33]. It can therefore

be expected that in the PEG-PDLLA-FAME/NVP hydrogels better phase separation is obtained than in the PEG-PTMC-FAME/NVP hydrogels which may explain the difference in swelling. PEG-PDLLA/PTMC-FAME/NVP hydrogels with a 400 g/mol hydrophobic segment show swelling ratios in between those of the hydrogels with 400 g/mol PDLLA and PTMC blocks. PEG-PDLLA/PTMC-FAME/NVP hydrogels with a 800 g/mol hydrophobic block display swelling ratios similar to those of PEG-PTMC-FAME/NVP hydrogels with a 800 g/mol hydrophobic segment.

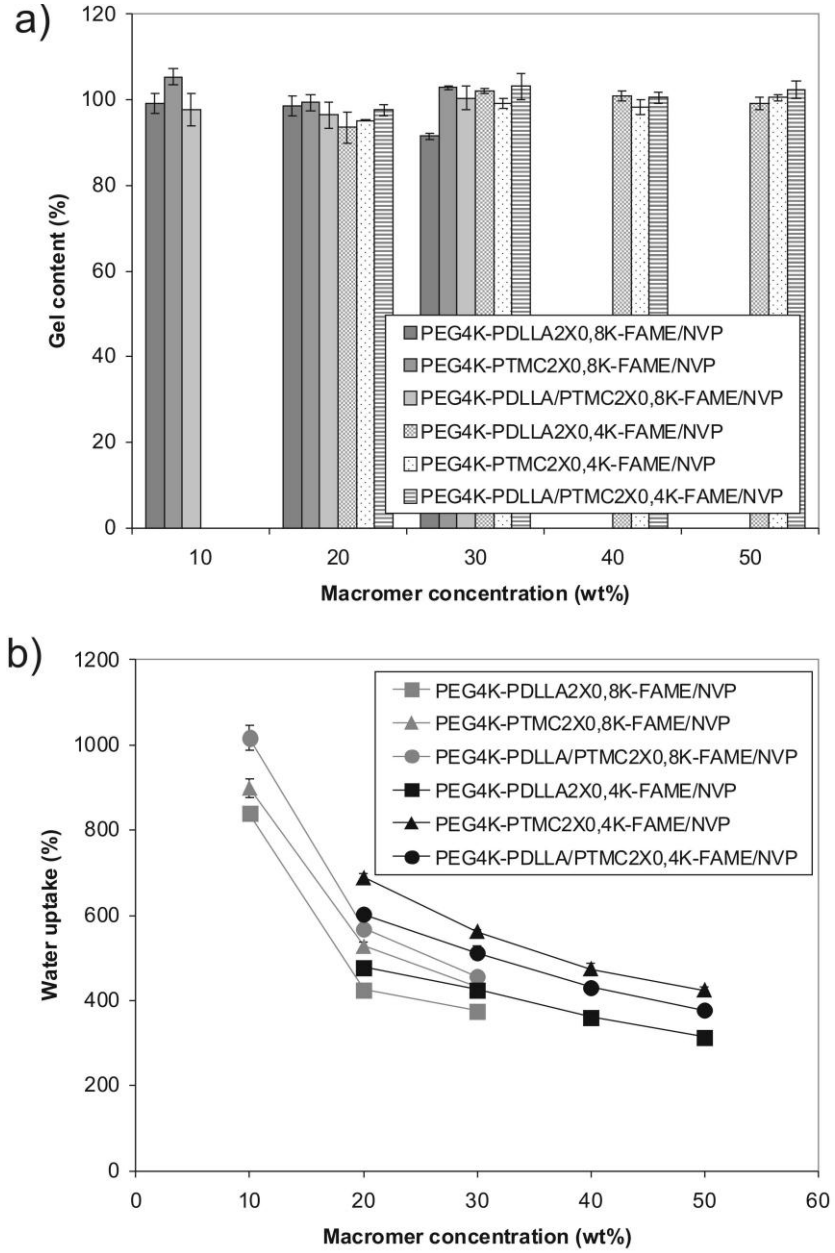

Figure 3. *Gel content (a) and water uptake (b) of PEG-PDLLA-FAME/NVP, PEG-PTMC-FAME/NVP and PEG-PDLLA/PTMC-FAME/NVP hydrogels.*

As all macromers could easily be dissolved and photo-crosslinked at a concentration of 30 wt%, hydrogels for further characterization and release studies were prepared from 30 wt% macromer solutions. The macromer concentration was kept constant to allow for comparison of hydrogels with different hydrophobic block compositions and lengths. It should be noted however, that Figure 3 illustrates that the macromer concentration can be used to tune hydrogel properties. In other studies it has been shown for example that hydrogel stiffness and protein release rates are influenced by the macromer concentration in the photo-crosslinked hydrogel [24].

It is known that PEG-PLA and PEG-PTMC block copolymers are thermosensitive [34, 35]. To study the thermosensitive behavior of the photo-crosslinked hydrogels prepared from these block copolymers, the water uptake of the gels prepared from 30 wt% macromer solutions was determined at different temperatures (Figure 4). For all the hydrogels prepared, water uptake decreased with increasing temperature. This is most likely caused by the decreasing solubility of PEG with increasing temperature [28]. For hydrogels with the shortest hydrophobic PDLLA or PTMC segments the dependence of the water uptake on temperature seems somewhat stronger (higher slope), most likely because of the higher PEG content. As was also shown in Figure 1; PEG-PTMC-FAME/NVP hydrogels take up more water than PEG-PDLLA-FAME/NVP hydrogels with the same length of the hydrophobic block. The swelling ratio of PEG4K-PDLLA/PTMC2X0.8K-FAME/NVP hydrogels is very similar to that of PEG4K-PTMC2X0.8K-FAME/NVP hydrogels, as was also shown in Figure 3.

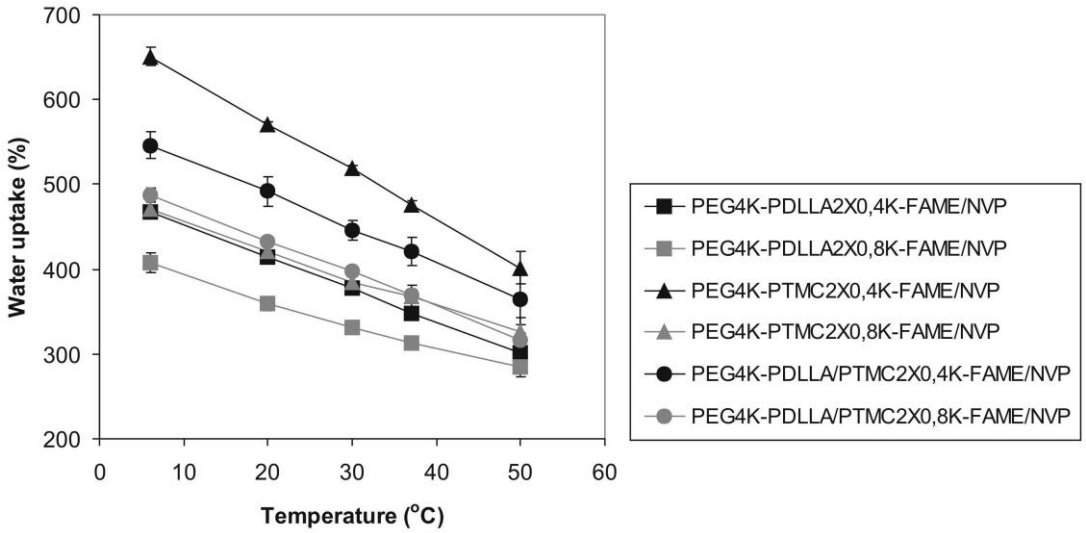

Figure 4. *Thermosensitive behavior of PEG-PDLLA-FAME/NVP, PEG-PTMC-FAME/NVP and PEG-PDLLA/PTMC-FAME/NVP hydrogels (prepared from 30 wt% macromer solutions in PBS).*

The mechanical properties of the hydrogels were studied by conducting rheology experiments at 37 ^{o}C. Stiff hydrogels with storage moduli varying from approximately 60 to 120 kPa were obtained (Table 3). The low loss moduli and low values of tan δ (G"/G') indicate that the hydrogels are highly elastic [36]. Although here we focus on the use of these hydrogels in protein delivery, they could also be interesting for application in tissue engineering. As it is known that the stiffness of a gel can significantly affect cell behavior [37] a system that can be optimized for a certain application is required. The stiffness of hydrogels presented here could be optimized for example by changing the macromer concentration in the crosslinked hydrogel or the block lengths or hydrophilic/hydrophobic ratio of the macromers.

Table 3. *Storage moduli (G'), loss moduli (G"), molecular weights between effective crosslinks (M_c) and mesh-sizes of PEG-PDLLA-FAME/NVP, PEG-PTMC-FAME/NVP and PEG-PDLLA/PTMC-FAME/NVP hydrogels (prepared from 30 wt% macromer solutions in PBS) after 1 d in PBS at 37 ^{o}C.*

	G' (kPa)	G" (kPa)	M_c (kg/mol)	Mesh-size (Å)
PEG4K-PDLLA2X0.4K-FAME/NVP	115 ± 4.4	3.04 ± 0.80	4.84 ± 0.15	89
PEG4K-PDLLA2X0.8K-FAME/NVP	107 ± 5.9	3.26 ± 0.68	5.56 ± 0.41	87
PEG4K-PTMC2X0.4K-FAME/NVP	69.5 ± 12.6	1.11 ± 0.22	6.29 ± 0.95	110
PEG4K-PTMC2X0.8K-FAME/NVP	93.5 ± 14.3	2.82 ± 0.89	6.35 ± 1.06	95
PEG4K-PDLLA/PTMC2X0.4K-FAME/NVP	63.8 ± 8.0	1.00 ± 0.33	7.20 ± 1.02	113
PEG4K-PDLLA/PTMC2X0.8K-FAME/NVP	59.3 ± 1.9	1.38 ± 0.29	6.63 ± 1.62	99

Among the gels with different hydrophobic block compositions, hydrogels with PDLLA blocks display the highest G' followed by the PTMC gels. The hydrogels with the PDLLA/PTMC copolymer hydrophobic blocks show the lowest stiffness. For the PEG-PTMC-FAME/NVP hydrogels a clear difference in G' can be observed for the two block lengths. The gels with the longer PTMC segments show the highest stiffness. For the hydrogels with PDLLA and PDLLA/PTMC copolymer hydrophobic blocks the differences between the hydrogels with different block lengths are small. These

observations are in agreement with the results from the swelling study where it was found that for PTMC the difference in swelling ratio between the different block lengths was higher than for the PDLLA and PDLLA/PTMC hydrogels.

The molecular weight between effective crosslinks was calculated from the measured storage moduli (Table 3). The calculated values range from 4.8 to 7.2 kg/mol, which is in agreement with the molecular weights of the macromers that were used to prepare the hydrogels (5.0 to 5.8 kg/mol). The hydrogel mesh-sizes were approximated from the molecular weight between crosslinks and the water uptake of the networks. The PEG-PDLLA-FAME/NVP hydrogels show the lowest molecular weights between effective crosslinks and the smallest mesh-sizes, which is in agreement with the low water uptake of these gels (Figure 3). The other four hydrogels all show somewhat higher, similar M_c values. For these hydrogels the mesh-sizes of the networks with 800 g/mol hydrophobic segments are somewhat smaller than the mesh-sizes of the networks with 400 g/mol hydrophobic segments.

To investigate the degradation of the hydrogels disk-shaped samples were incubated in PBS at 37 ^{o}C. At regular time intervals the mass of the swollen gels was determined and the swelling ratio calculated from this mass and the initial hydrogel mass after preparation. The results are summarized in Figure 5.

The degree of swelling did not change much as a function of time for the PEG-PTMC-FAME/NVP hydrogels, indicating no significant degradation at this time scale. This can be explained by the very slow *in vitro* degradation of PTMC [9]. The hydrolytic degradability of these hydrogels is shown by the fact that a PEG-PTMC-FAME/NVP hydrogel specimen immersed in a NaOH solution of pH 14 had dissolved completely within 1 d. For the PEG-PDLLA-FAME/NVP hydrogels the degree of swelling increased as a function of time. As the crosslink density decreases due to chain scission, the degree of swelling of the hydrogels increases. After 14 d the samples were too fragile to be weighed. The PEG-PDLLA/PTMC-FAME/NVP hydrogels displayed intermediate degradation behavior. These gels degrade faster than the PEG-PTMC-FAME/NVP gels, but slower than the PEG-PDLLA-FAME/NVP hydrogels.

These results clearly illustrate that by adjusting the composition of the hydrophobic blocks the degradation behavior of these photo-crosslinked hydrogels can be tuned. It should be noted that changing the molecular weight of the hydrophobic block has a limited effect on hydrogel degradation. For both the PEG-PDLLA-FAME/NVP and PEG-PDLLA/PTMC-FAME/NVP hydrogels similar degradation behavior is observed for the two different block lengths. These observations are in agreement with previous findings [7, 8], where it was shown that only large changes in the length of the hydrophobic

segments are able to significantly affect the degradation rate. The composition of the hydrophobic block is a more important factor.

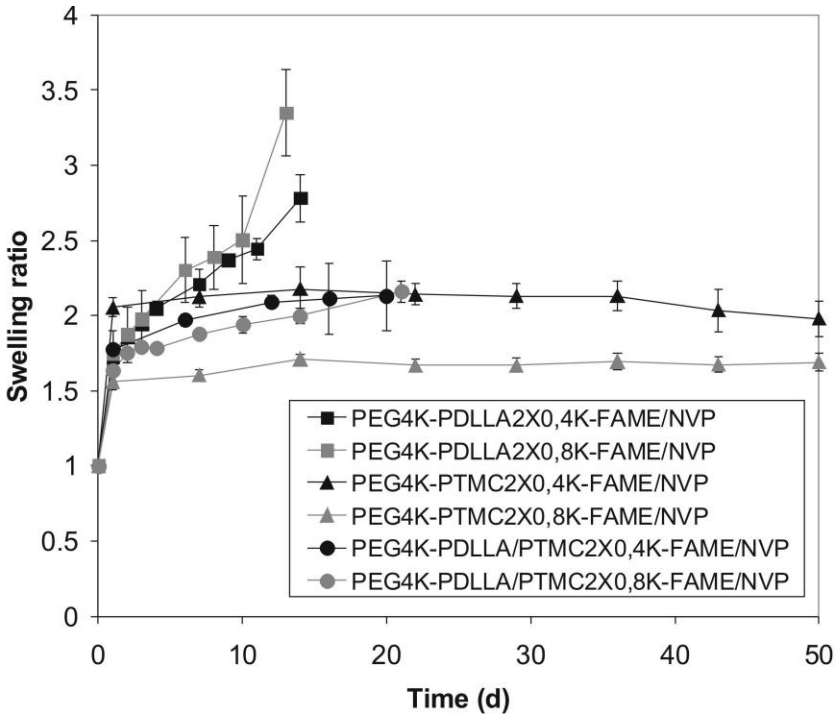

Figure 5. *Swelling ratio as a function of time for PEG-PDLLA-FAME/NVP, PEG-PTMC-FAME/NVP and PEG-PDLLA/PTMC-FAME/NVP hydrogels (prepared from 30 wt% macromer solutions in PBS).*

Protein release

The release of two model proteins, bovine serum albumin and lysozyme, from the prepared hydrogels was studied. The hydrogels could easily be loaded by mixing the proteins into the macromer solutions. The photo-initiator was dissolved in NVP and this solution was added to the macromer and protein solution in PBS prior to crosslinking. In case of albumin, precipitation of the protein was observed upon addition of NVP, implying that the protein was partly in the solid form during the photo-crosslinking reaction. Turbid, homogeneous dispersions were obtained. In case of lysozyme, no precipitation was observed. The results of the release studies are summarized in Figure 6 and Figure 7.

Albumin is released in a controlled and sustained way from the hydrogels and the initial burst release is very low, approximately 10 % (Figure 6). The PEG-PTMC-FAME/NVP hydrogels hardly show any degradation over the time scale of the release study (Figure 5) and the release of albumin from the PEG4K-PTMC2X0.4K-FAME/NVP hydrogel is diffusion controlled only (first-order kinetics, see insert in Figure 6). The release of

albumin from the more hydrophobic PEG4K-PTMC2X0.8K-FAME/NVP hydrogel is slower due to the lower swelling ratio of this gel. Apparently diffusion of albumin, a relatively large 66 kDa protein, in this hydrogel is restricted. The mesh-size calculated for the PEG4K-PTMC2X0.8K-FAME/NVP hydrogel is 95 Å (Table 3) which is close to the hydrodynamic diameter of albumin (72 Å). The mesh-size of the PEG4K-PTMC2X0.4K-FAME/NVP hydrogel was found to be 113 Å which explains why diffusion of albumin in this network is less restricted and release is faster.

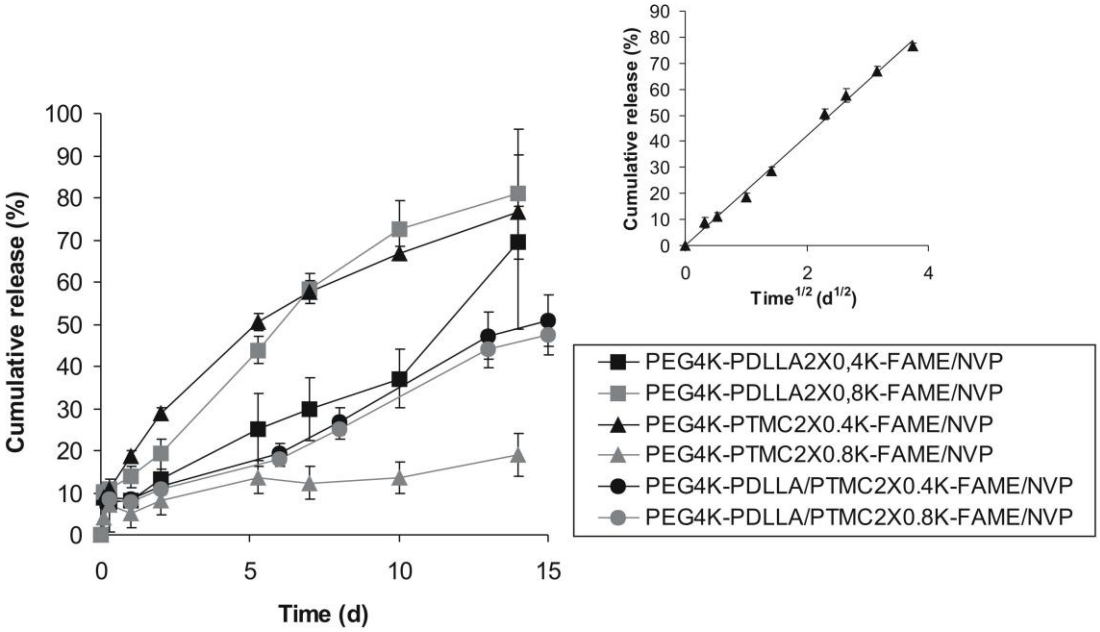

Figure 6. *Albumin release from PEG-PDLLA-FAME/NVP, PEG-PTMC-FAME/NVP and PEG-PDLLA/PTMC-FAME/NVP hydrogels (prepared from 30 wt% macromer solutions in PBS). The insert shows the cumulative release as a function of the square root of time for the PEG4K-PTMC2X0.4K-FAME/NVP hydrogels.*

The PEG-PDLLA-FAME/NVP and PEG-PDLLA/PTMC-FAME/NVP hydrogels do degrade over this time scale and therefore their release behavior is somewhat more complex (Figure 6), as both degradation and diffusion play a role here. Albumin is released slower from the PEG-PDLLA/PTMC-FAME/NVP hydrogels than from the PEG-PDLLA-FAME/NVP hydrogels. This is in agreement with the degradation behavior of the gels. The hydrogels with PDLLA segments degrade faster and show higher swelling ratios in time than the gels with PDLLA/PTMC segments (Figure 5). Albumin is released slightly faster from the PEG4K-PDLLA2X0.8K-FAME/NVP gels than from the PEG4K-PDLLA2X0.4K-FAME gels. Although these networks are more hydrophobic

and initially display a lower swelling ratio than the PEG4K-PDLLA2X0.4K-FAME/NVP hydrogels, degradation of these gels is somewhat faster (Figure 5) and therefore after a few days these gels have a larger swelling ratio than the gels with the short PDLLA block. For the hydrogels with PDLLA/PTMC hydrophobic segments the difference in albumin release rate is negligible for the two different segment lengths. These results demonstrate that for gels that do not degrade over the release period, the length of the hydrophobic segment can be used to control the release behavior. However, when the hydrogels do degrade over the release period, the composition of the hydrophobic block is much more important in controlling the release rates than the hydrophobic segment length.

Lysozyme is released from the hydrogels within 10 h (Figure 7). All hydrogels show similar release profiles. As lysozyme is a small protein (14 kDa, 41 Å) it can readily diffuse out of the hydrogels. The initial mesh-size of all hydrogels is much larger than the hydrodynamic diameter of lysozyme (Table 3) which explains why the protein can diffuse easily through these networks.

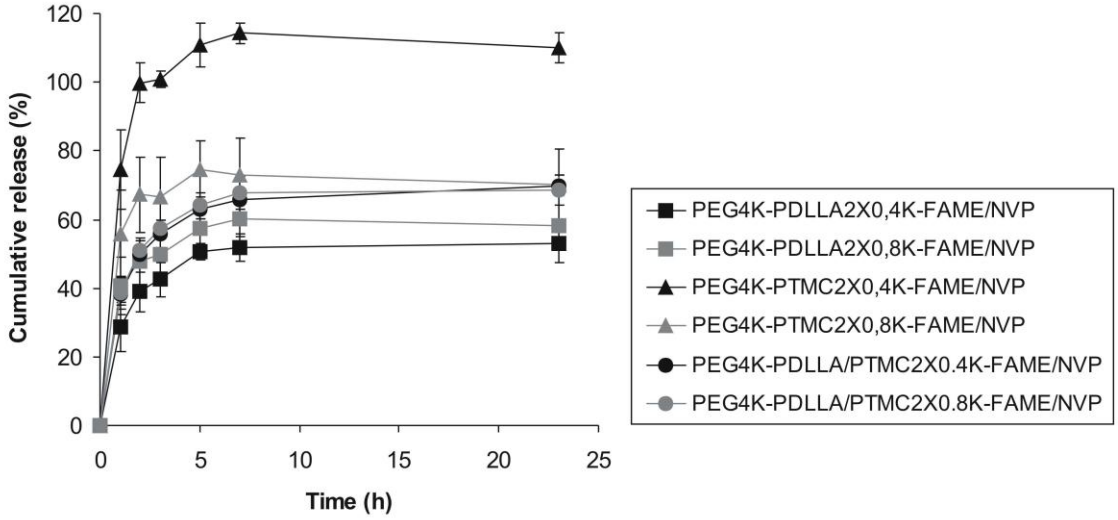

Figure 7. *Lysozyme release from PEG-PDLLA-FAME/NVP, PEG-PTMC-FAME/NVP and PEG-PDLLA/PTMC-FAME/NVP hydrogels (prepared from 30 wt% macromer solutions in PBS).*

Although all loaded lysozyme is released from the PEG4K-PTMC2X0.4K-FAME/NVP hydrogel, for all other hydrogel compositions lysozyme release is incomplete. A possible explanation may be that part of the lysozyme is conjugated to the polymer networks due the radical polymerization reaction [38]. As no precipitation of lysozyme was observed upon addition of the photo-initiator solution in NVP, lysozyme was in solution during the

polymerization reaction and side reaction with free radicals may have occurred. It might also be that lysozyme interacts with the network through hydrophobic or electrostatic interactions [39]. Lysozyme is a basic protein that is positively charged at neutral pH (isoelectric point at pH 11) and is known to adsorb to poly(lactic-co-glycolic acid) in PBS (pH 7.4) [40]. In contrast, albumin has an isoelectric point of 5.

The activity of the released lysozyme, determined using the *micrococcus lysodeikticus* assay, varied between 55 and 100 %. The loss in activity may again be caused by side reactions with the protein during radical polymerization or interaction of the protein with the matrix.

To obtain more insight in the role of the free radical polymerization in the incomplete lysozyme release, additional studies on the release of lysozyme from hydrogels prepared under different conditions were performed. For this the PEG4K-PDLLA2X0.4K-FAME/NVP hydrogel was used, as for this material the total release and lysozyme activity were lowest. The effects of the initiator type and concentration and the comonomer (NVP) concentration on total lysozyme release and activity were investigated (Table 4).

Table 4. *The effect of the type and amount of photo-initiator and the amount of NVP as a comonomer on the total amount of lysozyme and the activity of the lysozyme released from PEG4K-PDLLA2X0.4K-FAME/NVP hydrogels.*

Photo-initiator	Photo-initiatior concentration (wt%)	NVP content (wt%)	Total lysozyme release (%)	Lysozyme activity (%)
I2959	0.5	10	72.7 ± 2.3	70 ± 2
I2959	1	10	53.2 ± 5.9	57 ± 5
I2959	1	20	84.8 ± 2.9	73 ± 4
I651	1	10	89.4 ± 1.7	71 ± 0

By decreasing the photo-initiator concentration the free radical concentration is decreased, which may lead to less side reactions with lysozyme. The FAME end-groups are coupled to the hydrophobic segments of the macromer. This is why the radical polymerization is expected to take place in the hydrophobic domains. However, Irgacure 2959 is a relatively hydrophilic photo-initiator that is slightly water soluble. Free radicals are therefore also present in the hydrophilic phase were they can undergo side reactions with the protein. Irgacure 651 is a more hydrophobic photo-initiator that should stay in the hydrophobic phase and therefore limit the exposure of lysozyme to free radicals [38].

NVP copolymerizes with the fumarate end-groups in the radical polymerization reaction. It is known that if enough double bond-containing groups are present damage to proteins is limited [41]. Most likely the free radicals react rapidly with the double bonds instead of undergoing side reactions. It was therefore reasoned that a higher amount of NVP may lead to less side reactions with the protein. The complete release of lysozyme from PEG4K-PTMC0.4K-FAME/NVP (Figure 7) can be explained by a similar mechanism. As the PTMC blocks are quite short, it is likely that phase separation will no be extensive. Because of this, double bond-containing groups are present throughout the whole hydrogel thereby protecting the protein from side reactions with free radicals.

It was found that decreasing the initiator concentration, using a more hydrophobic initiator and increasing the NVP concentration all resulted in an increase of the total lysozyme release and lysozyme activity (Table 4). This supports the hypothesis that the limited lysozyme release and activity are related to the radical polymerization process. Especially increasing the NVP concentration and changing the initiator greatly increased the total amount of lysozyme released. The activity of the released lysozyme was increased to approximately 70 %.

Conclusion

Photo-crosslinked hydrogels were prepared from FAME-functionalized oligomers consisting of hydrophilic PEG segments and hydrophobic PTMC, PDLLA or PDLLA/PTMC copolymer segments. The degradation behavior and protein release profiles of the prepared hydrogels could be controlled by changing the composition of the hydrophobic segments. Albumin was released in a controlled way over a period of approximately 2 wk. Lysozyme release was much more rapid and incomplete. Careful optimization of photo-polymerization conditions can limit conjugation of proteins to the hydrogels and protein denaturation.

References

[1] N.A. Peppas, J.Z. Hilt, A. Khademhosseini, R. Langer, Hydrogels in biology and medicine: From molecular principles to bionanotechnology. Adv Mater 18(11) (2006) 1345-1360.

[2] W.E. Hennink, C.F. van Nostrum, Novel crosslinking methods to design hydrogels. Adv Drug Deliv Rev 54(1) (2002) 13-36.

[3] J. Elisseeff, K. Anseth, D. Sims, W. McIntosh, M. Randoplh, R. Langer, Transdermal photopolymerization for minimally invasive implantation. Proc Natl Acad Sci U S A 96 (1999) 3104-3107.

[4] K. Davis, Controlled release from crosslinked degradable networks. Crit Rev Ther Drug Carrier Syst 19(4-5) (2002) 385-423.

[5] N.E. Fedorovich, M.H. Oudshoorn, D. van Geemen, W.E. Hennink, J. Alblas, W.J.A. Dhert, The effect of photopolymerization on stem cells embedded in hydrogels. Biomaterials 30(3) (2009) 344-353.

[6] D.J. Quick, K.S. Anseth, DNA delivery from photocrosslinked PEG hydrogels: encapsulation efficiency, release profiles, and DNA quality. J Control Release 96(2) (2004) 341-351.

[7] A.S. Sawhney, C.P. Pathak, J.A. Hubbell, Bioerodible hydrogels based on photopolymerized poly(ethylene glycol)-co-poly(α-hydroxy acid) diacrylate macromers. Macromolecules 26(4) (1993) 581-587.

[8] J.L. West, J.A. Hubbell, Photopolymerized hydrogel materials for drug delivery applications. React Polym 25(2-3) (1995) 139-147.

[9] A.P. Pêgo, A.A. Poot, D.W. Grijpma, J. Feijen, In vitro degradation of trimethylene carbonate based (co)polymers. Macromol Biosci 2(9) (2002) 411-419.

[10] E. Bat, T.G. van Kooten, J. Feijen, D.W. Grijpma, Macrophage-mediated erosion of gamma irradiated poly(trimethylene carbonate) films. Biomaterials 30(22) (2009) 3652-3661.

[11] R. Chapanian, M.Y. Tse, S.C. Pang, B.G. Amsden, The role of oxidation and enzymatic hydrolysis on the in vivo degradation of trimethylene carbonate based photocrosslinkable elastomers. Biomaterials 30(3) (2009) 295-306.

[12] A.P. Pêgo, M.J.A. van Luyn, L.A. Brouwer, P.B. van Wachem, A.A. Poot, D.W. Grijpma, J. Feijen, In vivo behavior of poly(1,3-trimethylene carbonate) and copolymers of 1,3-trimethylene carbonate with D,L-lactide or ε-caprolactone: Degradation and tissue response. J Biomed Mater Res A 67A(3) (2003) 1044-1054.

[13] E. Bat, B.H.M. Kothman, G.A. Higuera, C.A. van Blitterswijk, J. Feijen, D.W. Grijpma, Ultraviolet light crosslinking of poly(trimethylene carbonate) for elastomeric tissue engineering scaffolds. Biomaterials 31(33) (2010) 8696-8705.

[14] C. Zhang, A. Aung, L.Q. Liao, S. Varghese, A novel single precursor-based biodegradable hydrogel with enhanced mechanical properties. Soft Matter 5(20) (2009) 3831-3834.

[15] H. Shin, J.S. Temenoff, A.G. Mikos, In vitro cytotoxicity of unsaturated oligo[poly(ethylene glycol) fumarate] macromers and their cross-linked hydrogels. Biomacromolecules 4(3) (2003) 552-560.

[16] D.W. Grijpma, Q. Hou, J. Feijen, Preparation of biodegradable networks by photo-crosslinking lactide, ε-caprolactone and trimethylene carbonate-based oligomers functionalized with fumaric acid monoethyl ester. Biomaterials 26(16) (2005) 2795-2802.

[17] J. Jansen, M.J. Boerakker, J. Heuts, J. Feijen, D.W. Grijpma, Rapid photo-crosslinking of fumaric acid monoethyl ester-functionalized poly(trimethylene carbonate) oligomers for drug delivery applications. J Control Release 147(1) (2010) 54-61.

[18] J. Heller, R.F. Helwing, R.W. Baker, M.E. Tutte, Controlled release of water-soluble macromolecules from bioerodible hydrogels. Biomaterials 4(4) (1983) 262-266.

[19] L.J. Suggs, E.Y. Kao, L.L. Palombo, R.S. Krishnan, M.S. Widmer, A.G. Mikos, Preparation and characterization of poly(propylene fumarate-co-ethylene glycol) hydrogels. J Biomater Sci Polym Ed 9(7) (1998) 653-666.

[20] A.S. Sarvestani, W. Xu, X. He, E. Jabbari, Gelation and degradation characteristics of in situ photo-crosslinked poly(L-lactide-co-ethylene oxide-co-fumarate) hydrogels. Polymer 48(24) (2007) 7113-7120.

[21] Q. Hou, D.W. Grijpma, J. Feijen, Preparation of hydrogels by photo-crosslinking of fumaric acid monoethyl ester (FAME) functionalized oligomers. J Control Release 101(1-3) (2005) 335-337.

[22] A. Hassner, V. Alexanian, Direct room temperature esterification of carboxylic acids. Tetrahedron Lett 19 (1978) 4475-4478.

[23] T.K.L. Meyvis, S.C. De Smedt, J. Demeester, W.E. Hennink, Rheological monitoring of long-term degrading polymer hydrogels. J Rheol 43(4) (1999) 933-950.

[24] R. Censi, T. Vermonden, M.J. van Steenbergen, H. Deschout, K. Braeckmans, S.C. De Smedt, C.F. van Nostrum, P. di Martino, W.E. Hennink, Photopolymerized thermosensitive hydrogels for tailorable diffusion-controlled protein delivery. J Control Release 140(3) (2009) 230-236.

[25] L.R.G. Treloar, Elasticity and related properties of rubbers. Rep Prog Phys 36(7) (1973) 755-826.

[26] T. Canal, N.A. Peppas, Correlation between mesh size and equilibrium swelling of polymeric networks J Biomed Mater Res 23(10) (1989) 1183-1193.

[27] S. Lu, K.S. Anseth, Release behavior of high molecular weight solutes from poly(ethylene glycol)-based degradable networks. Macromolecules 33(7) (2000) 2509-2515.

[28] J. Brandrup, E.H. Immergut, A. Abe, D.R. Bloch, Polymer Handbook, Wiley-Interscience New York, 1999.

[29] E.W. Merrill, K.A. Dennison, C. Sung, Partitioning and diffusion of solutes in hydrogels of poly(ethylene oxide). Biomaterials 14(15) (1993) 1117-1126.

[30] P.K. Smith, R.I. Krohn, G.T. Hermanson, A.K. Mallia, F.H. Gartner, M.D. Provenzano, E.K. Fujimoto, N.M. Goeke, B.J. Olson, D.C. Klenk, Measurement of protein using bicinchoninic acid. Anal Biochem 150(1) (1985) 76-85.

[31] P. Shih, B. Malcolm, S. Rosenberg, J. Kirch, A. Wilson, Reconstruction and testing of ancestral proteins. Methods Enzymol 224 (1993) 576-590.

[32] A.P. Pego, A.A. Poot, D.W. Grijpma, J. Feijen, Physical properties of high molecular weight 1,3-trimethylene carbonate and D,L-lactide copolymers. J Mater Sci Mater Med 14(9) (2003) 767-773.

[33] Z. Zhang, R. Kuijer, S.K. Bulstra, D.W. Grijpma, J. Feijen, The in vivo and in vitro degradation behavior of poly(trimethylene carbonate). Biomaterials 27(9) (2006) 1741-1748.

[34] B. Jeong, Y.H. Bae, D.S. Lee, S.W. Kim, Biodegradable block copolymers as injectable drug-delivery systems. Nature 388(6645) (1997) 860-862.

[35] S.Y. Kim, H.J. Kim, K.E. Lee, S.S. Han, Y.S. Sohn, B. Jeong, Reverse thermal gelling PEG-PTMC diblock copolymer aqueous solution. Macromolecules 40(15) (2007) 5519-5525.

[36] K.S. Anseth, C.N. Bowman, L. BrannonPeppas, Mechanical properties of hydrogels and their experimental determination. Biomaterials 17(17) (1996) 1647-1657.

[37] S. Nemir, J. West, Synthetic materials in the study of cell response to substrate rigidity. Ann Biomed Eng 38(1) (2010) 2-20.

[38] C.-C. Lin, S.M. Sawicki, A.T. Metters, Free-radical-mediated protein inactivation and recovery during protein photoencapsulation. Biomacromolecules 9(1) (2007) 75-83.

[39] M. van de Weert, W.E. Hennink, W. Jiskoot, Protein instability in poly(lactic-co-glycolic acid) microparticles. Pharm Res 17(10) (2000) 1159-1167.

[40] G. Jiang, B.H. Woo, F. Kang, J. Singh, P.P. DeLuca, Assessment of protein release kinetics, stability and protein polymer interaction of lysozyme encapsulated poly(lactide-co-glycolide) microspheres. J Control Release 79(1-3) (2002) 137-145.

[41] F. Gu, R. Neufeld, B. Amsden, Maintenance of vascular endothelial growth factor and potentially other therapeutic proteins bioactivity during a photo-initiated free radical cross-linking reaction forming biodegradable elastomers. Eur J Pharm Biopharm 66(1) (2007) 21-27.

Chapter 7

Controlling the kinetic chain length of the crosslinks in photo-polymerized biodegradable networks

Janine Jansen[1], Abdul Ghaffar[2,3], Thomas N.S. van der Horst[1], George Mihov[4], Sjoerd van der Wal[2,5], Jan Feijen[6] and Dirk W. Grijpma[1,7]

1) MIRA Institute for Biomedical Technology and Technical Medicine, Department of Biomaterials Science and Technology, Faculty of Science and Technology, University of Twente, P.O. Box 217, 7500 AE, Enschede, The Netherlands
2) Van't Hoff Institute for Molecular Sciences, Polymer-Analysis Group, University of Amsterdam, P.O. Box 94157, 1090 GD, Amsterdam, The Netherlands
3) Department of Chemistry, University of Engineering and Technology, Lahore, Pakistan.
4) DSM Ahead, P.O Box 18, 6160 MD, Geleen, The Netherlands
5) DSM Resolve R&D solutions, P.O Box 18, 6160 MD, Geleen, The Netherlands
6) MIRA Institute for Biomedical Technology and Technical Medicine, Department of Polymer Chemistry and Biomaterials, Faculty of Science and Technology, University of Twente, P.O. Box 217, 7500 AE, Enschede, The Netherlands
7) W.J. Kolff Institute, Department of Biomedical Engineering, University Medical Center Groningen, University of Groningen, Antonius Deusinglaan 1, 9713 AV, Groningen, The Netherlands

Abstract

Biodegradable polymer networks were prepared by photo-initiated radical polymerization of methacrylate functionalized poly(D,L-lactic acid) oligomers. The kinetic chains formed in this radical polymerization are the multifunctional crosslinks of the networks. These chains are carbon-carbon chains that remain after degradation. If their molecular weight is too high these poly(methacrylic acid) chains can not be excreted by the kidneys. The effect of the photo-initiator concentration and the addition of 2-mercaptoethanol as a chain transfer agent on the molecular weight of the kinetic chains was investigated. It was found that both increasing the initiator concentration and adding 2-mercaptoethanol decrease the kinetic chain length. However, the effect of adding 2-mercaptoethanol was much larger. A small amount of 2-mercaptoethanol is enough to decrease the kinetic chain length significantly. Some network properties such as the glass transition temperature and the swelling ratio in acetone are affected when the kinetic chain length is decreased.

Introduction

Photo-crosslinked biodegradable polymer networks are an interesting class of materials for biomedical applications, as photo-crosslinking is rapid and can be accomplished with minimal heat generation. Spatial and temporal control over the polymerization process allow for the fabrication of polymer matrices with complex shapes [1]. A wide range of substances and even cells can be entrapped in the networks [2]. Because of these advantageous characteristics, these materials have been studied frequently for application in drug delivery devices [3] and as scaffolding materials for tissue engineering [4].

Biodegradable polymer networks can be prepared by the photo-initiated crosslinking of (end-)functionalized degradable oligomers. Methacrylate derivatives have been most frequently used in functionalization reactions, although fumaric acid derivatives can also be attractive compounds for end-functionalization [5]. A network is formed through photo-initiated polymerization of the end-groups via an addition type polymerization reaction. The formed chains, also called kinetic chains, are carbon-carbon chains that remain present after degradation of the network. The size and character of these chains determine whether they can be removed from the body by renal clearance [6]. Water-soluble polymers with molecular weights up to 50 kg/mol are cleared by the kidneys within a few days [7, 8], while polymers with molecular weights over 200 kg/mol accumulate in the circulatory system and are not excreted by the kidneys [9, 10].

The kinetic chains in photo-crosslinked polymer networks have been the subject of a number of studies. The insoluble nature of the networks complicates these studies. Often

the networks are first degraded and the degradation products can then be characterized using different methods. For example, Burkoth and Burdick *et al*. [11, 12] analyzed the degradation products of their dimethacrylated sebacic acid networks using MALDI-TOF MS (matrix assisted laser desorption ionization – time of flight mass spectrometry) and GPC (gel permeation chromatography) to determine the kinetic chain length. Peters *et al*. [13] analyzed the degradation products of poly(ethylene glycol)-diacrylate (PEG-diacrylate) 2-ethylhexyl mono-acrylate copolymer networks using GPC to determine the kinetic chain length. Recently Ghaffar *et al*. [14] investigated the degradation products of polyester urethane acrylate networks in a similar manner. In another recent study Melchels *et al*. [15] used a different approach and determined the kinetic chain length of poly(D,L-lactic acid)-methacrylate (PDLLA-MA) networks by HR-MAS NMR (high resolution magic angle spinning nuclear magnetic resonance) analysis of solvent swollen networks.

As water soluble polymers that exceed a critical molecular weight can accumulate in the body, it is of great importance that the kinetic chain length of these networks can not only be measured, but can also be controlled and reduced. The kinetics of photo-crosslinking reactions are very complex [16] and therefore it is difficult to accurately predict the kinetic chain length [17]. However, several factors are known to affect the kinetic chain length in photo-initiated addition polymerizations. An increased initiation rate results in a decrease in the kinetic chain length [11, 12]. In photo-polymerization reactions the initiation rate can be increased by increasing the initiator concentration or the light intensity. Another parameter that can decrease the kinetic chain length is chain transfer [17, 18]. Thiols are very effective transfer agents, because of the labile S-H bond. In chain transfer to a thiol, the carbon-based radical on the growing chain abstracts a hydrogen atom from a thiol functional group to generate a thiyl radical. Rydholm *et al*. [17] prepared networks by reacting acrylates with thiols with different functionalities and have shown that an increase in thiol functional group concentration decreases the kinetic chain length.

While Rydholm *et al*. investigated the diverse properties of their very interesting family of network materials prepared with thiols with different functionalities, in this study our aim is to develop a practical general method, employing a mono-functional thiol, to control the kinetic chain length of photo-polymerized networks without altering other network properties to a large extent. The kinetic chain lengths of the multifunctional crosslinks of PDLLA-MA networks were investigated. The effect of the photo-initiator concentration and 2-mercaptoethanol as a transfer agent on the kinetic chain length was studied. 2-Mercaptoethanol was selected as a transfer agent since it is an antioxidant and

is frequently used in cell culture as a medium supplement [19]. The effect of decreasing the kinetic chain length on different network properties was studied.

Materials and methods

Materials

D,L-lactide was obtained from Purac Biochem (The Netherlands). Tin 2-ethylhexanoate ($Sn(Oct)_2$), trimethylol propane (TMP), glycerol, methacrylic anhydride, 5,5′-dithiobis (2-nitrobenzoic acid) (Ellman's reagent), N-methyl dibenzopyrazine methylsulfate (PMS), deuterated chloroform, trypsin and penicillin-streptomycin solution were purchased from Sigma Aldrich (U.S.A). Triethylamine (TEA) was obtained from Fluka (Switzerland). Irgacure 2959 (2-hydrox-1-[4-(2-hydroxyethoxy)phenyl]-2-methyl-1-propanone) was obtained from Ciba Specialty Chemicals (Switzerland). 2-Mercaptoethanol was purchased from Acros (Belgium). Phosphate buffered saline (PBS) was obtained from B. Braun (Germany). Deuterated methanol was obtained from Euriso-top (France). Dulbecco's modified Eagle's medium (DMEM) was purchased from Invitrogen (U.S.A.). XTT (2,3-bis-(2-methoxy-4-nitro-5-sulfophenyl)-2H-tetrazolium-5-carboxanilide) was obtained from Polysciences (U.S.A.). KOH was purchased from Merck (Germany). Newborn calf serum (NCS) was obtained from Lonza (Switzerland). Analytical grade dichloromethane (DCM) was obtained from Biosolve (The Netherlands). DCM was dried over CaH_2 and distilled. Other solvents were of technical grade and were used as received (Biosolve, the Netherlands).

Synthesis of star-shaped MA-functionalized PDLLA oligomers

Three-armed poly(D,L-lactide) oligomers were synthesized by ring opening polymerization of D,L-lactide in the presence of trimethylol propane or glycerol as a trifunctional initiator. D,L-lactide, TMP and $Sn(Oct)_2$ (approximately 0.2 mmol/mol monomer) as a catalyst were reacted in the melt at 130 °C for 48 h under argon. The monomer-to-initiator ratio was adjusted to yield oligomers with a targeted molecular weight of 1000 g/mol per arm and a total molecular weight of 3100 g/mol. The oligomers were functionalized with methacrylate end-groups by reacting methacrylic anhydride (MAAH) with the hydroxyl end-groups of the oligomers. An amount of oligomer was charged into a three-necked flask and dried for 2 h at 110 °C *in vacuo* and then cooled to room temperature under argon. The oligomer was dissolved in dry DCM and TEA was added. Methacrylic anhydride was added drop-wise to the vigorously stirred oligomer solution. Per mol of hydroxyl groups 1.2 moles of MAAH and TEA were used. The

coupling reaction was continued for 3 d. The macromers were purified by precipitation in cold isopropanol, washing with water and freeze-drying.
The oligomer molecular weights (M_n) and the degrees of functionalization were determined from ^{1}H-NMR spectra (Varian Inova 300 MHz NMR spectrometer). Deuterated chloroform was used as a solvent.

Photo-crosslinking of PDLLA-MA macromers

The macromers were dissolved in dichloromethane (1g/ml) and different amounts of Irgacure 2959 photo-initiatior and 2-mercaptoethanol were added. Three different initiatior concentrations were used: 0.2, 1 and 3 wt% (all with respect to macromer, corresponding to 1, 5 and 15 mol% with respect to the methacrylate end-groups). Five different 2-mercaptoethanol concentrations were used: 0.4, 0.7, 1.4, 2.9 and 5.8 wt% (all with respect to macromer, corresponding to 5, 10, 20, 40 and 80 mol% with respect to the methacrylate end-groups). These five solutions all contained 1 wt% photo-initiator. The macromer solutions were poured into Teflon moulds, covered with FEP (fluorinated ethylene propylene) foil and crosslinked for 15 min in an Ultralum crosslinking cabinet (365 nm, 3-5 mW/cm^2). Disked-shaped specimens with a diameter of approximately 10 mm and thickness of approximately 0.5 mm were obtained.
The specimens were dried overnight at 90 ^{o}C under a nitrogen flow. Specimens that were extracted for the studies on cytocompatibility and unreacted thiol concentrations were not dried at elevated temperature (see below).

Network degradation and analysis of the kinetic chains

Approximately 10 mg of each network specimen was immersed in 1 ml of 1 M KOH in a 10 ml glass vial which was internally lined with PTFE (poly(tetrafluoroethylene)). The mixture was then hydrolyzed at 120 ^{o}C, 3 bar for 20 h in a microwave instrument (Discover BenchMate, CEM).
After hydrolysis 1 mL of each hydrolyzed sample was acidified with 200 µL of 37 % HCl at 90 ^{o}C for a few minutes. The PMAA (poly(methacrylic acid)) precipitate and the supernatant (containing lactic acid, TMP, etc.) were dried overnight at 40 ^{o}C under an air flow. The dried hydrolysates (both precipitate and supernatant together) were re-dissolved in deuterated methanol. Samples of partially-hydrolyzed networks (hydrolyzed in 1 M KOH at room temperature) and networks hydrolyzed for 10 h in the microwave setup were also dissolved in deuterated methanol. ^{1}H-NMR spectra were recorded on a Bruker Avance 400 MHz NMR spectrometer.

For GPC analysis 0.2 ml of the hydrolyzed sample was diluted with 0.2 ml of the mobile phase (see below) and then the samples were neutralized (pH 7.4) with a few drops of 37 % HCl. The samples were filtered through a PTFE (0.45 µm) filter prior to injection.
The GPC experiments were performed on an HPLC (high performance liquid chromatography) system equipped with an in-line degasser, Model 600 pump, 717 plus TRI-SEC auto-sampler and Model 410 differential refractive index detector at 40 ^{o}C (all Waters).
The GPC separations were performed on PL aquagel-OH Guard (8µm, 50 × 7.5mm), PL aquagel-OH 50, 30 and 10 (each 8 µm, 300 × 7.5 mm) columns connected in series. The column oven temperature was adjusted to 45 ^{o}C. The mobile phase (0.2 M $NaNO_3$, 0.01 M NaH_2PO_4, pH ~ 7.0) was pumped at a flow rate of 1.0 ml/min. Narrow molecular weight poly(methacrylic acid) sodium salt (PMAA-Na) standards (M_p (the peak value of the molecular weight distribution) varying from 1.22×10^3 to 549×10^3 g/mol) were used to calibrate the GPC-dRI system. Data were recorded and chromatographic peaks were treated using the Empower 2 software (Waters). Calculations for the molar mass distribution (MMD) on the chromatographic peaks were executed using software written in-house in Excel 2003 (Microsoft). Highly pure water for mobile phase preparation was obtained by means of an Arium 611 Ultrapure (18.2 MΩ×cm) Water System (Sartorius AG).
Several low molecular weight GPC fractions were collected for analysis by MALDI-TOF MS. MALDI-TOF was performed using a Voyager-DE-RP MALDI-TOF spectrometer (Applied Biosystems) equipped with delayed extraction. A 337 nm UV nitrogen laser producing 2 ns pulses was used. Sinapinic acid was used as the matrix material and negative ions were detected. Collected GPC fractions were protonated with concentrated hydrochloric acid and dried. MALDI-TOF samples were prepared by dissolving the degradation products in a 50:50 mixture of acetonitrile and water containing 0.1 vol% TFA (trifluoroacetic acid) and mixing with the matrix material (approximately 1:1 sample to matrix ratio by volume).

Network characterization

To determine the gel content and swelling ratio in acetone, a network specimen (n=3) was weighed (m_0), swollen and extracted in acetone and weighed again (m_s). Then the specimen was dried at 90 ^{o}C under a nitrogen flow until constant weight. The mass of the dry network (m_1) was determined. Gel content is defined as:

$$\text{Gel content} = \frac{m_1}{m_0} \times 100\%$$

The swelling ratio was calculated using:

$$\text{Swelling ratio} = \frac{m_s}{m_0}$$

The thermal properties of the networks were evaluated using a Perkin-Elmer Pyris 1 differential scanning calorimeter (DSC). Samples were heated from 0 to 100 °C at a heating rate of 10 °C/min, quenched rapidly at 300 °C/min to 0 °C, and then a second heating scan was recorded after 5 min. The glass transition temperature (T_g) was taken as the midpoint of the heat capacity change in the second heating run.

To study degradation of the different PDLLA-MA networks, disk-shaped specimens (diameter = 10 mm, thickness = 0.5 mm) were immersed in 2 ml PBS containing 0.02 wt% NaN_3 as a bactericide. At different time points wet mass, dry mass, swelling ratio in acetone and gel content were determined. At a certain time point four specimens were taken out. Two specimens were weighed to determine the wet mass, dried at 90 ^oC under a nitrogen flow until constant weight, and then weighed again to determine the dry mass. Two other samples were swollen and extracted in acetone for 1 d, weighed to determine the swollen mass (m_s), and then dried and weighed again (m_1). All samples were also weighed prior to the degradation experiment (m_0). Swelling ratio and gel content were calculated as described above. The PBS was refreshed every 2 to 3 wk.

Ellman's reagent was used to determine the 2-mercaptoethanol concentrations in networks extracts [20]. Disk-shaped network specimens were extracted in PBS for 24 h directly after crosslinking. 100 µl of the network extracts and 100 µl of a 300 µM 5,5′-dithiobis(2-nitrobenzoic acid) solution in PBS were mixed in a 96 well plate. A 340 ATTC plate reader (SLT) was used to measure the absorption at a wavelength of 404 nm. A calibration curve was constructed using 2-mercaptoethanol.

Cytocompatibility of network extracts

Disk-shaped PDLLA-MA network specimens were dried at room temperature under vacuum for 2 d. The materials were disinfected in 70 % isopropanol (2×15 min) and washed with PBS (2×15 min). Samples were then extracted with serum free culture medium ((DMEM), 1 ml per 3 cm^2 surface area) at 37 °C for 24 h. The supernatants were

stored at −20 °C until further use. NIH 3T3 fibroblasts were cultured in T75 cell culture flasks in DMEM medium supplemented with 10 % newborn calf serum and 1 % penicillin/streptomycin. The cells were cultured for 1 d at 37 °C in a 5 % CO_2 atmosphere, trypsinized, and redispersed in medium (15×10^4 cells/ml). Cells were then seeded in 96 well tissue culture polystyrene (TCPS) plates at a density of 15×10^3 cells per well and cultured for 1 d. Then the medium was aspirated from the wells, and 50 μl of extract was added to the cells (n=3), followed by 50 μl of culture medium containing 20 % NCS. Normal culture medium (containing 10 % NCS) and 50 % v/v DMSO (dimethylsulfoxide) were used as controls. The cells were cultured at 37 °C, in a 5 % CO_2 atmosphere for 1 d. The metabolic activity of the cells was analyzed using the XTT assay. The medium was aspirated from the cells and replaced by 100 μl of fresh colorless medium and 50 μl of XTT solution (containing 1 mg/ml XTT and 0.38 mg/ml PMS). After 1 h of incubation, the absorbance was read on a 340 ATTC plate reader (SLT) at 450 nm with a reference wavelength of 620 nm.

Results and discussion

Synthesis and characterization of MA-functionalized PDLLA oligomers

Three-armed PDLLA oligomers were prepared by ring opening polymerization of D,L-lactide with a trifunctional initiatior. The obtained molecular weight, determined from the initiator to lactide ratio in ^{1}H-NMR spectra, was 3.4 kg/mol which is close to the intended molecular weight of 3.1 kg/mol.

The PDLLA oligomers were functionalized with methacrylate end-groups through reaction with methacrylic anhydride to obtain crosslinkable macromers (PDLLA-MA). The successful functionalization was confirmed by the appearance of the $=CH_2$, and $-CH_3$ peaks of the methacrylate at δ 5.65 and δ 6.21, and at δ 1.97 in ^{1}H-NMR spectra. The obtained degree of functionalization calculated from the $-CH_3$ of the methacrylate peak at δ 1.97 and the $-CH_3$ of TMP at δ 0.89 was 93 %.

Kinetic chains

PDLLA-MA networks were prepared by photo-polymerization of the synthesized macromers (Figure 1). The amount of photo-initiator and 2-mercaptoethanol, used as a transfer agent, were varied to investigate the effect on the kinetic chain length. It was anticipated that increasing the photo-initiator concentration and adding 2-mercaptoethanol would decrease the kinetic chain length of the networks.

2-Mercaptoethanol is an effective transfer agent because of the labile S-H bond it contains (Figure 2).

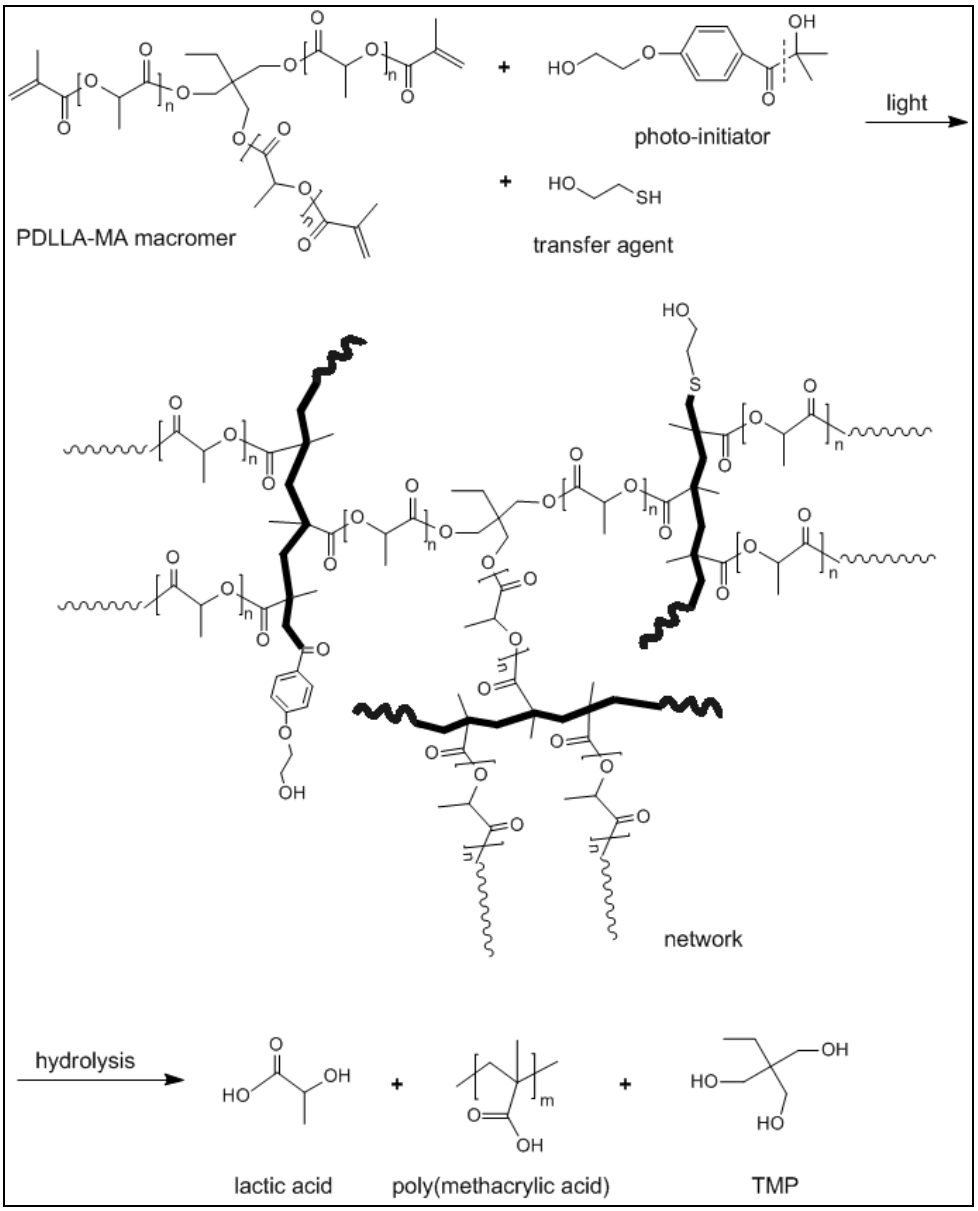

Figure 1. *Network formation and hydrolysis.*

To optimize the hydrolysis method the prepared networks were degraded in 1 M KOH at room temperature and for 10 and 20 h at 120 ^{o}C in a microwave instrument [14]. NMR spectroscopy was used to distinguish between lactic acid units attached to the poly(methacrylic acid) backbone and lactic acid units present in solution in the form of free lactic acid and oligomers.

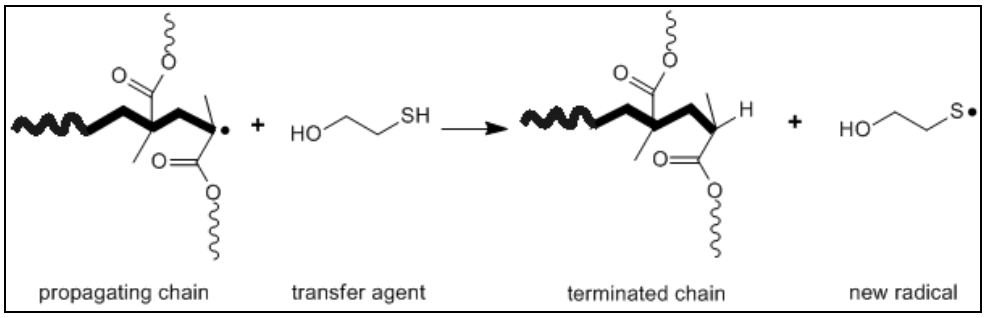

Figure 2. *Chain transfer to 2-mercaptoethanol.*

The overlay of ^{1}H-NMR spectra of the three-armed PDLLA oligomers and partially and fully hydrolyzed PDLLA-MA networks (Figure 3) shows clearly the cleavage of ester bonds as the degradation temperature and time increased. In case of the PDLLA oligomers (Figure 3a) peaks 4 and 5 belong to the CH protons of lactic acid, while peak 3 belongs to the methyl protons of lactic acid. The peaks 1 and 2 correspond to glycerol which was used as the initiator for the ring opening polymerization.

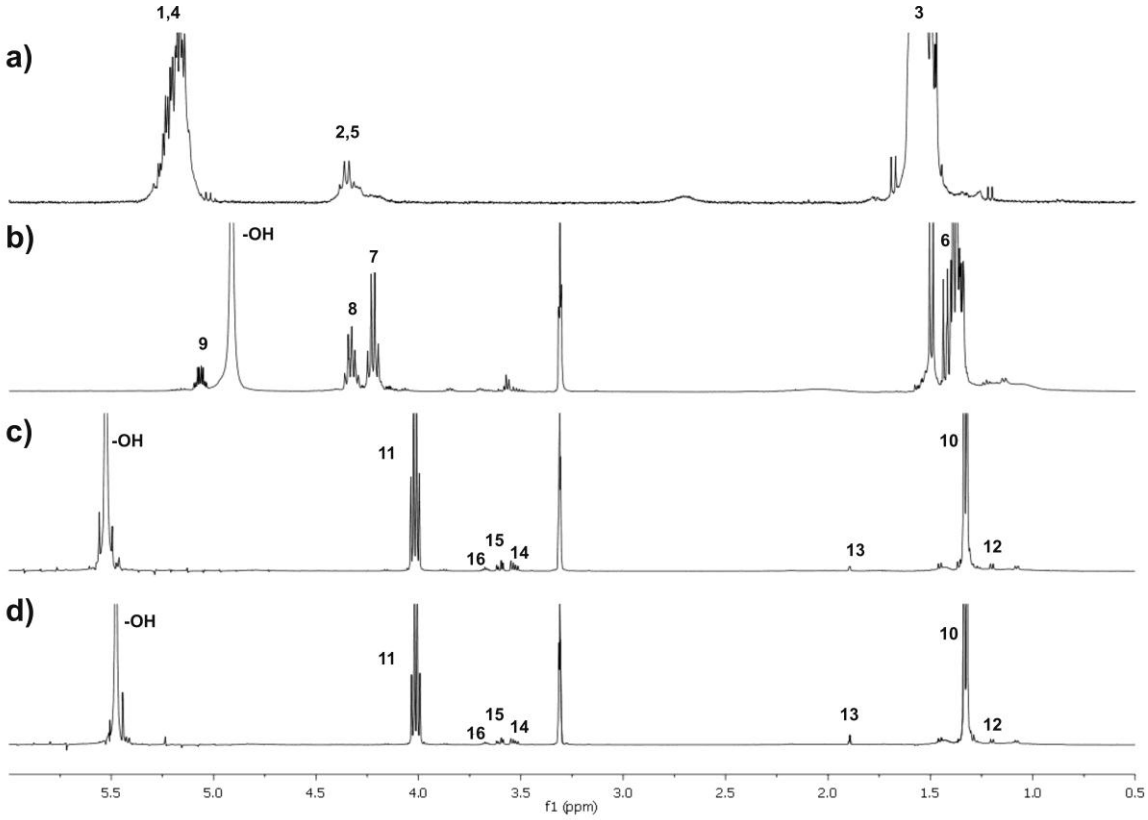

Figure 3. *An overlay of ^{1}H-NMR spectra (in d-chloroform (a) and d_4-methanol (b-d)) of the three-armed PDLLA oligomer (a), PDLLA-MA networks partially hydrolyzed at room temperature for two weeks (b) and PDLLA-MA networks hydrolyzed for 10 (c) and 20 h (d) in a microwave instrument.*

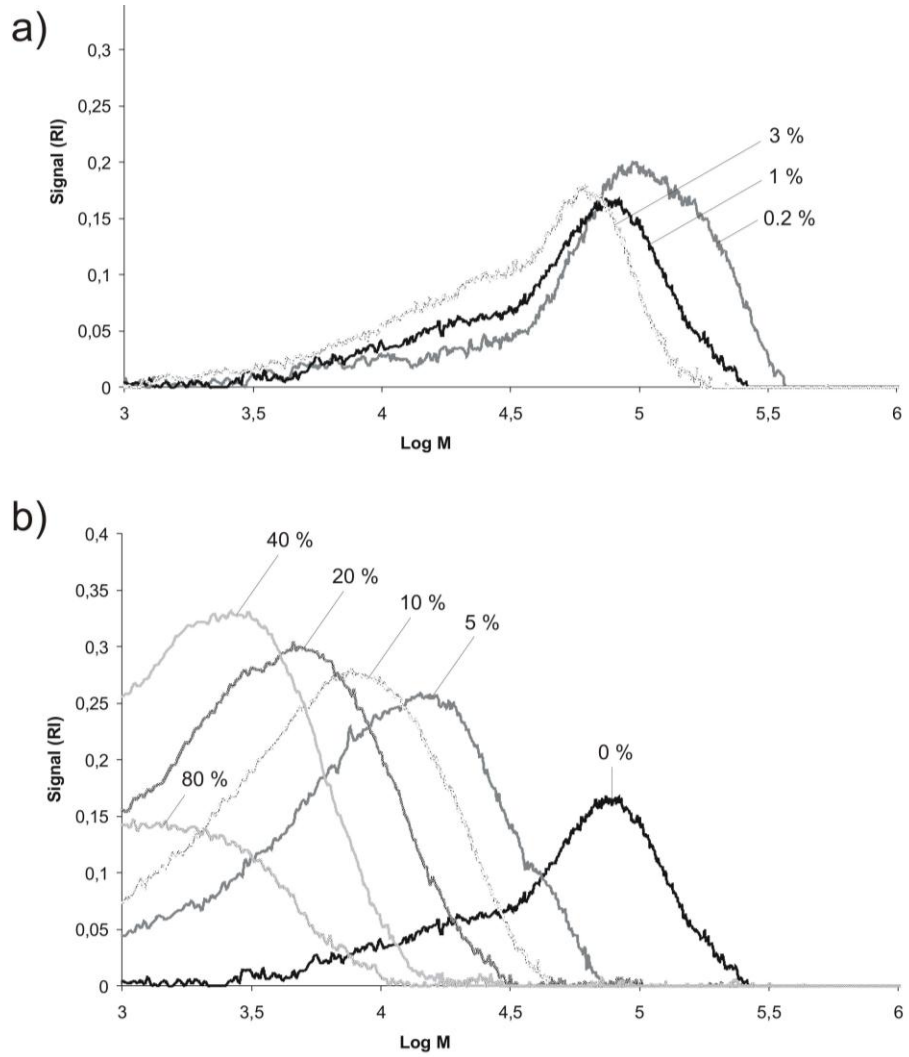

Figure 4. *GPC analysis of the products of microwave hydrolysis of PDLLA-MA networks prepared with different photo-initiator concentrations (a) and different 2-mercaptoethanol concentrations (b). Photo-initiator concentrations are indicated in weight percent with respect to macromer. 2-Mercaptoethanol concentrations are given in mole percent with respect to the methacrylate end-groups.*

In case of partially degraded networks (Figure 3b) peak 9 represents the CH group of lactic acid that is still attached to the methacrylate backbone, while peaks 7 and 8 represent free lactic acid (CH group) oligomers in the hydrolysis solution. Peak 6 represents different CH_3 groups of lactic acid units either attached to the methacrylate backbone or present as free monomers or oligomers in the hydrolysis solution. However hydrolysis at an elevated temperature and pressure (120 ^{o}C for 10 and 20 h, 3 bars) (Figure 3c and d) clearly shows only peak 11 for free lactic acid (CH group) and no noticeable peak for lactic acid attached to the methacrylate backbone. Peak 12 and 13

indicate the CH_3 and CH_2 groups of free polymethacrylic acid chains, respectively. Peaks 14, 15 and 16 indicate the presence of glycerol that in this case was used as an initiator in the ring opening polymerization reaction. Based on these results it was decided to hydrolyze all synthesized networks at 120 ^{o}C, 3 bar for 20 h in a microwave instrument to ensure complete hydrolysis.

The network degradation products were analyzed using GPC to determine the molecular weights of the kinetic chains. The results are summarized in Figure 4 and Table 1. When comparing the results for the different initiator concentrations it can be observed that increasing the initiator concentration results in a decrease in the kinetic chain length, but the effect is relatively small. Increasing the photo-initiator concentration from 0.2 to 3 wt% results in a decrease of M_n of the kinetic chains from 44×10^3 to 23×10^3 g/mol.

The effect of adding 2-mercaptoethanol as a transfer agent on the kinetic chain length is much larger. Adding 5 mol% 2-mercaptoethanol, 1 molecule per 20 methacrylate end-groups, results in a decrease in M_n of from 32×10^3 to 8×10^3 g/mol. The addition of more 2-mercaptoethanol decreases the molecular weight even further. So clearly, by adding small amounts of 2-mercaptoethanol as a transfer agent, the kinetic chain length of PDLLA-MA networks can be decreased.

Table 1. *Molecular weights of the kinetic chains of PDLLA-MA networks prepared with different photo-initiator and 2-mercaptoethanol concentrations.*

Initiator concentration (wt%)[a]	2-Mercaptoethanol concentration (mol%)[b]	M_n (g/mol)	M_w (g/mol)	PDI[c]	M_p (g/mol)[d]
0.2	-	44×10^3	110×10^3	2.5	97×10^3
1.0	-	32×10^3	72×10^3	2.3	74×10^3
3.0	-	23×10^3	52×10^3	2.3	62×10^3
1.0	5	8.0×10^3	18×10^3	2.2	14×10^3
1.0	10	5.3×10^3	10×10^3	2.0	7.7×10^3
1.0	20	[e]	[e]	[e]	4.6×10^3
1.0	40	[e]	[e]	[e]	2.6×10^3
1.0	80	[e]	[e]	[e]	$< 1\times10^3$

[a] With respect to macromer.

[b] With respect to methacrylate end-groups.

[c] Polydispersity index.

[d] M_p is the peak value of the molecular weight distribution.

[e] Could not be determined accurately due to low molecular weight resulting in incomplete separation by the columns (see Figure 4).

The effect of chain transfer on the polymer molecular weight can be described by the Mayo equation. A plot of $1/X_n$ (degree of polymerization) against the transfer agent concentration [S] divided by the monomer concentration [M] should result in a straight line [18]:

$$\frac{1}{X_n} = \frac{1}{(X_n)_0} + C_s \frac{[S]}{[M]}$$

The slope of the straight line is the chain transfer constant (C_s). $1/(X_n)_0$ is the value of $1/X_n$ in the absence of the transfer agent. When our data are plotted in this way (Figure 5 indeed a straight line is obtained ($R^2 = 0.995$). The chain transfer constant obtained for 2-mercaptoethanol and our PDLLA-MA macromer is 0.079.

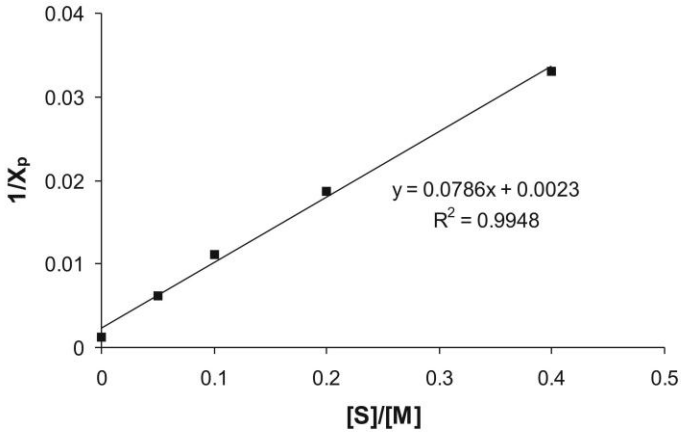

Figure 5. *Plot of $1/X_p$ against [S]/[M] to obtain the chain transfer constant for PDLLA-MA macromers and 2-mercaptoethanol. X_p is the peak value of the degree of polymerization distribution. These values were used since for the higher 2-mercaptoethanol concentrations X_n values could not be determined (Table 1).*

Low molecular weight fractions were collected from GPC for analysis by MALDI-TOF MS. Only low molecular weight GPC fractions were analyzed by MALDI-TOF-MS since it is known that MALDI-TOF-MS of high molecular weight poly(methacrylic acid) is hindered by the so-called mass discrimination effect [21]. The obtained spectra show a clear molecular weight distribution in agreement with the molecular weight of the fractions determined by GPC (Figure 6). For example, the GPC molecular weights of the fraction for which the MALDI-TOF-MS spectrum is shown in Figure 6 were below approximately 4.6×10^3 g/mol. Furthermore, the distance between the peaks corresponds to the molecular weight of methacrylic acid (86 g/mol), confirming that the degradation

products analyzed by GPC were indeed fully hydrolyzed poly(methacrylic acid) kinetic chains. No peaks with intervals corresponding to lactic acid (72 g/mol) were found indicating no evidence of the presence of lactic acid esters.

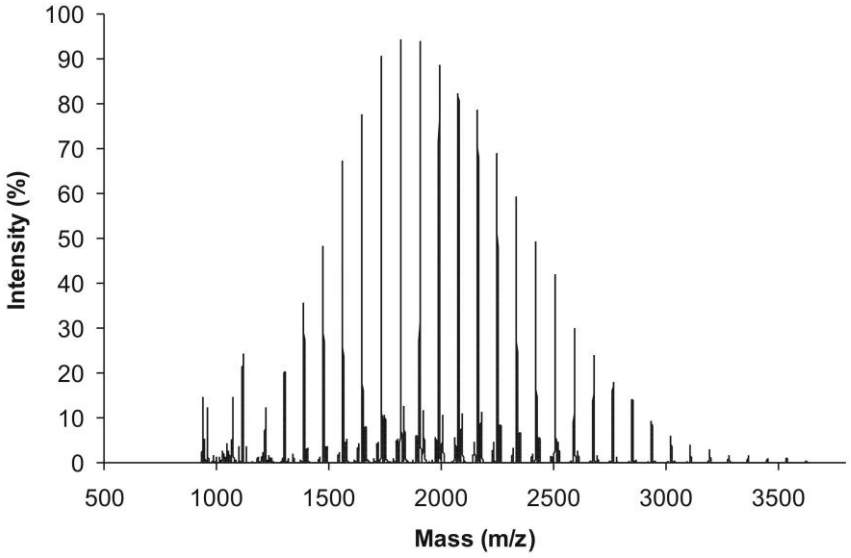

Figure 6. *MALDI-TOF MS spectrum of a low molecular weight GPC fraction (molecular weights below approximately 4.6×10^3 g/mol) of the degradation products of PDLLA-MA networks prepared with 20 mol% 2-mercaptoethanol.*

Network properties

Although controlling the kinetic chain length is very important when biodegradable photo-crosslinked polymer networks are used in biomedical applications, decreasing the kinetic chain length may affect important network properties. The effect of varying the photo-initiator concentration and adding 2-mercaptoethanol on the gel content, swelling behavior and glass transition temperature of the networks was investigated. The results are summarized in Table 2.

All networks showed gel contents above 90 % and no clear trend as a function of photo-initiator or 2-mercaptoethanol concentration was observed. From this it can be concluded that under all used conditions the photo-crosslinking process was effective and most macromer molecules were incorporated in the networks. The swelling ratio in acetone was similar for the networks with varying photo-initiator concentration. The photo-initiator concentration does not affect the crosslink density significantly. This can be explained by the fact that altering the photo-initiator concentration only has a small effect on the kinetic chain length. However, increasing the 2-mercaptoethanol concentration leads to a pronounced increase in swelling ratio and decrease in crosslink density. The

significant decrease in the kinetic chain length upon addition of 2-mercaptoethanol can explain this. The functionality of the crosslinks is lower (less polylactide chains attached to one poly(methacrylic acid) chain) for shorter kinetic chains resulting in a lower crosslink density. With respect to the glass transition temperature the same trends are observed. The T_g is a measure of crosslink density. A higher crosslink density results in a higher T_g [22]. For networks containing 2-mercaptoethanol it can be observed that the T_g decreases with increasing 2-mercaptoethanol concentrations. Any unreacted 2-mercaptoethanol present in the networks that was not removed during drying of the specimen at 90 ^oC may act as a plasticizer and also decrease the T_g somewhat.

Table 2. *Gel contents, equilibrium swelling ratios (in acetone) and glass transition temperatures of PDLLA-MA networks prepared with different concentrations of photo-initiator and 2-mercaptoethanol.*

Initiator concentration (wt%)[a]	2-Mercapto-ethanol concentration (mol%)[b]	Gel content (%)	Swelling ratio	T_g (^oC)
0.2	-	94.4 ± 0.5	1.99 ± 0.05	57.0
1.0	-	97.4 ± 1.4	2.20 ± 0.08	57.2
3.0	-	97.2 ± 0.8	2.07 ± 0.07	57.5
1.0	5	90.5 ± 0.8	2.07 ± 0.03	55.6
1.0	10	95.8 ± 1.4	2.34 ± 0.19	54.0
1.0	20	96.1 ± 1.4	2.70 ± 0.04	53.8
1.0	40	92.6 ± 3.0	3.01 ± 0.03	52.7
1.0	80	95.9 ± 1.8	3.27 ± 0.12	49.5

[a] With respect to macromer.

[b] With respect to methacrylate end-groups

Network degradation behavior is important for many biomedical applications. For example, in drug delivery systems, the degradation behavior of the networks can influence the release kinetics. Therefore, the influence of the kinetic chain length on network degradation was investigated. Degradation of crosslinked polymer networks is influenced by the network structure. For example, it has been shown that the mass loss behavior of thiol-acrylate networks, consisting of PEG-diacrylate and thiols of varying functionality, is influenced by the length of the poly(acrylic acid) kinetic chains [23].

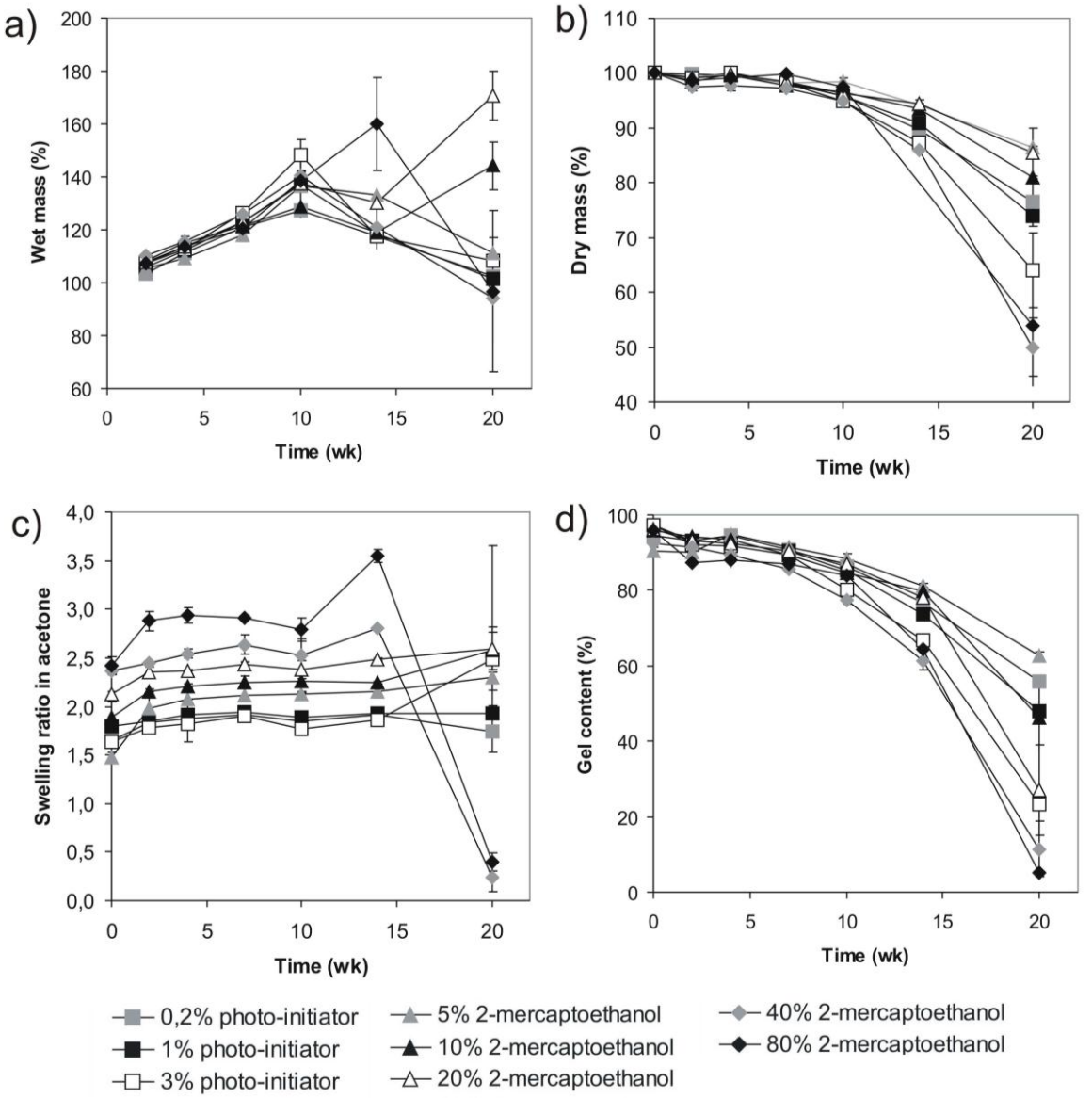

Figure 7. *Degradation of PDLLA-MA networks containing different amounts of photo-initiator (mass% with respect to macromer) and 2-mercaptoethanol (mol% with respect to methacrylate end-groups, all containing 1 wt% photo-initiator). Wet mass (a), dry mass (b), swelling ratio in acetone (c) and gel content (d) as a function of time.*

To investigate the degradation behavior, the wet mass, dry mass, swelling ratio in acetone and gel content of the different networks were followed in time (Figure 7). As was found in previous experiments, networks with shorter kinetic chains showed a higher swelling ratio in acetone. The networks containing different amounts of photo-initiator all showed a similar swelling ratio in acetone, since the amount of photo-initiator did not affect the kinetic chain length much. All materials show similar degradation behavior until approximately 10 wk. The wet mass of the networks steadily increases, while the dry

mass stays more or less constant. After 14 and especially 20 wk differences between the materials start to appear. Considering the networks prepared with different photo-initiator concentrations it can be seen that networks prepared with 3 wt% photo-initiatior seem to degrade somewhat faster than the networks prepared with 0.2 and 1 wt% photo-initiator. For the networks prepared with different amounts of 2-mercaptoethanol, especially the networks with the highest 2-mercaptoethanol concentrations, 40 and 80 mol%, show fast degradation. These two materials show the lowest dry mass and gel content after 20 wk of all the investigated materials. Lower molecular weight poly(methacrylic acid) chains have a smaller number of PDLLA chains that connect them to the rest of the network. Therefore, for networks prepared with higher 2-mercaptoethanol concentrations, the extent of degradation required before these poly(methacrylic acid) chains can go into solution is less. The degradation behavior of the networks prepared with 5, 10 and 20 wt% 2-mercaptoethanol is more similar to that of the networks prepared without 2-mercaptoethanol, although the networks containing 10 and 20 wt% 2-mercaptoethanol show a large increase in wet mass after 20 wk.

In a previous study a stronger dependence of mass loss on the kinetic chain length of the networks was reported [23]. This might be because, in the networks prepared in this study, multifunctional thiols were used, so changing the thiol concentration greatly alters the crosslink density of the networks. Furthermore the prepared PEG-based networks are much more hydrophilic than our PDLLA networks and therefore the length of the kinetic chain has a more direct influence on degree of swelling of the networks in water. For many applications it may be an advantage that for the more hydrophobic networks described in this study, the kinetic chain length can be decreased substantially without altering the degradation behavior of the material to a large extent.

It is possible that not all 2-mercaptoethanol added has reacted into the network. Therefore the prepared networks were extracted in PBS and the 2-mercaptoethanol concentrations in these extracts were determined (Table 3).

No 2-mercaptoethanol was detected in extracts from networks prepared with 5 or 10 mol% 2-mercaptoethanol. Most likely here all the 2-mercaptoethanol was incorporated into the networks, although there might be some unreacted 2-mercaptoethanol entrapped in the networks. In extracts from networks prepared with 20, 40 or 80 mol% 2-mercaptoethanol, 2-mercaptoethanol was indeed detected. For the networks prepared with more 2-mercaptoethanol the concentration in the extracts was higher. For these networks, clearly not al 2-mercaptoethanol was incorporated in the network. These results are in agreement with the study of Reddy *et al*. [24] who concluded from their modeling study on thiol-acrylate polymerizations that the final thiol conversion decreases with

increasing thiol/acrylate ratio in the initial mixture. Although only one to three percent of the 2-mercaptoethanol initially present was extracted from the networks, it is possible that more 2-mercaptoethanol did not react. It may be that 2-mercaptoethanol was physically entrapped in the hydrophobic networks and was therefore not extracted out of the networks. Extractable 2-mercaptoethanol may play a role in network cytocompatibility. While 2-mercaptoethanol is an antioxidant and is frequently used in cell culture as a medium supplement [19], it can reduce disulfide bonds and can therefore denature proteins.

Table 3. *2-Mercaptoethanol concentrations in network extracts*

[2-mercapto-ethanol] in network (mol%)[a]	[2-mercapto-ethanol] in network extracts (mM)	% of initial 2-mercaptoethanol
0	0	0
5	0	0
10	0	0
20	0.28	1.0
40	1.55	2.9
80	1.64	1.5

[a] With respect to methacrylate end-groups

PDLLA-MA networks are known to be cytocompatible [25]. To investigate whether this changes when the photo-initiator concentration is altered or 2-mercaptoethanol is added, a cytocompatibility experiment was performed. Network samples were extracted in culture medium. NIH 3T3 fibroblasts were cultured in the presence of this medium and the metabolic activity of the cells was determined using the XTT assay. The results are summarized in Figure 8.

As expected, cells cultured in the presence of DMSO showed significantly lower metabolic activity than cells cultured in normal culture medium. Although it is known that photo-initiators can be cytotoxic [26, 27] cells in contact with networks prepared with different photo-initiator concentrations showed metabolic activities comparable to the control. Most likely even for the networks prepared with 3 wt% photo-initiator the concentration of initiator in the extracts is low. Furthermore, Irgacure 2959 has been indicated as a relatively cytocompatible UV photo-initiator [26, 27].

For NIH 3T3 fibroblasts cultured in the presence of extracts from networks prepared with 5, 10 or 20 mol% 2-mercaptoethanol high metabolic activity was observed, comparable to cells cultured in normal culture medium. However, cells cultured in the presence of

extracts from networks prepared with 40 and especially, 80 mol% 2-mercaptoethanol, showed lower metabolic activity. These are also the materials for which significant amounts of 2-mercaptoethanol could be extracted from the networks (Table 3). Therefore is seems very likely that 2-mercaptoethanol released from the networks causes the toxicity of the extracts. However, also for networks prepared with only 5 or 10 mol% of 2-mercaptoethanol a significant decrease of the kinetic chain length was found (Table 1). Importantly, for these low concentrations no unreacted 2-mercaptoethanol was extracted from the networks (Table 3) and network extracts were found to be cytocompatible (Figure 8). If higher 2-mercaptoethanol concentrations are used, it may also be possible to extract unreacted 2-mercaptoethanol prior to implantation or to dry the samples at elevated temperature. If however, for a certain application the networks are loaded with a drug, this might not be feasible.

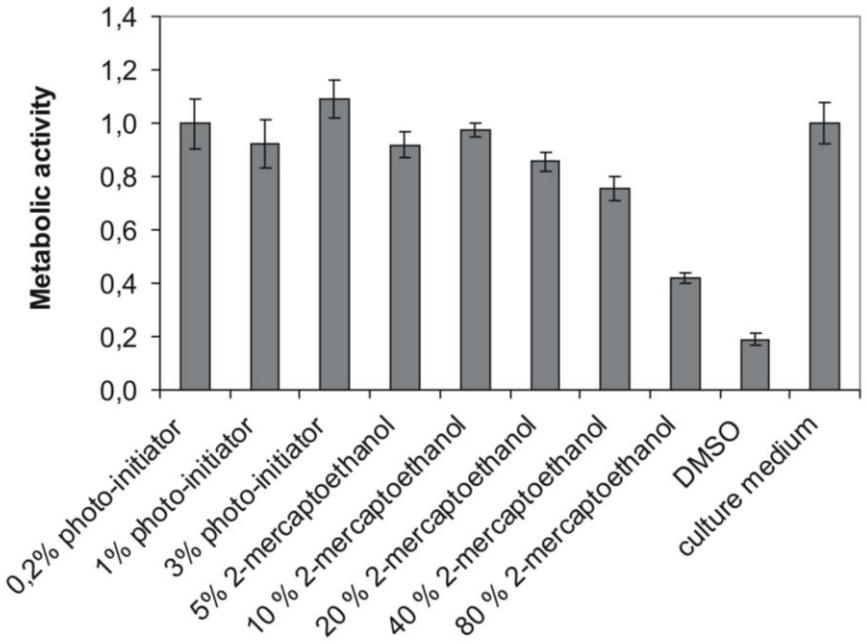

Figure 8. *XTT assay results. NIH 3T3 fibroblasts were cultured in medium containing extracts of PDLLA-MA networks. The networks were prepared with different amounts of photo-initiator and 2-mercaptoethanol. Values are relative to the control (culture medium). Photo-initiator concentrations are indicated in weight percent with respect to macromer. 2-Mercaptoethanol concentrations are given in mole percent with respect to the methacrylate end-groups.*

Conclusions

The kinetic chain length of PDLLA-MA networks can be decreased in a controlled way by adding 2-mercaptoethanol as a transfer agent. Some network properties such as the

glass transition temperature and the swelling ratio in acetone (crosslink density) are affected when the kinetic chain length is decreased. Only small amounts of 2-mercaptoethanol are required to significantly decrease the kinetic chain length. Large amounts should be avoided, since unreacted 2-mercaptoethanol that is extracted from the networks may be toxic to cells. To determine exactly which PMAA chain lengths allow excretion by the kidneys, *in vivo* studies with labeled PMAA are required.

Acknowledgements

We would like to acknowledge Tieme Stevens for performing the MALDI-TOF MS measurements.

References

[1] F.P.W. Melchels, J. Feijen, D.W. Grijpma, A review on stereolithography and its applications in biomedical engineering. Biomaterials 31(24) (2010) 6121-6130.

[2] S.J. Bryant, K.S. Anseth, Hydrogel properties influence ECM production by chondrocytes photoencapsulated in poly(ethylene glycol) hydrogels. J Biomed Mater Res 59(1) (2002) 63-72.

[3] K. Davis, Controlled release from crosslinked degradable networks. Crit Rev Ther Drug Carrier Syst 19(4-5) (2002) 385-423.

[4] J.L. Ifkovits, J.A. Burdick, Review: Photopolymerizable and degradable biomaterials for tissue engineering applications. Tissue Eng 13(10) (2007) 2369-2385.

[5] D.W. Grijpma, Q. Hou, J. Feijen, Preparation of biodegradable networks by photo-crosslinking lactide, ε-caprolactone and trimethylene carbonate-based oligomers functionalized with fumaric acid monoethyl ester. Biomaterials 26(16) (2005) 2795-2802.

[6] B.M. Brenner, T.H. Hostetter, H.D. Humes, Glomular permselectivity - barrier function based on discrimination of molecular-size and charge. Am J Physiol 234(6) (1978) F455-F460.

[7] T. Yamaoka, Y. Tabata, Y. Ikada, Distribution and tissue uptake of poly(ethylene glycol) with different molecular weights after intravenous administration to mice. J Pharm Sci 83(4) (1994) 601-606.

[8] T. Yamaoka, Y. Tabata, Y. Ikada, Comparision of body distribution of poly(vinyl alcohol) with other water-soluble polymers after intravenous administration. J Pharm Pharmacol 47(6) (1995) 479-486.

[9] Y. Murakami, Y. Tabata, Y. Ikada, Effect of the molecular weight of water-soluble polymers on accumulation at an inflammatory site following intravenous injection. Drug Deliv 3(4) (1996) 231-238.

[10] W.M. Ross, A.C. Martens, D.W. Vanbekkum, Polymethacrylic acid - Induction of lymphocytosis and tissue distribution. Cell Tissue Kinet 8(5) (1975) 467-477.

[11] J.A. Burdick, T.M. Lovestead, K.S. Anseth, Kinetic chain lengths in highly cross-linked networks formed by the photoinitiated polymerization of divinyl monomers: A gel permeation chromatography investigation. Biomacromolecules 4(1) (2003) 149-156.

[12] A.K. Burkoth, K.S. Anseth, MALDI-TOF characterization of highly cross-linked, degradable polymer networks. Macromolecules 32(5) (1999) 1438-1444.

[13] R. Peters, V.M. Litvinov, P. Steeman, A.A. Dias, Y. Mengerink, R. van Benthem, C.G. de Koster, S. van der Wal, P. Schoenmakers, Characterisation of UV-cured acrylate networks by means of hydrolysis followed by aqueous size-exclusion combined with reversed-phase chromatography. J Chromatogr A 1156(1-2) (2007) 111-123.

[14] A. Ghaffar, P.G. Verschuren, J.A.J. Geenevasen, T. Handels, J. Berard, B. Plum, A.A. Dias, P.J. Schoenmakers, S. van der Wal, Fast in vitro hydrolytic degradation of polyester urethane acrylate biomaterials: Structure elucidation, separation and quantification of degradation products. J Chromatogr A 1218(3) (2011) 449-458.

[15] F.P.W. Melchels, A.H. Velders, J. Feijen, D.W. Grijpma, Photo-cross-linked poly(D,L-lactide)-based networks. Structural characterization by HR-MAS NMR spectroscopy and hydrolytic degradation behavior. Macromolecules 43(20) (2010) 8570-8579.

[16] E. Andrzejewska, Photopolymerization kinetics of multifunctional monomers. Prog Polym Sci 26(4) (2001) 605-665.

[17] A.E. Rydholm, N.L. Held, C.N. Bowman, K.S. Anseth, Gel permeation chromatography characterization of the chain length distributions in thiol-acrylate photopolymer networks. Macromolecules 39(23) (2006) 7882-7888.

[18] G. Odian, Principles of Polymerization, Wiley-Interscience, 2004.

[19] S.M. Deneke, Current Topics in Cellular Regulation, Vol 36, Academic Press Inc, 2000, pp. 151-180.

[20] G.L. Ellman, Tissue sulfhydryl groups. Arch Biochem Biophys 82(1) (1959) 70-77.

[21] H. Matsubara, S. Hata, Y. Kondo, Y. Ishida, H. Takigawa, H. Ohtani, Characterization of cross-linking structures in UV-cured acrylic ester resin by MALDI-MS combined with supercritical methanolysis. Anal Sci 22(11) (2006) 1403-1407.

[22] T.G. Fox, S. Loshaek, Influence of molecular weight and degree of crosslinking on the specific volume and glass temperature of polymers. J Polym Sci 15(80) (1955) 371-390.

[23] A.E. Rydholm, S.K. Reddy, K.S. Anseth, C.N. Bowman, Controlling network structure in degradable thiol-acrylate biomaterials to tune mass loss behavior. Biomacromolecules 7(10) (2006) 2827-2836.

[24] S.K. Reddy, K.S. Anseth, C.N. Bowman, Modeling of network degradation in mixed step-chain growth polymerizations. Polymer 46(12) (2005) 4212-4222.

[25] F.P.W. Melchels, J. Feijen, D.W. Grijpma, A poly(D,L-lactide) resin for the preparation of tissue engineering scaffolds by stereolithography. Biomaterials 30(23-24) (2009) 3801-3809.

[26] S.J. Bryant, C.R. Nuttelman, K.S. Anseth, Cytocompatibility of UV and visible light photoinitiating systems on cultured NIH/3T3 fibroblasts in vitro. J Biomater Sci Polym Ed 11(5) (2000) 439-457.

[27] C.G. Williams, A.N. Malik, T.K. Kim, P.N. Manson, J.H. Elisseeff, Variable cytocompatibility of six cell lines with photoinitiators used for polymerizing hydrogels and cell encapsulation. Biomaterials 26(11) (2005) 1211-1218.

Chapter 8

Intraocular degradation behavior of crosslinked and linear poly(trimethylene carbonate) and poly(D,L-lactic acid)*

Janine Jansen[1], Steven A. Koopmans[2], Leonoor I. Los[2], Roelofje J. van der Worp[2], Johanna G. Podt[1], Johanna M.M. Hooymans[2], Jan Feijen[3] and Dirk W. Grijpma[1,4]

1) MIRA Institute for Biomedical Technology and Technical Medicine, Department of Biomaterials Science and Technology, Faculty of Science and Technology, University of Twente, P.O. Box 217, 7500 AE, Enschede, The Netherlands
2) W.J. Kolff Institute, Department of Ophthalmology, University Medical Center Groningen, Graduate School of Medical Sciences, University of Groningen, Antonius Deusinglaan 1, 9713 AV, Groningen, The Netherlands.
3) MIRA Institute for Biomedical Technology and Technical Medicine, Department of Polymer Chemistry and Biomaterials, Faculty of Science and Technology, University of Twente, P.O. Box 217, 7500 AE, Enschede, The Netherlands
4) W.J. Kolff Institute, Department of Biomedical Engineering, University Medical Center Groningen, University of Groningen, Antonius Deusinglaan 1, 9713 AV, Groningen, The Netherlands

*Biomaterials 32 (2011) 4994-5002.

Abstract

The intraocular degradation behavior of poly(trimethylene carbonate) (PTMC) networks and poly(D,L-lactic acid) (PDLLA) networks and of linear high molecular weight PTMC and PDLLA was evaluated. PTMC is known to degrade by enzymatic surface erosion *in vivo*, whereas PDLLA degrades by hydrolytic bulk degradation. Rod shaped specimens were implanted in the vitreous of New Zealand white rabbits for 6 or 13 wk. All materials were well tolerated in the rabbit vitreous. The degradation of linear high molecular weight PTMC and PTMC networks was very slow and no significant mass loss was observed within 13 wk. Only some minor signs of macrophage mediated erosion were found. The fact that no significant enzymatic surface erosion occurs can be related to the avascularity of the vitreous and the limited number of cells it contains. PDLLA samples showed more evident signs of degradation. For linear PDLLA significant swelling and a large decrease in molecular weight in time was observed and PDLLA network implants started to lose mass within 13 wk. Of the tested materials PDLLA networks seem to be most promising for long term degradation controlled intravitreal drug delivery since this material degrades without significant swelling. Furthermore the preparation method of these networks allows easy and efficient incorporation of drugs.

Introduction

Age-related macula degeneration (AMD) is the leading cause of blindness in the developed world [1]. Macula degeneration and other diseases of the posterior segment of the eye may require drug delivery to the posterior segment of the eye, which is challenging [2]. Topical ocular medications such as eye drops hardly reach the posterior segment and the blood-retinal barriers prevent most systemically delivered drugs from achieving therapeutic levels in the posterior segment of the eye. Pharmacologically, the most efficient way to deliver drugs to the posterior segment is direct administration into the vitreous. Following injection, drugs are cleared from the vitreous within days or weeks, depending on the drug. The repeated injections that are often required can be stressful for patients and might lead to complications such as endophthalmitis.

Several controlled release systems have been developed to achieve sustained intraocular drug levels [2-5]. Degradable inserts overcome the need to remove the implant after the drug is released. Ozurdex® (formerly Posurdex®, Allergan Inc.) [6] is the only degradable device for drug delivery to the posterior segment of the eye currently on the market. The injectable rod-shaped PLGA (poly(lactic-co-glycolic acid)) implant releases dexamethasone and is applied for the treatment of diabetic macular edema. Several other

degradable systems designed for drug delivery to the posterior segment of the eye are currently under investigation. Most often the focus in these studies is primarily on drug release or therapeutic effect. Only very few studies are available that provide details on the degradation behavior of the polymers which carry the drug in the eye. Most of the current literature on intraocular use of biodegradable polymers refers to poly(lactic acid) (PLA) or copolymers with glycolic acid (PLGA). Moritera *et al.* [7] and Giordano *et al.* [8] evaluated the intravitreal degradation of PLGA and PLA microspheres with and without drugs incorporated. For a few other materials initial studies regarding intravitreal behavior are available. Einmahl and Heller *et al*. [9-11] investigated the intravitreal degradation of two poly(ortho ester)s. Bruining *et al*. [12] studied the intravitreal behavior of poly(N-vinyl-2-pyrrolidone) networks designed for drug delivery applications. Hacker *et al*. [13] performed an initial two week intravitreal implantation study for their poly(propylene fumarate)/poly(N-vinyl-2-pyrrolidone) material. Silva-Cunha *et al*. [14] investigated the degradation of dexamethasone loaded ε-caprolactone intravitreal implants.

We set out to develop a system for controlled and sustained drug delivery to the posterior segment of the eye based on photo-crosslinked polymer networks. Polymer networks can be prepared by photo-polymerization of double bond-functionalized oligomers. The release profiles of these types of networks can be tuned by varying the crosslink density or by adjusting the network hydrophilicity [15-17]. Furthermore, networks can easily be loaded with drugs by dispersing or dissolving the drug in a liquid crosslinkable macromer or macromer solution prior to the crosslinking process. In this way, large amounts of drug can be loaded into a matrix efficiently. Samples with different shapes can simply be prepared using molds while crosslinked micro- and nanoparticles can be prepared by irradiating emulsions [18].

PTMC is a flexible, biocompatible polymer that has been shown to degrade by surface erosion *in vivo* [19, 20]. This can be an advantage in drug delivery applications since release patterns of surface-eroding polymers are closely related to the polymer degradation rate and independent of the size of the drug molecule [21]. It has been suggested that enzymes and reactive oxygen species secreted by phagocytic cells play an important role in the *in vivo* degradation of PTMC [22, 23]. It is not known whether this process also occurs in the vitreous as PTMC has never been applied in the vitreous before. The vitreous is a transparent gel that consists mostly of water (98-99 %), some macromolecules, such as glycosaminoglycans and collagens, and only a small number of cells [24]. Another characteristic of PTMC is that it degrades without the formation of

acidic compounds, which can be an advantage in protein delivery, since a drop in pH may lead to protein denaturation.

Poly(D,L-lactic acid) is a well known polymer that has been studied extensively for various biomedical applications [25] and has also been investigated for intravitreal delivery systems, mostly in the form of microspheres [26]. PDLLA degrades by bulk degradation into lactic acid.

In this study the intraocular degradation behavior of poly(trimethylene carbonate) (PTMC) networks was compared to that of poly(D,L-lactic acid) (PDLLA) networks. Besides the crosslinked polymers, also linear PTMC and PDLLA were investigated.

Materials and methods

Materials

Trimethylene carbonate (TMC) was purchased from Boehringer Ingelheim (Germany). D,L-lactide (DLLA) was purchased from Purac Biochem (The Netherlands). Tin 2-ethylhexanoate ($Sn(Oct_2)$), trimethylolpropane (TMP) and deuterated chloroform were obtained from Sigma Aldrich (U.S.A.). Methacryloyl chloride (MACl) was obtained from Alfa Aesar (Germany). Triethyl amine (TEA) and toluidine blue were purchased from Fluka (Switzerland). Irgacure 2959 (2-hydrox-1-[4-(2-hydroxyethoxy)phenyl]-2-methyl-1-propanone) was obtained from Ciba Specialty Chemicals (Switzerland). Phosphate buffered saline (PBS, pH 7.4) was purchased from B. Braun (Germany). Analytical grade dichloromethane (DCM) was obtained from Biosolve (The Netherlands). DCM was dried over CaH_2 and distilled. Other solvents were of technical grade and were used as received (Biosolve, the Netherlands). Oxybuprocaine 0.4 % eyedrops, phenylephrine 2.5 % eyedrops and povidone iodine 0.3 % eyedrops were obtained from the Hospital Pharmacy of the UMCG (The Netherlands). Ketamine was purchased from Alfasan (The Netherlands). Medetomidine was obtained from Janssen Pharmaceutica NV (Belgium). Tropicamide 2.5 % eyedrops were obtained from Thea Pharma NV (Belgium). Chloramphenicol 1 % ointment was purchased from Ratiopharm (The Netherlands). Buprenorphine was obtained from Scheringh Plough (U.S.A.). Paraformaldehyde was purchased from Polysciences Inc. (United Kingdom). Technovit 8100 was purchased from Heraeus Kulzer (Germany).

Implant preparation and characterization

Linear PTMC and PDLLA

High molecular weight poly(trimethylene carbonate) and poly(D,L-lactide) were synthesized in silanized glass ampoules. The ampoules were purged with argon and charged with trimethylene carbonate or D,L-lactide monomer (approximately 20 g) and stannous octoate as a catalyst. The system was switched to vacuum and dried for 15 min. Then the monomer mixture was molten (trimethylene carbonate at 55 ^{o}C, D,L-lactide at 130 ^{o}C) under argon and brought into Teflon tubes with an inner diameter of 0.8 mm using a syringe. The filled Teflon tubes were immersed in the monomer mixture. The system was cooled down and the ampoules were heat-sealed under vacuum. The polymerizations were conducted at 130 ^{o}C for 3 d. Then the ampoules were broken and the rod-shaped samples were taken out of the Teflon tubes and cut into pieces of approximately 5 mm.

The monomer conversion was determined from proton nuclear magnetic resonance (^{1}H-NMR) spectra (Varian Inova 300 MHz NMR spectrometer). Deuterated chloroform was used as a solvent.

Gel permeation chromatography (GPC) was used to obtain number average molecular weights (M_n), weight average molecular weights (M_w), polydispersity indexes (PDI) and intrinsic viscosities (η) of the polymers. The polymers were dissolved in chloroform, and GPC measurements were conducted with a Viscotek GPCmax VE-2001 GPC solvent/sample module equipped with a series of ViscoGEL columns and a TDA 302 triple detector array (light scattering detector, differential refractive index detector, four-capillary differential viscometer).

The glass transition temperatures of the polymers were determined using a Perkin Elmer Pyris 1 differential scanning calorimeter. Samples were heated at a heating rate of 10 °C/min and quenched rapidly at 300 °C/min. After 5 min a second heating scan was recorded. The glass transition temperature was taken as the midpoint of the heat capacity change in the second heating run.

PTMC and PDLLA networks

Three-armed poly(trimethylene carbonate) and poly(D,L-lactide) oligomers were synthesized by the ring opening polymerization of trimethylene carbonate and D,L-lactide respectively. The oligomer syntheses were carried out at a 20 to 60 gram scale. Trimethylol propane was used as a trifunctional initiator and stannous octoate was used as a catalyst. TMC or DLLA, TMP and stannous octoate (approximately 0.2

mmol/mol monomer) were reacted in the melt at 130 ^{o}C for 48 h under argon. The targeted molecular weight was 3100 g/mol for both oligomers, which corresponds to about 10 TMC units and about 7 DLLA units per arm. To achieve this, 30 mol TMC and 21 mol DLLA were added per mole of TMP.

Oligomers were functionalized with a methacrylic double bond by reacting methacryloyl chloride with the hydroxyl end-groups of the oligomers. In the coupling reaction the oligomers were used without purification. An amount of oligomer was charged into a three-necked flask and dried for 2 h at 110 ^{o}C *in vacuo* and then cooled to room temperature under argon. The oligomer was dissolved in dry DCM, triethylamine was added and the flask was cooled to 0 ^{o}C. Methacryloyl chloride was added drop-wise while the oligomer solution was stirred vigorously. Per mol of hydroxyl groups 1.2 moles of MACl and TEA were used. The coupling reaction was continued for 24 hours, letting the contents slowly warm up to room temperature. The TEA·HCl salt that had formed was removed by filtration. PTMC-MA macromers were purified by washing with water, precipitation in cold ethanol, and drying under vacuum. PDLLA-MA macromers were purified by precipitation in cold isopropanol, washing with water, and freeze drying.

The oligomer molecular weights (M_n) and the degrees of functionalization were determined from ^{1}H-NMR spectra.

The synthesized macromers were photo-crosslinked to prepare rod-shaped implants. PTMC-MA or PDLLA-MA macromers (1 g) and Irgacure 2959 photo-initiator (1 wt%, relative to macromer) were dissolved in dichloromethane (0.5 ml). The solution was brought into Teflon tubes with an inner diameter of 0.8 mm using a syringe.

Photo-crosslinking was carried out for 15 min at room temperature in a nitrogen atmosphere in an Ultralum crosslinking cabinet. Long-wave UV mercury lamps (365 nm) were used at 15 cm distance from the samples, resulting in an intensity of 3-5 mW/cm^2.

Samples were taken out of the Teflon tubes, dried at elevated temperature (90 ^{o}C) under a nitrogen flow to remove any remaining solvent and cut into pieces of approximately 5 mm.

To determine the gel content after crosslinking, network specimens (n=3) were weighed (m_0), extracted with acetone overnight and dried at 90 ^{o}C under a nitrogen flow until constant weight. The mass of the dry network (m_1) was then determined. Gel content is defined as:

$$\text{Gel content} = \frac{m_1}{m_0} \times 100\%$$

A correction was made for any dichloromethane that was left before crosslinking, by drying samples directly after crosslinking (without extraction).
A Perkin Elmer Pyris 1 differential scanning calorimeter was used to determine the glass transition temperatures of the networks as previously described.

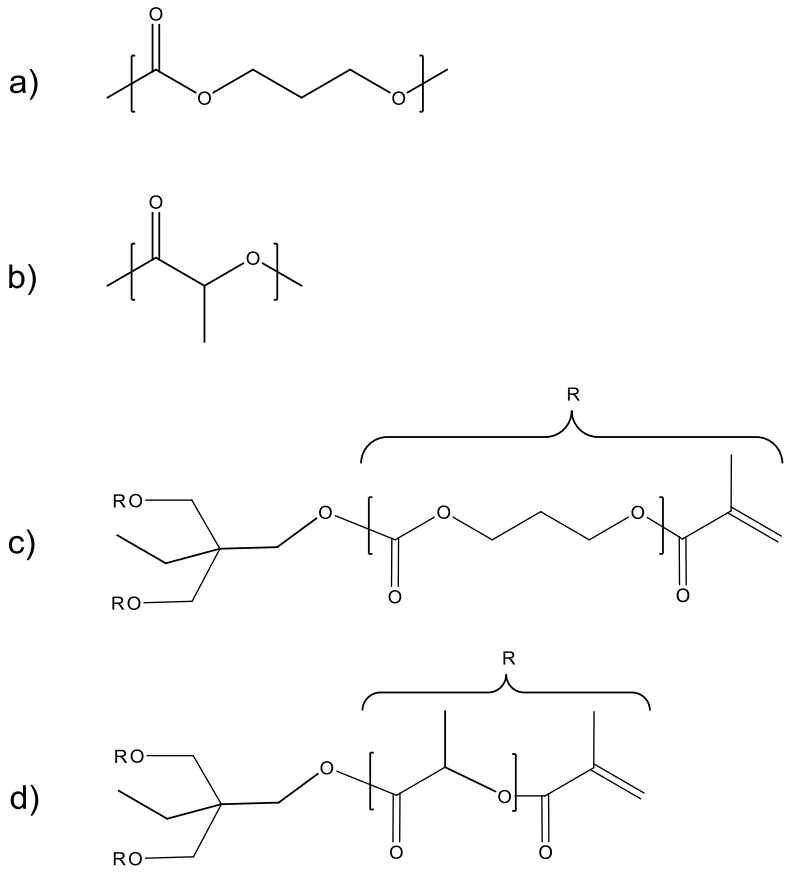

Figure 1. *Structural formulas of linear PTMC (a), linear PDLLA (b), a PTMC-MA macromer (c) and a PDLLA-MA macromer (d).*

Implantation

Linear PTMC and PDLLA and PTMC and PDLLA networks were implanted in the vitreous of 8 wk old female New Zealand white rabbits (1700-2200 g). The committee for animal experiments of the University Medical Center Groningen approved the animal experiment protocols. The experiments were conducted following national and European guidelines for animal experiments. The 24 rabbits were divided in two groups of 12 animals. The 12 animals of group 1 were housed in groups of 6. The 12 animals of group 2 were housed individually. The rabbits were fed standard food and water *ad libitum*. Each group of 12 rabbits was divided into four groups of three animals (n=3), one group for each material. Each rabbit received an implant in one eye. The other eye was used as a

reference. Clinical evaluation of group 1 was performed after 2 wk and 6 wk and the animals were sacrificed after 6 wk. Clinical evaluation of group 2 was performed after 5 wk, 8 wk and 13 wk and the animals were sacrificed after 13 wk.

The implants were disinfected with isopropanol (2 x 15 min), rinsed with sterile PBS (2 x 15 min) and immersed in sterile PBS until the implantation procedure (no longer than 1 d). The animals were anesthetized with ketamine (10-20 mg/kg) and medetomidine (0.2-0.5 mg/kg) injected subcutaneously. After anesthesia the animal was placed under a surgical microscope and a wire eyelid speculum was placed. A photograph was taken of the conjunctiva of the eye with a camera attached to the microscope to establish a basis for the redness of the conjunctiva. The conjunctiva was additionally anesthetized with oxybuprocaine 0.4 % eyedrops. The pupil was dilated with tropicamide and phenylephrine 2.5 % eyedrops. The conjunctiva cul de sac was disinfected with povidone iodine 0.3 % eyedrops. The conjunctiva was dissected from its insertion at the limbus in one quadrant with Wescott scissors. A stab incision was made 3-4 mm behind the limbus with a sclerotomy knife. The implant (diameter approximately 0.8 mm, length approximately 5 mm) was placed in a 20 G blunt cannula and the cannula was guided through the sclerotomy in a posterior direction until the tip of the cannula was visible behind the lens. A metal rod was inserted in the extraocular part of the cannula to push the implant into the vitreous body. A photograph was taken of the implant. The sclerotomy and the conjunctiva were sutured with a vicryl 8-0 resorbable suture (group 1) or a non-resorbable suture (group 2). Chloramphenicol 1 % ointment was applied once directly postoperative and twice a day during 7 d following surgery. Buprenorphine 0.01-0.05 mg/kg was given subcutaneous preoperatively, 1 h postoperatively and 12 h postoperatively as an analgesic.

One rabbit in group 2 had to be sacrificed 1 wk after implantation due to a spinal cord lesion. It is known that a spinal cord lesion can occur when a rabbit kicks its back legs in the air and the incident seemed unrelated to the implantation procedure. Because of the short implantation period, the eyes of this rabbit were not further evaluated and the rabbit was excluded from the study.

Clinical evaluation

After anesthesia (as described above) the animal was placed under the surgical microscope and an eyelid speculum was placed. A photograph was taken of the conjunctiva of the eye to evaluate the redness. The pupil was dilated with tropicamide and phenylephrine 2.5 % eyedrops. A photograph was taken of the implant through the operating microscope. A retinal examination was performed with indirect fundoscopy.

Results for conjunctival redness, corneal clarity, presence of posterior synechiae, dilated iris vessels, cells in the anterior chamber, clarity of the lens, vitreous cells and vitreous opacities were scored on a standard list.

Implant evaluation and histology

The animals were euthanized after 6 wk (group 1) or 13 wk (group 2) with 150 mg/kg nembutal intravenously. Prior to euthanization the eyes were examined as described above. From 2 out of 3 eyes per material group the samples were removed through the original sclerotomy. All eyes were enucleated, immediately fixed in 2 % paraformaldehyde solution and embedded in Technovit 8100. By means of a microtome, sections (4 μm thick) were taken along the direction of the implantation. The sections were stained with toluidine blue for evaluation by light microscopy.

The removed samples were immersed in PBS and their wet mass was determined. After drying at ambient temperature under vacuum, their dry mass was determined. Samples were examined by inverted light microscopy, μCT (micro-computed tomography) (GE eXplore Locus SP μCT scanner) and scanning electron microscopy (SEM, high resolution LEO 1550 SEM (Zeiss), operated at 0.5 kV).

Results and discussion

Implant preparation

Rod-shaped implants with a diameter of approximately 0.8 mm and a length of approximately 5 mm were prepared. Four different materials were used: linear, high molecular weight, PTMC and PDLLA and PTMC and PDLLA networks, prepared from PTMC-MA and PDLLA-MA macromers respectively.

To obtain rod-shaped high molecular weight PTMC and PDLLA implants, the respective monomers were polymerized in small Teflon tubes. The monomer conversion was calculated from ^{1}H-NMR spectra. The residual monomer content was 0.7 % for the PTMC implants and 2.3 % for the PDLLA implants. The rods were implanted without removal of the residual monomer. The amount of residual monomer is important, since it can influence the degradation profile of the polymer. Residual monomer is known to accelerate the degradation of PDLLA [27]. It seems likely that this effect is less important for PTMC, since the TMC monomer is water-soluble [20] and can readily diffuse out of the specimens. The number average molecular weights of the linear polymers were

468 kg/mol for PTMC and 209 kg/mol for PDLLA. The glass transition temperatures of PTMC and PDLLA were -17 ^{o}C and 55 ^{o}C respectively.

PTMC and PDLLA networks were prepared from three-armed methacrylate-functionalized oligomers. The molecular weights of the oligomers and the degrees of methacrylate functionalization of the macromers were calculated from ^{1}H-NMR spectra as described in previous studies [16, 28] and are summarized in Table 1. Rod shaped implants were prepared by photo-crosslinking the macromers in Teflon tubes. Crosslinked specimens with high gel contents were obtained (Table 1). Non-extracted specimens were used in the *in vivo* study.

Table 1. *Characteristics of PDLLA and PTMC networks.*

Material	Oligomer molecular weight (kg/mol)	Degree of methacrylate functionalization (%)	Gel content of photo-crosslinked network (%)	Network glass transition temperature (T_g, ^{o}C)
PTMC networks	2.9	91	97.1 ± 2.6	-7.9
PDLLA networks	3.2	93	95.5 ± 3.0	58

The rod diameters were determined from μCT images and are shown in Table 2. The diameters of the high molecular weight implants are very close to the inner diameter of the Teflon tubes (0.8 mm). The network specimens show a slightly smaller diameter, which may be due to polymerization shrinkage and because the macromers were crosslinked in solution.

Table 2. *Diameters of the prepared implants.*

Material	Rod diameter (mm)
High molecular weight PTMC	0.791 ± 0.009
PTMC networks	0.659 ± 0.006
High molecular weight PDLLA	0.779 ± 0.006
PDLLA networks	0.652 ± 0.014

Implantation and clinical evaluation

To evaluate the intraocular degradation behavior of the different specimens, they were implanted in the vitreous of New Zealand white rabbits. All implants were successfully placed into the vitreous body of the rabbits and no handling problems with the specimens occurred during the procedure. Directly after implantation and after 2, 5, 6, 8 and 13 wk

all implants could be observed through the lens of the eye (Figure 2). However, some of the specimens were difficult to find after 5 wk or more after the implantation, since they had moved to the peripheral part of the vitreous. Also images taken of the same eye at different time points indicate that the position of the implants in the vitreous had changed over time (Figure 2a and b).

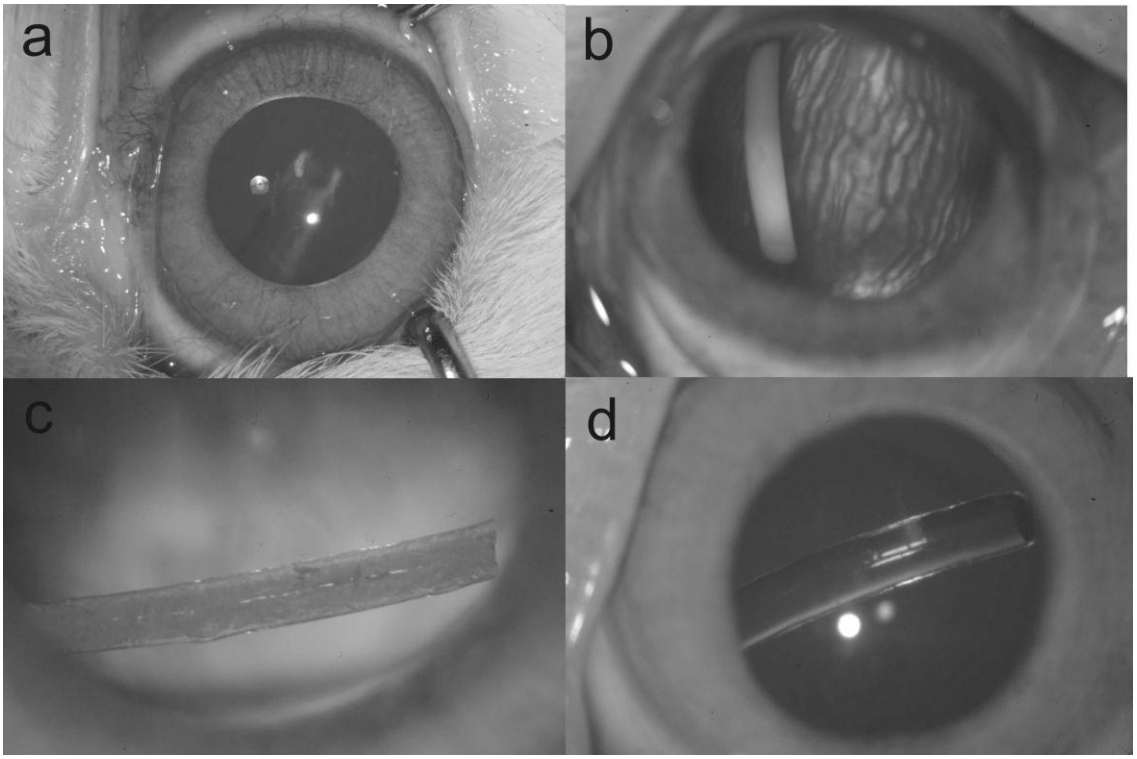

Figure 2. *PDLLA rod in the rabbit vitreous: just after implantation (a) and after 2 wk (b), PDLLA network rod 8 wk after implantation (c), PTMC rod 13 wk after implantation (d). Image b was made using a plano-concave contact lens that is put on the rabbit cornea to enable imaging of the retina.*

Since the implants could be observed through the lens, changes in appearance of the rods could easily be followed during the experiment. The PTMC rods (linear polymer and networks) remained transparent (Figure 2 d), whereas the specimens of linear PDLLA turned opaque within 2 wk (Figure 2 b) and in the PDLLA network specimens voids were observed (Figure 2 c). The number of voids and small cracks in the PDLLA network samples seemed to increase with implantation time. The structural integrity of all specimens was maintained during the study.

The response of the eyes was evaluated 2 and 6 wk after implantation for group 1 and 5, 8 and 13 wk after implantation for group 2. Some minor irregularities related to the implantation procedure were observed. In some rabbits, 5 out of 12 in group 1 and 1 out

of 12 in group 2, small scratches were observed on the back of the lens. This was most likely caused by the hollow needle, through which the sample was inserted. These scratches seemed to heal in time. Minor vitreous opacities were observed in 4 out of 12 rabbits in group 1. These opacities seem to represent a fibrous reaction along the track of the needle through the vitreous. In group 2, 2 out of 11 rabbits showed some mild redness around the suture. This might be related to the non-degradable suture used in this group, although after 13 wk no conjunctival redness was observed in any of the rabbits. A non-degradable suture was chosen since in the first group it was found that it could be difficult to find the location of the sclerotomy in the histological analysis. In 1 rabbit a fold or tear in the retina was observed which might have been caused by the needle. In 1 rabbit a small vitreous hemorrhage was observed, most likely also originating from the implantation procedure, which had disappeared after 13 wk.
Most importantly, eye examinations indicated no significant reaction to the implants at any time point.

Implant evaluation after explantation and histology

The animals were sacrificed after 6 wk (group 1) or 13 wk (group 2). For each material 2 of the 3 specimens per group were explanted for characterization. The other specimens were left in the eye to allow histological evaluation of the capsules around the implants. All eyes, including some reference eyes, were enucleated, embedded, microtomed, and stained for histological analysis. To asses the extent of degradation the masses and diameters of the explanted specimens were determined. Different imaging techniques were used to study the general appearance, interior, and surface structure of the specimens.
The PTMC implants (both linear polymer and networks) only show a very small decrease in dry mass after 6 wk and 13 wk (Figure 3). This is most likely caused by leaching of soluble components from the unextracted network samples and specimens of linear PTMC that contained a small amount of residual, water soluble, monomer. No decrease in implant diameter was observed as would be expected when surface erosion occurs. Also, no swelling of the specimens was observed upon implantation. Both linear PTMC and PTMC network specimens did not show any change in appearance after 6 wk and 13 wk in the rabbit vitreous (Figure 4).
For the specimens of linear PDLLA significant swelling was observed both after 6 and 13 wk (Figure 3 and Figure 4). No significant swelling was found when PDLLA specimens prepared from purified PDLLA without residual monomer were incubated in PBS (pH 7.4) at 37 ^{o}C *in vitro*. Therefore it is hypothesized that the swelling observed in

this *in vivo* study is related to the residual monomer in the implants. This is supported by the fact that extensive swelling of PDLLA samples containing residual monomer has been observed before [28]. The specimens of linear PDLLA did not show significant loss of mass after 6 and 13 wk (Figure 3).

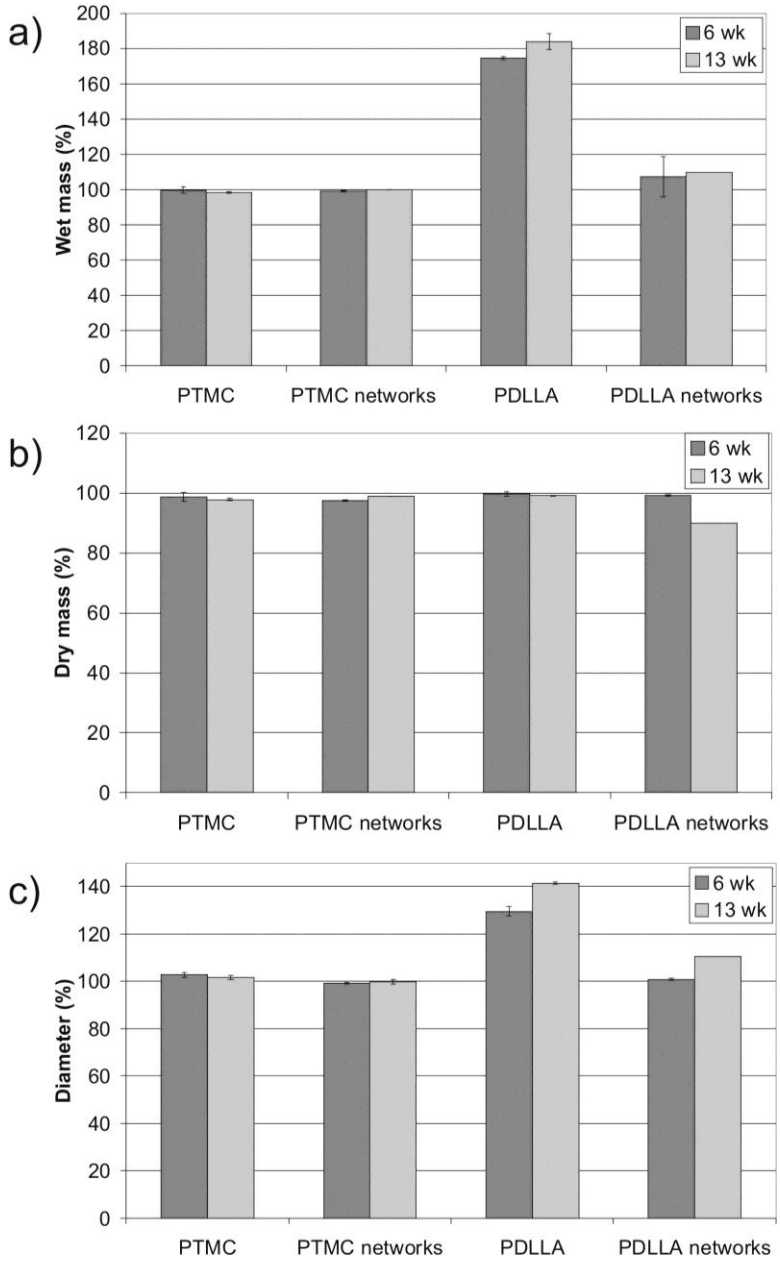

Figure 3. *Wet mass (a), dry mass (b) and rod diameter (c) after 6 wk and 13 wk in the rabbit vitreous. Wet mass and dry mass as percentages of the initial dry mass. Diameter determined from μCT images, percentage of initial dry diameter. For the specimens explanted after 13 wk only one PDLLA network specimen was available for analysis, since one rabbit was sacrificed after 1 wk because of a spinal cord lesion.*

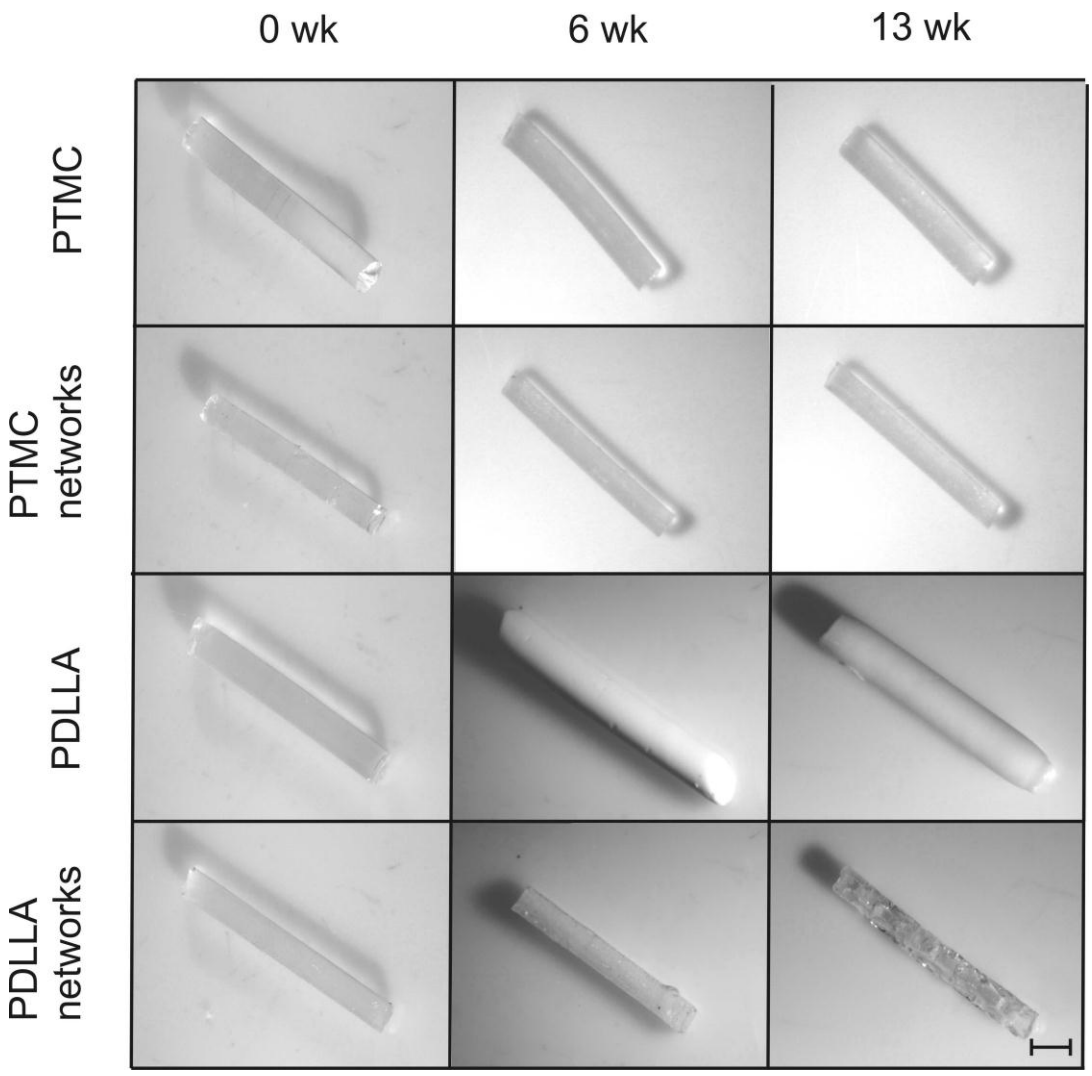

Figure 4. *Inverted light microscopy images of specimens before (left) and after implantation in the rabbit vitreous for 6 wk (middle) and 13 wk (right). Bar = 1 mm, the magnification is the same for all images in this figure. Shadows may make the samples look thicker or thinner than they are, especially for the transparent samples. The correct diameters can be found in Table 2 and Figure 3 (determined by μCT). This image is given to show the general appearance of the samples before and after implantation in the rabbit vitreous.*

The PDLLA network implants also showed no significant mass loss after 6 wk and after 13 wk mass loss was approximately 10 %. In a parallel *in vitro* experiment mass loss of PDLLA networks was 14 % after 12 wk in PBS (pH 7.4, 37 ^{o}C). In contrast to the specimens of linear PDLLA, the PDLLA network samples did not show extensive swelling. After implantation the PDLLA network specimens appeared less transparent than prior to their implantation. Also some large voids could be observed (Figure 4).

For many polymers that degrade by hydrolysis mass loss is preceded by a decrease in molecular weight. Therefore, GPC was used to determine the molecular weights of the linear polymers upon *in vivo* degradation. In our case the molecular weights of the explants could not be determined using triple detection because of the small amount of available material. For that reason, the peak values of the molecular weight distributions (M_p) were determined relative to polystyrene (Table 3). For PTMC a small decrease in the peak molecular weights was observed as a function of implantation time, this is most likely caused by hydrolytic chain scission of the PTMC chains. In previous *in vitro* studies it was found that the hydrolytic degradation of PTMC is very slow [29]. The molecular weights (M_p) determined for PDLLA indicate a stronger decrease in molecular weight after 6 wk and a slight decrease between 6 and 13 wk. In a previous *in vitro* study [28], where PDLLA samples (containing 1.7 % residual monomer) were degraded, a sharp decrease in molecular weight was observed within 10 wk, matching the observations in this *in vivo* study.

Table 3. *Molecular weight and polydispersity of linear PTMC and PDLLA before implantation and after 6 and 13 wk in the rabbit vitreous.*

	t (wk)	M_n (g/mol)	M_w (g/mol)	PDI	M_p [b] (g/mol)
PTMC	0	468×10^3	653×10^3	1.4	1.7×10^6
	6	[a]	[a]	[a]	1.4×10^6
	13	[a]	[a]	[a]	1.1×10^6
PDLLA	0	209×10^3	252×10^3	1.2	278×10^3
	6	[a]	[a]	[a]	78×10^3
	13	[a]	[a]	[a]	74×10^3

[a] Could not be determined accurately using triple detection due to the small amount of material.

[b] M_p is the peak value of the molecular weight distribution relative to poly(styrene).

The surfaces of the PTMC implants looked relatively smooth both before and after implantation in the rabbit vitreous, and no major signs of surface erosion were observed. Only some pits were found at the ends of PTMC rods explanted after 6 wk (Figure 5a) and after 13 wk. This might be a result of macrophage mediated erosion. The surface morphology resembles the morphology previously observed in macrophage mediated erosion of PTMC films [22]. In μCT analysis all PTMC implants, both linear polymers and networks, showed a homogeneous solid interior without any pores or voids.

In previous studies where specimens were implanted at other implantation sites, rapid degradation of PTMC by enzymatic surface erosion was observed. High molecular weight PTMC disks (M_n = 316 kg/mol) showed almost complete degradation within 3 wk upon subcutaneous implantation in rats [19]. In another study, a 60 % mass loss was observed for PTMC rods (M_n = 457 kg/mol) after 8 wk in the femur and tibia of rabbits [20]. The difference in the degradation behavior of PTMC in the vitreous and at other implantation sites might be explained by the avascularity of the vitreous and the limited number of cells it contains. The enzymes involved in the degradation of PTMC do not seem to be present in the vitreous.

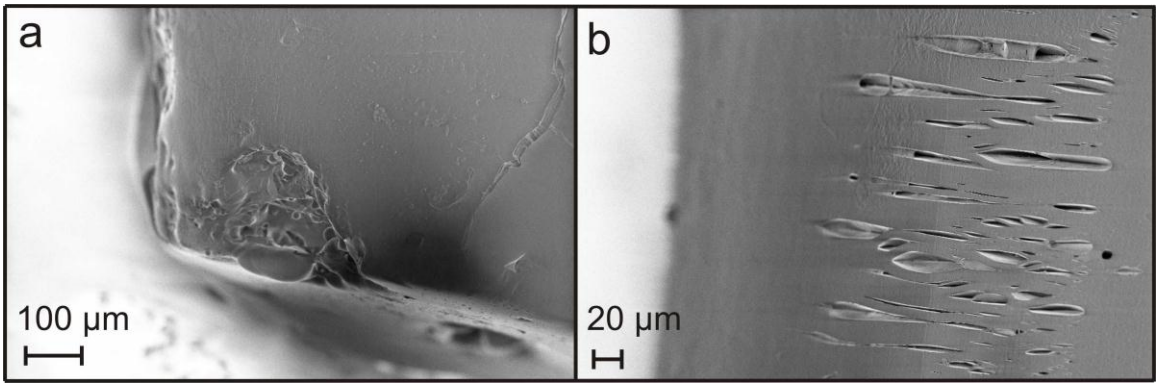

Figure 5. *SEM images of implant surfaces. Minor degradation at the end of a specimen of linear PTMC after 6 wk in the rabbit vitreous (a). Specimen of linear PDLLA after 13 wk in the rabbit vitreous (b).*

The surfaces of PDLLA network specimens looked relatively smooth before and after implantation in the rabbit vitreous. The surfaces of specimens of linear PDLLA looked smooth before implantation and after 6 wk. Some small fissures were observed in one specimen of linear PDLLA explanted after 13 wk (Figure 5b).

Analysis by µCT revealed small pores in the center of the specimens of linear PDLLA explanted after 13 wk (Figure 6). Specimens explanted after 6 wk had a homogeneous interior. Inhomogeneous degradation of PDLLA specimens has been observed before [30] and can be explained by the fact that degradation products formed close to the surface of the specimen can dissolve in the surrounding medium more easily than degradation products formed in the centre of the specimen. This leads to a higher concentration of carboxylic end-groups in the centre and autocatalysis of ester degradation. This inhomogeneous degradation process could be clearly visualized using µCT imaging.

In the μCT images of PDLLA network specimens large pores were found in the specimens explanted after 6 and 13 wk (Figure 6). The number of pores increased over time and the external shape of the rods became irregular.

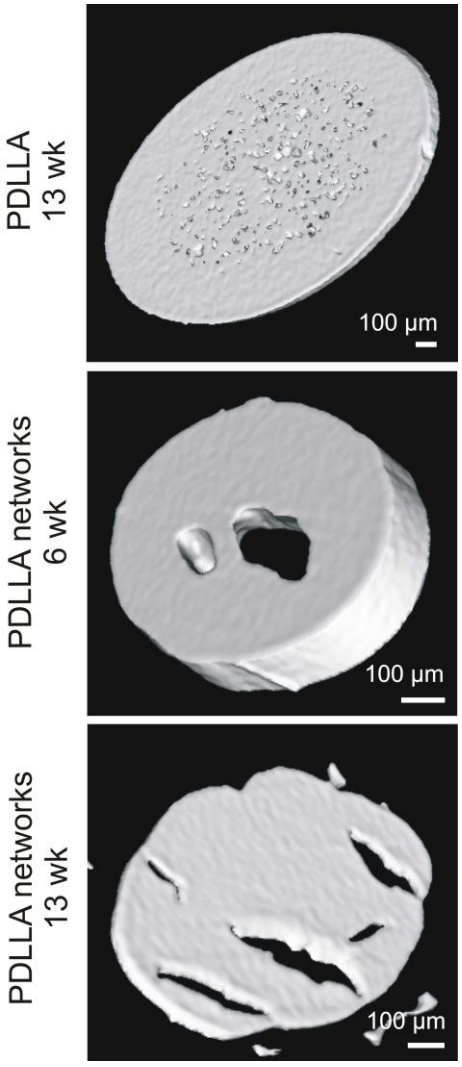

Figure 6. *μCT cross-sections through a specimen of linear PDLLA implanted for 13 wk and PDLLA network specimens implanted for 6 and 13 wk.*

Histology results indicate no cellular reaction to any of the implants after 6 wk. Very thin fibrous capsules were observed around the implants (Figure 7). Also, the retinas looked normal. After 13 wk thin capsules with only few cells were found around the implants and again the retinas looked normal. For the specimens of linear PTMC and the PTMC networks after 13 wk some inflammatory cells were observed in the vitreous in accordance with a foreign body reaction to the implant. Also, in the eye containing a PTMC implant, few giant cells that had phagocytosed some biomaterial were found in the

vitreous. These observations match well with the minor signs of degradation found for the PTMC rods (Figure 5a).

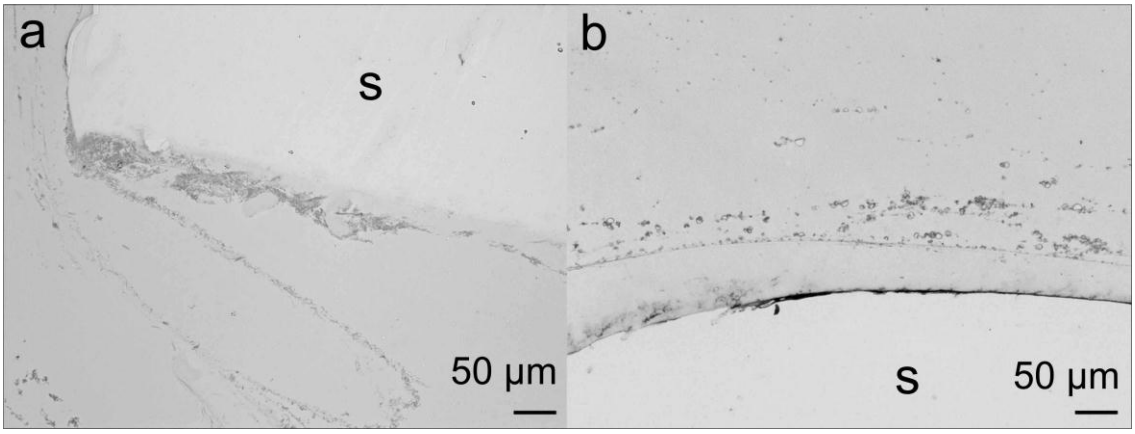

Figure 7. *Capsule around PTMC network specimen (s) after 6 wk in the rabbit vitreous, magnification 20x (a) and capsule around PDLLA network specimen (s) after 13 wk in the rabbit vitreous, magnification 20x (b).*

Conclusions

Crosslinked PTMC and PDLLA networks and linear PTMC and PDLLA were well tolerated in the rabbit vitreous. The degradation of linear PTMC and PTMC networks was very slow and comparable to the non-enzymatic *in vitro* situation. No significant mass loss was observed within 13 wk. Only minor signs of surface erosion were found for linear PTMC. PDLLA samples showed stronger signs of degradation. For linear PDLLA a large decrease in molecular weight was observed and PDLLA network implants started to lose mass within 13 wk. It can be concluded that linear PDLLA and PDLLA networks might be well-suited for degradable (degradation-controlled) drug release systems in the vitreous. PDLLA networks seem to be promising for long term degradation controlled intravitreal drug delivery since this material shows a suitable degradation rate without significant swelling. Furthermore these networks can easily be loaded with drugs and network properties such as the crosslink density can be adjusted to obtain optimal drug release profiles. Longer term studies are required to investigate the reaction of the eye when the mass loss of the PDLLA network implants increases and more degradation products are released into the vitreous.

Acknowledgements

We would like to acknowledge Sigrid Schüller-Ravoo for her help with the comparative *in vitro* degradation study and Mark Smithers for performing the SEM analysis.

References

[1] C. Bunce, W. Xing, R. Wormald, Causes of blind and partial sight certifications in England and Wales: April 2007-March 2008. Eye 24(11) (2010) 1692-1699.

[2] A. Urtti, Challenges and obstacles of ocular pharmacokinetics and drug delivery. Adv Drug Deliv Rev 58(11) (2006) 1131-1135.

[3] M.J. Colthurst, R.L. Williams, P.S. Hiscott, I. Grierson, Biomaterials used in the posterior segment of the eye. Biomaterials 21(7) (2000) 649-665.

[4] E. Eljarrat-Binstock, J. Pe'er, A. Domb, New techniques for drug delivery to the posterior eye segment. Pharm Res 27(4) (2010) 530-543.

[5] S.S. Lee, P. Hughes, A.D. Ross, M.R. Robinson, Biodegradable implants for sustained drug release in the eye. Pharm Res 27(10) (2010) 2043-2053.

[6] J.A. Haller, F. Bandello, R. Belfort Jr, M.S. Blumenkranz, M. Gillies, J. Heier, A. Loewenstein, Y.-H. Yoon, M.-L. Jacques, J. Jiao, X.-Y. Li, S.M. Whitcup, Randomized, sham-controlled trial of dexamethasone intravitreal implant in patients with macular edema due to retinal vein occlusion. Ophthalmology 117(6) (2010) 1134-1146.

[7] T. Moritera, Y. Ogura, Y. Honda, R. Wada, S.H. Hyon, Y. Ikada, Microspheres of biodegradable polymers as a drug-delivery system in the vitreous. Invest Ophthalmol Vis Sci 32(6) (1991) 1785-1790.

[8] G.G. Giordano, P. Chevezbarrios, M.F. Refojo, C.A. Garcia, Biodegradation and tissue reaction to intravitreous biodegradable poly(D,L-lactic-co-glycolic) acid microspheres. Curr Eye Res 14(9) (1995) 761-768.

[9] S. Einmahl, F. Behar-Cohen, C. Tabatabay, M. Savoldelli, F. D'Hermies, D. Chauvaud, J. Heller, R. Gurny, A viscous bioerodible poly(ortho ester) as a new biomaterial for intraocular application. J Biomed Mater Res 50(4) (2000) 566-573.

[10] S. Einmahl, S. Ponsart, R.A. Bejjani, F. D'Hermies, M. Savoldelli, J. Heller, C. Tabatabay, R. Gurny, F. Behar-Cohen, Ocular biocompatibility of a poly(ortho ester) characterized by autocatalyzed degradation. J Biomed Mater Res A 67A(1) (2003) 44-53.

[11] J. Heller, Ocular delivery using poly(ortho esters). Adv Drug Deliv Rev 57(14) (2005) 2053-2062.

[12] M.J. Bruining, P.S. Edelbroek-Hoogendoorn, H.G.T. Blaauwgeers, C.M. Mooy, F.H. Hendrikse, L.H. Koole, New biodegradable networks of poly(N-vinylpyrrolidinone) designed for controlled nonburst degradation in the vitreous body. J Biomed Mater Res A 47(2) (1999) 189-197.

[13] M.C. Hacker, A. Haesslein, H. Ueda, W.J. Foster, C.A. Garcia, D.M. Ammon, R.N. Borazjani, J.F. Kunzler, J.C. Salamone, A.G. Mikos, Biodegradable fumarate-based drug-delivery systems for ophthalmic applications. J Biomed Mater Res A 88A(4) (2009) 976-989.

[14] A. Silva-Cunha, S.L. Fialho, M.-C. Naud, F. Behar-Cohen, Poly(ε-caprolactone) intravitreous devices: an in vivo study. Invest Ophthalmol Vis Sci 50(5) (2009) 2312-2318.

[15] K. Davis, Controlled release from crosslinked degradable networks. Crit Rev Ther Drug Carrier Syst 19(4-5) (2002) 385-423.

[16] J. Jansen, M.J. Boerakker, J. Heuts, J. Feijen, D.W. Grijpma, Rapid photo-crosslinking of fumaric acid monoethyl ester-functionalized poly(trimethylene carbonate) oligomers for drug delivery applications. J Control Release 147(1) (2010) 54-61.

[17] A.S. Sawhney, C.P. Pathak, J.A. Hubbell, Bioerodible hydrogels based on photopolymerized poly(ethylene glycol)-co-poly(α-hydroxy acid) diacrylate macromers. Macromolecules 26(4) (1993) 581-587.

[18] D. Missirlis, N. Tirelli, J.A. Hubbell, Amphiphilic hydrogel nanoparticles. Preparation, characterization, and preliminary assessment as new colloidal drug carriers. Langmuir 21(6) (2005) 2605-2613.

[19] A.P. Pêgo, M.J.A. van Luyn, L.A. Brouwer, P.B. van Wachem, A.A. Poot, D.W. Grijpma, J. Feijen, In vivo behavior of poly(1,3-trimethylene carbonate) and copolymers of 1,3-trimethylene carbonate with D,L-lactide or ε-caprolactone: Degradation and tissue response. J Biomed Mater Res A 67A(3) (2003) 1044-1054.

[20] Z. Zhang, R. Kuijer, S.K. Bulstra, D.W. Grijpma, J. Feijen, The in vivo and in vitro degradation behavior of poly(trimethylene carbonate). Biomaterials 27(9) (2006) 1741-1748.

[21] O.S. Kluin, H.C. van der Mei, H.J. Busscher, D. Neut, A surface-eroding antibiotic delivery system based on poly-(trimethylene carbonate). Biomaterials 30(27) (2009) 4738-4742.

[22] E. Bat, T.G. van Kooten, J. Feijen, D.W. Grijpma, Macrophage-mediated erosion of gamma irradiated poly(trimethylene carbonate) films. Biomaterials 30(22) (2009) 3652-3661.

[23] R. Chapanian, M.Y. Tse, S.C. Pang, B.G. Amsden, The role of oxidation and enzymatic hydrolysis on the in vivo degradation of trimethylene carbonate based photocrosslinkable elastomers. Biomaterials 30(3) (2009) 295-306.

[24] J. Sebag, The vitreous: Structure, function and pathobiology, Springer-Verlag, New York, 1989.

[25] B.D. Ratner, A.S. Hofmann, F.J. Schoen, J.E. Lemons, Biomaterials Science, Elsevier, 2004.

[26] R. Herrero-Vanrell, I.T. Molina-Martinez, PLA and PLGA microparticles for intravitreal drug delivery: an overview. J Drug Deliv Sci Technol 14(1) (2007) 11-17.

[27] S.-H. Hyon, K. Jamshidi, Y. Ikada, Effects of residual monomer on the degradation of D,L-lactide polymer. Polym Int 46(3) (1998) 196-202.

[28] F.P.W. Melchels, A.H. Velders, J. Feijen, D.W. Grijpma, Photo-cross-linked poly(D,L-lactide)-based networks. structural characterization by HR-MAS NMR spectroscopy and hydrolytic degradation behavior. Macromolecules 43(20) (2010) 8570-8579.

[29] A.P. Pêgo, A.A. Poot, D.W. Grijpma, J. Feijen, In vitro degradation of trimethylene carbonate based (co)polymers. Macromol Biosci 2(9) (2002) 411-419.

[30] S.M. Li, H. Garreau, M. Vert, Structure property relationships in the case of the degradation of massive aliphatic poly-(α-hydroxy acids) in aqueous-media .1. poly(D,L-lactic acid). J Mater Sci Mater Med 1(3) (1990) 123-130.

Supporting information

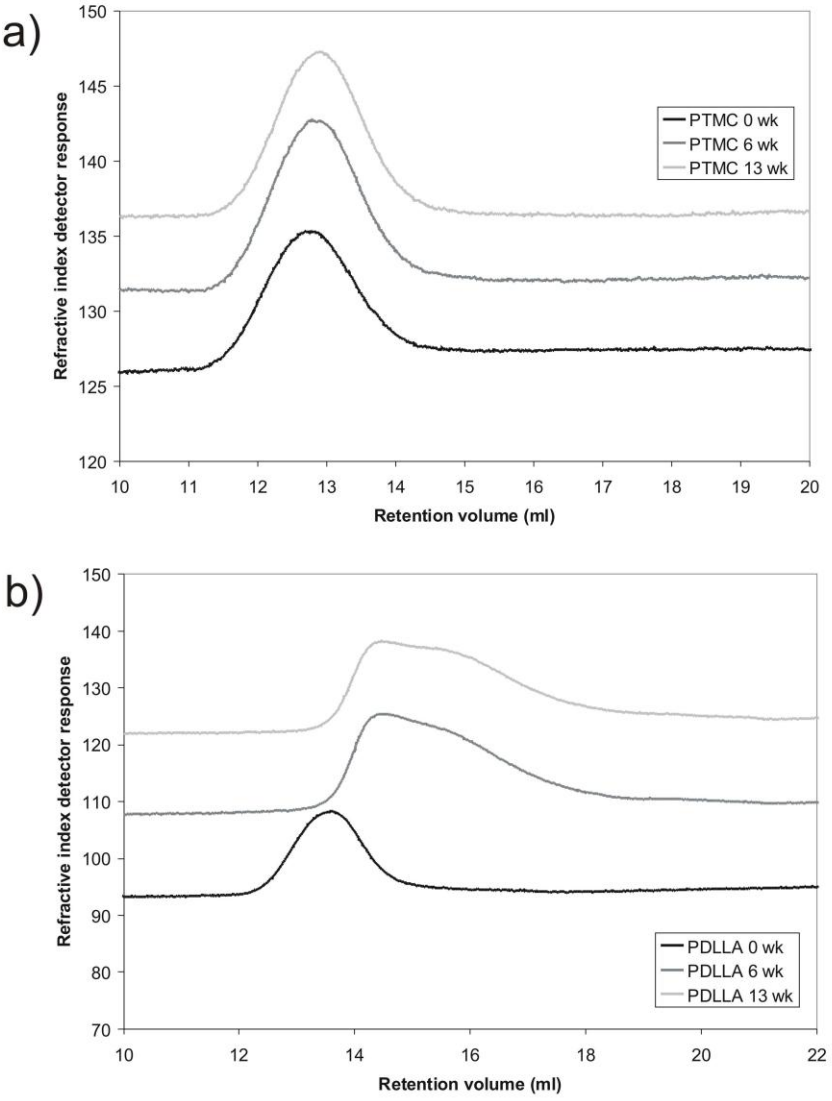

Figure 8. *GPC profiles of linear PTMC (a) and PDLLA (b) before implantation and after 6 and 13 wk in the rabbit vitreous.*

Chapter 9

The preparation of photo-crosslinked microspheres from fumaric acid monoethyl ester- and methacrylate-functionalized poly(D,L-lactic acid) oligomers

Janine Jansen[1], Gert-Jan A. ter Boo[1], George Mihov[2], Jan Feijen[3] and Dirk W. Grijpma[1,4]

1) MIRA Institute for Biomedical Technology and Technical Medicine, Department of Biomaterials Science and Technology, Faculty of Science and Technology, University of Twente, P.O. Box 217, 7500 AE, Enschede, The Netherlands
2) DSM Ahead, P.O Box 18, 6160 MD, Geleen, The Netherlands
3) MIRA Institute for Biomedical Technology and Technical Medicine, Department of Polymer Chemistry and Biomaterials, Faculty of Science and Technology, University of Twente, P.O. Box 217, 7500 AE, Enschede, The Netherlands
4) W.J. Kolff Institute, Department of Biomedical Engineering, University Medical Center Groningen, University of Groningen, Antonius Deusinglaan 1, 9713 AV, Groningen, The Netherlands

Abstract

Photo-crosslinked microspheres could readily be prepared from methacrylate-functionalized poly(D,L-lactic acid) oligomers. To allow the preparation of photo-crosslinked microspheres from fumaric acid monoethyl ester-functionalized poly(D,L-lactic acid) oligomers, N-vinyl-2-pyrrolidone (NVP) was required as a comonomer. The amount of NVP added and the microsphere hardening time prior to photo-crosslinking were carefully optimized to obtain non-aggregated crosslinked microspheres. These microspheres could be loaded with hydrophilic drugs using double emulsion solvent evaporation methods and hold promise for application in drug delivery.

Introduction

Photo-crosslinked polymer networks are interesting for drug delivery applications due to their versatility [1]. By adjusting factors such as the crosslink density and network hydrophilicity, drug release profiles can be tuned. Many of the studies on drug delivery systems based on photo-crosslinked polymer networks, performed in our group [2-5] and by others [6, 7], focus on disk- or rod-shaped devices. For several applications however, it would be advantageous if the release system is injectable. To achieve this photo-crosslinked microspheres could be used.

Several researchers investigated the preparation and application of photo-crosslinked micro- and nanoparticles. Most of these studies were focused on hydrophilic particles; so-called nano- or microgels [8, 9]. Also more hydrophobic photo-crosslinked microspheres were investigated. These could be prepared by photo-polymerization of aerosol droplets [10, 11] or emulsions [12].

Here we describe the preparation of photo-crosslinked microspheres from fumaric acid monoethyl ester- and methacrylate-functionalized poly(D,L-lactic acid) oligomers. These were made using the emulsion solvent evaporation method and subsequent photo-crosslinking.

Materials and methods

Materials

D,L-lactide (DLLA) was purchased from Purac Biochem (The Netherlands). Trimethylol propane (TMP), tin 2-ethylhexanoate ($Sn(Oct)_2$), methacrylic anhydride, triethyl amine (TEA), fumaric acid monoethyl ester (FAME) and polyvinyl alcohol (PVA) (80 % hydrolyzed, M_w = 9,000 to 10,000) were purchased from Sigma Aldrich (U.S.A.). 4-Dimethylaminopyridine (DMAP) and analytical grade chloroform were purchased from

Merck (Germany). 1,3-Dicyclohexylcarbodiimide (DCC) and N-vinyl-2-pyrrolidone (NVP) were obtained from Fluka (Switzerland). Analytical grade dichloromethane (DCM) was purchased from Biosolve (The Netherlands). DCM was dried over CaH_2 and distilled. Other solvents were of technical grade and were used as received. Irgacure 819 (BAPO, bis (2,4,6-trimethylolbenzoyl)-phenylphosphineoxide) was purchased from Ciba Specialty Chemicals (Switzerland).

Synthesis and characterization of 3-armed MA- and FAME-functionalized PDLLA oligomers

Three-armed poly(D,L-lactide) oligomers were synthesized by ring opening polymerization of D,L-lactide in the presence of trimethylol propane (TMP) as a trifunctional initiator. DLLA, TMP and $Sn(Oct)_2$ (approximately 0.2 mmol/mol monomer) as a catalyst were reacted in the melt at 130 ^{o}C for 48 h under argon. The targeted molecular weight was 9100 g/mol corresponding to approximately 21 D,L-lactide units per arm. To achieve this, 63 mol of monomer was used per mol of initiator.

The oligomers were functionalized with FAME end-groups by coupling fumaric acid monoethyl ester to the hydroxyl termini of the oligomers [13, 14]. An amount of oligomer was charged into a three-necked flask and dried for 2 h at 110 ^{o}C *in vacuo* and cooled to room temperature under argon. The oligomers were dissolved in dried DCM, and after addition and dissolution of FAME the system was further cooled to 0 ^{o}C. Then a dichloromethane solution of DCC and DMAP was added drop-wise to the vigorously stirred oligomer solution. In the coupling reaction, 1.2 moles of FAME and DCC and 0.03 moles of DMAP were used per mole of hydroxyl end-groups. The coupling reaction was continued overnight, letting the contents slowly warm up to room temperature. After completion of the reaction, the formed dicyclohexylurea was removed by filtration. The macromers were purified by precipitation in cold isopropanol, washing with water and freeze-drying.

The oligomers were functionalized with methacrylate end-groups by reacting methacrylic anhydride (MAAH) with the hydroxyl end-groups of the oligomers. An amount of oligomer was charged into a three-necked flask and dried for 2 h at 110 °C *in vacuo* and then cooled to room temperature under argon. The oligomer was dissolved in dry DCM and TEA was added. Methacrylic anhydride was added drop-wise to the vigorously stirred oligomer solution. Per mol of hydroxyl groups 1.2 moles of MAAH and TEA were used. The coupling reaction was continued for 3 d. The macromers were purified by precipitation in cold isopropanol, washing with water and freeze-drying.

The oligomer molecular weights (M_n) and the degrees of functionalization were determined from ^{1}H-NMR spectra (Varian Inova 300 MHz NMR spectrometer). Deuterated chloroform was used as a solvent.

The macromers are labeled as PDLLA 3X3K-FAME or PDLLA 3X3K-MA, in which 3 is the number of arms (the same for all macromers) and 3K is the molecular weight per arm (3000 g/mol).

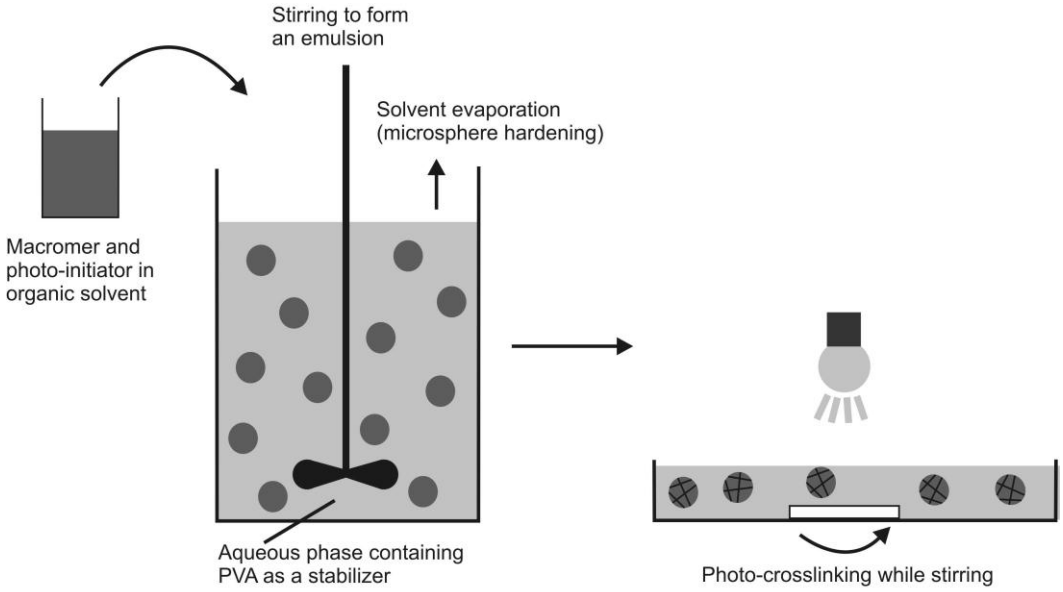

Figure 1. *Schematic representation of the preparation of photo-crosslinked microspheres.*

Preparation of photo-crosslinked PDLLA-MA microspheres

The emulsion solvent evaporation method was used to prepare microspheres from PDLLA 3X3K-MA macromers (Figure 1). First 0.5 g of macromer was dissolved in 3.5 ml chloroform. Subsequently, this solution was added drop-wise to 25 ml of a PVA solution (2 w/v %) in distilled water and the mixture was stirred for 5 min at 200 rpm using a magnetic stirrer. Subsequently, 200 ml of distilled water was added to adjust the final volume of the outer water phase and 3 h of stirring using a mechanical stirrer (400 rpm) was performed to allow the solvent to evaporate. The microspheres were washed three times with distilled water to remove residual PVA. Finally, the microspheres were freeze-dried.

Crosslinked PDLLA-MA microspheres were prepared by the same method as used for the preparation of their uncrosslinked counterparts. Now, 1 wt% Irgacure 819 photo-initiator (with respect to the macromer) was added to the macromer solution in chloroform. Photo-crosslinking was performed (after 3 h of solvent evaporation) in a

Petri dish while stirring, using an Ultralum crosslinking cabinet (365 nm, 3-5 mW/cm^2, 15 min).

Preparation of photo-crosslinked PDLLA-FAME microspheres

Uncrosslinked PDLLA 3X3K-FAME microspheres were prepared in the same way as PDLLA 3X3K-MA microspheres.

For the preparation of crosslinked PDLLA 3X3K-FAME microspheres dichloromethane was used to dissolve the macromers and 1 wt% Irgacure 819 photo-initiator (with respect to the macromer) was added to the macromer solution. NVP (20 wt% with respect to macromer) was added as a comonomer. The total amount of solvent (DCM + NVP) was kept constant at 3.5 ml. Crosslinking was performed after 1.5 h of solvent evaporation. The crosslinking conditions were the same as for the PDLLA 3X3K-MA microspheres.

Microsphere characterization

Microspheres were imaged using a light microscope (Nikon Eclipse E600 Fluorescence Microscope) and NIS-Elements F3.0 software including scale bars. Microsphere sizes were determined using ImageJ software, a public domain imaging program. The average sizes and size distribution of the microspheres were determined by measuring 100 spheres each time. The number mean diameter (D_n), volume mean diameter (D_v) and polydispersity index (PDI) of the microspheres were calculated using to the following equations:

$$D_n = \frac{\sum_{i=1}^{k} n_i D_i}{\sum_{i=1}^{k} n_i} \qquad D_v = \frac{\sum_{i=1}^{k} n_i D_i^4}{\sum_{i=1}^{k} n_i D_i^3} \qquad PDI = \frac{D_v}{D_n}$$

In these equations, D_i is the diameter of the microspheres, and n_i is the number of microspheres of that diameter.

Crosslinking was assessed by adding acetone to the prepared microspheres and using light microscopy to observe whether dissolution or swelling occurred in the solvent.

The thermal properties of macromers, uncrosslinked microspheres and crosslinked microspheres were evaluated using a Perkin Elmer Pyris 1 differential scanning calorimeter. Microspheres were dried under vacuum at room temperature prior to the measurements. Samples were heated from −0 °C to 100 °C at a heating rate of 10 °C/min and quenched rapidly at 300 °C/min to −0 °C. After 5 min a second heating scan was

recorded. The glass transition temperature (T_g) was taken as the midpoint of the heat capacity change in the second heating run.
Scanning electron microscopy (SEM; Philips XL30 operated at 2-10 kV) was used to study the microspheres. Samples were sputter coated with gold prior to analysis.

Results and discussion

Synthesis and characterization of 3-armed MA- and FAME-functionalized PDLLA oligomers

Three-armed PDLLA oligomers were prepared by ring opening polymerization of D,L-lactide with a trifunctional initiatior. The obtained molecular weight, determined from the initiator to lactide ratio in ^{1}H-NMR spectra, was close to the intended molecular weight (Table 1). The PDLLA oligomers were functionalized with FAME or methacrylate end-groups to obtain crosslinkable macromers. The obtained degrees of functionalization (p), calculated from ^{1}H-NMR spectra, where above 90 % (Table 1).

Table 1. *Characteristics of the prepared macromers.*

Macromer	M_n (kg/mol per arm)	p (%)
PDLLA 3X3K-MA	2.8	93
PDLLA 3X3K-FAME	2.8	92

Preparation and characterization of photo-crosslinked PDLLA-MA and PDLLA-FAME microspheres

Microspheres were prepared from the synthesized macromers using the emulsion solvent evaporation method. Crosslinked PDLLA-MA microspheres could be obtained by adding Irgacure 819 photo-initiator to the macromer solution in chloroform used in the emulsion solvent evaporation process and 15 min of crosslinking at 365 nm. Upon addition of acetone to these microspheres, they did not dissolve but only swelled (Figure 3), illustrating that they were indeed crosslinked.

Table 2. *Microsphere size and polydispersity.*

Macromer	Solvent	Crosslinked	D_n (μm)	D_v (μm)	PDI
PDLLA-3X3K-MA	chloroform	no	87	103	1.2
PDLLA-3X3K FAME	chloroform	no	99	129	1.3
PDLLA-3X3K-MA	chloroform	yes	130	144	1.1
PDLLA-3X3K-FAME /20%NVP	dichloromethane	yes	141	192	1.4

Microsphere sizes and size distributions are given in Table 2 and Figure 2. It can be seen that the crosslinked PDLLA-MA microspheres are somewhat larger than the uncrosslinked PDLLA-MA microspheres. This may be related to the photo-crosslinking process. Also, the photo-crosslinked PDLLA-MA microspheres were somewhat irregular in shape which can be seen most clearly in the SEM image in Figure 6. The thermal properties of the macromers and microspheres were determined by DSC. It was found that the glass transition temperature of the uncrosslinked microspheres is lower than that of the macromers. This may be due to some PVA or other impurities left in the microspheres that act as a plasticizer and thereby decrease the T_g. When the uncrosslinked and crosslinked PDLLA-MA microspheres are compared, the crosslinked microspheres show a higher T_g. This is in line with the fact that the T_g increases with increasing crosslink density [15].

Photo-crosslinking of PDLLA-FAME microspheres was not successful initially. This can be explained by the low reactivity of the FAME end-groups. It is known that a suitable comonomer is needed to allow rapid photo-polymerization of FAME end-groups [4]. Therefore, NVP, which is known to be suitable comonomer, was added to the macromer solution in chloroform. NVP does not only dissolve in chloroform, but also in water. It therefore diffuses out of the microspheres when these harden out as the chloroform evaporates. Careful optimization was required before photo-crosslinked PDLLA-FAME microspheres could be obtained. When too little NVP was added, or the microspheres were hardened out for too long times, no NVP was left at the time that crosslinking was preformed, and the microspheres did not crosslink at all. On the other hand, when too much NVP was present, or the microspheres did not harden out long enough, they did crosslink, but aggregation occurred (Figure 4). To solve these issues; chloroform was replaced by a more volatile solvent, dichloromethane. This allowed for shorter hardening times to limit diffusion of NVP out of the microspheres. In this way photo-crosslinked microspheres could be prepared with 20 wt% NVP after 1.5 h microsphere hardening time and 15 min of photo-crosslinking (Figure 5).

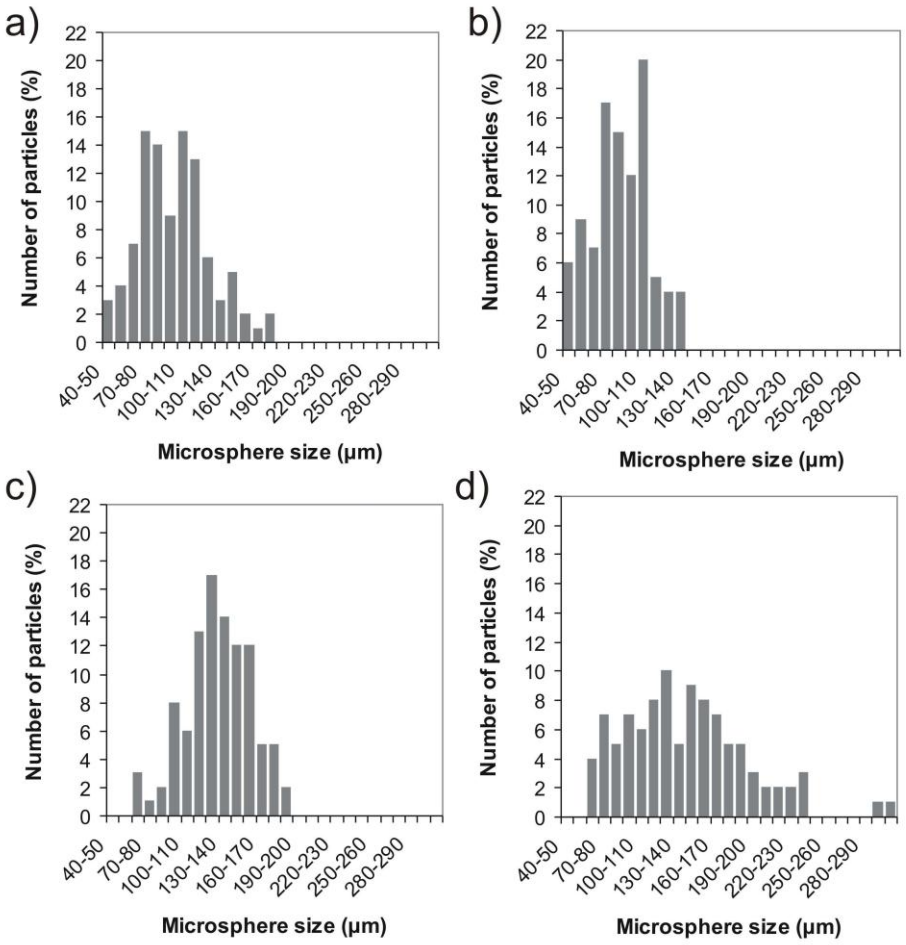

Figure 2. *Particle size distributions of uncrosslinked PDLLA-MA microspheres (a), uncrosslinked PDLLA-FAME microspheres (b), crosslinked PDLLA-MA microspheres (c) and crosslinked PDLLA-FAME microspheres, prepared with 20 % NVP (d).*

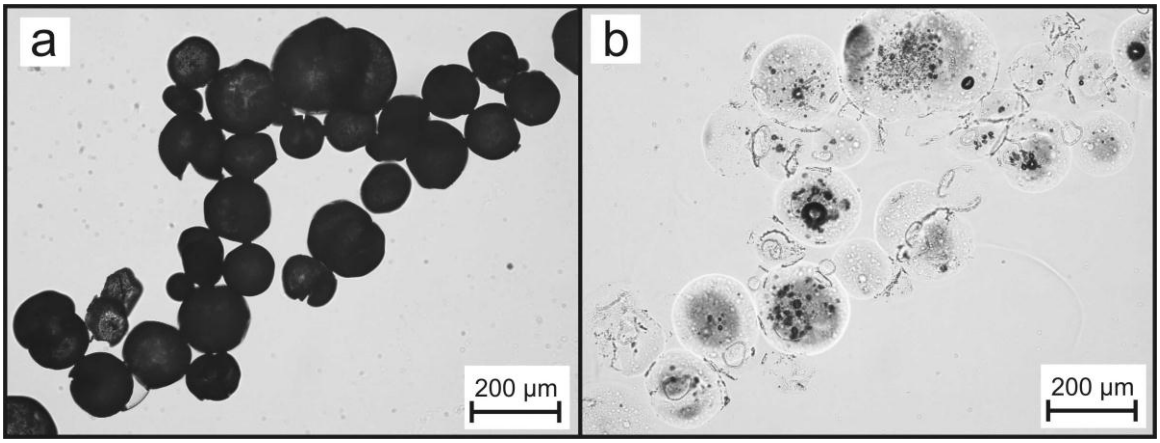

Figure 3. *Photo-crosslinked PDLLA 3X3K-MA microspheres before (a) and directly after (b) exposure to acetone.*

Table 3. *Glass transition temperatures of PDLLA-MA and PDLLA-FAME macromers, uncrosslinked microspheres and crosslinked microspheres.*

	T_g (°C)
PDLLA-3X3K-MA macromer	46.2
PDLLA-3X3K-MA uncrosslinked microspheres	28.3
PDLLA-3X3K-MA crosslinked microspheres	30.7
PDLLA-3X3K-FAME macromer	47.7
PDLLA-3X3K-FAME uncrosslinked microspheres	30.3
PDLLA-3X3K-FAME/20% NVP crosslinked microspheres	43.4

As for the PDLLA-MA microspheres, the crosslinked PDLLA-FAME microspheres are larger than their uncrosslinked counterparts (Table 2 and Figure 2). The high T_g of the crosslinked microspheres indicates not only that the microspheres are indeed crosslinked, but also that copolymerized NVP is present. PVP, the polymer of NVP, has a T_g of approximately 179 ^{o}C [16].

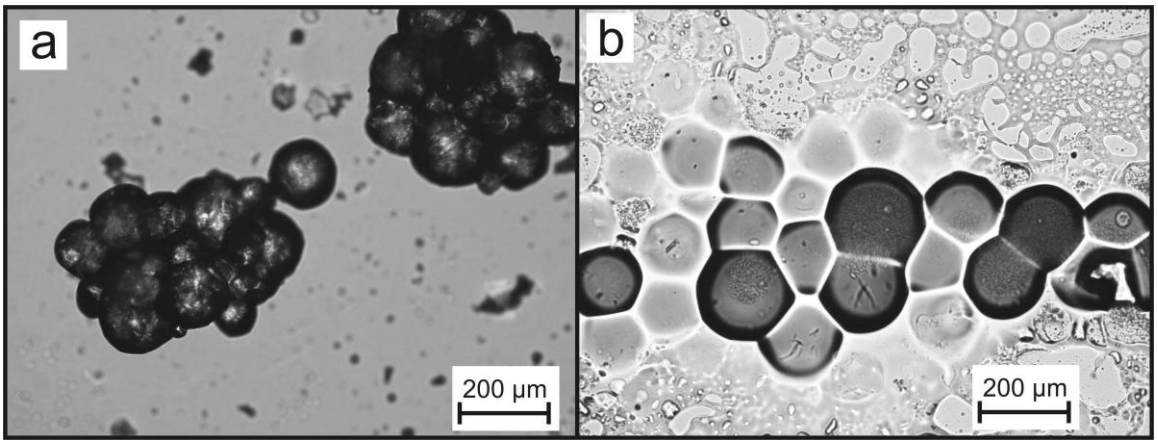

Figure 4. *PDLLA 3X3K-FAME microspheres prepared using 73 % of NVP and crosslinking after 3 h of solvent evaporation. Before (a) and after (b) exposure to acetone.*

Initial experiments have shown that using a double emulsion solvent evaporation method, hydrophilic drugs could be incorporated into photo-crosslinked PDLLA-MA and PDLLA-FAME microspheres. Further studies need to be performed to investigate the effect of the photo-crosslinking process and the matrix composition on the release of model drugs and proteins.

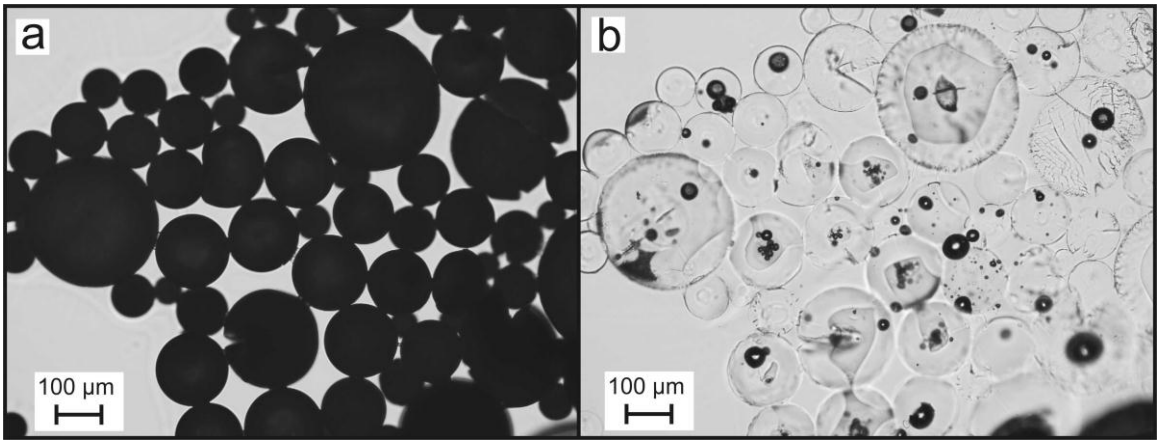

Figure 5. *Photo-crosslinked PDLLA 3X3K-FAME microspheres prepared using 20 %. NVP. After 1.5 h of microsphere hardening crosslinking was performed. Before (a) and after (b) exposure to acetone.*

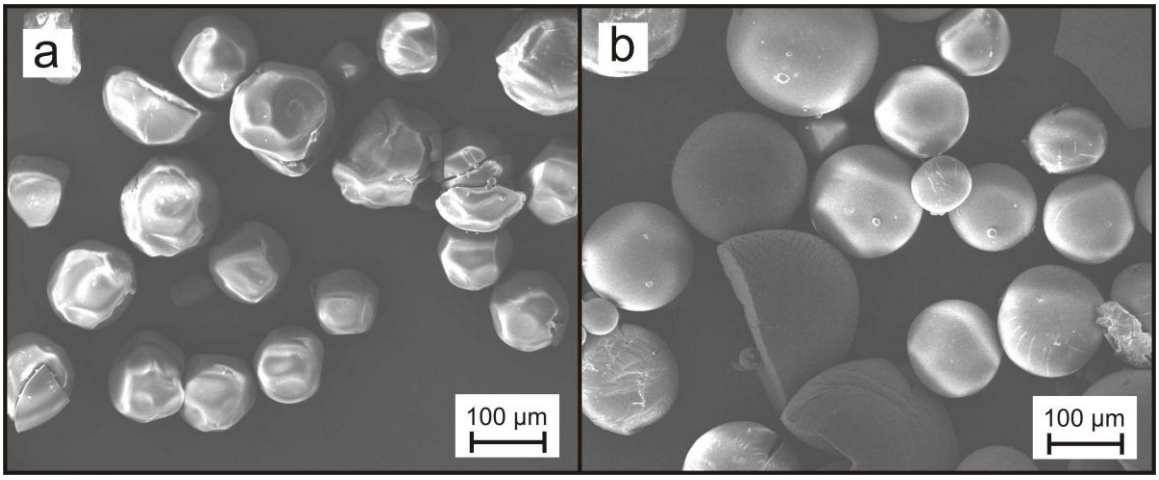

Figure 6. *SEM images of photo-crosslinked PDLLA 3X3K-MA microspheres (a) and photo-crosslinked PDLLA 3X3K-FAME microspheres prepared with 20 % NVP (b).*

Conclusions

Photo-crosslinked PDLLA-MA and PDLLA-FAME microspheres were successfully prepared. In the case of the PDLLA-FAME macromers, NVP was used as a comonomer and careful optimization of the preparation process was needed to obtain crosslinked microspheres without significant aggregation. The prepared photo-crosslinked microspheres may be attractive as an injectable controlled release system.

References

[1] B. Baroli, Photopolymerization of biomaterials: issues and potentialities in drug delivery, tissue engineering, and cell encapsulation applications. J Chem Technol Biot 81(4) (2006) 491-499.

[2] Chapter 5 of this thesis.

[3] Chapter 6 of this thesis.

[4] J. Jansen, M.J. Boerakker, J. Heuts, J. Feijen, D.W. Grijpma, Rapid photo-crosslinking of fumaric acid monoethyl ester-functionalized poly(trimethylene carbonate) oligomers for drug delivery applications. J Control Release 147(1) (2010) 54-61.

[5] J. Jansen, M.B. Bosman, M.J. Boerakker, J. Feijen, D.W. Grijpma, Photo-crosslinked poly(trimethylene carbonate)-fumarate/N-vinyl pyrrolidone networks for the controlled release of proteins. J Control Release 148(1) (2010) e79-e80.

[6] B. Amsden, Review of osmotic pressure driven release of proteins from monolithic devices. J Pharm Pharm Sci 10(2) (2007) 129-143.

[7] A. Haesslein, M.C. Hacker, A.G. Mikos, Effect of macromer molecular weight on in vitro ophthalmic drug release from photo-crosslinked matrices. Acta Biomater 4(1) (2008) 1-10.

[8] D. Missirlis, N. Tirelli, J.A. Hubbell, Amphiphilic hydrogel nanoparticles. Preparation, characterization, and preliminary assessment as new colloidal drug carriers. Langmuir 21(6) (2005) 2605-2613.

[9] J.K. Oh, R. Drumright, D.J. Siegwart, K. Matyjaszewski, The development of microgels/nanogels for drug delivery applications. Prog Polym Sci 33(4) (2008) 448-477.

[10] C. Esen, G. Schweiger, Preparation of monodisperse polymer particles by photopolymerization. J Colloid Interface Sci 179(1) (1996) 276-280.

[11] Z. Gao, E. Grulke, A. Ray, Synthesis of monodisperse polymer microspheres by photopolymerization of microdroplets. Colloid Polym Sci 285(8) (2007) 847-854.

[12] A.A. Dias, A. Petit, Microparticles comprising a crosslinked polymer. Patent (2006).

[13] D.W. Grijpma, Q. Hou, J. Feijen, Preparation of biodegradable networks by photo-crosslinking lactide, ε-caprolactone and trimethylene carbonate-based oligomers functionalized with fumaric acid monoethyl ester. Biomaterials 26(16) (2005) 2795-2802.

[14] A. Hassner, V. Alexanian, Direct room temperature esterification of carboxylic acids. Tetrahedron Lett 19 (1978) 4475-4478.

[15] T.G. Fox, S. Loshaek, Influence of molecular weight and degree of crosslinking on the specific volume and glass temperature of polymers. J Polym Sci 15(80) (1955) 371-390.

[16] J. Brandrup, E.H. Immergut, A. Abe, D.R. Bloch, Polymer Handbook, Wiley-Interscience New York, 1999.

Summary

In this thesis the potential of photo-crosslinked polymer networks for intraocular drug delivery is described. Patients with diseases of the back of the eye would benefit considerably from the development of drug delivery systems that can provide sustained intraocular delivery for months to years. Due to their versatility, photo-crosslinked polymer networks are an interesting class of materials for application in drug delivery systems. Photo-crosslinked polymer networks are often prepared from oligomers that are end-functionalized with double bond-containing groups. Many of the networks described in this thesis were prepared from oligomers functionalized with fumaric acid monoethyl ester (FAME). The possibilities of preparing photo-crosslinked polymer networks using these end-groups were explored.

Chapter 1 briefly describes the aim and outline of this thesis. In **Chapter 2** an introduction to biodegradable photo-crosslinked polymer networks is given. A number of intraocular drug delivery systems is described that are commercially available or currently under investigation. Several examples of the application of biodegradable photo-crosslinked polymer networks in drug delivery systems are presented.

In **Chapter 3** the preparation of photo-crosslinked polymer networks from poly(trimethylene carbonate) (PTMC) oligomers end-functionalized with FAME is described. Due to the low reactivity of the FAME end-groups these macromers crosslink slowly compared to methacrylate end-functionalized oligomers. To overcome this, two reactive diluents were selected: N-vinyl-2-pyrrolidone (NVP), a hydrophilic comonomer, and vinyl acetate (VAc), a hydrophobic comonomer. It was indeed found that the copolymerization reactions were much faster than homopolymerization of the FAME end-groups. The hydrophilicity of the networks could by varied by mixing NVP and VAc at different ratios. Extracts of the prepared networks were compatible with NIH 3T3 fibroblasts. For an initial release study vitamin B12, used as a hydrophilic model drug, was incorporated in the network films in the form of solid particles. The drug could be released from the networks in a controlled and sustained way over a period of several months. Release rates could be tuned by varying network hydrophilicity and macromer molecular weight. A more hydrophilic and less densely crosslinked network resulted in faster release.

In **Chapter 4** the release of two model proteins, lysozyme and bovine serum albumin, from networks prepared from the same PTMC-FAME macromers is described. Here, only NVP was applied as a comonomer and macromers of different molecular weights were prepared to vary the network mesh-size. Remarkably, the proteins were released fastest from the networks with the smallest mesh-size, probably due to osmotic pressure induced microcracks. The networks prepared from the macromers with higher molecular weights were found to be most suited for the controlled release of proteins over longer periods of time.

The networks described in **Chapters 3** and **4** were prepared from PTMC-based macromers. Due to the very slow hydrolytic degradation of PTMC (in the absence of enzymes), these networks hardly degraded over the release period. To enable the release of large proteins, possibly larger than the network mesh-size, faster degrading materials were used.

Chapter 5 is focused on the preparation of photo-crosslinked polymer networks from FAME-functionalized poly(D,L-lactic acid) (PDLLA) oligomers. The molecular weight of the oligomers and the NVP content were varied to obtain networks with different mesh-sizes and hydrophilicities. Again two model proteins, lysozyme and albumin, were incorporated in the network films as solid particles and their release was studied. The proteins were released from the networks in a controlled and sustained way over periods of a few weeks to a few months. It was found that by changing the NVP content and macromer molecular weight, degradation behavior and protein release profiles of the prepared networks could be tuned. The more hydrophilic and less densely crosslinked networks released the proteins at a faster rate. Although active lysozyme was released from the networks over the complete release period, lysozyme release was often incomplete. This was most likely caused by electrostatic and/or hydrophobic interactions between the positively charged protein and the degrading polymer network.

In **Chapter 6** the preparation of photo-crosslinked hydrogels is described. The hydrogels were prepared from FAME-functionalized triblock oligomers with a hydrophilic poly(ethylene glycol) middle block. The hydrophobic blocks consisted of PTMC, PDLLA or a copolymer of the two monomers. Hydrogels could easily be prepared by irradiation of aqueous solutions of the macromers in the presence of a photo-initiator and NVP as a comonomer. The length and composition of the hydrophobic blocks were varied to tune degradation and protein release profiles. Lysozyme was released from the hydrogels within one day, whereas albumin, a larger protein, was released over a period of a few weeks. In the networks described in **Chapters 3**, **4** and **5**, the model drugs were incorporated as solid particles. This minimized the contact between the sensitive drug

molecules and the free radicals present during the photo-crosslinking process. In the case of the hydrogels described in **Chapter 6** however, the proteins were dissolved in the aqueous macromer solutions and side reactions with free radicals occurred. This resulted in incomplete protein release. It was found however, that careful optimization of the photo-polymerization conditions could limit conjugation of proteins to the hydrogels as well as protein denaturation.

In **Chapter 7** attention is paid to an issue that is important for all degradable photo-crosslinked polymer networks designed for biomedical applications: the kinetic chain. Kinetic chains form during the radical polymerization and are the multifunctional crosslinks of the networks. These chains are carbon-carbon chains that remain after degradation. If their molecular weight is too high they can not be excreted by the kidneys. Photo-crosslinked polymer networks were prepared from methacrylate functionalized PDLLA oligomers. The networks were degraded completely and the molecular weight distributions of the kinetic chains were determined. The effect of the photo-initiator concentration and the addition of 2-mercaptoethanol as a chain transfer agent on the molecular weight of the kinetic chains was investigated. It was found that both increasing the initiator concentration and adding 2-mercaptoethanol decrease the kinetic chain length. However, the effect of adding 2-mercaptoethanol was much larger. A small amount of 2-mercaptoethanol is enough to decrease the kinetic chain length significantly. Some network properties such as the glass transition temperature and the swelling ratio in acetone are affected when the kinetic chain length is decreased.

Chapter 8 describes the intraocular degradation behavior of linear and crosslinked PTMC and PDLLA. Rod-shaped samples were implanted in the vitreous of rabbits and the degradation process was followed in time. PTMC is known to degrade by enzymatic surface erosion *in vivo*, whereas PDLLA degrades by hydrolytic bulk degradation. All materials were well tolerated in the rabbit vitreous. The degradation of linear high molecular weight PTMC and PTMC networks was very slow and no significant mass loss was observed within 13 wk. Only some minor signs of macrophage mediated erosion were found. The fact that no significant enzymatic surface erosion occurs can be related to the avascularity of the vitreous and the limited number of cells it contains. PDLLA samples showed more evident signs of degradation. For linear PDLLA, significant swelling and a large decrease in molecular weight in time were observed and PDLLA network implants started to lose mass within 13 wk. Of the tested materials PDLLA networks seem to be most promising for long term degradation controlled intravitreal drug delivery since this material degrades without significant swelling. Furthermore the preparation method of these networks allows easy and efficient incorporation of drugs.

For many applications, including intraocular drug delivery, it is advantageous if a drug delivery system can simply be injected. Therefore, the possibilities of preparing microspheres out of the developed materials were investigated in **Chapter 9**. Microspheres were prepared from FAME- and methacrylate-functionalized PDLLA oligomers using the emulsion solvent evaporation method. To allow the preparation of photo-crosslinked microspheres from FAME-functionalized PDLLA oligomers, NVP was needed as a comonomer. The amount of NVP added and the microsphere hardening time prior to photo-crosslinking were carefully optimized to obtain crosslinked microspheres without aggregation. The microspheres could be loaded with hydrophilic drugs using the double emulsion solvent evaporation method and hold promise for application in drug delivery.

The work described in this thesis demonstrates that photo-crosslinked polymer networks with diverse properties can be prepared from FAME-functionalized oligomers. By varying factors such as the crosslink density and network hydrophilicity, release profiles could be tuned. Model proteins could be released in a controlled way over periods of a few months. Therefore the prepared networks hold promise for the intraocular delivery of protein drugs. Importantly, an initial *in vivo* study indicated that photo-crosslinked polymer networks are well tolerated in the rabbit vitreous. However, there also remain challenges that need to be solved. Due to their large size and relative instability the controlled release of proteins remains challenging. Side reactions may occur during the network formation process and interactions of the protein with the polymer matrix may lead to incomplete protein release. It was shown that side reactions can be minimized if the network preparation process is optimized carefully, but these issues need further attention in the future. *In vivo* release studies with one of the networks that displayed attractive release profiles could be a next step towards an intraocular drug delivery system based on photo-crosslinked polymer networks.

Samenvatting

Dit proefschrift is gericht op de vervaardiging van polymere netwerken met verschillende hydrofiliciteit en dichtheid met behulp van foto-polymerisatie en de bestudering van de relatie tussen de netwerkeigenschappen en medicijnafgifte. Patiënten met een aandoening aan het achterste gedeelte van het oog zouden veel baat hebben bij de ontwikkeling van een afgiftesysteem dat een medicijn kan afgeven in het oog gedurende een periode van een aantal maanden tot een jaar. Door hun veelzijdigheid zijn polymere netwerken gemaakt met behulp van foto-polymerisatie een interessante groep materialen voor toepassing in afgiftesystemen voor medicijnen. Polymere netwerken worden vaak gemaakt door foto-polymerisatie van oligomeren met eind-gefunctionaliseerde, dubbele binding-bevattende groepen. Veel van de netwerken beschreven in dit proefschrift zijn gemaakt van oligomeren gefunctionaliseerd met fumaarzuur monoethyl ester (FAME). De mogelijkheden van het gebruik van deze eindgroepen bij het maken van polymere netwerken met behulp van fotopolymerisatie werden verkend.

Hoofdstuk 1 beschrijft het doel van het onderzoek en geeft een kort overzicht van het proefschrift. In **Hoofdstuk 2** wordt een korte introductie over biodegradeerbare polymere netwerken gemaakt met behulp van foto-polymerisatie gegeven. Een aantal intraoculaire afgiftesystemen dat momenteel op de markt is of wordt onderzocht wordt beschreven. Er worden verschillende voorbeelden gegeven van de toepassing van biodegradeerbare polymere netwerken gemaakt met behulp van foto-polymerisatie in afgiftesystemen voor medicijnen.

In **Hoofdstuk 3** wordt de synthese beschreven van polymere netwerken vanuit poly(trimethyleen carbonaat) (PTMC) oligomeren, gefunctionaliseerd met FAME eindgroepen met behulp van foto-polymerisatie. Door de lage reactiviteit van de FAME eindgroepen foto-polymeriseren deze macromeren langzaam vergeleken met oligomeren gefunctionaliseerd met methacrylaat eindgroepen. Om dit op te lossen werden twee reactieve oplosmiddelen geselecteerd: N-vinyl-2-pyrrolidon (NVP), een hydrofiel comonomeer, en vinyl acetaat (VAc), een hydrofoob comonomeer. De copolymerisatie reacties waren inderdaad veel sneller dan de homopolymerisatie van de FAME eindgroepen. De hydrofiliciteit (wateropname) van de netwerken kon worden gevarieerd door mengsels van NVP en VAc in verschillende verhoudingen te gebruiken. Extracten van de netwerken waren compatibel met NIH 3T3 fibroblasten. Voor een initieel afgifte

experiment werd vitamine B12, gebruikt als een hydrofiel modelmedicijn, ingemengd in de netwerk films in de vorm van vaste deeltjes. Vitamine B12 werd op een gecontroleerde manier afgegeven uit de netwerken gedurende een periode van een aantal maanden. De afgiftesnelheid kon worden aangepast door de hydrofiliciteit van de netwerken of het molecuulgewicht van de macromeren te variëren. Een hydrofieler netwerk en een netwerk met een lagere dichtheid resulteerden in snellere afgifte.

In **Hoofdstuk 4** wordt de afgifte van twee modeleiwitten, lysozym en albumine, uit netwerken gemaakt van dezelfde PTMC-FAME macromeren beschreven. Alleen NVP werd hier gebruikt als comonomeer en macromeren met verschillende molecuulgewichten werden gebruikt om de dichtheid van de netwerken te variëren. Opmerkelijk was dat de eiwitten het snelst werden afgegeven uit de netwerken met de hoogste dichtheid. Waarschijnlijk veroorzaakte osmotische druk kleine scheurtjes in deze netwerken. De netwerken gemaakt van macromeren met een hoger molecuulgewicht bleken het beste geschikt om eiwitten gedurende langere periodes af te geven.

De netwerken beschreven in **Hoofdstukken 3** en **4** werden gemaakt van macromeren gebaseerd op PTMC. Door de zeer langzame hydrolytische degradatie van PTMC (in afwezigheid van enzymen) degradeerden deze netwerken nauwelijks tijdens de afgifteperiode. Om de afgifte van grotere eiwitten, wellicht eiwitten die groter zijn dan de maaswijdte van het netwerk, mogelijk te maken werden sneller degraderende materialen gebruikt.

Hoofdstuk 5 is gericht op het maken van polymere netwerken door middel van foto-polymerisatie van FAME-gefunctionaliseerde poly(D,L-lactide) (PDLLA) oligomeren. Het molecuulgewicht van de oligomeren en de hoeveelheid NVP werden gevarieerd om netwerken te verkrijgen met verschillende netwerkdichtheden en hydrofiliciteit. Opnieuw werden twee modeleiwitten, lysozym en albumine, ingemengd in de netwerkfilms in de vorm van vaste deeltjes en werd hun afgifte bestudeerd. De eiwitten werden op een gecontroleerde manier uit de netwerken afgegeven gedurende een periode van een paar weken tot een paar maanden. Er werd gevonden dat door de hoeveelheid NVP en het molecuulgewicht van de oligomeren te variëren, degradatiegedrag en afgifteprofielen konden worden aangepast. De meer hydrofiele netwerken en de netwerken met een lagere dichtheid gaven de eiwitten sneller af. Hoewel tijdens de gehele periode actief lysozym werd afgegeven, was de afgifte vaak niet compleet. Dit werd waarschijnlijk veroorzaakt door elektrostatische of hydrofobe interacties tussen het positief geladen eiwit en het degraderende polymeernetwerk.

In **Hoofdstuk 6** wordt de synthese van hydrogelen met behulp van foto-polymerisatie beschreven. De hydrogelen werden gemaakt van FAME-gefunctionaliseerde triblok-

oligomeren met een hydrofiel poly(ethyleen glycol) middenblok. De hydrofobe blokken bestonden uit PTMC, PDLLA of een copolymeer van de twee monomeren. Hydrogelen konden eenvoudig worden gemaakt door waterige oplossingen van de macromeren te belichten in de aanwezigheid van een foto-initiator en NVP als comonomeer. De lengte en samenstelling van de hydrofobe blokken werden gevarieerd om het degradatiegedrag en de afgifteprofielen te beïnvloeden. Lysozym werd binnen één dag afgegeven uit de hydrogelen, terwijl albumine, een groter eiwit, gedurende een periode van een aantal weken werd afgegeven. In de netwerken beschreven in **Hoofdstukken 3-5** werden de eiwitten ingemengd in de vorm van vaste deeltjes. Dit resulteerde in minimaal contact tussen de gevoelige medicijnen en de vrije radicalen die aanwezig zijn tijdens de foto-polymerisatiereactie. In het geval van de hydrogelen beschreven in **Hoofdstuk 6** werden de eiwitten opgelost in waterige macromeeroplossingen en vonden er nevenreacties met de vrije radicalen plaats. Dit resulteerde in incomplete afgifte. Er werd wel gevonden dat, door de foto-polymerisatieomstandigheden nauwkeurig te optimaliseren, conjugatie van het eiwit aan de hydrogel en eiwit denaturatie konden worden beperkt.

In **Hoofdstuk 7** wordt aandacht geschonken aan een onderwerp dat belangrijk is voor alle afbreekbare polymere netwerken gemaakt met foto-polymerisatie die zijn ontworpen voor biomedische toepassingen: de kinetische keten. Kinetische ketens worden gevormd tijdens de radicaal polymerisatie en zijn de multifunctionele verknopingspunten van het netwerk. Deze ketens zijn koolstof-koolstof ketens die achterblijven na degradatie van het netwerk. Als het molecuulgewicht te hoog is kunnen ze niet worden uitgescheiden door de nieren. Polymere netwerken werden gemaakt door middel van foto-polymersatie van methacrylaat-gefunctionaliseerde PDLLA oligomeren. De netwerken werden volledig afgebroken en de molecuulgewichtsverdelingen van de kinetische ketens werden bepaald. Het effect van de foto-initiatorconcentratie en het toevoegen van 2-mercaptoethanol als een ketenoverdrachtsmiddel op het molecuulgewicht van de kinetische ketens werd onderzocht. Er werd gevonden dat zowel het verhogen van de foto-initiator concentratie als het toevoegen van 2-mercaptoethanol de kinetische ketenlengte verkleinde, waarbij het effect van het toevoegen van 2-mercaptoethanol veel groter was dan het verhogen van de foto-initiator concentratie. Een kleine hoeveelheid 2-mecaptoethanol is genoeg om de kinetische ketenlengte significant te verkleinen. Een aantal netwerkeigenschappen zoals de glasovergangstemperatuur en het zwelgedrag in aceton werden beïnvloed als de kinetische ketenlengte werd verkleind.

Hoofdstuk 8 beschrijft het intraoculaire degradatiegedrag van lineair PTMC en PDLLA en PTMC en PDLLA netwerken gemaakt met behulp van foto-polymerisatie. Kleine specimens in de vorm van cylinders werden geïmplanteerd in het glasvocht van het oog

van konijnen en het degradatieproces werd gevolgd in de tijd. Het is bekend dat PTMC *in vivo* degradeert door middel van enzymatische oppervlakte erosie, terwijl PDLLA degradeert door middel van hydrolytische bulk degradatie. Alle materialen werden goed verdragen in het glasvocht van de konijnen. De degradatie van hoog molecuulgewicht PTMC en PTMC netwerken was erg langzaam en er werd geen significante afname in massa gevonden na 13 weken. Er werden alleen wat zeer kleine tekenen van degradatie door macrofagen gevonden. Het feit dat er geen significante enzymatische oppervlakte erosie plaats vindt kan zijn gerelateerd aan de afwezigheid van bloedvaten in het glasvocht van het oog en het beperkte aantal cellen dat daar aanwezig is. De PDLLA specimens lieten duidelijkere tekenen van degradatie zien. Voor lineair PDLLA werden een significante zwelling en een grote afname in het molecuulgewicht in de tijd waargenomen. PDLLA netwerk specimens lieten een afname in massa zien binnen 13 weken. Van de geteste materialen lijken PDLLA netwerken het meest veelbelovend voor lange termijn, degradatie gecontroleerde medicijnafgifte in het glasvocht omdat dit materiaal degradeert zonder significant te zwellen. Bovendien laat de methode waarmee deze specimens gemaakt zijn belading met medicijnen op een eenvoudige en efficiënte manier toe.

Voor veel toepassingen, inclusief intraoculaire medicijnafgifte, is het gunstig als een afgiftesysteem eenvoudigweg kan worden geïnjecteerd. Daarom werden de mogelijkheden om microbolletjes te maken vanuit de ontwikkelde materialen onderzocht in **Hoofdstuk 9**. Microbolletjes werden gemaakt van FAME- en methacrylaat-gefunctionaliseerde oligomeren. Hierbij werd gebruik gemaakt van een emulsie-techniek. Om het mogelijk te maken microbolletjes te maken van FAME-gefunctionaliseerde PDLLA oligomeren was NVP opnieuw nodig als comonomeer. De hoeveelheid NVP en de tijd die de deeltjes kregen om uit te harden voor de foto-polymersatiereactie werden nauwkeurig geoptimaliseerd om verknoopte microbolletjes te verkrijgen zonder aggregatie. De microbolletjes konden worden beladen met een hydrofiel medicijn door gebruik te maken van een dubbele emulsie-techniek en zijn veelbelovend voor toepassing in medicijnafgifte.

Het werk beschreven in dit proefschrift toont aan dat polymere netwerken met uiteenlopende eigenschappen kunnen worden bereid door foto-polymerisatie van FAME-gefunctionaliseerde oligomeren. Door factoren zoals de netwerkdichtheid en de hydrofiliciteit van de netwerken te variëren konden afgifteprofielen worden aangepast. Modeleiwitten konden worden afgegeven gedurende periodes van een aantal maanden. De gemaakte netwerken zijn daarom veelbelovend voor de afgifte van therapeutische eiwitten in het oog. In een initiële *in vivo* studie werd bovendien aangetoond dat de

polymere netwerken gemaakt met behulp van foto-polymerisatie goed werden verdragen in het glasvocht van konijnen. Desondanks zijn er nog een aantal belangrijke uitdagingen die aandacht vragen. Door hun grote formaat en relatief geringe stabiliteit blijft de gecontroleerde afgifte van eiwitten uitdagend. Nevenreacties kunnen plaatsvinden tijdens de foto-polymerisatie en interacties van het eiwit en de polymere matrix kunnen leiden tot incomplete afgifte. Er werd aangetoond dat nevenreacties kunnen worden geminimaliseerd als het foto-polymerisatie proces zorgvuldig wordt geoptimaliseerd, maar aandacht voor deze belangrijke punten blijft nodig in de toekomst. *In vivo* afgiftestudies met één van de netwerken die aantrekkelijke afgifteprofielen lieten zien kunnen een volgende stap zijn in de richting van een intraoculair afgiftesysteem gebaseerd op polymere netwerken gemaakt met behulp van foto-polymerisatie.

Dankwoord

Na bijna vier jaar is het dan zover: mijn proefschrift is af en ik ben toe aan het schrijven van het dankwoord. Misschien wel het lastigste stukje schrijfwerk, omdat ik besef dat dit deel het vaakst gelezen zal worden. Mijn promotietraject was niet alleen erg leerzaam maar vooral ook erg leuk. De afgelopen jaren is er geen dag geweest dat ik met tegenzin op mijn fiets stapte om naar de universiteit te gaan. De mensen die hieraan een bijdrage hebben geleverd wil ik hier graag bedanken.

Als eerste bedank ik natuurlijk mijn promotors: professor Jan Feijen en professor Dirk W. Grijpma. Van de één maakte ik tijdens mijn promotietrajact het emiritaat mee, van de ander de oratie. Professor Feijen, van harte bedankt voor al uw hulp, suggesties en vertrouwen in mij. Het was een eer één van uw laatste promovendi te zijn. Dirk, naast promotor ook mijn dagelijks begeleider. Ik waardeer het erg dat je me vrij hebt gelaten om mijn eigen keuzes te maken. Toch kon ik altijd bij je binnenlopen en stond je klaar als ik je hulp nodig had. Je hebt me veel geleerd over het schrijven van artikelen en het op een positieve en heldere manier presenteren van mijn resultaten, waarvoor dank.

Mijn project werd gefinancierd door DSM, maar dat was niet de enige inbreng in mijn onderzoek vanuit Geleen. George Mihov en Mark Boerakker speelden hierin een belangrijke rol. Dear George, thank you very much for all your input during the last two years. Many of your ideas and suggestions helped me in my studies. I should also thank you for all the paperwork you did to get my chapters and articles approved for publication. I am looking forward to seeing you in my committee on the 26th of January. Beste Mark, ook jij natuurlijk van harte bedankt voor al je input. Na een zeer prettige samenwerking van twee jaar ging je “helaas” hogerop binnen een ander onderdeel van DSM. Ik wil ook graag Jean Heuts en Peter Tummers van DSM Resolve bedanken voor hun hulp bij de FTIR metingen die zijn terug te vinden in hoofdstuk 3. The half yearly meetings at DSM were also very useful to me thanks to the many questions and suggestions I received from DSM employees. Many thanks to Aylvin Dias, Ken Messier, Mark Hendriks, Jens Thies and all other DSM people that were somehow involved in my project.

Graag wil ik ook Steven Koopmans, Leonie Los, Corien van der Worp, Corina van der Burgt, professor Anneke Hooymans en de mensen van het dierenlab van het UMCG bedanken voor de prettige samenwerking. Ik heb erg veel geleerd op de dagen die ik in

Groningen was en de studie heeft geresulteerd in een mooi artikel (hoofdstuk 8 van dit proefschrift). Helaas is het afgiftesysteem voor patiënten met macula degeneratie er nog niet gekomen, maar ik denk dat we wel een stap in de goede richting hebben gezet.
Many thanks also to Abdul Ghaffar and professor Sjoerd van der Wal of the UVA for the cooperation that resulted in Chapter 7 of this thesis. Thanks to your sophisticated analysis techniques I learned a lot about the structure of my networks. I appreciated the always very hospitable receptions in Amsterdam.
Ook verschillende deskundige mensen binnen de UT leverden een bijdrage aan mijn project. Ik bedank graag Thieme Stevens (MALDI-TOF), Clemens Padberg (photo-DSC), Mark Smitters (SEM) en Bianca Snellink-Ruel (NMR). Ook dank aan de heren van TCO voor alle reparaties en het maken van Teflon mallen, glaswerk en de (oude) photo-DSC opstelling.
Graag wil ik ook professor Piet Dijkstra, professor Johan Engbersen, André Poot en Dimitris Stamatialis bedanken voor alle nuttige opmerkingen en suggesties tijdens de vakgroep presentaties. André, ook van harte bedankt voor je advies op gebied van de meer biologisch getinte onderdelen van mijn onderzoek. Piet, ik kijk uit naar je kritische vragen op 26 januari. Johan zal die dag als voorzitter alles in goede banen leiden. Ook daarvoor alvast veel dank.
Graag bedank ik ook Anita Podt voor al haar hulp met de microCT en de GPC. Sandra Teixeira, thank you very much for your help with the cell culture experiments described in Chapter 3. Hetty, bedankt voor je deskundige hulp bij computer gerelateerde problemen. Marc, bedankt voor je ondersteuning op het gebied van veiligheidszaken. Zlata, bedankt voor al je hulp met de bestellingen. En natuurlijk Karin, bedankt voor al je hulp met het papierwerk en vooral ook voor al het andere wat je doet voor de groep.
In de afgelopen vier jaar heb ik vijf studenten mogen begeleiden bij hun bachelor of master opdracht. Voor mij één van de leukste bezigheden in mijn tijd als promovendus. Ik ben erg trots dat veel van jullie werk is terug te vinden in dit proefschrift en wil jullie van harte bedanken voor jullie inzet en enthousiasme. Mirjam Bosman was mijn allereerste student. Een bacheloropdracht duurt maar drie maanden, maar toch hebben we van je werk een mooi kort hoofdstuk (hoodfstuk 4) kunnen maken. Daarna kwamen tegelijk nog twee bachelorstudenten: Martijn Tibbe en Thomas van der Horst. Martijn, jouw werk gaf aanzet tot het onderzoek beschreven in hoofdstuk 5. Thomas, jouw project was een onderdeel van de samenwerking met Amsterdam en was de aanleiding voor het onderzoek beschreven in hoofdstuk 7. Daarna kwam Mike Geven, jouw project was een zijstapje en is daarom niet terug te vinden in dit proefschrift. Ik hoop dat iemand in de groep nog eens aan de slag gaat met de mooie afbreekbare crosslinker die je hebt

gemaakt. Als laatste kwam Gert-Jan ter Boo, een master student die zich ging bezig houden met het maken van microdeeltjes van de materialen die ik heb ontwikkeld. Jouw werk is te vinden in hoofdstuk 9. Leuk dat je nu ook zelf verder gaat als promovendus, en nog wel in Zwitserland!

In het lab was het altijd een gezellige boel met de collega-aio's en postdocs en met de vele studenten die kwamen en gingen. Erhan, Ferry en Siggi hebben mij alles geleerd over polymere netwerken, PTMC en praktische zaken in het lab. Dankzij jullie kwam ik in een gespreid bedje terecht waarvoor heel veel dank! Siggi, ook nog bedankt voor je bijdrage aan de vergelijkende in vitro studie bij hoofdstuk 8. Helaas gedroegen de netwerken zich niet zoals we hadden gehoopt. Erhan, it was an honor to be your paranimf. I wish you and Arzu all the best with your postdoc in the USA. Ferry, mijn afstudeerbegeleider, toen ik tijdens mijn afstudeeronderzoek kennis maakte met de fumaraten had ik me niet kunnen voorstellen dat ik er ooit een proefschrift over zou schrijven. Na een rustige periode werd het gelukkig weer lekker druk in lab ZH 283. Erwin, fantastisch dat je terug kwam! Ik kan me geen betere lab en kantoor genoot wensen dan jij. Leuk dat je mijn paranimf wilt zijn. Shahriar, although your style of working did not always make my life as a lab chief easy, I enjoyed our discussions about polymer networks and admire you creativity. Xiaolin, unfortunately your project is a cooperation with Amsterdam and you will move there soon. You will be missed in the lab for sure. Sebastien, we have only worked together in the lab for a short while. Your knowledge of organic chemistry and your great sense of humor and positive spirit were welcomed by everyone. Graag bedank ik ook Sandra, Kasia, Vincent, Alfredo, Nynke, Melissa, Laura en alle studenten die kort of wat langer werkten in ons lab.

Toen ik tijdens mijn afstuderen terecht kwam op kantoor ZH 248 stond het nog bekend als het kippenhok. Inmiddels deel ik het kantoor met drie heren, maar dat is gelukkig niet ten koste gegaan van de perfecte sfeer. Erwin, Frits, Mark, Wei, Lanti, Ingrid (dankzij jou maakte ik ooit kennis met PBM), Alfredo, Anita K en Astrid, bedankt voor de gezelligheid.

Ik denk met veel plezier terug aan alle activiteiten die werden georganiseerd de afgelopen jaren. Tijdens de studiereizen, triathlons, groepsuitjes, het zeilweekend, pubquizen, barbecues en tijdens de lunch en koffiepauzes was het altijd gezellig dankzij alle fijne collega's. Niels, jouw droge humor wordt nog steeds gemist tijdens de koffiepauzes. Ook je kennis van nutteloze RTL boulevard feitjes is onnavolgbaar. Wat betreft de slechte woordgrappen moest je het toch afleggen tegen Hans. Hans, ik bewonder je tomeloze energie. Wie wint er nou zonder enige training de triathlon? Met Sytze maakte ik een prachtige roadtrip naar Las Vegas na een congres in Salt Lake City. Wat bewaar ik daar

mooie herinneringen aan! Jos, jij staat altijd klaar voor iedereen. Ook bedankt voor alle leuke pubquiz avondjes die je de afgelopen jaren organiseerde. Met al die mannen in de groep was ik blij dat Dimitrios wat gezellige dames meenam toen hij bij onze groep kwam. Marlon, bedankt voor alle gespreken over onze toekomstplannen. Ik waardeer je betrokkenheid en interesse. Leuk dat je mijn paranimf wilt zijn! Verder wil ik hier ook graag Lydia, Martin, Gregory, Jung Seok, Rong, Chao, Dewi, Marloes, Kim, Andries, Bade, Kishore, Nazely, Suvi, Di Zhou, Hongzi Du, Arkadi, Federico en Guoying Si bedanken.

Tijdens mijn promotie ben ik ongeveer anderhalf jaar bestuurslid geweest bij het Female Faculty Network Twente (FFNT). Ik heb erg veel geleerd van de activiteiten die we hebben georganiseerd maar vooral ook van het samenwerken met de andere bestuursleden. Angelika, Liudvika, Wietske, Genie, Laura, Marcella, Monique en Marjolein, heel veel dank daarvoor!

Naast het onderzoek was er gelukkig ook tijd voor ontspanning. Liesbeth en Jobke, bedankt voor alle broodnodige en vooral gezellige uurtjes in het sportcentrum. Jammer dat ik net die ene keer dat Hans en Andries gingen winnen bij yoga moest missen…

Veel van mijn vrienden zijn ook bezig met hun promotieonderzoek, op verschillende plekken in Nederland, of zelfs daarbuiten. Ik heb het altijd erg prettig gevonden om ervaringen te kunnen delen. Bart R., Theun, Jetty, Erwin, Jobke, Bart B. en Marjolein, heel veel succes met jullie onderzoek. Ik kijk er naar uit lekker achterover te leunen tijdens jullie verdediging.

Graag wil ik ook mijn ouders, schoonouders, zus, zwager, opa's, oma's en andere familieleden bedanken voor hun interesse in mijn onderzoek, ook al was het soms erg ver van jullie bed. Ik kijk ernaar uit om jullie op 26 januari te zien zitten op de eerste rij. Lieve pap en mam, bedankt dat jullie mij altijd hebben gestimuleerd om te doen wat ik leuk vind en me de mogelijkheden hebben gegeven om mijn dromen na te jagen. En ja opa en oma, nu ben ik eindelijk uitgestudeerd en kan ik aan een "echte baan" beginnen.

Als laatste bedank ik Bas, voor de mooie tijd de afgelopen vier jaar, waarin we allebei aan ons promotieonderzoek werkten. Ook naast het werk hebben we samen veel avonturen beleefd en ik kijk uit naar nog veel meer mooie avonturen in de toekomst. Ik hou van je!

Janine